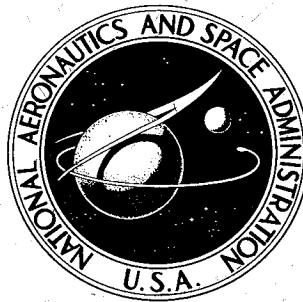


CASE FILE COPY

NASA TECHNICAL
REPORT



NASA TR R-187

NASA TR R-187

FLUID OSCILLATIONS IN THE CONTAINERS OF A SPACE VEHICLE AND THEIR INFLUENCE UPON STABILITY

by Helmut F. Bauer

George C. Marshall Space Flight Center

Huntsville, Alabama

FLUID OSCILLATIONS IN THE CONTAINERS OF A SPACE
VEHICLE AND THEIR INFLUENCE UPON STABILITY

By Helmut F. Bauer

George C. Marshall Space Flight Center
Huntsville, Alabama

NATIONAL AERONAUTICS AND SPACE ADMINISTRATION

For sale by the Office of Technical Services, Department of Commerce,
Washington, D.C. 20230 -- Price \$3.00

TABLE OF CONTENTS

	Page
SUMMARY	1
SECTION I. INTRODUCTION	2
SECTION II. OSCILLATION OF A FRICTIONLESS LIQUID IN CYLINDRICAL CONTAINERS	4
A. The Basic Equations	4
B. Free Oscillations	6
C. Forced Oscillations	8
SECTION III. THE MECHANICAL MODEL	29
A. Discussion	29
B. The Mechanical Model for the Description of Liquid Motion . .	29
SECTION IV. INFLUENCE OF PROPELLANT SLOSHING UPON THE STABILITY OF A SPACE VEHICLE	40
A. Equations of Motion	40
B. Stability Boundaries of a Space Vehicle with a Simple Control System	43
C. Stability Boundaries for Space Vehicles with Two Containers And Simple Control System or Quarter Tank Arrangement. . .	53
SECTION V. CONCLUSION	55
FIGURES	59
APPENDIX	101
TABLES	127

LIST OF ILLUSTRATIONS

Figure	Title	Page
1.	Coordinate System and Tank Geometry.	59
2.	Eigen Frequency Parameter for Containers of Circular, Annular and Quarter-Circular Cross Section (ξ_{mn})	60
3.	Wave Form of Free Fluid Surface Before First and Second Resonance.	61
4.	Free Surface Displacement For Various Excitation Frequency Ratios (in Circular Cylindrical Container). . . .	62
5.	Magnification Function of Free Surface Displacement of a Liquid in a Circular Cylindrical Container.	63
6.	Magnification Function of the Liquid Force in a Circular Cylindrical Container	64
7.	Magnification Function of the Liquid Moment in a Circular Cylindrical Container	65
8.	Wave Form of the Free Fluid Surface in a Circular Cy- lindrical Quarter Container. (First Eigen Frequency at 5.5 rad/sec, Second Eigen Frequency at 6.2 rad/sec	66
9.	Magnification Function of Liquid Force in a Circular Cylindrical Quarter Container (Excitation Along x-axis)	67
10.	Magnification Function of Liquid Moment in a Circular Cylindrical Quarter Container (Excitation Along x-axis)	68
11.	Magnification Function of Liquid Force in Circular Cylindrical Quarter Container (Rotational Excitation About y-axis).	69
12.	Magnification Function of Liquid Moment in Circular Cylindrical Quarter Container (Rotational Excitation About y-axis).	70

LIST OF ILLUSTRATIONS (CONT'D)

Figure	Title	Page
13.	Magnification Function of Liquid Force in a Circular Cylindrical Quarter Container (Roll Excitation About z-axis)	71
14.	Magnification Function of Liquid Moment in a Circular Cylindrical Quarter Container (Roll Excitation About z-axis)	72
15.	Magnification Function of Liquid Moment in a Circular Cylindrical Quarter Container (Roll Excitation About z-axis)	73
16.	Mechanical Model	74
17.	Magnitude and Location of Sloshing (Modal) Masses For Circular Cylindrical Container	75
18.	Ratio of Modal Masses to Liquid Mass	76
19.	Magnitude and Location of Sloshing (Modal) Masses For Circular Cylindrical Quarter Container	77
20.	Location of Non-Oscillating Mass	78
21.	Moment of Inertia of Disk	79
22.	Magnification Function of Liquid Force in Circular Cylindrical Container. (Liquid Height $h = 1.40$ m, ▲ Floating Baffles, ■ Ring Baffles.)	80
23.	Phase of Liquid Force in Circular Cylindrical Container	81
24.	Magnification Function of Free Fluid Surface Displacement in Circular Cylindrical Container	82
25.	Phase of Free Fluid Surface Displacement in Circular Cylindrical Container	83
26.	For the Determination of the Damping Factor	84
27.	Test Set-Up	85
28.	View Inside the Container With Baffles and Level Gauges	86

LIST OF ILLUSTRATIONS (CONT'D)

Figure	Title	Page
29.	Effective Moment of Inertia of Liquid in Completely Filled Closed Container.	87
30.	Coordinate System of Space Vehicle	88
31.	Stability Boundaries of Rigid Space Vehicle With Simple Control System	89
32.	Stability Boundaries of Rigid Space Vehicle With Additional Ideal Accelerometer Control (Influence of Gain Value of the Accelerometer)	90
33.	Stability Boundaries of Rigid Space Vehicle With Additional Accelerometer Control of Various Eigen Frequencies	91
34.	Stability Boundaries of Rigid Space Vehicle With Additional Accelerometer Control of Various Vibrational Characteristics.	92
35.	Stability Boundaries of Rigid Space Vehicle With Additional Accelerometer Control.(Influence of the Location of the Accelerometer).	93
36.	Stability Boundaries of a Rigid Space Vehicle With Additional Accelerometer Control.(Influence of the Control Frequency).	94
37.	Stability Boundaries of a Rigid Space Vehicle With Additional Accelerometer Control. (Influence of the Control Damping)	95
38.	Stability Boundaries of a Rigid Space Vehicle With Additional Accelerometer Control.(Influence of the Gain Value of the Accelerometer).	96
39.	Stability Boundaries of a Rigid Space Vehicle With Additional Accelerometer Control (Without Sloshing of the Propellant).	97
40.	Stability Boundaries of a Rigid Space Vehicle With Simple Control System and Propellant Sloshing in Two Tanks	98
41.	Stability Boundaries of a Rigid Space Vehicle With Simple Control System in Four Tanks.	99

LIST OF ILLUSTRATIONS (CONCL'D)

Figure	Title	Page
42.	Stability Boundaries of a Rigid Space Vehicle With Simple Control System in Four Tanks	100

LIST OF TABLES

Table	Title	Page
1.	Cylindrical Tank With Ring Sector Cross-Section	128
2.	Circular Cylindrical Sector Tank	130
3.	Cylindrical Container with Circular and Quarter Cross Section	132
4.	Roots of $J'_{2m}(\epsilon_{mn}) = 0$	133
5.	Mechanical Model	134
6.	Damping Factor γ_s For Constant Excitation Amplitude $X_0 = 2.5\text{cm}$	136

LIST OF SYMBOLS

SYMBOL	DEFINITION
r, φ, z	Cylindrical coordinates
t	Time
$\Phi = \phi_o + \phi$	Velocity potential
ϕ	Disturbance potential
ϕ_o	Potential of rigid body
ρ	Mass density of liquid
p	Pressure
a	Outer tank radius
b	Inner tank radius
$k = b/a$	Diameter ratio
h	Liquid height
g	Longitudinal acceleration (in z-direction)
$\omega_{mn} = \omega$	Eigen frequency of liquid
Ω	Forced circular frequency
$\eta = \frac{\Omega}{\omega}$	Frequency ratio
x_o	Amplitude of excitation in x-direction
y_o	Amplitude of excitation in y-direction
Θ_o	Amplitude of rotational excitation about y-axis
χ_o	Amplitude of rotational excitation about x-axis
F	Liquid force

LIST OF SYMBOLS (CONT'D)

SYMBOL	DEFINITION
M	Liquid moment
\bar{z}	Free fluid surface displacement, measured from the undisturbed position
u_r, u_ϕ, w	Flow velocities
$J_{m/2\alpha}, Y_{m/2\alpha}$	Bessel functions of order $\frac{m}{2\alpha}$ of first and second kind
ξ_{mn}	Roots of $\Delta_{m/2\alpha}(\xi) = 0$; ' differentiation with respect to argument
ϵ_{mn}	Roots of $J'_{m/2\alpha}(\epsilon) = 0$
$C_{m/2\alpha}$	(Eq. 13)
I	Moment of inertia
$2\pi\alpha \equiv \bar{\alpha}$	Vertex angle of container
c	Damping coefficient
m_n	Mass of n th sloshing mode
m_0	Nonvibrating rigid mass
I_0	Moment of inertia of nonvibrating rigid mass about its center of gravity
h_0	Distance of nonvibrating rigid mass below center of gravity of undisturbed fluid
h_n	Distance of n th sloshing mass above center of gravity of undisturbed fluid
k_n	Spring constant of n th mode
c_n	Damping coefficient of n th mode

LIST OF SYMBOLS (CONT'D)

SYMBOL	DEFINITION
γ_n	Damping number of nth mode
y_n	Displacement of sloshing mass of nth mode
I_d	Moment of inertia of disc
c_d	Damping coefficient of disc damper
I_{rigid}	Moment of inertia of solidified liquid
Ψ	Angle of disc relative to tank bottom
T	Kinetic energy
V	Potential energy
D	Dissipation function
q_i	Generalized coordinates
Q_i	Generalized forces
I_f	Effective moment of inertia
\bar{c}	Effective damping coefficient
m_s	Mass of sloshing mode
y	Translation of space vehicle
F	Thrust
φ	Rotational deviation from standard trajectory
β	Engine deflection
k	Radius of gyration

LIST OF SYMBOLS (CONCLUDED)

SYMBOL	DEFINITION
$\xi_s = x_s/k$	Location of sloshing mass
$\xi_E = x_E/k$	Distance of swivel point of engine to origin
$\nu_s = \omega_s/\omega_c$	Ratio of frequencies of liquid to control system
a_0, a_1	Gain values of attitude control system
g_2	Gain value of accelerometer
A_i	Indicated acceleration perpendicular to longitudinal axis of space vehicle
$\nu_a = \omega_a/\omega_c$	Ratio of frequencies of accelerometer to control system
ξ_a	Damping number of accelerometer
$\xi_a = x_a/k$	Location number of accelerometer
$\mu = m_s/m$	Ratio of sloshing mass to total mass of vehicle
ω_c	Control frequency
ζ_c	Control damping number
$\xi_d = x_d/k$	Coordinate of instantaneous center of rotation
$\lambda = gg_2$	Gain parameter of accelerometer
p_λ	Phase coefficients
η_ν	Generalized coordinate of ν th bending mode
Y_ν	ν th bending mode
$Y_{G\nu}$	Derivative of ν th bending mode at the location of the gyro

FLUID OSCILLATIONS IN THE CONTAINERS OF A SPACE VEHICLE AND THEIR INFLUENCE UPON STABILITY

By

Helmut F. Bauer

SUMMARY

With the increasing size of space vehicles and their larger tank diameters, which lower the natural frequencies of the propellants, the effects of propellant sloshing upon the stability of the vehicle are becoming more critical. Especially since at launch, usually more than ninety per cent of the total mass is in the form of liquid propellant. With increasing diameter, the oscillating propellant masses and the corresponding forces increase. Furthermore, the Eigen frequencies of the propellant become smaller and shift closer to the control frequency of the space vehicle. To obtain smaller sloshing masses and higher Eigen frequencies, the cylindrical containers can be divided by radial or circular walls. Another possibility is the clustering of tanks with smaller diameters, which has the disadvantage of a weight penalty. For stability investigations the influence of the oscillating propellant must be determined. For this reason, forces and moments of the propellant with a free surface performing forced oscillations in a container must be known. To obtain the Eigen frequencies and mode shapes of the liquid, forced oscillations of a frictionless fluid in a cylindrical container of circular ring sector cross section are treated. The assumption of frictionless liquid is justified, since only very small damping is provided by the friction at the tank walls. In a cylindrical container, the lower part of the liquid performs the forced oscillation like a rigid body and only the liquid in the immediate vicinity of the free surface moves independently. With increasing mode number, this motion penetrates less deeply into the liquid. The oscillating propellant can be represented as a spring-mass-system, in which location and magnitude of the model values are determined to give the same forces and moments as the liquid. In this mechanical model, linear damping can be introduced. The magnitude of this damping, which is provided by wall friction and possibly additional baffles, is obtained by experiments.

After the introduction of the mechanical model for the propellants, the derivation of the equations of motion presents no problem. The influence of propellant sloshing is then determined by stability boundaries. To minimize this influence, various methods can be used: First, subdivision of propellant containers of which the oscillating liquid

masses are decreased and distributed to different modes and the Eigen frequencies are increased; second, proper location of the propellant containers; third, appropriate choice of the control system, such as gain values and additional control elements; and fourth, the introduction of additional baffles into the propellant, to disturb the flow field and create larger damping.

This paper gives the results of theoretical studies for the response of the liquid in an arbitrary cylindrical ringsector container, derives the model for the most frequent tank forms and presents stability boundaries for various control systems.

SECTION I. INTRODUCTION

The present trend in modern space technology toward large vehicles presents numerous new problems not encountered in the development of smaller missiles. For example, propellant sloshing may be established by the motion of a space vehicle. Such propellant oscillations are of importance for there is a possibility of extreme amplitudes if the excitation frequency is in the neighborhood of one of the natural frequencies of the fuel.

Since more than 90 per cent of the total weight at take-off is liquid propellant, the influence of propellant sloshing upon the stability of the vehicle becomes more critical, especially with increasing tank diameter, because the oscillating propellant masses and propellant forces increase very rapidly. Furthermore, the Eigen frequencies of the propellant decrease with increasing propellant tank diameter and are getting closer to the control frequency of the space vehicle. For this reason, there will be a continuous excitation of propellant and the influence of propellant sloshing upon stability has to be investigated.

To obtain smaller sloshing masses, one can subdivide the cylindrical tanks by either radial or circular walls. Another possibility is the clustering of tanks of smaller diameter. This, however, has structural and weight disadvantages. If a space vehicle, due to an atmospheric disturbance, deviates from its original trajectory, it should be quickly returned to its preprogrammed flight path. This is performed by the control and guidance system and is executed by swiveling the thrust of the space vehicle. A poorly designed control system can therefore continuously excite the motion of the propellant in the tanks. For this reason, force and moments of the liquid in performing harmonic oscillations in a cylindrical container must be determined and their influence upon the stability must be investigated. The exact solution of this problem is too complicated. To obtain the values of the Eigen frequencies, the mode shapes, and the sloshing masses of the vibration modes, the liquid vibration is treated for free and forced oscillations of a frictionless fluid in a circular cylindrical ring sector tank. The assumption of a frictionless liquid is justified since the damping due to friction at the tank walls is usually of very small magnitude.

In a cylindrical container the largest part of the liquid performs the forced motion, like a rigid body. Only the liquid in the immediate vicinity of the free fluid surface oscillates by itself. This motion penetrates approximately one radius into the liquid surface for the lowest Eigen frequencies. For higher Eigen frequencies, the penetration becomes smaller.

For stability investigations of space vehicles, the motion perpendicular to the trajectory is of main importance. For this reason we will restrict our investigation to these motions. Free and forced vibrations in the form of translatory, rotational or roll excitation of the container will be treated. In these motions the boundary conditions will be linearized. This has, besides the simplification for the solution, the advantage that solutions of different excitations can be superimposed. The fact that the liquid is considered irrotational results in the representation of the velocity vector of a fluid particle as a gradient of a velocity potential. Since the fluid is incompressible, the velocity potential must be a solution of the Laplace equation which does not explicitly contain the time. This means that the flow in the container is determined at any instant by the boundary conditions at that time.

The oscillating liquid can be represented as a spring-mass system for which the magnitude and location of the oscillating liquid masses and corresponding spring constants must be determined. They must have the same Eigen frequencies and exert the same forces and moments as the actual fluid.

At the Eigen frequencies of the propellant, the solutions of the potential theory exhibit singularities. The oscillation of the propellant, however, is damped by wall and internal friction indicating that an investigation of damped fluid vibration would be necessary. Especially in the region of resonance where fluid forces occur which are a multiple of the inertial force, an exact knowledge of these values is important. The analytical treatment of damped fluid oscillations, especially in containers with stiffener rings and baffles, presents insurmountable difficulties. The mechanical model therefore serves for the introduction of linear damping. The magnitude of the damping is determined by experiments.

After the introduction of the mechanical model, the derivation of the equations of motion of the space vehicle represents no further difficulty. The elastic behavior of the space vehicle can also be included in the analysis. With increasing length of the vehicles, these elastic effects play a more important role. Finally, the influence of the propellant oscillations upon the stability of the space vehicle is investigated. The questions of how to design a control system and where one should place an additional control accelerometer to minimize baffle requirements and to enhance the stability of the vehicle with respect to propellant sloshing are answered. The influence of tank geometry, the location of a propellant container as well as the gain values, and the vibrational characteristics of a control accelerometer upon the stability boundaries are investigated. This is performed by varying the different parameters and by determining the stability boundaries with the usual criteria of Hurwitz.

The problem of free fluid oscillations in a circular cylindrical container was treated in 1829 by Poisson. Because the theory of Bessel functions was at that time unavailable, the result was not completely interpreted [1]. In the year 1876, Rayleigh [2] gave the solution for free fluid oscillations in rectangular and cylindrical tanks of circular cross section. In recent years, the problem of forced fluid oscillations has grown in importance [3]. Graham and Rodrigue [4] determined the forced vibration of liquid in rectangular containers while Lorell [5] gave the flow of a fluid in a two-dimensional rectangular container and cylindrical tank of circular cross section for translational excitation. At almost the same time, reports about forced fluid oscillations in cylindrical tanks [6, 7, 8, 9] began to appear at various companies in the United States. Fluid oscillations in a cylindrical tank with annular [10] and elliptic [11] cross section have also been treated. Budiansky [12] used integral equation techniques to determine fluid oscillations in horizontal, circular cylindrical, and spherical containers. The first Eigen frequency can also be obtained by an approximation method [13] if one considers the liquid of small fluid heights as a compound pendulum. For large liquid heights, the Eigen frequency can be approximated by substituting the liquid body by an equivalent circular cylindrical liquid mass of equal volume and equal free fluid surface area.

All circular cylindrical containers can be obtained from the results of the fluid oscillations in circular cylindrical ring sector tanks. The mechanical model is presented only for the most important practical container geometries such as circular containers and four quarter containers.

SECTION II. OSCILLATION OF A FRICTIONLESS LIQUID IN CYLINDRICAL CONTAINERS

An exact solution of the problem of fluid oscillations with a free fluid surface in a container is practically impossible. Since at first we are interested only in the mechanical values of the system, namely, the Eigen frequencies of the liquid and the sloshing masses, we assume for simplification that the flow field can be considered frictionless, irrotational, and incompressible. With the results of this theory, a mechanical model can be derived in which damping can be included. Since the cylindrical propellant containers will be divided by radial or concentric walls to decrease the oscillating propellant masses, we will discuss the fluid oscillations in a cylindrical container with circular annular sector cross section (Fig. 1). From the results of this analysis, we can obtain by limit considerations the solutions for container forms which are most important in practice.

A. THE BASIC EQUATIONS

Because of the assumption of irrotational flow, the velocity \vec{v} can be represented as a gradient of the velocity potential Φ . For an incompressible medium, Φ must be a solution of the Laplace equation [14].

$$\Delta\Phi = 0 \tag{1}$$

The introduction of the potential Φ has the advantage that all interesting values such as velocity and pressure can be obtained with one single function. The velocity distribution is derived by differentiation with respect to the spatial coordinates, and the pressure p follows from the unstationary Bernoulli equation

$$\frac{\partial \Phi}{\partial t} + \frac{1}{2} v^2 + \frac{p}{\rho} + gz = 0. \quad (2)$$

Here g is the longitudinal acceleration of the container. To solve equation 1, the boundary conditions of the problem have to be derived. At the tank walls the normal velocities of liquid and wall are equal.

$$\frac{dT}{dt} = \left(\frac{\partial}{\partial t} + \vec{v} \cdot \text{grad} \right) T = 0. \quad (3)$$

In addition, there is the boundary condition at the free fluid surface. If the equation of such a surface at which the pressure $p = 0$ is described by

$$z = \bar{z}(x, y, t),$$

then it is for liquid particles at the surface

$$T \equiv z - \bar{z}(x, y, t) = 0. \quad (4)$$

With equation 3 this results in the linearized form $\frac{\partial \bar{z}}{\partial t} = \frac{\partial \Phi}{\partial z}$ and represents the kinematic condition. From the linearized Bernoulli equation 2, we obtain with the pressure $p = 0$ at the free fluid surface,

$$\bar{z} = -\frac{1}{g} \frac{\partial \Phi}{\partial t}, \quad (5)$$

from which, by elimination of \bar{z} , we finally obtain

$$\frac{\partial^2 \Phi}{\partial t^2} + g \frac{\partial \Phi}{\partial z} = 0 \quad (6)$$

for the free surface condition. Besides simplification in the treatment for the solution, linearization of the problem has the advantage that various cases can be superimposed.

For the free oscillations of incompressible, frictionless and irrotational liquid in a fixed container with a free fluid surface, we obtain the equations

$$\Delta\Phi = 0$$

$$\frac{\partial\Phi}{\partial n} = 0 \quad \text{at the container walls.} \quad (7)$$

$$\frac{\partial^2\Phi}{\partial t^2} + g \frac{\partial\Phi}{\partial z} = 0 \quad \text{at the free fluid surface.}$$

If the container performs forced oscillations, then the basic equations can also be represented in simple form. In this case, the boundary conditions at the tank walls must also be linearized. The solution of the Laplace equation is built by the potential of the motion of the container without a free fluid surface (which is assumed to be small) and the disturbance potential ϕ which is caused by the disturbance of the free fluid surface.

$$\Phi(x, y, z, t) = \phi_0(x, y, z, t) + \phi(x, y, z, t). \quad (8)$$

Both functions ϕ_0 and ϕ satisfy the Laplace equation. The normal derivative of the velocity potential Φ must be equal to the normal velocity of the container wall. From this we conclude that the normal derivative of the disturbance potential must be equal to zero at the container walls.

The equations for the solution of forced oscillations are therefore

$$\Delta\Phi = 0$$

$$\frac{\partial\Phi}{\partial n} = \text{Normal velocity of container wall.} \quad (9)$$

$$\frac{\partial^2\Phi}{\partial t^2} + g \frac{\partial\Phi}{\partial z} = 0 \quad \text{at free fluid surface.}$$

B. FREE OSCILLATIONS

We start with the free oscillations to find the Eigen solutions needed for the series expansion of the solution of the forced oscillations. The flow field of the fluid of a liquid with free fluid surface in a cylindrical container of circular annular sector cross section and with a vertex angle $2\pi\alpha$ and a flat tank bottom is obtained from the solution of the Laplace equation $\Delta\phi = 0$ with the linearized boundary conditions.

$$\frac{\partial \phi}{\partial z} = 0 \quad \text{at the bottom of the container } z = -h$$

$$\frac{\partial \phi}{\partial r} = 0 \quad \text{at the circular cylindrical tank walls } r = a, b \quad (10)$$

$$\frac{1}{r} \frac{\partial \phi}{\partial \varphi} = 0 \quad \text{at the sector walls } \varphi = 0, 2\pi\alpha$$

$$\frac{\partial^2 \phi}{\partial t^2} + g \frac{\partial \phi}{\partial z} = 0 \quad \text{at the free fluid surface } z = 0$$

With the assumption of the product solution of the form

$$\phi(r, \varphi, z) = R(r) G(\varphi) Z(z),$$

the solution can be found to be

$$\phi = e^{i\omega t} \{C_1 \cos \nu \varphi + C_2 \sin \nu \varphi\} [\{C_3 \cosh \lambda z + C_4 \sinh \lambda z\} \{C_5 J_\nu(\lambda r) + C_6 Y_\nu(\lambda r)\} + \{C_7 z + C_8\} \{C_9 r^\nu + C_{10} r^{-\nu}\}]. \quad (11)$$

The velocity potential which satisfies the boundary conditions at the container walls is

$$\phi(r, \varphi, z, t) = \sum_m \sum_n A_{mn} e^{i\omega_{mn} t} \cos\left(\frac{m}{2\alpha} \varphi\right) \frac{\cosh\left[\xi_{mn} \left(\frac{z}{a} + \frac{h}{a}\right)\right]}{\cosh\left[\xi_{mn} \frac{h}{a}\right]} C_{\frac{m}{2\alpha}}\left(\xi_{mn} \frac{r}{a}\right). \quad (12)$$

Here the abbreviations are

$$C_{\frac{m}{2\alpha}}\left(\xi_{mn} \frac{r}{a}\right) \equiv C(\rho) = \frac{J_{\frac{m}{2\alpha}}(\rho)}{Y'_{\frac{m}{2\alpha}}(\xi_{mn})} - \frac{J'_{\frac{m}{2\alpha}}(\xi_{mn}) Y_{\frac{m}{2\alpha}}(\rho)}{Y'_{\frac{m}{2\alpha}}(\xi_{mn})} \quad (13)$$

The values ξ_{mn} are the positive roots of the equation

$$\Delta_{\frac{m}{2\alpha}} = \frac{J'_{\frac{m}{2\alpha}}(\xi) Y'_{\frac{m}{2\alpha}}(k\xi)}{Y'_{\frac{m}{2\alpha}}(\xi)} - \frac{J'_{\frac{m}{2\alpha}}(k\xi) Y'_{\frac{m}{2\alpha}}(\xi)}{Y'_{\frac{m}{2\alpha}}(\xi)} = 0, \quad (14)$$

in which $k = b/a$ is the diameter ratio of the inner and outer tank wall. The unknown constants A_{mn} can be obtained from the initial conditions. The equation for the Eigen

values of the liquid is obtained from the free surface condition 10.

$$\omega_{mn}^2 \equiv \omega^2 = \frac{g}{a} \xi_{mn} \tanh \left(\xi_{mn} \frac{h}{a} \right). \quad m, n = 0, 1, 2 \dots \quad (15)$$

It can be seen that the Eigen frequencies of the liquid increase with the square root of the longitudinal acceleration and that they decrease with increasing tank diameter. For large container diameters, the Eigen frequencies are small. This is of great disadvantage in designing a space vehicle control system. It indicates that, with increasing tank diameter, the Eigen frequencies of the propellant are dangerously close to the control frequency which usually exhibits small values in the order of 0.2 to 0.5 cycles/sec. A possibility for the increase of the Eigen frequencies exists in the change of the container geometry. This is expressed by the value ξ_{mn} .

For large values of the liquid height h/a , the square of the Eigen value $\omega^2 \approx \frac{g\xi_{mn}}{a}$ is practically independent of the fluid height; and expresses that the ratio $\omega/\sqrt{g/a}$ changes its value only for small fluid heights $h/a < 1$. For higher mode shapes, this value stays constant $\sqrt{\xi_{mn}}$ to very small values of h/a then decreases rapidly toward zero. (Fig. 2)

C. FORCED OSCILLATIONS

For a stability investigation of the total space vehicle, fluid forces and moments due to oscillations of the vehicle about its trajectory, that is, translational motion perpendicular to the flight trajectory or rotational about the longitudinal and latitudinal axis, have to be known. We therefore investigate the case that the propellant container performs forced oscillations. Since the liquid follows the motion of the tank wall in the lower part of the container like a rigid body and since in the vicinity of the surface the fluid performs independent oscillations, it makes sense to split the potential Φ into the potential of the rigid body motion ϕ_0 (liquid without free fluid surface) and a disturbance potential ϕ which is caused by the free surface motion.

1. Translational Motion of the Container. We start with the special case that the excitation is parallel to the container wall. For this case the boundary conditions are

$$\frac{\partial \Phi}{\partial r} = i\Omega x_0 e^{i\Omega t} \cos \varphi \quad \text{at the circular cylindrical tank walls } r = a, b.$$

$$\frac{\partial \Phi}{\partial z} = 0 \quad \text{at the bottom of the container } z = -h$$

$$\frac{1}{r} \frac{\partial \Phi}{\partial \varphi} = 0 \quad \text{at the sector wall } \varphi = 0 \quad (16)$$

$$\frac{1}{r} \frac{\partial \Phi}{\partial \varphi} = -i\Omega x_0 e^{i\Omega t} \sin 2\pi\alpha \quad \text{at the sector wall } \varphi = 2\pi\alpha$$

and $\frac{\partial^2 \Phi}{\partial t^2} + g \frac{\partial \Phi}{\partial z} = 0$ at the free fluid surface $z = 0$

By extracting the container motion

$$\Phi = \{ \phi + i\Omega x_0 r \cos \varphi \} e^{i\Omega t}, \quad (17)$$

one obtains the boundary conditions for the disturbance potential which are homogeneous at the container walls.

$$\frac{\partial \phi}{\partial r} = 0 \quad \text{for } r = a, b$$

$$\frac{\partial \phi}{\partial z} = 0 \quad \text{for } z = -h$$

$$\frac{1}{r} \frac{\partial \phi}{\partial \varphi} = 0 \quad \text{for } \varphi = 0, 2\pi\alpha$$

$$g \frac{\partial \phi}{\partial z} - \Omega^2 \phi = i\Omega^3 x_0 r \cos \varphi \quad \text{for } z = 0$$

For this reason the disturbance potential $\phi(r, \varphi, z)$ which satisfies the Laplace equation has the same form as 12. Omitting the double summation and indices for a more lucid presentation, and introducing the abbreviations

$$\bar{\varphi} = \frac{m}{2\alpha} \varphi, \quad \xi = \xi_{mn} \frac{z}{a}, \quad \rho = \xi_{mn} \frac{r}{a} \quad \text{and} \quad \kappa = \xi_{mn} \frac{h}{a},$$

the disturbance potential is

$$\phi(r, \varphi, z) = A \cos \bar{\varphi} C(\rho) \frac{\cosh(\kappa + \xi)}{\cosh \kappa} \quad (18)$$

To determine from the condition of the free fluid surface the still unknown coefficients A_{mn} , the right hand side of this boundary condition has to be expanded into a series where $\cos \varphi$ is represented as the Fourier series

$$\cos \varphi = \sum_{m=0}^{\infty} a_m \cos \bar{\varphi} \quad \text{with} \quad a_0 = \frac{\sin \bar{\alpha}}{\bar{\alpha}}, \quad a_m = \frac{2\bar{\alpha}(-1)^{m+1} \sin \bar{\alpha}}{(m^2 \pi^2 - \bar{\alpha}^2)}. \quad (\bar{\alpha} = 2\pi\alpha) \quad (19)$$

The function r is represented as a Bessel series

$$r = \sum_{n=0}^{\infty} b_{mn} C(\rho) \quad (20)$$

where

$$b_{mn} = \frac{a \int_{k\xi_{mn}}^{\xi_{mn}} \rho^2 C(\rho) d\rho}{\xi_{mn} \int_{k\xi_{mn}}^{\xi_{mn}} \rho C^2(\rho) d\rho} = \frac{2a N_2(\xi_{mn})}{\left[\frac{4}{\pi^2 \xi_{mn}^2} - k^2 C^2(k\xi_{mn}) \right] - \frac{m^2}{4a^2 \xi_{mn}^2} \left[\frac{4}{\pi^2 \xi_{mn}^2} - C^2(k\xi_{mn}) \right]} \quad (21)$$

The coefficients A_{mn} become

$$A_{mn} = \frac{i\Omega a_m b_{mn} x_o \eta^2}{(1-\eta^2)}$$

where $\eta = \frac{\Omega}{\omega}$ is the ratio of the exciting frequency to the Eigen frequency. The velocity potential Φ for translational container excitation in x - direction is then

$$\Phi(r, \varphi, z, t) = i\Omega x_o e^{i\Omega t} \left\{ r \cos \varphi + \frac{a_m b_{mn} C(\rho) \eta^2 \cosh(\kappa + \xi)}{(1-\eta^2) \cosh \kappa} \cos \bar{\varphi} \right\}. \quad (22)$$

The first term (potential of the rigid body) satisfies the boundary conditions at the tank walls while the second part (disturbance potential) vanishes at the tank walls. The free surface condition is satisfied by both parts of the formula. The free surface displacement, the pressure-and velocity-distribution, as well as the forces and moments of the liquid, can be determined from the potential by differentiations and integrations with respect to the time-and spatial coordinates.

The surface displacement of the propellant which is measured from the undisturbed position of the liquid is

$$\bar{z} = \frac{\Omega^2}{g} x_o e^{i\Omega t} \left\{ r \cos \varphi + \frac{a_m b_{mn} C(\rho) \eta^2}{(1-\eta^2)} \cos \bar{\varphi} \right\}. \quad (23)$$

The pressure in a depth (-z) is

$$p = -\bar{\rho} \frac{\partial \Phi}{\partial t} - g \bar{\rho} z = \bar{\rho} \Omega^2 x_o e^{i\Omega t} \left[r \cos \varphi + \frac{a_m b_{mn} \eta^2 \cosh(\kappa + \xi) C(\rho) \cos \bar{\varphi}}{(1-\eta^2) \cosh \kappa} \right] - \bar{\rho} g z. \quad (24)$$

At the outer container wall $r = a$, the function $C(\rho) = 2/\pi \xi_{mn}$, while at the inner container wall, $r = b$, the function $C(\rho)$ has a value $C(k\xi_{mn})$. At the sector walls $\varphi = 0$, $\varphi = \bar{\alpha}$, the cosine assumes the value 1, respectively $(-1)^m$. The pressure distribution at the tank bottom is obtained from 24 with $z = -h$ ($\xi = -\kappa$).

By integration of the appropriate components of the pressure distributions, the liquid forces and moments can be obtained. The resulting force in x-direction is therefore

$$F_x = \int_0^{\bar{\alpha}} \int_{-h}^0 (ap_a - bp_b) \cos \varphi d\varphi dz - \int_b^a \int_{-h}^0 p_{\varphi=\bar{\alpha}} \sin \bar{\alpha} dr dz. \quad (25)$$

Here the first integral represents a contribution of the pressure distribution at the circular container walls, and the second integral stems from the pressure distribution at the sector walls. With the mass of the liquid $m = \bar{\rho} \pi a^2 h \alpha (1-k^2)$ the fluid force becomes

$$F_x = m\Omega^2 x_o e^{i\Omega t} \left[1 + 2 \frac{(-1)^{m+1} a_m b_{mn} \sin \bar{\alpha} \eta^2 \tanh \kappa}{\bar{\alpha} a (1-k^2) (1-\eta^2) \kappa} \left\{ N_o(\xi_{mn}) \right. \right. \\ \left. \left. + \frac{\bar{\alpha}^2}{(\pi^2 m^2 - \bar{\alpha}^2)} \left[\frac{2}{\pi \xi_{mn}} - kC(k\xi_{mn}) \right] \right\} \right]. \quad (26)$$

The force components in y-direction is governed by

$$F_y = \int_0^{\bar{\alpha}} \int_{-h}^0 (ap_a - bp_b) \sin \varphi d\varphi dz + \int_b^a \int_{-h}^0 p_{\varphi=\bar{\alpha}} \cos \bar{\alpha} dr dz - \int_b^a \int_{-h}^0 p_{\varphi=0} dr dz \quad (27)$$

and results in

$$F_y = -2m\Omega^2 x_o e^{i\Omega t} \frac{a_m b_{mn} \eta^2 [1 - (-1)^m \cos \bar{\alpha}] \tanh \kappa}{-a\bar{\alpha} (1-k^2) (1-\eta^2) \kappa} \left\{ N_o(\xi_{mn}) \right. \\ \left. + \frac{\bar{\alpha}^2}{(\pi^2 m^2 - \bar{\alpha}^2)} \left[\frac{2}{\pi \xi_{mn}} - kC(k\xi_{mn}) \right] \right\}. \quad (28)$$

Here (see Table 1)

$$N_o(\xi_{mn}) = \frac{1}{\xi_{mn}} \int_{k\xi_{mn}}^{\xi_{mn}} C(\rho) d\rho. \quad (29)$$

The first term,

$$m\Omega^2 x_o e^{i\Omega t},$$

in 26 represents the inertial force of the propellant that is the force of the solidified liquid. The fluid moments M_y and M_x with respect to the point $(0, 0, -h/2)$ are given by

$$M_y = \int_0^{\bar{\alpha}} \int_{-h}^0 (ap_a - bp_b) \left(\frac{h}{2} + z\right) \cos\varphi d\varphi dz + \int_0^{\bar{\alpha}} \int_b^a p_c r^2 \cos\varphi d\varphi dr - \int_b^a \int_{-h}^0 p_{\varphi=\bar{\alpha}} \sin\bar{\alpha} \left(\frac{h}{2} + z\right) dr dz \quad (30)$$

and

$$M_x = - \int_0^{\bar{\alpha}} \int_{-h}^0 (ap_a - bp_b) \left(\frac{h}{2} + z\right) \sin\varphi d\varphi dz - \int_0^{\bar{\alpha}} \int_b^a p_c r^2 \sin\varphi d\varphi dr + \int_b^a \int_{-h}^0 \left(\frac{h}{2} + z\right) p_{\varphi=0} dr dz - \int_b^a \int_{-h}^0 \left(\frac{h}{2} + z\right) p_{\varphi=\bar{\alpha}} \cos\bar{\alpha} dr dz. \quad (31)$$

M_y is the moment about an axis passing through point $(0, 0, -h/2)$ parallel to the y-axis while M_x is the moment about an axis parallel to the x-axis through the same point. In these formulas, the first integral again represents the contribution of the pressure distribution at the circular cylindrical tank walls. The second integral is the contribution of the bottom pressure while the remaining integrals represent the pressure contribution at the sector walls to the moment. After the integration has been performed, the moments of the liquid are

$$M_y = m\Omega^2 a x_o e^{i\Omega t} \left[\frac{1+k^2}{4h/a} \left(1 + \frac{\sin\bar{\alpha} \cos\bar{\alpha}}{\bar{\alpha}}\right) + \frac{\sin\bar{\alpha}}{\bar{\alpha}} \frac{(-1)^{m+1} a_m b_{mn} \eta^2}{\alpha(1-\eta^2)(1-k^2)\xi_{mn}} \cdot \left\{ \left[\tanh \kappa + \frac{2}{\kappa} \left(\frac{1}{\cosh \kappa} - 1 \right) \right] \left[N_o(\xi_{mn}) + \frac{\bar{\alpha}^2}{(\pi^2 m^2 - \bar{\alpha}^2)} \left[\frac{2}{\pi \xi_{mn}} - kC(k\xi_{mn}) \right] + \frac{2\bar{\alpha}^2 \xi_{mn}^2 N_2(\xi_{mn})}{(\pi^2 m^2 - \bar{\alpha}^2) \kappa \cosh \kappa} \right] \right\} \right. \\ \left. + \frac{2mga}{3} \frac{(1-k^3)}{(1-k^2)} \frac{\sin\bar{\alpha}}{\bar{\alpha}} \right]. \quad (32)$$

$$\begin{aligned}
M_x = & -m\Omega^2 a x_o e^{i\Omega t} \left[\frac{(1+k^2)}{4h/a} \frac{\sin^2 \bar{\alpha}}{\bar{\alpha}} - \frac{1}{\bar{\alpha}} \frac{a}{m} \frac{b}{mn} \frac{[1-(-1)^m \cos \bar{\alpha}] \eta^2}{(1-\eta^2)(1-k^2) \xi_{mn} \alpha} \cdot \left\{ \left[\tanh \kappa + \frac{2}{\kappa} \cdot \right. \right. \right. \\
& \cdot \left. \left(\frac{1}{\cosh \kappa} - 1 \right) \right] \left[N_o(\xi_{mn}) + \frac{\bar{\alpha}^2}{(\pi^2 m^2 - \bar{\alpha}^2)} \left[\frac{2}{\pi \xi_{mn}} - kC(k \xi_{mn}) \right] \right] + \frac{2\bar{\alpha}^2 \xi_{mn}^2 N_2(\xi_{mn})}{(\pi^2 m^2 - \bar{\alpha}^2) \kappa \cosh \kappa} \left. \right\} \right] \\
& - \frac{2mga}{3} \frac{(1-k^3)}{(1-k^2)} \frac{(1-\cos \bar{\alpha})}{\bar{\alpha}}. \quad (33)
\end{aligned}$$

Since the reference axis does not pass through the center of gravity of the undisturbed liquid, the last term in the moment formula represents the static moment of the liquid.

The velocity distribution is in radial direction

$$u_r = \frac{\partial \Phi}{\partial r} = -i\Omega x_o e^{i\Omega t} \left[\cos \varphi + \frac{a}{m} \frac{b}{mn} \frac{\eta^2 \xi_{mn} \cosh(\kappa + \xi)}{(1-\eta^2) a \cosh \kappa} C'(\rho) \cos \bar{\varphi} \right], \quad (34a)$$

in angular direction

$$u_\varphi = \frac{1}{r} \frac{\partial \Phi}{\partial \varphi} = -i\Omega x_o e^{i\Omega t} \left[\sin \varphi + \frac{a}{m} \frac{b}{mn} \frac{\eta^2 (m/2\alpha) \cosh(\kappa + \xi)}{r(1-\eta^2) a \cosh \kappa} C(\rho) \sin \bar{\varphi} \right], \quad (34b)$$

and in axial direction

$$w = \frac{\partial \Phi}{\partial z} = i\Omega x_o e^{i\Omega t} \frac{a}{m} \frac{b}{mn} \frac{\eta^2 \xi_{mn} \sinh(\kappa + \xi)}{a(1-\eta^2) \cosh \kappa} C(\rho) \cos \bar{\varphi}. \quad (34c)$$

In the equations for the pressure, forces, moments and velocity distribution of the liquid, the term for the solidified liquid is represented as a single term and not as a series. This results in a faster convergence of the results. The velocity distribution in the container is obtained by omitting the first term in the braces, that is, omitting the term $\cos \varphi$ for the radial velocity component of u_r and $\sin \varphi$ for the angular component of u_φ . To know completely the response of the liquid to a translational motion the excitation in y-direction also has to be treated. The procedure is only slightly different from that of excitation of the translational excitation in x-direction and makes a comprehensive investigation unnecessary. The flow field of the liquid with respect to forced oscillation of the container in y-direction is again obtained from the solution of the potential equation 1. The boundary conditions at the tank walls are, for this case

$$\frac{\partial \Phi}{\partial r} = i\Omega y_o e^{i\Omega t} \sin \varphi \quad \text{at the tank walls } r = a, b.$$

$$\frac{\partial \Phi}{\partial z} = 0 \quad \text{at the tank bottom } z = -h$$

$$\frac{1}{r} \frac{\partial \Phi}{\partial \varphi} = i\Omega y_0 e^{i\Omega t} \quad \text{at the sector wall } \varphi = 0$$

$$\frac{1}{r} \frac{\partial \Phi}{\partial \varphi} = i\Omega y_0 e^{i\Omega t} \cos \bar{\alpha} \quad \text{at the sector wall } \varphi = 2\pi\alpha$$

By transformation similar to the one previously used, the container motion can be eliminated. This is performed by substituting $x_0 \cos \varphi$ of the previous transformation by $y_0 \sin \varphi$. For the determination of the unknown coefficients, A_{mn} , $\sin \varphi$ has to be expanded into a Fourier series

$$\sin \varphi = \sum_{m=0}^{\infty} c_m \cos \bar{\varphi} \quad \text{with } c_0 = \frac{1 - \cos \bar{\alpha}}{\bar{\alpha}}, c_m = \frac{2\bar{\alpha} [(-1)^m \cos \bar{\alpha} - 1]}{(m^2 \pi^2 - \bar{\alpha}^2)}. \quad (35)$$

The velocity potential finally is

$$\Phi(r, \varphi, z, t) = i\Omega y_0 e^{i\Omega t} \left\{ r \sin \varphi + \frac{c_m b_{mn} \eta^2 \cosh(\kappa + \zeta)}{(1 - \eta^2) \cosh \kappa} C(\rho) \cos \bar{\varphi} \right\} \quad (36)$$

The terms of the double summation vanish at the tank walls while the term $i\Omega y_0 r \sin \varphi e^{i\Omega t}$ satisfies the boundary conditions at the tank walls. Both satisfy the free surface condition. The corresponding results are presented in Table 1. The velocity distribution for excitation in y-direction is obtained from 34 by substituting y_0 for x_0 and c_m instead of a_m in the double series. Furthermore, one has to substitute in the velocity component u_r the value $\cos \varphi$ by $\sin \varphi$ and in u_φ the value $\sin \varphi$ by $-\cos \varphi$.

2. Rotational Oscillations. Besides translational oscillations, a space vehicle also performs rotational oscillations. Therefore, rotational excitation of the containers about the origin of the coordinate system, which is now placed in the middle between the tank bottom and the undisturbed fluid surface on the vertex axis of the tank, must also be performed. If θ_0 is the rotational amplitude about the y-axis and if χ_0 is the amplitude about the x-axis, the boundary conditions are expressed by

$$\frac{\partial \Phi}{\partial r} = \left\{ \begin{array}{l} -i\Omega \theta_0 e^{i\Omega t} z \cos \varphi \\ -i\Omega \chi_0 e^{i\Omega t} z \sin \varphi \end{array} \right\} \quad \text{at the tank walls } r = a, b.$$

$$\frac{\partial \Phi}{\partial z} = \left\{ \begin{array}{l} i\Omega \theta_0 e^{i\Omega t} r \cos \varphi \\ i\Omega \chi_0 e^{i\Omega t} r \sin \varphi \end{array} \right\} \quad \text{at the tank bottom } z = -\frac{h}{2}$$

$$\frac{1}{r} \frac{\partial \Phi}{\partial \varphi} = \left\{ \begin{array}{l} 0 \\ -i\Omega \chi_0 e^{i\Omega t} z \end{array} \right\} \quad \text{at the tank sector wall } \varphi = 0$$

$$\frac{1}{r} \frac{\partial \Phi}{\partial \varphi} = \begin{Bmatrix} i\Omega \theta_o e^{i\Omega t} z \sin \bar{\alpha} \\ -i\Omega \chi_o e^{i\Omega t} z \cos \bar{\alpha} \end{Bmatrix} \quad \text{at the tank sector wall } \varphi = 2\pi\alpha$$

$$\frac{\partial^2 \phi}{\partial t^2} + g \frac{\partial \phi}{\partial z} = 0 \quad \text{at the free fluid surface } z = +\frac{h}{2}$$

By elimination of the rigid body potential ϕ_o with

$$\Phi = \left[-i\Omega r z \begin{Bmatrix} \theta_o \cos \varphi \\ \chi_o \sin \varphi \end{Bmatrix} + \phi \right] e^{i\Omega t},$$

the boundary conditions at the tank side walls ($r=a$, b , and $\varphi = 0, 2\pi\alpha$) can be made homogeneous. The solution of the Laplace equation which satisfies these tank wall conditions is

$$\phi = [A \cosh \xi + B \sinh \xi] C(\rho) \cos \bar{\varphi}. \quad (37)$$

Because of the moving tank bottom two hyperbolic functions appear. From the boundary conditions for the tank bottom and the free fluid surface, one obtains with the series expansions of $\cos \varphi$, $\sin \varphi$ and r

$$A_{mn} = \frac{ab_{mn} \eta^2}{\xi_{mn} (1-\eta^2) \cosh \kappa} \left[2 \sinh \left(\frac{\kappa}{2} \right) - \left(\frac{\kappa}{2} + \gamma \right) \cosh \left(\frac{\kappa}{2} \right) \right] \begin{Bmatrix} a_m \\ c_m \end{Bmatrix}. \quad (38a)$$

$$B_{mn} = \frac{ab_{mn} \eta^2}{\xi_{mn} (1-\eta^2) \cosh \kappa} \left[\left(\gamma - \frac{\kappa}{2} \right) \sinh \left(\frac{\kappa}{2} \right) - 2 \cosh \left(\frac{\kappa}{2} \right) \right] \begin{Bmatrix} a_m \\ c_m \end{Bmatrix}. \quad (38b)$$

The abbreviation $\gamma = g \xi_{mn} / a \Omega^2$ equals the reciprocal of the frequency ratio η^2 for large liquid fillings. With this the velocity potential is

$$\Phi(r, \varphi, z, t) = i\Omega e^{i\Omega t} \begin{Bmatrix} \theta_o \\ \chi_o \end{Bmatrix} \left[\begin{Bmatrix} -rz \cos \varphi \\ -rz \sin \varphi \end{Bmatrix} + (A \cosh \xi + B \sinh \xi) C(\rho) \cos \bar{\varphi} \right]. \quad (39)$$

The term in the front of the double series satisfies the boundary conditions at the container side walls while the terms of the double series vanish there. The double series, together with the terms in front of it, satisfies the boundary conditions at the tank bottom and at the free liquid surface. The corresponding results are given in Table 1.

Here the forces contain, in the space-fixed coordinate system, the weight component as the first term. The displacement \bar{z}^* of the free fluid surface in tank fixed coordinates is obtained by subtracting from the displacement \bar{z} of the space-fixed system the value due to container rotation

$$\bar{z}^* = \bar{z} - \left\{ \begin{array}{l} r \cos \varphi \theta_0 e^{i\Omega t} \\ r \sin \varphi \chi_0 e^{i\Omega t} \end{array} \right\}.$$

For design of the roll control system, the knowledge of the response of the liquid due to roll excitation, $\varphi = \varphi_0 e^{i\Omega t}$, is important. The origin of the coordinate system is again placed in the undisturbed free fluid surface. This results in a simpler representation of that part of the solution which depends on z . The boundary conditions are

$$\frac{\partial \Phi}{\partial r} = 0 \quad \text{at container walls } r = a, b,$$

$$\frac{\partial \Phi}{\partial z} = 0 \quad \text{at the tank bottom } z = -h,$$

$$\frac{1}{r} \frac{\partial \Phi}{\partial \varphi} = i\Omega r \varphi_0 e^{i\Omega t} \quad \text{at the sector walls } \varphi = 0, \bar{\alpha},$$

$$\frac{\partial^2 \Phi}{\partial t^2} + g \frac{\partial \Phi}{\partial z} = 0 \quad \text{at the free fluid surface } z = 0.$$

However, these boundary conditions cannot, as in the previous cases, be satisfied by one potential but by two potentials,

$$\phi_1 = \phi_1(r, \varphi), \quad \phi = \phi(r, \varphi, z).$$

$$\Phi(r, \varphi, z, t) = [\phi_0(r, \varphi) + \phi(r, \varphi, z)] e^{i\Omega t}.$$

Both functions satisfy the Laplace equation. $\phi_0(r, \varphi)$ is determined such that it satisfies the boundary conditions at the tank side walls $r = a, b$ and $\varphi = 0, 2\pi\alpha$. The solution represents nothing but the flow in an infinitely long tank. With the help of the disturbance potential $\phi(r, \varphi, z)$, we take care of the boundary conditions at the tank bottom and at the free surface. The boundary conditions for the functions ϕ_0 and ϕ are given by

$$\frac{\partial \phi_0}{\partial r} = 0 \quad \text{at the tank walls } r = a, b.$$

$$\frac{\partial \phi_0}{\partial \varphi} = i\Omega \varphi_0 r^2 \quad \text{at the sector walls } \varphi = 0, 2\pi\alpha$$

and

$$\frac{\partial \phi}{\partial r} = 0 \quad \text{at the tank walls } r = a, b$$

$$\frac{\partial \phi}{\partial \varphi} = 0 \quad \text{at the sector walls } \varphi = 0, 2\pi\alpha$$

$$\frac{\partial \phi}{\partial z} = 0 \quad \text{at the tank bottom } z = -h$$

$$g \frac{\partial \phi}{\partial z} - \Omega^2 \phi = \Omega^2 \phi_0 \quad \text{at the free fluid surface } z = 0.$$

From the equation $\Delta \phi_0 = 0$, one obtains the Poisson equation

$$\Delta \phi_1 = -4i\Omega \phi_0 (\varphi - \pi\alpha) \quad \text{with } \phi_0 = i\Omega^2 \varphi_0 r^2 (\varphi - \pi\alpha) + \phi_1.$$

The boundary conditions are then

$$\frac{\partial \phi_1}{\partial r} = -2i\Omega \varphi_0 r (\varphi - \pi\alpha) \quad \text{for } r = a, b.$$

$$\frac{\partial \phi_1}{\partial \varphi} = 0 \quad \text{for } \varphi = 0, 2\pi\alpha.$$

A solution that satisfies the last boundary conditions in φ has the form

$$\phi_1(r, \varphi) = \sum_{m=0}^{\infty} R_m(r) \cos \bar{\varphi}.$$

Introducing these into the Poisson differential equation, we obtain an infinite number of ordinary differential equations for the function $R_m(r)$ if on the right hand side the function φ is represented as a cosine series.

$$\varphi - \pi\alpha = \sum_{m=0}^{\infty} p_m \cos \bar{\varphi} \quad \text{with } p_0 = 0, \quad p_{2m} = 0, \quad p_{2m-1} = -\frac{4\bar{\alpha}}{\pi^2} \frac{1}{(2m-1)^2}. \quad (40)$$

The obtained differential equations are

$$\frac{d^2 R_0}{dr^2} + \frac{1}{r} \frac{dR_0}{dr} = 0$$

$$\frac{d^2 R_{2m}}{dr^2} + \frac{1}{r} \frac{dR_{2m}}{dr} - \frac{m^2}{\alpha^2 r^2} R_{2m} = 0 \quad \text{for } m = 1, 2, \dots$$

$$\frac{d^2 R_{2m-1}}{dr^2} + \frac{1}{r} \frac{dR_{2m-1}}{dr} - \frac{(2m-1)^2}{4\alpha^2 r^2} R_{2m-1} = \frac{16i\Omega \varphi_0 \bar{\alpha}}{\pi^2} \frac{1}{(2m-1)^2} \quad \text{for } m = 1, 2, \dots$$

They have for $\alpha \neq 1/4, 3/4$ with the boundary conditions in r the solutions

$$R_0(r) = 0$$

$$R_{2m}(r) = 0$$

$$R_{2m-1}(r) = \frac{8i\Omega\varphi_0 a^2 \bar{\alpha}^2}{\pi(2m-1)[(2m-1)^2 \pi^2 - \bar{\alpha}^2]} \left\{ \left(\frac{r}{a}\right)^{\frac{2m-1}{2\alpha}} \frac{(1-k)^{\frac{2m-1}{2\alpha}+2}}{\frac{2m-1}{2\alpha}} - \left(\frac{a}{r}\right)^{\frac{2m-1}{2\alpha}} \frac{(1-k)^{\frac{2m-1}{2\alpha}}}{(1-k)} - \frac{(k^2 - k^{\frac{2\alpha}{2\alpha}}) k^{\frac{2\alpha}{2\alpha}}}{\frac{2m-1}{2\alpha}} - \frac{2\bar{\alpha}}{\pi(2m-1)} \left(\frac{r}{a}\right)^2 \right\}.$$

The solution $\phi_0(r, \varphi)$ is for $\alpha \neq 1/4$ and $3/4$:

$$\phi_0(r, \varphi) = i\Omega\varphi_0 r^2(\varphi - \pi\alpha) + \frac{8i\Omega\varphi_0 a^2 \bar{\alpha}}{\pi} \cdot \frac{\cos \bar{\varphi}}{(2m-1)[(2m-1)^2 \pi^2 - 4\bar{\alpha}^2]} \cdot \left\{ \left(\frac{r}{a}\right)^{\frac{2m-1}{2\alpha}} \frac{(1-k)^{\frac{2m-1}{2\alpha}+2}}{\frac{2m-1}{2\alpha}} - \left(\frac{a}{r}\right)^{\frac{2m-1}{2\alpha}} \frac{(k^2 - k^{\frac{2\alpha}{2\alpha}}) k^{\frac{2\alpha}{2\alpha}}}{\frac{2m-1}{2\alpha}} - \frac{2\bar{\alpha}}{\pi(2m-1)} \left(\frac{r}{a}\right)^2 \right\}.$$

This represents an infinite series in m . It is $\bar{\varphi} = \frac{2m-1}{2\alpha} \varphi$.

The solution of the equation $\Delta\phi = 0$, which satisfies the homogeneous boundary conditions of the container walls, is given by

$$\phi(r, \varphi, z) = D \frac{\cosh(\kappa + \zeta)}{\cosh \kappa} C(\rho) \cos \bar{\varphi}.$$

Introducing the Fourier series for φ in the function $\phi_0(r, \varphi)$ and satisfying the boundary conditions at the free surface, one obtains with the Bessel series the constants D_{mn} . It is

$$D_{2m} = 0$$

$$m = 0, 1, 2, \dots$$

$$D_{2m-1n} = \frac{8i\Omega\varphi_0 a^2 \bar{\alpha}^2 \eta^{*2}}{\pi(2m-1) [(2m-1)^2 \pi^2 - 4\bar{\alpha}^2] (1-\eta^{*2})} \left\{ \frac{l_{2m-1n} (1-k^{\frac{2m-1}{2\alpha}})^{-q_{2m-1n}}}{(1-k^{\frac{2m-1}{2\alpha}})} - \frac{(k^2 - k^{\frac{2m-1}{2\alpha}})k}{\frac{\pi(2m-1)}{2\bar{\alpha}}} g_{2m-1n} \right\}$$

The solution of $\Delta \phi = 0$ is therefore

$$\phi(r, \varphi, z) = \frac{8i\Omega\varphi_0 a^2 \bar{\alpha}^2}{\pi} \cdot \frac{\eta^{*2} C^*(\rho^*) \cosh(\xi^* + \kappa^*) \cos \bar{\varphi}}{(2m-1) [\pi^2 (2m-1)^2 - 4\bar{\alpha}^2] (1-\eta^{*2}) \cosh \kappa^*} \cdot \left\{ \frac{l_{2m-1n} (1-k^{\frac{2m-1}{2\alpha}})^{-q_{2m-1n}} (k^2 - k^{\frac{2m-1}{2\alpha}})k}{(1-k^{\frac{2m-1}{2\alpha}})} - \frac{\pi(2m-1)}{2\bar{\alpha}} g_{2m-1n} \right\}.$$

Here the ξ_{mn} are roots of $C'_{\frac{2m-1}{2\alpha}} = 0$.

The values g_{2m-1n} , h_{2m-1n} , l_{2m-1n} , q_{2m-1n} are the coefficients of the Bessel series

$$\left(\frac{r}{a}\right)^2 = \sum_{n=0}^{\infty} g_{2m-1n} C^*(\rho^*) .$$

$$\left(\frac{a}{r}\right)^2 = \sum_{n=0}^{\infty} h_{2m-1n} C^*(\rho^*)$$

$$\left(\frac{r}{a}\right)^{\frac{2m-1}{2\alpha}} = \sum_{n=0}^{\infty} l_{2m-1n} C^*(\rho^*)$$

$$\left(\frac{a}{r}\right)^{\frac{2m-1}{2\alpha}} = \sum_{n=0}^{\infty} q_{2m-1n} C^*(\rho^*) .$$

where $C^*(\rho^*) = C \frac{2m-1}{2\alpha} \left(\xi_{2m-1n} \frac{r}{a} \right)$ and $\int_{k \xi_{2m-1n}}^{\xi_{2m-1n}} \rho^* C^{*2}(\rho^*) d\rho^* = I^*$

$$g_{2m-1n} = \int_{k \xi_{2m-1n}}^{\xi_{2m-1n}} \rho^{*3} C^*(\rho^*) d\rho^* / \xi_{2m-1n}^2 I^*$$

$$h_{2m-1n} = \xi_{2m-1n}^2 \int_{k \xi_{2m-1n}}^{\xi_{2m-1n}} C^*(\rho^*) \frac{d\rho^*}{\rho^*} / I^*$$

$$l_{2m-1n} = \int_{k \xi_{2m-1n}}^{\xi_{2m-1n}} \rho^{*\frac{2m-1}{2\alpha} + 1} C^*(\rho^*) d\rho^* / \xi_{2m-1n}^{\frac{2m-1}{2\alpha}} I^*$$

$$q_{2m-1n} = \xi_{2m-1n}^{\frac{2m-1}{2\alpha}} \int_{k \xi_{2m-1n}}^{\xi_{2m-1n}} \rho^{*(1 - \frac{2m-1}{2\alpha})} C^*(\rho^*) d\rho^* / I^*$$

The velocity potential finally is

$$\begin{aligned} \Phi(r, \psi, z, t) = i\Omega \varphi_0 e^{i\Omega t} a^2 \left\{ \left(\frac{r}{a} \right)^2 (\varphi - \pi\alpha) + \frac{8\bar{\alpha} \cos \bar{\varphi}}{\pi (2m-1) [\pi^2 (2m-1)^2 - 4\bar{\alpha}^2]} \right. \\ \left[\frac{\left(\frac{r}{a} \right)^{\frac{2m-1}{2\alpha}} (1-k)^{\frac{2m-1}{2\alpha} + 2} - \left(\frac{a}{r} \right)^{\frac{2m-1}{2\alpha}} (k^2 - k)^{\frac{2m-1}{2\alpha}} k^{\frac{2m-1}{2\alpha}}}{(1-k)^{\frac{2m-1}{2\alpha}}} - \frac{2\bar{\alpha}}{\pi (2m-1)} \left(\frac{r}{a} \right)^2 \right] + \\ \frac{8\bar{\alpha}^2 C^*(\rho^*) \eta^{*2} \cosh(\xi^* + \kappa^*) \cos \bar{\varphi}}{\pi (2m-1) [\pi^2 (2m-1)^2 - 4\bar{\alpha}^2] (1-\eta^{*2}) \cosh \kappa^*} \left[\frac{l_{2m-1n} (1-k)^{\frac{2m-1}{2\alpha} + 2}}{(1-k)^{\frac{2m-1}{2\alpha}}} \right. \\ \left. \left. - \frac{q_{2m-1n} (k^2 - k)^{\frac{2m-1}{2\alpha}} k^{\frac{2m-1}{2\alpha}}}{(1-k)^{\frac{2m-1}{2\alpha}}} - \frac{\pi (2m-1)}{2\bar{\alpha}} g_{2m-1n} \right] \right\} \quad (41) \end{aligned}$$

The first term satisfies the boundary conditions at the sector walls while the infinite series vanishes there term by term. In the boundary conditions at the tank wall $r = a$, $r = b$, the double series vanishes term by term, and the simple summation together with the first term vanishes after differentiation with respect to the radius r . The corresponding results obtained from this velocity potential are represented in Table 1. In the moment about the z -axis, one recognizes that the first term represents nothing but the moment of the solidified liquid. By omitting the double series, the moment of the liquid in a infinitely long container is obtained. As already mentioned, the results are only valid as long as the apex angle $\alpha \neq 1/4$ and $\alpha \neq 3/4$. In these cases, the nonhomogeneous solution of the differential equation exhibits resonance conditions with the solution of the homogeneous differential equation for the function $R_1(r)$ in the case $m = 1$ and $R_3(r)$ in the case $m = 2$. In the case of a cylindrical container with a cross section in the form of a circular quarter ring,

$$R_1(r) = C_1 r^2 + D_1 r^{-2} + \frac{2}{\pi} i \Omega \varphi_0 r^2 \ln r.$$

All other solutions of the differential equations in R_m remain the same. Here the integration constants C_1 and D_1 are obtained with the boundary conditions for r . For this tank form the velocity potential, the free surface displacement, and the pressure distribution are obtained by introducing $\alpha = 1/4$ and by substituting for the term of the index $m=1$ in the simple series the value

$$\frac{1}{\pi} \left[1 + \frac{2k^4}{1-k^4} \ln k + 2 \ln \left(\frac{r}{a} \right) \right] \left(\frac{r}{a} \right)^2 - \frac{2k^4 \ln k}{1-k^4} \left(\frac{a}{r} \right)^2 \cos 2\varphi.$$

The term for $m = 1$ in the double series in substituting by

$$\frac{1}{\pi} \sum_{n=0}^{\infty} \frac{\left[2\beta_n + g_n \left(\frac{2k^4 \ln k}{1-k^4} - 1 \right) + \frac{2k^4 \ln k}{1-k^4} h_n \right] \cosh(\kappa_2 + \zeta_2) C_2(\rho_2) \eta_2^2 \cos 2\varphi}{(1-\eta_2^2) \cosh \kappa_2}$$

where the values β_n are the coefficients of the series expansion

$$\left(\frac{r}{a} \right)^2 \ln \left(\frac{r}{a} \right) = \sum_{n=0}^{\infty} \beta_n C_2(\rho_2)$$

and are

$$\beta_n = \frac{\int_b^a r^3 \ln \left(\frac{r}{a} \right) C_2 \left(\xi_{2n} \frac{r}{a} \right) dr}{a^2 \int_b^a r C_2^2 \left(\xi_{2n} \frac{r}{a} \right) dr}.$$

The terms h_n and g_n are coefficients of the expansions

$$\left(\frac{r}{a}\right)^2 = \sum_{n=0}^{\infty} g_n C_2(\rho_2)$$

$$\left(\frac{a}{r}\right)^2 = \sum_{n=0}^{\infty} h_n C_2(\rho_2)$$

and are

$$g_n = \frac{\int_b^a r^3 C_2\left(\xi_{2n} \frac{r}{a}\right) dr}{a^2 \int_b^a r C_2^2\left(\xi_{2n} \frac{r}{a}\right) dr}$$

$$h_n = \frac{a^2 \int_b^a C_2\left(\xi_{2n} \frac{r}{a}\right) \frac{dr}{r}}{\int_b^a r C_2^2\left(\xi_{2n} \frac{r}{a}\right) dr}.$$

3. Special Cases. Containers of circular cross section are most frequently used in missiles and space vehicles. With increasing diameter of the containers, a subdivision of the tanks by longitudinal walls to decrease the sloshing propellant masses can hardly be avoided. For instance, a cylindrical container could be divided into four quarter tanks. A concentric container also could be of some advantage since, by proper selection of the diameter ratio, the liquid oscillations could be brought into favorable phase relations so that the influence upon the total stability could be partially cancelled. Fluid oscillations in a cylindrical container of annular cross section have been treated [10]. The following will be restricted to the treatment of cylindrical containers of sector circular and quarter circular cross section. The forces and moments of the liquid are given in Tables 2 and 3.

a. Sector tank. Let the ratio $k = b/a$ of the inner to the outer tank diameter approach zero; then we obtain the results which are due to the fluid motion in a cylindrical container of circular sector cross section. Here the determinant

$$\Delta_{\frac{m}{2\alpha}}(\xi) = 0$$

$$\text{becomes } J'_{\frac{m}{2\alpha}}(\xi) = 0$$

the zeros of which are denoted by ϵ_{mn} . The expansion functions $C(\rho)$ become simply the Bessel functions $J(\rho) \equiv J_{\frac{m}{2\alpha}}\left(\epsilon_{mn} \frac{r}{a}\right)$, and the coefficients b_{mn} are given in the simple form

$$b_{mn} = \frac{a \int_0^{\epsilon_{mn}} \rho^2 J(\rho) d\rho}{\epsilon_{mn} \int_0^{\epsilon_{mn}} \rho J^2(\rho) d\rho} =$$

$$2a \frac{\frac{\Gamma(m/4\alpha+3/2)}{\Gamma(m/4\alpha-1/2)} \sum_{\mu=0}^{\infty} \frac{(m/2\alpha+2\mu+1)\Gamma(m/4\alpha+\mu+1/2)}{\Gamma(m/4\alpha+\mu+5/2)} J_{m/2\alpha+2\mu+1}(\epsilon_{mn})}{\epsilon_{mn} (1-m^2/4\alpha^2\epsilon_{mn}^2) J_{m/2\alpha}^2(\epsilon_{mn})} \quad (42)$$

$$m, n = 0, 1, 2, \dots$$

In the force component the singular solution at $r = 0$ must be omitted. Therefore, the value $2/\pi \xi_{mn} - kC(k\xi_{mn})$ in the forces and moments is replaced by $J(\epsilon_{mn})$. The expression $N_0(\xi_{mn})$ will be substituted by $L_0(\epsilon_{mn})$ since $\int C(\rho) d\rho$ is replaced by $\int J(\rho) d\rho$. The same is valid for N_1 and N_2 which are replaced by L_1 and L_2 . The velocity potential, the free fluid surface displacement, the force and moment components are represented for the various excitation forms in Table 2.

In the case of roll excitation, the results for the flow of the liquid in a circular sector tank can be obtained from the previous results of a container of circular ring sector cross section by introducing $k=0$ and substituting for l_{2m-1n} the value f_{2m-1n} and for g_{2m-1n} the value e_{2m-1n} . These are coefficients of the expansions.

$$\left(\frac{r}{a}\right)^{2\alpha} = \sum_{n=0}^{\infty} f_{2m-1n} \frac{J_{2m-1}}{2\alpha} \left(\epsilon_{2m-1n} \frac{r}{a}\right)$$

$$\left(\frac{r}{a}\right)^2 = \sum_{n=0}^{\infty} e_{2m-1n} \frac{J_{2m-1}}{2\alpha} \left(\epsilon_{2m-1n} \frac{r}{a}\right)$$

Again the results are valid only if $\alpha \neq 1/4, 3/4$. For $\alpha = 1/4$ one substitutes, in the velocity potential the free fluid surface displacement of the liquid and in the pressure distribution for the first term ($m = 1$) in the simple summation the value

$$\frac{1}{\pi} \left(\frac{r}{a}\right)^2 \left\{ 2 \ln \left(\frac{r}{a}\right) + 1 \right\} \cos 2\varphi.$$

The term for $m = 1$ in the double series is replaced by

$$\frac{1}{\pi} \sum_{n=0}^{\infty} \frac{(2f_n - e_n) \cosh(\kappa_2 + \zeta_2) \eta_2^2}{(1 - \eta_2^2) \cosh \kappa_2} J_2(\rho_2) \cos 2\varphi.$$

Here the values f_n are the coefficients of the series expansion

$$\left(\frac{r}{a}\right)^2 \ln \left(\frac{r}{a}\right) = \sum_{n=0}^{\infty} f_n J_2\left(\epsilon_{2m} \frac{r}{a}\right)$$

$$\text{with } f_n = \frac{\int_0^a r^3 \ln\left(\frac{r}{a}\right) J_2\left(\epsilon_{2m} \frac{r}{a}\right) dr}{a^2 \int_0^a r J_2^2\left(\epsilon_{2m} \frac{r}{a}\right) dr}$$

and the coefficients e_n are obtained from the expansion

$$\left(\frac{r}{a}\right)^2 = \sum_{n=0}^{\infty} e_n J_2\left(\epsilon_{2m} \frac{r}{a}\right) dr$$

with

$$e_n = \frac{\int_0^a r^3 J_2\left(\epsilon_{2m} \frac{r}{a}\right) dr}{a^2 \int_0^a r J_2^2\left(\epsilon_{2m} \frac{r}{a}\right) dr}.$$

b. Circular cylindrical container. For a cylindrical container of circular cross section, α must be taken to be one. This represents a tank with a side wall in the $\varphi = 0$ plane from $r = 0$ to $r = a$. The values a_m, b_{mn}, c_m are therefore

$$a_0 = 0 \quad a_m = 0 \quad a_2 = \lim_{\alpha \rightarrow 1} \left\{ - \frac{\alpha \sin 2\pi\alpha}{\pi (1-\alpha^2)} \right\} = 1 \quad (43)$$

$$c_0 = 0 \quad c_{2m} = 0 \quad c_{2m-1} = -\frac{8}{\pi} \frac{1}{[(2m-1)^2 - 4]} \quad m = 1, 2, 3, \dots \quad (44)$$

The value c_2 also vanishes. The limit is

$$c_2 = \lim_{\alpha \rightarrow 1} \left\{ \frac{\alpha (\cos 2\pi\alpha - 1)}{\pi (1-\alpha^2)} \right\} = 0.$$

To obtain the solution for the circular cylindrical container, one chooses the excitation in x-direction at which the side wall does not disturb the motion. For this reason, only the expression b_{2n} is needed. Considering the singularity of the gamma-function at the argument zero and the recursion formula of the Bessel function

$$xJ'_v(x) - vJ_v(x) = -xJ_{v+1}(x)$$

from which for $x = \epsilon_n$ as a root of the equation $J'_1(\epsilon_n) = 0$ we obtain the value $\epsilon_n J_2(\epsilon_n) = J_1(\epsilon_n)$. The expression b_{2n} finally is

$$b_{2n} = \frac{2a}{(\epsilon_n^2 - 1) J_1(\epsilon_n)} \quad (45)$$

The velocity potential for translational excitation in x-direction is therefore

$$\Phi(r, \varphi, z, t) = i\Omega x_0 e^{i\Omega t} \cos\varphi \left\{ \frac{r}{a} + 2 \frac{J_1(\rho)\eta^2 \cosh(\kappa + \zeta)}{(\epsilon_n^2 - 1) J_1(\epsilon_n) \cosh\kappa(1 - \eta^2)} \right\}. \quad (46)$$

The natural frequencies of the liquid in cylindrical container of free fluid surface and circular cross section are given by

$$f_n = \frac{\omega_n}{2\pi} = \frac{1}{2\pi} \sqrt{\frac{g}{a} \epsilon_n \tanh\left(\epsilon_n \frac{h}{a}\right)}.$$

The zeros of the first derivative of the Bessel function of first kind and first order are

$$\epsilon_0 = 1.8412, \epsilon_1 = 5.3314, \epsilon_2 = 8.5363, \epsilon_3 = 11.7060.$$

As can be seen from the formula and from the numerical result represented in Figure 2, the natural frequency of the liquid in a partially filled container changes considerably at constant longitudinal acceleration only for small liquid height ($h/a < 1$).

This is true because the hyperbolic tangent practically assumes the value one for values of $(h/a) > 1$. The natural frequency increases proportionally to the square root of the longitudinal acceleration g . Furthermore, it can be seen that the Eigen frequency of the fluid with increasing radius a changes its value like $1/\sqrt{a}$. This indicates that for increasing tank diameter, the natural frequency of the liquid becomes smaller. From the free fluid surface displacement z (Table 3) one concludes that the first term represents the displacement with respect to small excitation frequency. For these the surface displacement of the liquid (neglecting terms of Ω^4) is a plane of the form $r \cos \varphi$, since the required pressure is replaced by the static pressure. With increasing excitation amplitudes x_0 , the free surface amplitude becomes larger, while for increasing longitudinal acceleration of the container the disturbances of the free surface become smaller. The wave form of the free fluid surface for excitation frequencies Ω before the first and second resonance is presented in Figure 3. The surface displacement of the liquid for various frequency ratios is given in Figure 4. Here the given curves for the displacement correspond to the indicated points of frequencies in the magnification function for the displacement of the free fluid surface at the container wall (Fig. 5).

In the fluid force the limit value is

$$\lim_{\substack{\alpha \rightarrow 1 \\ m \rightarrow 2}} \left\{ (-1)^{m+1} \frac{\sin 2\pi\alpha}{\pi\alpha} \left[\frac{4\alpha^2}{(m^2 - 4\alpha^2)} J_{\frac{m}{2\alpha}}(\epsilon_{mn}) + L_0(\epsilon_{mn}) \right] \right\} = J_1(\epsilon_n).$$

A similar result is obtained for the moment where $L_2(\epsilon_n) = J_1(\epsilon_n)/\epsilon_n^2$

and
$$\lim_{\substack{\alpha \rightarrow 1 \\ m \rightarrow 2}} \left[(-1)^{m+1} \frac{\sin 2\pi\alpha}{\pi\alpha} \frac{8\alpha^2}{(m^2 - 4\alpha^2)} \right] = 2.$$

In the force the first term again can be identified as the inertial force of the liquid (Fig. 6), while the first term in the moment represents the moment with respect to the shifting of the center of gravity of the liquid for small frequencies (Ω^4 terms neglected) (Fig. 7). For surface displacement proportional to $r \cos \varphi$ in which the surface assumes an angle α from its undisturbed position, the shifting of the center of gravity is

$$x_s = \frac{a^2 \operatorname{tg} \alpha}{4h}.$$

Here, $\operatorname{tg} \alpha = \ddot{x}/g$. The contribution of this part to the total moment of the liquid is therefore

$$M_y = mgx_s = -m\ddot{x}a/4 \frac{h}{a}.$$

The shifting of the center of gravity in vertical direction can be neglected, because it is represented by a term of the second order. The velocity potential for rotational excitation $\Theta = \Theta_0 e^{i\Omega t}$ is

$$\Phi(r, \varphi, z, t) = -i\Omega\theta_0 e^{i\Omega t} a^2 \cos \varphi \left\{ \frac{r}{a} \frac{z}{a} + 2 \frac{J_1(\rho)\eta^2}{\epsilon_n(\epsilon_n^2 - 1)J_1(\epsilon_n) \cosh \kappa(1 - \eta^2)} \cdot \left[\left(\gamma + \frac{\kappa}{2} \right) \cosh \left(\frac{\kappa}{2} + \zeta \right) - 4\gamma \sinh \frac{\kappa}{2} \sinh \zeta - 2 \sinh \left(\frac{\kappa}{2} - \zeta \right) \right] \right\} \quad (47)$$

The free surface remains horizontal for very small and infinitely large excitation frequencies. The wave form of the free surface is presented in Figure 4 for various frequency ratios. Figure 5 shows the magnification function of the free surface at the tank wall. The force component is shown in Figure 6, and the first term in the force represents only the weight of the liquid. In the moment the first term again represents the contribution of shifting of the center of gravity of the liquid for small excitation frequencies. The free surface in that case remains horizontal and has, with respect to the tank bottom, an angle $\alpha = \Theta_0$. The shifting of the center of gravity therefore is ($\operatorname{tg} \alpha \approx \alpha$)

$$\frac{a^2 \operatorname{tg} \alpha}{4h} = \frac{a\theta_0 e^{i\Omega t}}{4h/a}.$$

The contribution of the shifting of the center of gravity to the moment about the center of gravity of the undisturbed liquid (origin of the coordinate system) is therefore

$$M_y = - \frac{mga\theta_0 e^{i\Omega t}}{4h/a}.$$

The magnification function of the moments are represented in Figure 7.

c. Container with quarter circular cross section. The results for the liquid motion in a container of a quarter circular cross section are obtained by substituting into the equations of Para. a. $\alpha = 1/4$. With this the velocity potential results in

$$\Phi(r, \varphi, z, t) = i\Omega x_o e^{i\Omega t} \left\{ r \cos \varphi + \frac{a_m b_{mn} \cos 2m\varphi \cosh(\kappa + \zeta) J_{2m}(\rho) \eta^2}{(1 - \eta^2) \cosh \kappa} \right\} \quad (48)$$

where

$$a_o = \frac{2}{\pi}, \quad a_m = \frac{(-1)^{m+1}}{\pi(m^2 - 1/4)}, \quad b_{mn} = \frac{16a_{mn}(\epsilon_{mn}^2 - 1/4)}{(\epsilon_{mn}^2 - 4m^2) J_{2m}^2(\epsilon_{mn})} \cdot \sum_{\mu=0}^{\infty} \frac{J_{2m+2\mu+1}(\epsilon_{mn})}{(2m+2\mu-1)(2m+2\mu+3)}.$$

The values ϵ_{mn} are the roots of the equation $J'_{2m}(\epsilon_{mn}) = 0$. For a container of circular symmetric cross section the orthogonality conditions of the trigonometric functions are responsible for the appearance of only one class of resonances in the forced oscillations. Here, also, as in the sector tanks the other class appears. The results of the liquid motion in this tank are shown in Table 3. Table 4 represents the roots in the equation $J'_{2m}(\epsilon_{mn}) = 0$. From these it is recognized that the zero root is larger than the first (because of $J'_0 = -J_1$). This indicates that the zero Eigen frequency is larger than the first Eigen frequency. Figure 2 exhibits the ratio $f_{mn}/\sqrt{g/a}$. They present essentially the same behavior as the frequencies in a cylindrical tank of circular or annular cross section except that the Eigen frequencies are slightly larger than those of the circular cylindrical container and that they are closer together. Figure 8 represents the wave form of the free surface for excitation in x-direction with forcing frequencies in front and shortly before first resonance ($\omega_{10} = 5.5$ 1/sec.) as well as between first and second resonance ($\omega_{00} = 6.2$ 1/sec.) and shortly after second resonance. In the liquid force and moments, the values for L_o and L_2 are

$$L_o = \frac{2}{\epsilon_{mn}} \sum_{\mu=0}^{\infty} J_{2m+2\mu+1}(\epsilon_{mn}),$$

$$L_2 = \frac{2(4m^2 - 1)}{\epsilon_{mn}} \sum_{\mu=0}^{\infty} \frac{J_{2m+2\mu+1}(\epsilon_{mn})}{(2m+2\mu-1)(2m+2\mu+3)}.$$

In the force F_x , the first term again can be identified as inertial force of the fluid (Fig. 9). The last term in the moment represents the static moment (Fig. 10).

The velocity potential for rotational excitation $\theta = \theta_o e^{i\Omega t}$ becomes

$$\Phi(r, \varphi, z, t) = -i\Omega \theta_o e^{i\Omega t} \left\{ rz \cos \varphi - [A \cosh \zeta + B \sinh \zeta] J_{2m}(\rho) \cos 2m\varphi \right\}. \quad (49)$$

Here the values A_{mn} , B_{mn} are the corresponding expressions 38a and 38b if one substitutes the appropriate values for a_m , b_{mn} , and for ξ_{mn} the values ϵ_{mn} . The first term in the force represents the force component with respect to the weight of the liquid. The magnification function is shown in Figure 11, while that for the moment is represented in Figure 12. For roll excitation of the container $\varphi = \varphi_0 e^{i\Omega t}$, the velocity potential is

$$\begin{aligned} \Phi(r, \varphi, x, t) = i\Omega \varphi_0 e^{i\Omega t} \left\{ r^2 \left(\varphi - \frac{\pi}{4} \right) + \frac{2a^2 \cos[(4m-2)\varphi]}{\pi(2m-1)[(2m-1)^2 - 1]} \left[\left(\frac{r}{a} \right)^{4m-2} - \frac{(r/a)^2}{(2m-1)} \right] \right. \\ \left. + \frac{2a^2}{\pi} \left(\frac{r}{a} \right)^2 \left[\ln\left(\frac{r}{a}\right) + \frac{1}{2} \right] \cos 2\varphi + \frac{2a^2}{\pi} \frac{[f_{2m-1n} - e_{2m-1n}(2m-1)]\eta_1^{*2} J_{4m-2}(\rho_1^*)}{(2m-1)[(2m-1)^2 - 1](1-\eta_1^{*2}) \cosh \kappa_1^*} \right. \\ \left. \cosh(\kappa_1^* + \xi_1^*) \cos(4m-2)\varphi + \frac{a^2}{\pi} \frac{(2f_n - e_n) \cosh(\kappa_1^* + \xi_1^*) \eta_1^{*2} J_2(\rho_1^*) \cos 2\varphi}{(1-\eta_1^{*2}) \cosh \kappa_1^*} \right\}. \quad (50) \end{aligned}$$

Here the values $\bar{\epsilon}_n$ are the roots of the equation $J_2'(\bar{\epsilon}_n) = 0$ while the values $\bar{\epsilon}_{2m-1n}$ are solutions of the equation $J_{4m-2}'(\bar{\epsilon}_{2m-1n}) = 0$. Furthermore, it is

$$f_n = -\frac{8}{(\bar{\epsilon}_n^2 - 4) J_2^2(\bar{\epsilon}_n)} \sum_{\mu=0}^{\infty} \frac{J_{2\mu+4}(\bar{\epsilon}_n)}{(\mu+1)(\mu+3)}$$

$$e_n = \frac{4}{(\bar{\epsilon}_n^2 - 4) J_2(\bar{\epsilon}_n)}$$

$$f_{2m-1n} = \frac{4(2m-1)}{[\bar{\epsilon}_{2m-1n}^2 - 4(2m-1)^2] J_{4m-2}(\bar{\epsilon}_{2m-1n})}$$

and

$$\begin{aligned} e_{2m-1n} &= \frac{2m\bar{\epsilon}_{2m-1n}(2m-1)}{(m-1)[\bar{\epsilon}_{2m-1n}^2 - 4(2m-1)^2] J_{4m-2}^2(\bar{\epsilon}_{2m-1n})} \\ &\cdot \sum_{\mu=0}^{\infty} \frac{(4m+2\mu-1) J_{4m+2\mu-1}(\bar{\epsilon}_{2m-1n})}{(2m+2\mu-2)(2m+2\mu-1)(2m+\mu)(2m+\mu+1)}. \end{aligned}$$

One recognizes from all these results that only one-half of the natural frequencies appear. Figures 13 through 15 illustrate the various magnification functions for the forces and moments of the liquid. Here the value L_0 , L_1 , and L_2 are

$$L_0 = \frac{2}{\bar{\epsilon}_{2m-1n}} \sum_{\mu=0}^{\infty} J_{4m+2\mu-1}(\bar{\epsilon}_{2m-1n}).$$

$$L_1 = \frac{2m-1}{\bar{\epsilon}_{2m-1n}} \sum_{\mu=0}^{\infty} \frac{(4m+2\mu-1) J_{4m+2\mu-1}(\bar{\epsilon}_{2m-1n})}{(2m+\mu-1)(2m+\mu)} .$$

$$L_2 = \frac{2(4m-1)(4m-3)}{\bar{\epsilon}_{2m-1n}} \sum_{\mu=0}^{\infty} \frac{J_{4m+2\mu-1}(\bar{\epsilon}_{2m-1n})}{(4m+2\mu+1)(4m+2\mu-3)} .$$

SECTION III. THE MECHANICAL MODEL

A. DISCUSSION

Since in the frictionless liquid the magnification function exhibits singularities at the resonances, all previous results are not applicable as long as the exciting frequency is too close to the Eigen frequencies. In the vicinity of these, finite values occur which influence the stability of the space vehicle considerably. Especially at the lower Eigen frequencies of the propellant, liquid forces occur which are a multiple of the inertial forces of the propellant. An exact solution of damped liquid vibrations is practically impossible. However, a good approximation can be obtained by treating each vibration mode of the liquid as a degree of freedom and representing it as a spring-mass system. Since the mode shapes are not considerably changed by the small damping of the liquid, magnitude and location of the spring constants and sloshing masses can be derived from the results of the previous paragraph. In this mechanical model, damping can be introduced in a simple way in form of linear viscous damping. Actually the forced damped fluid oscillations represent a nonlinear vibration problem. Since the treatment of a nonlinear system of many degrees of freedom represents considerable difficulty, equivalent linear damping is introduced. From this, the magnification functions and their phases can be numerically determined for various damping factors and will be compared with experimental values. This way the equivalent linear damping factor of the liquid is obtained. In the following, the mechanical model will be derived only for the most important practical container arrangements. The determination of the various elements of the model will be exercised in paragraph 2 of this section.

B. THE MECHANICAL MODEL FOR THE DESCRIPTION OF LIQUID MOTION

In an oscillating container the liquid oscillates only in close proximity of the free fluid surface, while in the lower part of the container, it follows the motion like a rigid body. This indicates that the sloshing mass m_n corresponding to the appropriate vibration mode and the corresponding springs with stiffness $k_n/2$ (with which the slosh mass is fixed at the tank wall at a distance h_n from the center of gravity of the undisturbed liquid) have to be attached in the proximity of the free fluid surface ($h_1 \rightarrow h_2$). This happens with increasing order of vibration modes. The nonvibrating liquid in the lower part of the container is described by a mass m_0 and a moment of inertia I_0 . This mass is attached rigidly to the container at a height h_0 below the center of gravity of

the liquid. (Fig. 16)

To make the mechanical model equivalent to the original fluid system, the sum of the model mass must equal the total liquid mass.

$$m = m_o + \sum_{n=1}^{\infty} m_n .$$

For small oscillations, the center of gravity of the liquid shifts horizontally only in the first approximation. Therefore

$$m_o h_o = \sum_{n=1}^{\infty} m_n h_n$$

must be satisfied.

The spring constant, k_n , is chosen in such a fashion that its ratio to the mass of the sloshing mode represents the square of the Eigen frequency

$$\omega_{n-1}^2 = \frac{k_n}{m_n} .$$

For rotational excitation about the origin, not all of the liquid participates in the motion, but a part of it remains completely at rest. So, a frictionlessly mounted massless disc with a moment of inertia, I_d , must be introduced at the origin. Thus, the effective moment of inertia of the liquid becomes

$$I_f = I_{\text{rigid}} - I_d = I_o + m_o h_o^2 + \sum_{n=1}^{\infty} m_n h_n^2$$

Linear damping is introduced in the model by attaching two dampers with the damping coefficients $c_n/2$ between the mass of the n th vibration mode and the tank wall. In addition, one must introduce a damper, c_d , between the disc and tank bottom, since, for rotational excitation of a nonfrictionless liquid, more fluid participates in the motion than for a frictionless one. The magnitude of the damping coefficients can be approximately determined from torsional vibration experiments of a completely filled, closed container of equal liquid height. The damping coefficient, c_n , will be obtained from forced vibration experiments of the free fluid surface. The linear damping terms are introduced in the usual form ($c_n = 2m_n \omega_n \gamma_n$) where γ_n represents the damping factor. The equations of motion of the model are now derived with the help of the Lagrange equations. For this reason one determines the kinetic and potential energy as well as the dissipation function. If one considers y_n as the displacement of the sloshing mass, m_n , with respect to the container wall, with y the tank displacement in y -direction, with φ the rotation about the z -axis, and with ψ the rotation of the disc with respect to the tank bottom, the kinetic energy will be:

$$T = \frac{m_o}{2} (\dot{y} + h_o \dot{\phi})^2 + \frac{1}{2} I_o \dot{\phi}^2 + \frac{1}{2} \sum_{n=1}^{\infty} m_n (\dot{y}_n + \dot{y} + h_n \dot{\phi})^2 + \frac{1}{2} I_d (\dot{\phi} + \dot{\psi})^2 .$$

The first two terms represent the kinetic energy of the mass, m_o , which is rigidly connected with the container. The series describes the kinetic energy of the various modal masses, m_n , while the last term represents only the kinetic energy of the disc. The dissipation function is

$$D = \frac{1}{2} \sum_{n=1}^{\infty} c_n \dot{y}_n^2 + \frac{1}{2} c_d \dot{\psi}^2 = \sum_{n=1}^{\infty} m_n \omega_n \gamma_n \dot{y}_n^2 + \frac{1}{2} c_d \dot{\psi}^2 ,$$

where the sum represents the contribution of the dash pots between the modal masses m_n and the container, and the last term is due to the damper between disc and tank bottom.

The potential energy is

$$V = \frac{1}{2} g \varphi^2 m_o h_o - \frac{1}{2} g \varphi^2 \sum_{n=1}^{\infty} m_n h_n - g \varphi \sum_{n=1}^{\infty} m_n y_n + \frac{1}{2} \sum_{n=1}^{\infty} k_n y_n^2 .$$

Here, the first term represents the potential energy due to the lifting of the mass, m_o , during rotation, while the second and third terms describe the same fact for the modal masses. The last term is the accumulated energy in the springs. The first two terms in the potential energy will cancel each other due to the condition of the center of mass law.

The equations of motion are derived from the Lagrange equation

$$\frac{d}{dt} \left(\frac{\partial T}{\partial \dot{q}_i} \right) + \frac{\partial D}{\partial \dot{q}_i} + \frac{\partial V}{\partial q_i} = Q_i .$$

If one considers y , φ , ψ and y_n as generalized coordinates and

$$Q_y = -F_y, \quad Q_\varphi = -M_z, \quad Q_\psi = 0, \quad \text{and} \quad Q_{y_n} = 0$$

as generalized forces, the equations of motion are then

$$m_o (\ddot{y} + h_o \ddot{\phi}) + \sum_{n=1}^{\infty} m_n (\ddot{y}_n + \ddot{y} + h_n \ddot{\phi}) = -F_y . \quad (51)$$

$$I_o \ddot{\phi} + m_o h_o^2 \ddot{\phi} - g \sum_{n=1}^{\infty} m_n y_n + \sum_{n=1}^{\infty} m_n h_n (\ddot{y}_n + h_n \ddot{\phi}) + I_d (\ddot{\phi} + \ddot{\psi}) = -M_z. \quad (52)$$

$$I_d (\ddot{\psi} + \ddot{\phi}) + c_d \dot{\psi} = 0. \quad (53)$$

$$m_n (\ddot{y}_n + h_n \ddot{\phi}) + 2m_n \gamma_n \omega_n \dot{y}_n + k_n y_n - m_n g \phi = 0. \quad (54)$$

The first equation is the force equation, the second is the moment equation, and the third describes the motion of the disc, while the last one represents the equation of motion of the nth modal sloshing mass. With these equations, the forces, F_y , and the moment, M_z , can be determined for the particular excitations by introducing the results of the equation of motion of the modal masses into the other equations. Instead of the spring-mass system, a pendulum system could also have been applied.

1. Solution of the Equations of the Model. Introducing the values $\phi = 0$ $\psi = 0$ into the equations of motion, that is, considering the case of translation with $y = y_o e^{i\Omega t}$, one obtains from the equation of the modal masses, m_n ,

$$y_n = \frac{-\ddot{y}/\omega^2}{1 - \eta_{n-1}^2 + 2i\gamma_n \eta_{n-1}} \quad \ddot{y}_n = \frac{\eta_{n-1}^2 \ddot{y}}{1 - \eta_{n-1}^2 + 2i\gamma_n \eta_{n-1}}.$$

With this, the force (eq. 51) is obtained to be

$$F_y = -m\ddot{y} \left[1 + \sum_{n=1}^{\infty} \frac{m_n}{m} \cdot \frac{\eta_{n-1}^2}{(1 - \eta_{n-1}^2 + 2i\gamma_n \eta_{n-1})} \right] \quad (55)$$

and from equation 52, one obtains the moment to be

$$M_z = -m\ddot{y} \sum_{n=1}^{\infty} \frac{m_n}{m} \frac{(g/\omega^2 + h_n \eta_{n-1}^2)}{(1 - \eta_{n-1}^2 + 2i\gamma_n \eta_{n-1})}. \quad (56)$$

In the case of rotation about the z-axis, it is $y = 0$, $\phi = \phi_o e^{i\Omega t}$, and $\psi = \psi_o e^{i\Omega t}$. One obtains for the motion of the modal mass, m_n , from equation 54

$$y_n = \frac{(h_n \eta_{n-1}^2 + g/\omega^2) \phi}{(1 - \eta_{n-1}^2 + 2i\gamma_n \eta_{n-1})},$$

and from equation 51 the force

$$F_y = -m\ddot{\phi} \sum_{n=1}^{\infty} \frac{m_n}{m} \frac{(h_n \eta_{n-1}^2 + g/\omega_{n-1}^2)}{(1 - \eta_{n-1}^2 + 2i\gamma_n \eta_{n-1})} , \quad (57)$$

while from equation 52 the moment is obtained to be

$$M_z = \ddot{\phi} \left\{ \left[I_o + I_d + m_o h_o^2 + \sum_{n=1}^{\infty} m_n h_n^2 \right] - m \sum_{n=1}^{\infty} \frac{m_n}{m} \frac{(\eta_{n-1}^2 h_n^2 + g^2/\eta_{n-1}^2 \omega_{n-1}^4 + 2gh_n/\omega_{n-1}^2)}{(1 - \eta_{n-1}^2 + 2i\gamma_n \eta_{n-1})} \right\} + I_d \ddot{\psi} .$$

As could be expected, the moment due to translational displacement, $y_o = 1$, is equal to the force due to the rotation, $\phi_o = 1$. Assuming that ψ can be approximated from considerations of a completely filled and closed container, one obtains, by suppressing the liquid oscillations at the free fluid surface ($y_n = 0$), from the equation

$$I_{\text{rigid}} \ddot{\phi} + I_d \ddot{\psi} = 0 . \quad (58)$$

$$I_d (\ddot{\phi} + \ddot{\psi}) + c_d \dot{\psi} = 0 . \quad (59)$$

From this we obtain

$$\ddot{\psi} = - \frac{\ddot{\phi}}{\{1 + (c_d/\Omega I_d)^2\}} + \frac{(c_d/I_d)\dot{\phi}}{\{1 + (c_d/\Omega I_d)^2\}} . \quad (60)$$

With this, the moment of the damped model is given by

$$M_z = \ddot{\phi} \left\{ \left[I_o + m_o h_o^2 + \sum_{n=1}^{\infty} m_n h_n^2 + I_d \left(1 - \frac{\Omega^2 I_d^2}{\Omega^2 I_d^2 + c_d^2} \right) \right] + m \sum_{n=1}^{\infty} \frac{m_n}{m} \frac{\left(\frac{2gh_n}{\omega_{n-1}^2} + \frac{g^2}{\omega_{n-1}^4 \eta_{n-1}^2} + h_n^2 \eta_{n-1}^2 \right)}{(1 - \eta_{n-1}^2 + 2i\gamma_n \eta_{n-1})} \right\} + \frac{c_d \Omega^2 I_d^2}{(c_d^2 + \Omega^2 I_d^2)} \dot{\phi} . \quad (61)$$

The mechanical model, as it was derived here, is valid only for containers of rotational symmetry, that is, for tanks with circular and annular cross sections. It can also be applied to a tank arrangement of four-quarter containers, which are gaining more importance and are of special interest. Since the side forces of four-quarter containers, perpendicular to the direction of excitation, cancel each other and since the same is true for the moments about the axis of excitation, the same model can be applied. One has only to consider that the square of the Eigen frequency is

$$\omega_{mn}^2 = \frac{k_{mn}}{m_{mn}}$$

and the total mass of the liquid is given by

$$m = m_o + \sum_{m=1}^{\infty} \sum_{n=1}^{\infty} m_{mn}.$$

The number of mode shapes is increased considerably, since the infinite number of mode shapes in φ -direction must be added to those in r -direction. This is expressed by the double index.

The equations of motion are:

$$\begin{aligned} m_o (\ddot{y} + h_o \ddot{\varphi}) + \sum_{m=1}^{\infty} \sum_{n=1}^{\infty} m_{mn} (\ddot{y}_{mn} + h_{mn} \ddot{\varphi}) &= -F_y \\ (m_o h_o^2 + I_o) \ddot{\varphi} + \sum_{m=1}^{\infty} \sum_{n=1}^{\infty} m_{mn} h_{mn} (\ddot{y}_{mn} + h_{mn} \ddot{\varphi}) - I_d (\ddot{\varphi} + \ddot{\psi}) - g \sum_{m=1}^{\infty} \sum_{n=1}^{\infty} m_{mn} y_{mn} &= -M_z \\ I_d (\ddot{\varphi} + \ddot{\psi}) + c_d \dot{\psi} &= 0. \end{aligned}$$

$$\ddot{y}_{mn} + h_{mn} \ddot{\varphi} + 2\omega_{m-1n-1} \gamma_{mn} y_{mn} + \omega_{m-1n-1}^2 y_{mn} - g\varphi = 0. \quad (m, n = 1, 2, \dots)$$

From this, similar results for the forces and moments can be obtained as in the previous case.

2. Determination of the Mechanical Values. After we have derived and solved the mechanical model, the mechanical values have to be determined. This determination will be performed by comparing the values of the undamped mechanical model with the results of the ideal liquid motion (II, C, 3, b and II, C, 3, c). However, some of these results must be brought into a form that compares with the mechanical model by certain series expansions of Bessel functions and their zeros of the first derivative. In the following, the determination of the mechanical values will be performed for a container with circular cross section. For containers with annular and four-quarter circular cross section, the results can be obtained in a similar way and are presented in Table 5.

Comparison of the forces due to translatory excitation of the undamped ($\gamma_n = 0$) mechanical model (eq. 55) with the force of the liquid (Table 3),

$$F_y = -m\ddot{y} \left\{ 1 + 2 \sum_{n=1}^{\infty} \frac{\tanh \kappa \cdot \eta_{n-1}^2}{\kappa (\epsilon_{n-1}^2 - 1) (1 - \eta_{n-1}^2)} \right\}, \quad (62)$$

results in the ratio of the modal mass m_n to the total mass of the liquid m

$$\frac{m_n}{m} = \frac{2 \tanh(\epsilon_{n-1} \frac{h}{a})}{(\epsilon_{n-1} \frac{h}{a}) (\epsilon_{n-1}^2 - 1)} \cdot \quad n = 1, 2, \dots \quad (63)$$

Comparison of the moments requires a transformation of the liquid moment with

$$\frac{1}{4} = 2 \sum_{n=1}^{\infty} \frac{1}{\epsilon_{n-1}^2 (\epsilon_{n-1}^2 - 1)}$$

and

$$1 - \frac{1}{\cosh \kappa} = \tanh \kappa \tanh \frac{\kappa}{2} \quad (64)$$

It is

$$M_z = -m\ddot{y} \sum_{n=1}^{\infty} \frac{2 \tanh \kappa}{\kappa (\epsilon_{n-1}^2 - 1)} \frac{\frac{g}{\omega_{n-1}^2} + \frac{h}{2} \eta_{n-1}^2 [1 - \frac{4}{\kappa} \tanh \frac{\kappa}{2}]}{(1 - \eta_{n-1}^2)} \cdot \quad (65)$$

Comparison with equation 56 results in the already obtained mass ratio m_n/m and the height ratio

$$\frac{h_n}{h} = \frac{1}{2} \left[1 - \frac{4}{\epsilon_{n-1} \frac{h}{a}} \tanh \left(\frac{\epsilon_{n-1}}{2} \frac{h}{a} \right) \right] \cdot \quad (66)$$

For rotational excitation the liquid force is, by omitting the part due to gravity,

$$F_y = -m\ddot{\phi} \sum_{n=1}^{\infty} \frac{2 \tanh \kappa}{\kappa (\epsilon_{n-1}^2 - 1)} \frac{\frac{g}{\omega_{n-1}^2} + \frac{h}{2} \eta_{n-1}^2 [1 - \frac{4}{\kappa} \tanh(\frac{\kappa}{2})]}{(1 - \eta_{n-1}^2)} \cdot \quad (67)$$

In comparison with equation 57 the force of the mechanical model results, as one would expect, in the same ratios m_n/m and h_n/h . The moment of the ideal liquid will be transformed with the help of the effective moment of inertia I_f for ideal liquid in a completely filled and closed container into the form

$$M_z = -m\ddot{\phi} \left\{ a^2 I_f + \sum_{n=1}^{\infty} \frac{2 \tanh \kappa}{\kappa (\epsilon_{n-1}^2 - 1)} \frac{\left[\frac{g^2}{\eta_{n-1}^2 \omega_{n-1}^4} + \frac{gh}{\omega_{n-1}^2} (1 - \frac{4}{\kappa} \tanh \frac{\kappa}{2}) + \frac{h^2 \eta_{n-1}^2}{4} (1 - \frac{4}{\kappa} \tanh \frac{\kappa}{2})^2 \right]}{(1 - \eta_{n-1}^2)} \right\} \quad (68)$$

This was obtained with the series expansion equation 64. The moment of inertia of the ideal liquid is

$$I_f = ma^2 \left\{ \frac{1}{12} \left(\frac{h}{a} \right)^2 + \frac{1}{4} - 8 \sum_{n=1}^{\infty} \frac{[1 - \frac{2}{\kappa} \tanh(\frac{\kappa}{2})]}{\epsilon_{n-1}^2 (\epsilon_{n-1}^2 - 1)} \right\}. \quad (69)$$

The terms in front of the summation represent the moment of inertia of the rigid circular cylinder, while the infinite sum represents the fact that we deal with a liquid. Comparison with the mechanical model must again result in the ratios m_n/m and h_n/h . In the same manner, one can obtain the mechanical values for containers of annular and four-quarter circular cross section. The results of these investigations are given in Table 5.

The magnitude of the modal masses and their locations depend only on the geometry of the container. Thus, one will expect that the influence of the liquid propellant upon the stability of the total vehicle will be mainly determined by the tank geometry. Since the liquid nearly always sloshes in the vicinity of the free fluid surface, the absolute magnitude of the modal masses at moderate fluid heights ($(h/a) > 2$) would be independent of the filling. With increasing Eigen frequency, the disturbances penetrate less deeply into the liquid. This means that the modal masses of higher sloshing modes approach more and more the free fluid surface (Fig. 17). For decreasing fluid heights, the location of the modal mass shifts to the immediate vicinity of the center of gravity of the liquid.

The mass ratio m_n/m increases with decreasing liquid height, h ; that is, in long containers where the ratio of fluid heights to container radius is large, only a small amount of the total liquid participates in the oscillation. In short tanks, a larger amount of the liquid oscillates (Fig. 18). Figure 17 and equation 63 show that for containers with circular cross section, the first modal mass represents the main part of the oscillating mass. In a circular cylindrical tank, the mass of the second sloshing mode is usually less than 3 per cent of the first mode. Only for small liquid heights ($(h/a) < 1$), the second modal mass will reach a value of 8.4 per cent of that of the first. At this point, one must prove that the free surface displacement at the tank wall is always smaller than the liquid height, since otherwise the solutions will no longer be valid. In the container of annular circular cross section, the magnitude of the modal mass depends also on the diameter ratio. In the most unfavorable case of $k = (b/a) \approx 0.45$, the mass of the second sloshing mode is about 12 per cent of that of the first one. Again, we can conclude from this that, for stability investigations, the masses of higher sloshing modes, which are usually well separated from critical frequencies of the space vehicle, can be neglected. For four-quarter tanks, the situation is different, since due to the tank geometry, other vibration modes appear. Figure 19 shows that the mass of the consecutive sloshing mode still represents 43 per cent of the first one, indicating that in stability investigations this second mode can no longer be neglected. A comparison

of the three main container forms now shows clearly that the masses of the sloshing modes are definitely influenced by the geometry of the tanks. A comparison of the magnitudes of the oscillating modal masses shows that a propellant container with a circular cross section is the least favorable one. Here the oscillating mass is about $1.43 \bar{\rho} a^3$. By separating the tanks with inner tank walls the oscillating mass can be reduced in two ways. By choosing a concentric wall with half the tank diameter ($k = 0.5$), one obtains for the modal mass a value of about $0.96 \bar{\rho} a^3$ if only the outer tank is filled, and $1.14 \bar{\rho} a^3$ if both tanks are filled. Here one should notice that the phase relations of the propellant in these two tanks in the important frequency range decrease the effective mass rather than increase it. A much more favorable situation is obtained by subdivision of the tank with radial walls, for instance, by subdividing into four-quarter tanks. Here the modal mass belonging to the first Eigen frequency is only $0.46 \bar{\rho} a^3$; that is, it is only about a third of the value of the circular cylindrical tank. If all modal masses in the four-quarter tank arrangement were added and the sum were compared with the circular cylindrical tank, it would only total about half of the mass. It can be concluded that subdivision of tanks into sector tanks has great advantage with respect to the prevention of the effect of propellant sloshing upon the stability of the total vehicle. Furthermore, it has the advantage that the vibrating masses are distributed to various sloshing modes. This means they have their largest influence at different frequencies.

The non-oscillating mass m_0 is located a little below the center of gravity of the liquid (Fig. 20). The spring constant k_n is given by the equation $k_n = \omega_{n-1}^2 m_n$. The moment of inertia of the disc for containers with circular and annular cross section is given in Figure 21. For decreasing liquid height, the moment of inertia increases with decreasing diameter ratio.

After the introduction of the linear damping terms into the mechanical model, damping can be introduced into the theory of liquid motion. In the solution of the mechanical model, we have introduced in place of the resonance terms $(1 - \eta_{n-1}^2)$ the values $(1 - \eta_{n-1}^2 + 2i\gamma_n \eta_{n-1})$. Performing this with the formulas of the results of the ideal liquid (62), (65), (67), and (68), one obtains the results for the damped liquid motion. In Figure 22, the magnification function, $|F_y/y_0|$, of the force for the translatory excitation is given with the damping factor γ_n as a parameter. The parabola is the force if we consider the liquid as rigid. From there, it can be seen that, in the first resonance, very large forces can appear and that they are a multiple of the inertial force. Figure 23 shows the phase of the force. Introducing the experimental results into these figures will lead to the equivalent linear damping coefficients by comparison with the theoretical curves. Other possibilities for determination of the damping can be obtained by measuring the surface displacement, pressure distribution, and the moments and their phases (Fig. 24 and 25). With these, we obtain the same results as with the force measurements. The free surface displacement measurement will be obtained at the tank walls in the plane of excitation.

Another method, which represents an approximate determination of the damping directly from the experimental results, can also be applied. Since we are particularly interested in the magnitude in the vicinity of the first resonance, we consider the magnification function about the first resonance. Its maximum will be close to the natural frequency if the damping $\gamma_n = \gamma$ is small. The amplitude at the natural frequency is $1/2 \gamma \sqrt{1-\gamma^2}$ which for small damping can be approximated by $1/2 \gamma$. Since the damping factor not only depends on the maximum height of the magnification function but also on its width, one chooses on the response curve at the height $1/2 \gamma \sqrt{2}$ the points P_1 and P_2 for which

$$\frac{1}{2\gamma\sqrt{2}} = \frac{\eta^2}{\sqrt{(1-\eta^2)^2 + 4\gamma^2\eta^2}},$$

(Fig. 26). This is a biquadratic equation for which η_1 and η_2 can be determined. It is $\eta_2 - \eta_1 = \Delta\eta \approx 2\gamma$. The results obtained in this manner are in agreement with those obtained from the measured experimental values as read off from the theoretical curves.

An experimental program using a 105-inch diameter container yielded the following:

- a. Theoretical results have been verified.
- b. Approximate values for the equivalent damping of the liquid have been obtained.
- c. The efficiency of various damping devices has been determined.
- d. The effect of the difference of the viscosities of the conventional propellants compared with the viscosity of water could be neglected.

The container is mounted on a carriage which was excited harmonically with constant amplitude (Fig. 27 and 28). The nearly conical tank bottom part is substituted in the theoretical investigations by an equivalent circular cylinder whose length is determined by the volume of the conical part. The forced frequency is varied up to 1.9 cycles. Since the viscosity of the conventional propellants is similar to that of water and does not show an important influence, water was used for the experiments.

With these results, the damping of the modal masses can be determined. Only the moment of inertia and the damping of the disc are missing. For these we go back to equations (52) and (53) and set the displacement y_n of the modal masses m_n equal to zero; that is, we consider the completely closed container. With the formula of the moment (58), the effective moment of inertia, $I_{f, \sim}$ of the liquid, which is given for ideal liquid by the formula (69), will be substituted by I_f . Furthermore, there is an additional term due to the damping of the liquid in the completely closed container which is of the form $\bar{c} \dot{\phi}$, as can be concluded by the comparison with the moment of the mechani-

cal model (61). The values, \bar{I}_f and \bar{c} , will be obtained by torsion spring experiments of the completely closed fuel container. They depend upon the properties of the liquid, the tank geometry, and the number and size of baffles in the tank. For the determination of the values of the mechanical model, I_d and c_d , we consider the equation (58), which with (60) can be written in this form,

$$\bar{I}_f \ddot{\phi} + \bar{c} \dot{\phi} = 0 .$$

Here

$$\bar{I}_f = I_{\text{rigid}} - \frac{I_d}{1 + (c_d / \Omega I_d)^2}$$

and

$$\bar{c} = \frac{c_d}{1 + (c_d / \Omega I_d)^2} .$$

Once the values \bar{I}_f of the effective moment of inertia and \bar{c} of the effective damping have been experimentally determined, the moment of inertia, I_d , of the disc and the damping coefficient, c_d , can be obtained. One determines from the above equations

$$I_d = I_{\text{rigid}} - \bar{I}_f \left[1 + \frac{\bar{c}^2}{\Omega^2 (I_{\text{rigid}} - \bar{I}_f)^2} \right]$$

and

$$c_d = \bar{c} \left[1 + \frac{\bar{c}^2}{\Omega^2 (I_{\text{rigid}} - \bar{I}_f)^2} \right] .$$

For small damping, the term $\bar{c} \dot{\phi}$ in the moment can be omitted and the effective moment of inertia can be assumed to be of the form (69) as obtained by the theory of potential flow. Figure 29 shows the effective moment of inertia for a completely filled and closed container with circular and annular cross section. For small and large fluid heights, the effective moment of inertia approaches the value of a rigid body. For increasing diameter ratio k , the minimum (which is located approximately at a place where the height equals the outer diameter) shifts in direction of larger fluid heights and has a larger value. In the container with circular cross section, it is located at a fluid height $h \approx 1.72a$ and the moment of inertia is only 16 per cent of that of the rigid body. Results of the damping measurements are given in Table 6. There the damping values, which have been obtained from the free surface displacement, have a considerable scatter. This is caused by the disturbed flow field around the baffles. The damping values have been obtained from three different fluid heights: $h_1 = 1.40$ meter, $h_2 = 1.65$ meter, $= 2.70$ meter. At the last two fluid heights, 3-inch wide stiffener rings have been attached in the tank. As one can conclude from the results of the mechanical model, the modal mass for a fluid height, h_1 , is about 42 per cent of the liquid mass, 33 per cent at the fluid height, h_2 , and about 28 per cent for the fluid height, h_3 . This,

of course, has an influence on the results of the damping values. Furthermore, the location and width of the baffle have a decisive influence upon the damping factor.

SECTION IV. INFLUENCE OF PROPELLANT SLOSHING UPON THE STABILITY OF A SPACE VEHICLE

The motion of the liquid propellant in the tanks of a space vehicle represents a potential hazard for stability and control due to its low natural frequencies which are usually very close to the control frequency. The stability of a space vehicle can be tremendously influenced by this propellant sloshing. The possibility of the destabilizing effect of the propellant is investigated by variation of parameters. The propellant motion in the containers will be described by the mechanical model as derived in Section III. The stability boundaries are given by the necessary damping values of the propellant along the vehicle. The influence of tank geometry (which essentially determines the magnitude of the modal masses of the liquid), the influence of the location of the tank, and the influence of the various gain values of the control system are investigated. Also, the influence of additional control elements upon stability will be studied. To simplify the computation, aerodynamic effects and the inertia of the swivel engines will be neglected. As shown in the previous section, the first modal mass of the liquid is sufficient in circular symmetric containers to describe the motion of the propellant; higher modal masses have practically no influence on stability. Only in the four-quarter tank arrangement, the two lower modal masses have to be considered. This seems necessary because the second modal mass can no longer be neglected with respect to the first one.

The control moments will be produced by swivel engines. In the following, a space vehicle is treated with a simple control system and additional control by an accelerometer. The coordinate system has its origin at the center of gravity of the undisturbed space vehicle. The accelerated coordinate system is substituted by an inertial system such that the space vehicle is subjected to an equivalent field of acceleration (Fig. 30). The centrifugal and Coriolis forces, which result from a rotation, will be neglected. Furthermore, the acceleration in direction of the trajectory, the mass, and the moment of inertia will be considered constant. The following investigations are restricted to the interaction of translatory, y , and rotational motion, φ , as well as the propellant oscillations, y_n , and bending vibrations, η_n , in the plane. For simplification, the so-called disc motion is omitted. It is assumed that only half of the thrust is available for control purposes. In the numerical procedure, the bending vibrations will not be treated.

A. EQUATIONS OF MOTION

The equation of motion perpendicular to the trajectory is with m as the total mass of the space vehicle, m_λ as the modal mass of the propellant, φ as the deviation of the attitude angle, F the thrust, and β as the swivel angle:

$$m\ddot{y} + \sum_{\lambda} m_{\lambda} \ddot{y}_{\lambda} - F\varphi - \frac{F}{2} \beta + F \sum_{\nu} \eta_{\nu} Y'_{E\nu} = 0. \quad (70)$$

The factor 1/2 in the control term is there because only half of the thrust is available for control purposes. The displacement of the modal mass, m_{λ} of the propellant with respect to the tank wall is denoted by y_{λ} . The transversal displacement of the space vehicle from its trajectory is given by y . The last term in the equation represents the generalized translatory force of the thrust with respect to bending. The term η_{ν} denotes the generalized bending coordinate of the ν th bending mode, and $Y'_{E\nu}$ represents the slope of that mode at the swivel point of the engines.

In the containers in which the sloshing is not considered, the mass of the structure and the propellant being considered as rigid is denoted by m' per unit length. I'_0 is the moment of inertia of the structure about the center of gravity of the cross section, $m_{o\lambda}$ is the nonsloshing mass of the liquid in the container λ , and $x_{o\lambda}$ is its distance from the center of gravity. Furthermore, $I_{o\lambda}$ is the moment of inertia of the nonsloshing mass about its center of gravity and x_{λ} is the location of the modal masses. Considering I as the effective moment of inertia of the vehicle about its center of gravity, the equation of motion with respect to pitching (with respect to the center of gravity of the vehicle) is obtained

$$I\ddot{\varphi} + \frac{F}{2} x_E \beta + \sum_{\lambda} (m_{\lambda} x_{\lambda} \ddot{y}_{\lambda} - g m_{\lambda} y_{\lambda}) - F \sum_{\nu} (x_E Y'_{E\nu} - Y_{E\nu}) \eta_{\nu} = 0. \quad (71)$$

Here, it is

$$I = \int (x^2 m'_a + I'_0) dx + \sum_{\lambda} (m_{o\lambda} x_{o\lambda}^2 + I_{o\lambda}) + \sum_{\lambda} m_{\lambda} x_{\lambda}^2 \equiv mk^2.$$

The term x_E is the distance of the swivel point of the engines from the origin and k is the radius of gyration of the vehicle. The last term of this equation represents the generalized force of the thrust with respect to bending. $Y_{E\nu}$ is the lateral displacement of the ν th bending mode at the location of the swivel point. In the further treatment, it is useful to refer all length to the radius of gyration $k = \sqrt{I/m}$.

The equation of the modal sloshing mass is

$$\ddot{y}_{\lambda} + 2\omega_{\lambda} \gamma_{\lambda} \dot{y}_{\lambda} + \omega_{\lambda}^2 y_{\lambda} - x_{\lambda} \ddot{\varphi} - g\varphi + \ddot{y} + \sum_{\nu} (Y_{\nu\lambda} \ddot{\eta}_{\nu} + g Y'_{\lambda\nu} \eta_{\nu}) = 0, \quad (72)$$

where λ represents either the number of containers and/or the various modes of the liquid in the containers. The term ω_{λ} represents the natural circular frequency of the

liquid and γ_λ represents the damping factor. The longitudinal acceleration is $g = F/m$. The slope of the ν th bending mode at the location of the modal mass is $Y'_{\nu\lambda}$.

As space vehicles increase in size, the bending frequency approaches more and more the control frequency and the lower Eigen frequencies of the propellant. This indicates that in many cases the bending vibrations can no longer be neglected. The equation of the ν th bending mode is

$$\ddot{\eta}_\nu + \omega_\nu g_\nu \dot{\eta}_\nu + \omega_\nu^2 \eta_\nu + \sum_\lambda \frac{m_\lambda}{M_B} (Y_\lambda \ddot{y}_\lambda + g y_\lambda Y'_\lambda) - \frac{g}{2M_B/m} Y_\nu E^\beta = 0. \quad (73)$$

Here ω_ν represents the natural circular frequency of the ν th bending mode and g_ν the corresponding structural damping, which usually is proportional to the amplitude (restoring force) of the elastic system and in phase with the velocity of the vibration. Here it is represented as linear viscous damping. This was preferred to avoid complex coefficients in the stability polynomial. It is also justified for small damping since the structural damping shows its largest influence only in the vicinity of the bending frequency. The generalized mass, M_B , is

$$M_B = \int m'_a Y_\nu^2 dx + \int I'_o Y_\nu'^2 dx + \sum_\lambda (m_{o\lambda} Y_{o\lambda\nu}^2 + I_{o\lambda} Y_{o\lambda\nu}'^2 + m_\lambda Y_{\lambda\nu}^2),$$

where $Y_{o\lambda\nu}$ and $Y'_{o\lambda\nu}$ represent the displacement and slope of the ν th bending mode at the location of the λ th nonoscillating liquid mass.

Actually, the control equation cannot be written as a linear equation. However, translatory and rotational vibrations usually occur at small frequencies where the control elements can be considered as essentially linear. Nonlinearities usually occur at higher frequencies, as a cause of saturation of amplifiers, and limited output of velocities. Without wind disturbances, the control equation can be written in the form

$$f_1(\beta) = f_2(\varphi, A_i),$$

where f_1 and f_2 are functions depending on the form of the system. In linear form one can write these as

$$\sum_\nu p_\nu \beta^{(\nu)} = \sum_\nu a_\nu \varphi_i^{(\nu)} + g_2 A_i.$$

Here p_ν are the so-called phase lag coefficients, and φ_i is the indicated deviation from the trajectory as indicated by the gyro. A_i represents the indicated acceleration normal to the longitudinal axis of the vehicle. It is:

$$\varphi_i = \varphi - \sum_\nu \eta_\nu Y'_{\nu G},$$

where $Y'_{\nu G}$ is the slope of the ν th bending mode at the location of the gyro. For a rigid space vehicle where the elastic behavior of the structure is neglected, it is sufficient to use

$$\beta = a_0 \varphi + a_1 \dot{\varphi} + g_2 A_i \quad (74)$$

Here the last term with a gain value g_2 is proportional to the indicated acceleration perpendicular to the longitudinal axis of the vehicle and is obtained by a measurement with the help of an accelerometer. The term g_2 is a measure of the strength with which the accelerometer influences the control system. In this form of the control equation, the time derivatives of the control angle, β , which with increasing frequency, cause increasing phase lags, have been neglected. This is justified because of the small magnitude of control and propellant frequencies.

The accelerometer is described by the equation

$$\frac{\ddot{A}_i}{\omega_a^2} + \frac{2\zeta_a}{\omega_a} \dot{A}_i + A_i = \ddot{y} - x_a \ddot{\varphi} - g\varphi + \sum_{\nu} (\ddot{\eta}_{\nu} Y_{\nu a} + g\eta_{\nu} Y'_{\nu a}) \quad (75)$$

Here ω_a is the natural circular frequency of the accelerometer, ζ_a its damping factor, and x_a its location. The displacement, $Y_{\nu a}$, of the ν th bending mode at the accelerometer location will be set equal to zero if a rigid space vehicle is considered. For an ideal accelerometer it is $\omega_a \gg 1$ and for a rigid space vehicle, the equation of the accelerometer is simplified to

$$A_i = \ddot{y} - x_a \ddot{\varphi} - g\varphi \quad (76)$$

B. STABILITY BOUNDARIES OF A SPACE VEHICLE WITH A SIMPLE CONTROL SYSTEM

To obtain the main results of the influence of the propellant sloshing on the stability with minimum numerical effort, we will first treat the equations of motion and the propellant as free to oscillate in one tank only. This is justified in many vehicles, since the propellant masses in the other tanks are sometimes considerably smaller. It is also justified in the same way for the Saturn vehicle whose booster tanks consist of many containers with smaller diameters. Here, the sum of these sloshing masses is relatively below the one of the large second stage tank. Sometimes for tanks with lighter propellant (such as liquid hydrogen) whose density is only a fraction of that of liquid oxygen, its modal mass, compared with the heavy propellant, can be neglected. Furthermore, we will consider the space vehicle as rigid ($\eta_{\nu} = 0$). If one introduces the value $\eta_{\nu} = 0$ into equations 70, 71, 72, 74 and 75 and chooses only one equation, 72, we obtain the equations of motion of a rigid space vehicle with additional control by an accelerometer. With the usual assumption for solution of the form $e^{s\omega_c t}$, where s is the complex frequency $s = \sigma + i\omega$, the differential equations are transformed into

homogeneous algebraic equations.

$$\begin{vmatrix}
 y & \varphi & y_s & A_i \\
 s^2 \omega_c^2 & -g \left(1 + \frac{a_0}{2} + \frac{a_1}{2} s \omega_c \right) & \mu s^2 \omega_c^2 & -\frac{\lambda}{2} \\
 0 & s^2 \omega_c^2 + \frac{g x_E}{2k^2} (a_0 + a_1 s \omega_c) & -\frac{\mu}{k^2} (x_s \omega_c^2 s^2 + g) & \frac{\lambda x_E}{2k^2} \\
 s^2 \omega_c^2 & -(x_s \omega_c^2 s^2 + g) & \omega_c^2 s^2 + 2\omega_c \omega_s \gamma_s s + \omega_s^2 & 0 \\
 -s^2 \omega_c^2 & (x_a \omega_c^2 s^2 + g) & 0 & \frac{s^2 \omega_c^2}{\omega_a^2} + \frac{2\xi_a \omega_c s}{\omega_a} + 1
 \end{vmatrix} = 0 \quad (77)$$

Here, $\lambda = gg_2$ and $\mu = m_s/m$ is the ratio of the sloshing mass in the container to the total mass of the vehicle. For nontrivial solutions, the coefficient determinant 77 with which we obtain the characteristic polynomial in s must vanish.

$$\sum_{i=0}^6 B_i s^i = 0.$$

The coefficients, B_i , are represented as polynomials of ξ_s and γ_s and are

$$\begin{aligned}
 B_6 &= k_{17} + k_{18} \xi_s^2 \\
 B_5 &= k_{13} + 2k_{14} \gamma_s + k_{15} \xi_s + k_{16} \xi_s^2 \\
 B_4 &= k_9 + 2k_{10} \gamma_s + k_{11} \xi_s + k_{12} \xi_s^2 \\
 B_3 &= k_6 + 2k_7 \gamma_s + k_8 \xi_s \\
 B_2 &= k_3 + 2k_4 \gamma_s + k_5 \xi_s \\
 B_1 &= k_1 + 2k_2 \gamma_s \\
 B_0 &= k_0.
 \end{aligned} \quad (78)$$

Here the location of the modal mass, $\xi_s = x_s/k$, (with respect to the center of gravity) and the damping factor, γ_s , are extracted since they are the ones with which the stability of the vehicle can be influenced. The representation of the stability boundaries

will be in these coordinates. It presents not only the magnitude of the required damping in the tanks, but also its location. The abbreviations k_j ($j=0, 1, 2, \dots, 18$) depend on the frequency and damping factors, and gain values of the control system, as well as on the mass ratio, μ , and the vibrational characteristics of the accelerometer. With the notations ζ_c as the damping factor of the control system, ω_c as the circular frequency of the control system, $\omega_c^2 = \omega_{co}^2 / (1 - \frac{\lambda}{2} - \lambda x_E x_a / 2k^2)$ and ω_{co} as the circular frequency of the control system without accelerometer ($\omega_{co}^2 = g x_E a_o / 2k^2$) and $\xi_E = x_E / k$, $\xi_a = x_a / k$ as the distance with respect to the radius of gyration, and $\nu_s = \omega_s / \omega_c$, $\nu_a = \omega_a / \omega_c$ as the ratios of the Eigen frequencies and the value $\Lambda = 1 - \frac{\lambda}{2} (1 + \xi_E \xi_a)$ the coefficients k_j are with

$$a_1 = \frac{2 \zeta_c a_o}{\omega_c}, \frac{g x_E a_1}{2k^2} = 2 \zeta_c \omega_c \left(1 - \frac{\lambda}{2} - \frac{\lambda}{2} x_E x_a\right) \quad (79)$$

$$k_0 = \Lambda \left[\nu_s^2 + \frac{2\mu \Lambda}{a_o \xi_E^2} \right]$$

$$k_1 = 2\Lambda \left(\zeta_c + \frac{\xi_a}{\nu_a} \right) \left[\frac{2\mu \Lambda}{a_o \xi_E^2} + \nu_s^2 \right]; \quad k_2 = \Lambda \nu_s$$

$$k_3 = \Lambda \left\{ \frac{1}{\nu_a} \left(\frac{1}{\nu_a} + 4\zeta_c \xi_a \right) \left(\frac{2\mu \Lambda}{a_o \xi_E^2} + 1 \right) + 1 - \mu + \nu_s^2 - \frac{\mu \lambda \xi_a}{a_o \xi_E} \right\} \quad (80)$$

$$k_4 = 2\nu_s \Lambda \left(\zeta_c + \frac{\xi_a}{\nu_a} \right), \quad k_5 = \frac{\mu \Lambda}{a_o \xi_E} (a_o^{-2+\lambda})$$

$$k_6 = 2\zeta_c \frac{\nu_s^2}{a \nu_a} + \Lambda \left\{ \frac{4\mu \zeta_c \Lambda}{a_o \xi_E^2 \nu_a^2} + 2(1-\mu) \frac{\xi_a}{\nu_a} + 2\zeta_c \left(1 - \mu + \frac{\nu_s^2}{\nu_a^2} \right) \right\}$$

$$k_7 = \Lambda \left\{ \nu_s + 4\zeta_c \xi_a \frac{\nu_s}{\nu_a} + \frac{\nu_s}{\nu_a^2} \right\}, \quad k_8 = \frac{2\mu \Lambda}{\nu_a \xi_E} \left\{ \zeta_c \nu_a + \xi_a - \frac{2\zeta_a}{a_o} \right\}$$

$$k_9 = \frac{\nu_s^2}{\nu_a^2} - \frac{\lambda}{2} \mu + \frac{\Lambda(1-\mu)}{\nu_a^2} [1 + 4\zeta_c \xi_a \nu_a + \nu_a^2]$$

$$k_{10} = \frac{2\nu_s}{\nu_a^2} [\zeta_c \Lambda + \xi_a \nu_a], \quad k_{11} = \frac{\Lambda \mu}{\xi_E a_o \nu_a^2} [a_o + 4\zeta_c \xi_a a_o \nu_a - 2] - \frac{\mu \lambda}{2} (\xi_E + \xi_a)$$

$$k_{12} = \mu \left(\frac{\lambda}{2} - 1 \right), \quad k_{13} = \frac{2(1-\mu)}{\nu_a^2} [\zeta_a \nu_a + \zeta_c \Lambda], \quad k_{14} = \frac{\nu_s}{\nu_a^2}$$

$$k_{15} = \frac{2\mu \Lambda \zeta_c}{\xi_a \nu_a^2}, \quad k_{16} = -\frac{2\mu \xi_a}{\nu_a}, \quad k_{17} = \frac{1-\mu}{\nu_a^2}, \quad k_{18} = -\frac{\mu}{\nu_a^2}.$$

The parameters are as follows:

- a. $\mu = m_s/m =$ ratio of modal mass of liquid over total mass of space vehicles
- b. $\zeta_c =$ control damping factor
- c. $\nu_s = \omega_s/\omega_c =$ frequency ratio of undamped propellant frequency to undamped control frequency
- d. $\gamma_s =$ damping factor of propellant
- e. $\nu_a = \omega_a/\omega_c =$ frequency ratio of undamped accelerometer frequency to undamped control frequency.
- f. $\zeta_a =$ damping factor of accelerometer
- g. $\lambda = gg_2 =$ product of longitudinal accelerometer of the vehicle and gain value of the accelerometer
- h. $\xi_a = x_a/k =$ ratio of the coordinate of the accelerometer location to radius of gyration of the space vehicle
- i. $\xi_s = x_s/k =$ ratio of the coordinate of the location of the modal mass of the propellant to radius of gyration of the space vehicle, and
- j. $a_o =$ gain value of the attitude control system.

The stability boundaries are characterized by the roots s of which at least for one the real part will be zero, while the others are stable roots. This is with Hurwitz theorem for a stability polynomial of the n th degree

$$B_n = 0, \quad H_{n-1} = 0$$

where H_{n-1} represents the Hurwitz determinant of the form

$$H_{n-1} = \begin{vmatrix} B_1 & B_3 & B_5 & \dots\dots\dots \\ B_0 & B_2 & B_4 & \dots\dots\dots \\ 0 & B_1 & B_3 & \dots\dots\dots \\ 0 & B_0 & B_2 & \dots\dots\dots \\ \dots\dots\dots \end{vmatrix} \quad (n-1) \text{ lines and columns}$$

Representing the stability boundaries in the (ξ_s, γ_s) - plane, the Hurwitz determinant $H_5 = 0$ results in

$$\sum_{j=0}^5 C_j(\xi_s) \gamma_s^j = 0, \quad (81)$$

where the functions $C_j(\xi_s)$ are polynomials in ξ_s . $C_0(\xi_s) = 0$ is the stability boundary for the undamped liquid. It represents the intersection points with the ξ_s -axis. For all points (ξ_s, γ_s) above the stability boundary, one obtains stability. Because of $B_n = 0$, the stability is interrupted at the left and at the right. This means that only within these boundaries stability is guaranteed. From $B_6 = 0$ it is recognized that the corresponding stability boundaries to the right and left are given in the form of straight lines perpendicular to the ξ_s -axis. It is

$$\xi_s = \pm \sqrt{-\frac{k_{17}}{k_{18}}} = \pm \frac{\sqrt{1-\mu}}{\mu} \quad (82)$$

For most vehicles, these boundaries play no practical role. Substitution of $\xi_s = \gamma_s = 0$ into the Hurwitz determinants determines whether the origin is in the stable or instable region. A necessary and sufficient condition for stability is [15]:

a. The coefficients

$$B_n, B_{n-1}, B_{n-3}, \dots > 0$$

$$B_1, B_0 > 0 \text{ for even } n$$

$$B_0 > 0 \text{ for odd } n$$

b. The Hurwitz determinant

$$H_{n-1}, H_{n-3}, \dots > 0$$

$$H_3 > 0 \text{ if } n \text{ is even}$$

$$H_2 > 0 \text{ if } n \text{ is odd}$$

In the numerical evaluation, the distance of the swivel point from the center of gravity of the vehicle was chosen, $x_E = 12.5$ -meters and the radius of gyration $k = 12.5$ meters. The total length of the space vehicle is 56.5-meters. If an accelerometer was used for additional control its location was at $x_a = -6$ meters (in front of the center of gravity).

1. Rigid Space Vehicle Without Accelerometer Control. Using control without an accelerometer ($\lambda = 0$) (a simple attitude control system) results in a stability polynomial of fourth degree. The coefficients B_j would be obtained from (77) and (80) if one introduces $\omega_a = \infty$ and $\lambda = 0$ ($B_6 = B_5 = 0$), the stability boundaries due to $B_n = 0$ again are straight lines, $\xi_s = \pm \sqrt{(1-\mu)}$. The stability boundary from the Hurwitz

determinant $H_{n-1} = 0$ (here $H_3 = 0$ or $B_1 B_2 B_3 = B_2 B_3^2 + B_1^2 B_4$) is

$$(K_1 + K_2 \xi_s + K_3 \xi_s^2) + 2\gamma_s (K_4 + K_5 \xi_s + K_6 \xi_s^2) + 4\gamma_s^2 (K_7 + K_8 \xi_s + K_9 \xi_s^2) + 8\gamma_s^3 = 0, \quad (83)$$

where

$$K_1 = k_1 k_3 k_6 - k_1^2 k_9 - k_0 k_6^2$$

$$K_2 = k_1 k_5 k_6 + k_1 k_3 k_8 - 2k_0 k_6 k_8 - k_1^2 k_{10}$$

$$K_3 = k_1 k_5 k_8 - k_0 k_8^2 - k_1^2 k_{11}$$

$$K_4 = k_1 k_4 k_6 + k_2 k_3 k_6 + k_1 k_3 k_9 - 2k_0 k_6 k_7 - 2k_1 k_2 k_9$$

$$K_5 = k_2 k_5 k_6 + k_1 k_5 k_7 + k_1 k_4 k_8 + k_2 k_3 k_8 - 2k_0 k_1 k_8 - 2k_1 k_2 k_{10}$$

$$K_6 = k_2 k_5 k_8 - 2k_1 k_2 k_{11}$$

$$K_7 = k_2 k_4 k_6 + k_1 k_4 k_7 + k_2 k_3 k_7 - k_0 k_7^2 - k_2^2 k_9$$

$$K_8 = k_2 k_5 k_7 + k_2 k_4 k_8 - k_2^2 k_{10}$$

$$K_9 = k_2^2 k_{11}$$

$$K_{10} = k_2 k_4 k_{11}.$$

The points of intersection of this stability boundary with the ξ_s - axis are obtained by setting $\gamma_s = 0$ and solving the quadratic equation in

$$K_1 + K_2 \xi_s + K_3 \xi_s^2 = 0.$$

The roots

$$\xi_1 = - \left| \xi_d \right|$$

$$\xi_2 = \left| \xi_d \right| (1-\mu) / a_o \nu_s^2,$$

give a first indication for the critical area. Here $1/a_o \nu_s^2$ is considered to be of small magnitude. This assumption is satisfied in most cases if the control frequency is far enough away from the Eigen frequency of the liquid. Therefore, the result expresses that the stability boundary for small values of $1/a_o \nu_s^2$ intersects the ξ_s - axis in the vicinity of the center of gravity (origin) and the instantaneous center of rotation $\xi_d = x_d/k$.

One can see that ξ_2 becomes, due to the factor of $1-\mu$, sensitive to changes of $1/a_0\nu_s^2$. This indicates that for decreasing gain values, a_0 , the intersection point shifts toward the tail of the vehicle. The same behavior occurs if $\nu_s = \omega_s/\omega_c$ decreases. This means that, for decreasing Eigen frequency of the liquid or increasing control frequency, damping must be applied in the aft section of the space vehicle. Figure 31 indicates that the danger zone for instability of the vehicle is located approximately between the center of gravity and the center of instantaneous rotation. In this zone the propellant must be more or less damped, depending on the magnitude of the modal mass of the liquid. For increasing modal mass, not only more damping is needed in the danger zone, but also more damping is required to maintain stability. This is most unfavorable if the control frequency is below the Eigen frequency of the propellant, that is, if $\nu_s < 1.0$. For $\nu_s > 2$, the wall friction ($\gamma_s = 0.01$) is already sufficient to guarantee stability.

The change of the control damping ξ_c indicates that, for increasing subcritical damping $\xi_c < 1$, the stability in the danger zone will be diminished while, for increased supercritical damping $\xi_c > 1$, the stability is enhanced. This means that less damping is necessary in the container to maintain stability in the case $\xi_c > 1$. No additional baffles are required in the danger zone if the mass ratio $\mu = 0.1$, and the control damping $\xi_c \leq 0.5$ or $\xi_c \geq 2.0$. This means that, for these values and the parameters $\nu_s = 2.5$ and $a_0 = 3.5$, the wall friction in the container is sufficient to maintain stability.

Another important question of great interest for the design of a large space vehicle is the choice of the form of the propellant containers. As seen from Sections II and III, the tank geometry plays an important role for the modal masses and the natural frequencies of the propellant. Containers with large diameters exhibit small natural frequencies which are often too close to the control frequency. Of course, the magnitude of the modal mass magnifies considerably this unfavorable effect upon the stability. Clustering of numerous smaller containers not only increases the natural frequencies of the propellant (due to smaller diameters), but also reduces the modal masses which is a much more important effect. In addition to weight saving and the slight increase of the natural frequencies, subdivision of tanks by sector walls has the advantage of distributing the modal masses to different vibration modes of the liquid. To summarize: with increasing mass, stability decreases. The influence of the Eigen frequency change of the propellant with fixed modal mass is such that a decrease of the natural frequency increases the danger zone toward the end of the vehicle and requires more local damping in the propellant. With increasing natural frequency of the liquid, the influence of the propellant sloshing on the stability of the vehicle diminishes more and more. Wall friction is already sufficient to maintain stability.

The gain value, a_0 , of the attitude control system shows, for decreasing magnitude, a decrease of stability in addition to a small enlargement of the danger zone toward the end of the vehicle.

2. Rigid Space Vehicle With Ideal Accelerometer Control. Introducing into the control system an additional control element in the form of an ideal accelerometer ($\omega_a \gg \omega_c$), proper choice of the gain value, g_2 , which determines the influence of the accelerometer in the control system, can minimize the danger zone. This indicates that the possibility of an instability due to the propellant sloshing in a container can be considerably diminished (Fig. 32). Because of $\nu_a \gg 1$, the coefficients of the stability polynomial are $B_6 = B_5 = 0$, and one obtains again a stability polynomial of fourth degree. The same formulas are valid as in the previous case except that in the values, k_j , the appropriate terms with λ have to be considered. The boundaries $B_4 = 0$ are again straight lines,

$$\xi_s = \frac{1}{2\mu(\lambda-2)} \left\{ \mu\lambda(\xi_E + \xi_a) \pm \sqrt{\mu^2\lambda^2(\xi_E + \xi_a)^2 - 16\mu\left(\frac{\lambda}{2} - 1\right) \left[1 - \mu - \frac{\lambda}{2} - \frac{\lambda}{2}(1-\mu)\xi_E \cdot \xi_a\right]} \right\},$$

$$\sqrt{1 - \frac{1}{4\mu^2(\lambda-2)^2} \left\{ \mu\lambda(\xi_E + \xi_a) \pm \sqrt{\mu^2\lambda^2(\xi_E + \xi_a)^2 - 16\mu\left(\frac{\lambda}{2} - 1\right) \left[1 - \mu - \frac{\lambda}{2} - \frac{\lambda}{2}(1-\mu)\xi_a \xi_E\right]} \right\}^2} \quad (84)$$

which are parallel to the γ_s -axis. For values, $\lambda = gg_2 < 1$, the danger zone is located approximately behind the center of instantaneous rotation and shifts with decreasing gain value g_2 toward a zone between the center of gravity and center of instantaneous rotation. The stability decreases, which means more damping in the tank is necessary for increasing $\lambda > 1$. This means that, for stronger influence of the accelerometer in the control system, the danger zone shifts in front of the center of instantaneous rotation and increases with increasing gain value toward the nose of the vehicle. For propellant containers in this location, strong damping must be applied to obtain stability. For values, $\lambda = 1.5$, the vehicle is instable if the tank with 10 per cent slosh mass is located in front of the center of instantaneous rotation, and if no additional baffles are applied. For containers behind the center of instantaneous rotation, the vehicle is stable. Furthermore, one recognizes that $\lambda = 1.0$ represents the most favorable gain value. In this case the danger zone shrinks to a small region around the center of instantaneous rotation.

The change of the other parameters, such as the slosh mass ratio μ , the frequency ratio $\nu_s = \omega_s/\omega_c$, the control system damping ζ_c , as well as the gain value a_0 of the attitude system, exhibits the same influence as the previous case. An enlargement of the danger zone toward the end of the vehicle occurs for large control frequencies and also for small propellant frequencies ($\nu_s < 1$), even in the most favorable case $\lambda = 1.0$. The addition of an accelerometer introduces another important parameter: its location ξ_a . For $\lambda = 1$, the most favorable case for an ideal accelerometer, the influence of its location upon stability of the space vehicle is unimportant. For other values g_2 , the location of the accelerometer has considerable influence upon stability. The strong effect of the accelerometer in the control system ($\lambda > 1.5$) exhibits strong instability if the container is located behind the center of instantaneous rotation with the accelerometer being in front of the center of gravity. Propellant sloshing in those tanks

located in front of the center of instantaneous rotation will make the vehicle unstable if the accelerometer is in front of the center of gravity. For decreasing values $g_2 < 1/g$, the stability behavior of the vehicle approaches that of a rigid vehicle without additional accelerometer control. These results are too optimistic since every accelerometer has its own vibrational characteristics which must be considered.

3. Rigid Space Vehicle With Real Accelerometer Control. The dynamic behavior of an accelerometer, and its natural frequency and damping factor ζ_a , have a non-negligible influence upon the overall stability of the vehicle. From the results of equations 78 and 80, it is recognized that the stability polynomial is of sixth degree. Therefore, the stability boundaries are given by $H_5 = 0$, and $B_6 = 0$ (equations 81 and 82).

The main influence arises from the natural frequency of the accelerometer. In the numerical evaluation, two circular frequencies $\omega_a = 55;12$ rad/sec are considered for the accelerometer. Figure 33 indicates that, for decreasing accelerometer frequency (with a damping factor, $\zeta_a = \sqrt{2}/2$) the danger zone increases from the center of instantaneous rotation toward the end of the vehicle. The influence of increasing liquid mass has the same effect as previously with the exception that it is very much amplified for small Eigen frequencies of the accelerometer; a large amount of damping is required in the container in order to obtain stability of the space vehicle. For the natural frequency of the accelerometer of $\omega_a = 55$ rad/sec, wall friction is already sufficient to maintain stability. For small natural frequencies of the accelerometer, propellant sloshing is even excited. This means that the situation is more unfavorable with an accelerometer than in the case without one. The damping required in such a case would be about three to four times as much as in the case without additional accelerometer control. This indicates that the natural frequency of the accelerometer should be chosen as large as possible. To recognize the influence of the accelerometer characteristics, we consider the effect of the changes of the Eigen frequency, ω_a , the damping factor, ζ_a , and the coordinate of location, x_a , upon the stability of the space vehicle. For increasing natural frequency of the accelerometer $\omega_a < \omega_s$, an increase of the danger zone is obtained, and more damping is required in the container to maintain stability. Above the natural frequency of the propellant, a decrease of the danger zone and enhanced stability can be observed. This means that less damping is required to maintain stability. The larger the frequency ratio $\nu_a/\nu_s = \omega_a/\omega_s$, the less damping is required in the continuously decreasing danger zone. The influence of the frequency, ω_a and the damping factor, ζ_a , of the accelerometer can be seen in Figure 34. The increase of ζ_a enlarges the danger zone and requires more damping in the propellant container. This effect is more pronounced the smaller the Eigen frequency of the accelerometer. From a damping factor ζ_a or greater, which is about twice the critical damping, one recognizes, in the case $\omega_a = 12$ rad/sec, that a further increase of the damping factor decreases the danger zone slightly from the back and slightly enhances the stability. A very important parameter in the design of a control system of a space vehicle is the location, ξ_a , of an additional control element in the form of an accelerometer. The influence of this value can be seen in Figure 35. An accelerometer location behind the center of gravity of the

vehicle must be avoided. Shifting the accelerometer toward the nose of the vehicle enhances the stability. An increase of the control frequency ω_c (Fig. 36) below the natural frequency of the propellant ($\nu_s > 1$) increases the danger zone toward the tail of the vehicle. For $\omega_a = 55$ rad/sec, the required damping in the liquid for maintaining stability of the vehicle is relatively small ($\gamma_s = 0.005$ and less). The influence of the control damping ζ_c is given by the fact that, for increasing subcritical control damping $\zeta_c < 1$, the danger zone decreases and the stability increases, while for supercritical damping $\zeta_c > 1$, the stability becomes more unfavorable (Fig. 37). The influence of the propellant frequency being below the control frequency indicates again the enlarged danger zone which stretches nearly from the center of instantaneous rotation toward the end of the vehicle. Increasing propellant frequency leads to a decreasing danger zone and less required damping. Approaching the Eigen frequency of the accelerometer makes the vehicle more unstable and increases the danger zone toward the end of the vehicle. The gain value, a_0 , has only small influence upon the stability. Its gain growth increases stability slightly and decreases the danger zone some. Of important influence upon stability is the gain value, g_2 , of the accelerometer because it presents the strength of the accelerometer in the control system. Figure 38 exhibits this influence for two accelerometer frequencies. For an Eigen frequency of the accelerometer of $\omega_a = 55$ rad/sec, one recognized similar behavior as in the ideal accelerometer case. For values of $\lambda = 1.5$, an increase of $\lambda = gg_2$ exhibits an increase in stability and decrease of the danger zone between the center of instantaneous rotation and the center of gravity of the vehicle. For further increase of λ , the danger zone shifts in front of the center of instantaneous rotation. With increasing λ , more damping is required in the propellant container in that zone to maintain stability. For an accelerometer with small Eigen frequency, the situation is quite different. For increasing gain value, g_2 , the stability constantly decreases. Here, the influence of the accelerometer favors instability. It not only increases the danger zone toward the end of the vehicle, but it also requires considerably more damping in the tank. It even requires more damping as in the case $\lambda = 0$ (without accelerometer control). From this one can again conclude that large accelerometer frequency is required to stabilize the vehicle with respect to propellant sloshing in the tank. The conclusion can also be made that the danger zone is located between the center of instantaneous rotation and the center of gravity, and that it can be diminished by an additional control element in the form of an accelerometer whose Eigen frequency and location have to be properly chosen. These results are valid only for the rigid vehicle, in which the sloshing propellant mass in one container is much larger than that in the other tanks. With more than one sloshing mass of equal magnitude, the results will probably look different. Furthermore, it has to be mentioned that the bending vibration of the vehicle has an effect on the propellant sloshing as well as on the choice of the accelerometer characteristics and its location. If the control frequency and the first bending frequency are sufficiently separated from each other, then the location of an accelerometer requires negative displacement of the bending modes if the bending modes are normalized at the tail of the vehicle. This indicates, that, for the control of the first two bending modes, an approximate location of the accelerometer in front of the center of gravity is appropriate. This location would also be favorable from

the standpoint of propellant sloshing. From the point of view of rigid body control which restricts the gain values to certain values (Fig. 39), care must be taken.

C. STABILITY BOUNDARIES FOR SPACE VEHICLES WITH TWO CONTAINERS AND SIMPLE CONTROL SYSTEM OR QUARTER TANK ARRANGEMENT

Considering a rigid space vehicle with a simple control system of the form $\beta = a_0 \varphi + a_1 \dot{\varphi}$ and the liquid in two tanks free to oscillate, one has to substitute into the equations 70, 71, and 72 for $\nu = 0$ and $\lambda = 1$ and 2. Introducing again into the thus obtained differential equations the time dependency, $e^{s\omega_c t}$, one obtains for nontrivial solutions the determinant:

$$\begin{vmatrix} s^2 \omega_c^2 & -g - \frac{g}{2} (a_0 + a_1 \omega_c s) & \mu_1 \omega_c^2 s^2 & \mu_2 \omega_c^2 s^2 \\ 0 & s^2 \omega_c^2 + \frac{g x_E}{2k^2} (a_0 + a_1 s \omega_c) & -\frac{\mu_1}{k^2} (x_1 \omega_c^2 s^2 + g) & -\frac{\mu_2}{k^2} (x_2 \omega_c^2 s^2 + g) \\ s^2 \omega_c^2 & - (x_1 \omega_c^2 s^2 + g) & s^2 \omega_c^2 + 2\gamma_1 \omega_c \omega_1 s + \omega_1^2 & 0 \\ s^2 \omega_c^2 & - (x_2 \omega_c^2 s^2 + g) & 0 & \omega_c^2 s^2 + 2\gamma_2 \omega_c \omega_2 s + \omega_2^2 \end{vmatrix} = 0. \quad (85)$$

Here $\mu_1 = m_1/m$ and $\mu_2 = m_2/m$ are the modal masses in the two containers or the first two modal masses in the quarter tank arrangement. The evaluation of the above determinant results in a stability polynomial of the sixth degree. To represent the stability boundaries in the two-dimensional case, the damping factors in the two containers are set to be equal ($\gamma_1 = \gamma_2 = \gamma_s$). Furthermore, one chooses the distance of the rear container (1) to the front container (2) to be of value ℓ . Therefore, it is $x_1 = x_s$, $x_2 = x_s + \ell$. The stability boundaries again are obtained from $H_5 = 0$, $B_6 = 0$. The last condition again represents, in the $(\xi_s - \gamma_s)$ - plane, parallel straight lines to the γ_s - axis which in most cases have no practical meaning. It is when $\xi_\ell = \ell/k$

$$\xi_{1:2} = \frac{\left\{ -\mu_2 \xi_\ell \pm \sqrt{[1 - (\mu_1 + \mu_2)] [\mu_1 + \mu_2 - \mu_1 \mu_2 \xi_\ell^2]} \right\}}{\sqrt{(\mu_1 + \mu_2)^2 - \left\{ -\mu_2 \xi_\ell \pm \sqrt{[1 - (\mu_1 + \mu_2)] [\mu_1 + \mu_2 - \mu_1 \mu_2 \xi_\ell^2]} \right\}^2}}$$

The main purpose of this investigation is to treat two circular cylindrical containers in tandem arrangement with the modal slosh masses being considered approximately equal. Figure 40 gives the results for two containers of equal volume and with a modal mass distance of 4.2-meters. The danger zone as a whole shifts slightly toward the end of the vehicle and the required damping in the containers is approximately the same as that of a vehicle with one container with double the modal slosh mass. The results of the

change of parameters are similar to those in the stability investigation with one propellant container. Enlarging the distance between the two propellant containers, however, one recognizes that the danger zone in which damping has to be provided will shift with nearly unchanged magnitude toward the tail of the vehicle. Furthermore, it indicates that a little less local damping is required. This is an important result because it expresses that - for a multi-stage space vehicle in which the forward modal mass location is constant during first stage flight time and the other mass location is shifting away from this - the entire rear part of the vehicle must be provided with appropriate baffles.

With clustered circular cylindrical containers whose modal masses are at the same height, a considerable reduction of modal propellant masses is obtained as compared to a single circular cylindrical container of equal volume. Furthermore, the natural frequency of the propellant is slightly increased by clustering tanks. For p containers, the natural frequency of the liquid is proportional to the fourth root of the number of containers.

$$\frac{f_n^{(p)}}{f_n^{(1)}} = \sqrt[4]{p} \sqrt{\frac{\tanh'(\epsilon_n \sqrt{p} h/a)}{\tanh'(\epsilon_n h/a)}} \quad (86)$$

The total mass of the propellant reduces proportionally to the reciprocal value of the square root of the number of containers:

$$\frac{m_s^{(p)}}{m_s^{(1)}} = \frac{1}{\sqrt{p}} \frac{\tanh(\epsilon_n \sqrt{p} h/a)}{\tanh(\epsilon_n h/a)} \quad (87)$$

In clustered containers a smaller total mass of the liquid oscillates with higher frequency; that is, μ is smaller and ω_s is a little larger, both enhancing stability. The influence of the various parameters is the same as in the case of one container with a simple control system. Because of structural reasons and due to the increased weight of the containers, the clustering of propellant containers has some disadvantages. Change in tank geometry can minimize the influence of propellant sloshing upon stability; that is, by subdividing the tanks, the magnitude of the modal slosh masses can be reduced and the slosh frequencies can be increased. We consider two possibilities for the subdivision of the circular cylindrical containers. For example, one would expect that by properly using a concentric wall to subdivide a tank, the phase relation of the modal masses in the inner and outer tank could be tuned to minimize the effect of propellant sloshing upon stability. To accomplish this, the magnitude of modal masses in the inner tank and in the annular ring tank should be approximately equal. At a diameter ratio of $k = b/a \approx 0.77$, the modal masses of the two containers are approximately equal. Unfortunately, their frequencies are not very favorable. Therefore, one does not obtain the optimal cancellation of the effect of these two propellant motions. At the

diameter ratio of $k = 0.5$ the phases are very favorable; however, the modal masses working against each other are only of the ratio 1:5. For the diameter ratios $k = 0.3$, 0.5 and 0.7 , the required damping in the containers for maintaining the stability is approximately 12:9.8. The behavior of the various parameters is similar to the case of one container. The other possibility of reducing the influence of propellant sloshing on the stability of the space vehicle is to subdivide the tanks with radial walls. The most important form of a subdivision by sector walls is the four-quarter tank arrangement. In this tank arrangement, the second modal mass of the propellant also must be considered in the treatment of stability. This tank arrangement has the great advantage that only about one-third of the propellant mass oscillates. The second modal mass in the four-quarter tank arrangement is about 43 per cent of that of the first. Therefore, it must be considered in stability investigations. Compared with a space vehicle with circular cylindrical container, a four-quarter tank arrangement requires only half the damping. The overall stability is, therefore, considerably enhanced. The results for the four-quarter tank arrangement can be seen in Figures 41 and 42. For increasing modal mass, more damping is required. Again, the danger zone is located between the center of gravity and the center of instantaneous rotation. Increase of subcritical control damping decreases stability while the increase of supercritical damping increases stability. For increasing control frequency, the danger zone enlarges toward the end of the space vehicle, and a larger local damping is required to maintain stability. The influence of the Eigen frequency of the propellant is similar to the case of a space vehicle with one propellant container. If the natural frequencies of the propellant are below control frequency, the propellant has to be strongly damped in the enlarged danger zone. Small gain values, a_0 , require more baffling in an enlarged danger zone.

SECTION V. CONCLUSION

In the stability consideration of large liquid propelled space vehicles, the influence of propellant sloshing has to be considered in the dynamic treatment. To eliminate instability caused by propellant oscillations, several possibilities can be applied: first, subdivision of the propellant containers in which the oscillating liquid masses are decreased and distributed to different modes, thereby increasing the Eigen frequency of the propellant; second, proper location of the propellant container; third, appropriate choice of the control system, proper choice of gain values and additional control elements; and fourth, introduction of baffles into the liquid to disturb the flow field.

For the determination of the flow field of the propellant in a circular cylindrical ring sector tank, the linearized equations and boundary conditions are treated with the liquid of a free fluid surface. The liquid has been considered incompressible, non-viscous, and irrotational.

The behavior of the liquid in circular cylindrical sector tank containers with circular cross section, annular cross section or one-quarter circular cross section can

be obtained by limit considerations. The natural frequencies of the liquid are indirectly proportional to the square root of the tank diameter and decrease with increasing tank diameter. Furthermore, they increase with the longitudinal acceleration of the space vehicle. The influence upon the Eigen frequencies of the liquid by the tank geometry is exhibited by the value ξ_{mn} . The Eigen values are influenced less by concentric walls but exhibit quite a change if radial walls are introduced in a tank. The influence of the liquid height upon the Eigen frequencies is only noticeable if the liquid height is less than the tank radius. For decreasing liquid heights the natural frequency of the propellant tends toward zero. As in a mechanical vibration system, the magnitude of the surface displacement, the forces and moments of the liquid are increasing with increasing exciting frequency before the first resonance. For a frequency band around the Eigen frequencies of the propellant, violent liquid motion takes place in the container. Behind the resonances the magnification functions decrease again. To introduce a damping into the results of an ideal flow theory a mechanical model (spring-mass system) is derived which describes the motion of the propellant for the stability investigations. By introduction of each vibration mode as an independent degree of freedom, and by comparison of the results of the ideal fluid theory with those of the mechanical model, the spring constants as well as the magnitude and location of the masses of the mechanical model are obtained. Magnitude and location of the masses depend on the container geometry and the liquid height; therefore, the influence of the liquid propellant upon the stability of a space vehicle has been affected by the container geometry. Since the liquid particularly oscillates only in the vicinity of the free fluid surface, the absolute values of the masses for fluid heights larger than the tank diameter are independent of the tank filling. With increasing Eigen frequency the disturbances shift further toward the free fluid surface. The mass ratio of the modal mass to the total liquid mass increases with decreasing fluid height. This ratio indicates that in a long container for which the ratio of the fluid height to the tank diameter is large, only a small amount of the total liquid participates in the propellant sloshing. In short containers a large amount of propellant participates in these vibrations. For decreasing liquid heights the location of the modal mass shifts into the immediate vicinity of the center of gravity of the liquid. The nonvibrating mass is located close to the center of gravity of the liquid. In containers of symmetrical circular cross section, the first modal mass represents the main part of the oscillating propellant. The second modal mass, in the case of a container of circular or annular cross section, represents only 3 per cent, respectively, 12 per cent of the first modal mass. This indicates that for stability investigations these and higher modal masses can be neglected. For a four-quarter tank arrangement the mass of the second mode has to be considered since it represents still 43 per cent of the first modal mass. A decrease of the modal masses can, obviously be performed by subdividing the container using radial and concentric walls. It has been shown that the subdivision by radial walls is much more effective. In the case of four-quarter containers the vibrating liquid mass is reduced to more than half of that of a cylindrical container of circular cross section. Another advantage is exhibited by the fact that the vibrating masses are distributed to various vibrating modes and the Eigen frequency is slightly increased.

The nonlinear damping of the liquid is introduced into the forced vibrations as equivalent linear damping, which is determined by experiments.

For the determination of the magnitude and location of the required damping in the containers, one treats the stability of the vehicle by considering the equations of motion for translation, pitching about the center of gravity of the vehicle, the oscillating propellant and the control system. With the usual solution in the form of $e^{s\omega_c t}$, the characteristic polynomial is obtained and is treated with the Hurwitz criterion. Here the stability boundaries are best determined in terms of the location of the modal masses and the damping factor of the propellant liquid. Not only the magnitude of the damping, but also its location, is obtained.

The results of the investigation of a rigid space vehicle with a simple control system and one propellant container in which the liquid is considered to oscillate, show that along the vehicle a danger zone for instabilities appears. This is located between the center of gravity and the center of instantaneous rotation. In this location the propellant must be more or less damped according to the magnitude of the modal mass of the propellant. To avoid this, the container with large modal mass should be located behind the center of gravity. If the natural frequencies of the propellant are in the proximity of the control frequency, which is sometimes the case with large containers, then the danger zone increases further behind the center of gravity toward the end of the vehicle. Therefore, the Eigen frequencies of the propellant should be as far above the control frequency as possible. The change of the control system damping exhibits, with increasing subcritical damping, a decrease in stability, and with increasing supercritical damping, enhanced stability in the danger zone. Decrease of the attitude control value, a_0 , results in a small decrease in stability.

The introduction of an accelerometer as an additional control element into the control system can enhance the stability considerably if the vibrational characteristics, the location of the accelerometer, and its gain value are chosen appropriately.

Here the location, the Eigen frequency, and the gain value of the accelerometer play an important role. With properly chosen accelerometer characteristics, the danger zone can be reduced to a small region about the center of instantaneous rotation. If the gain value of the accelerometer is smaller, the danger zone expands into the direction of the center of gravity. If it is too large, the danger zone shifts in front of the center of instantaneous rotation and requires comparatively large damping in the propellant containers. Here the accelerometer is located in front of the center of gravity and its natural frequency is appropriately separated from the control frequency. If the latter is not the case, the propellant sloshing is excited and strong damping is required in the tanks. The mounting of an accelerometer behind the center of gravity must be avoided. Increasing damping factor of the accelerometer requires more damping in the containers located in the danger zone.

With two containers in the tandem tank arrangement, the danger zone shifts with increasing distance of the modal masses toward the end of the space vehicle. With increasing flight time, the distance of the modal masses increases (which takes place during the draining of the first stage containers). Therefore, the total rear part of the vehicle has to be provided with appropriate damping in order to maintain stability.

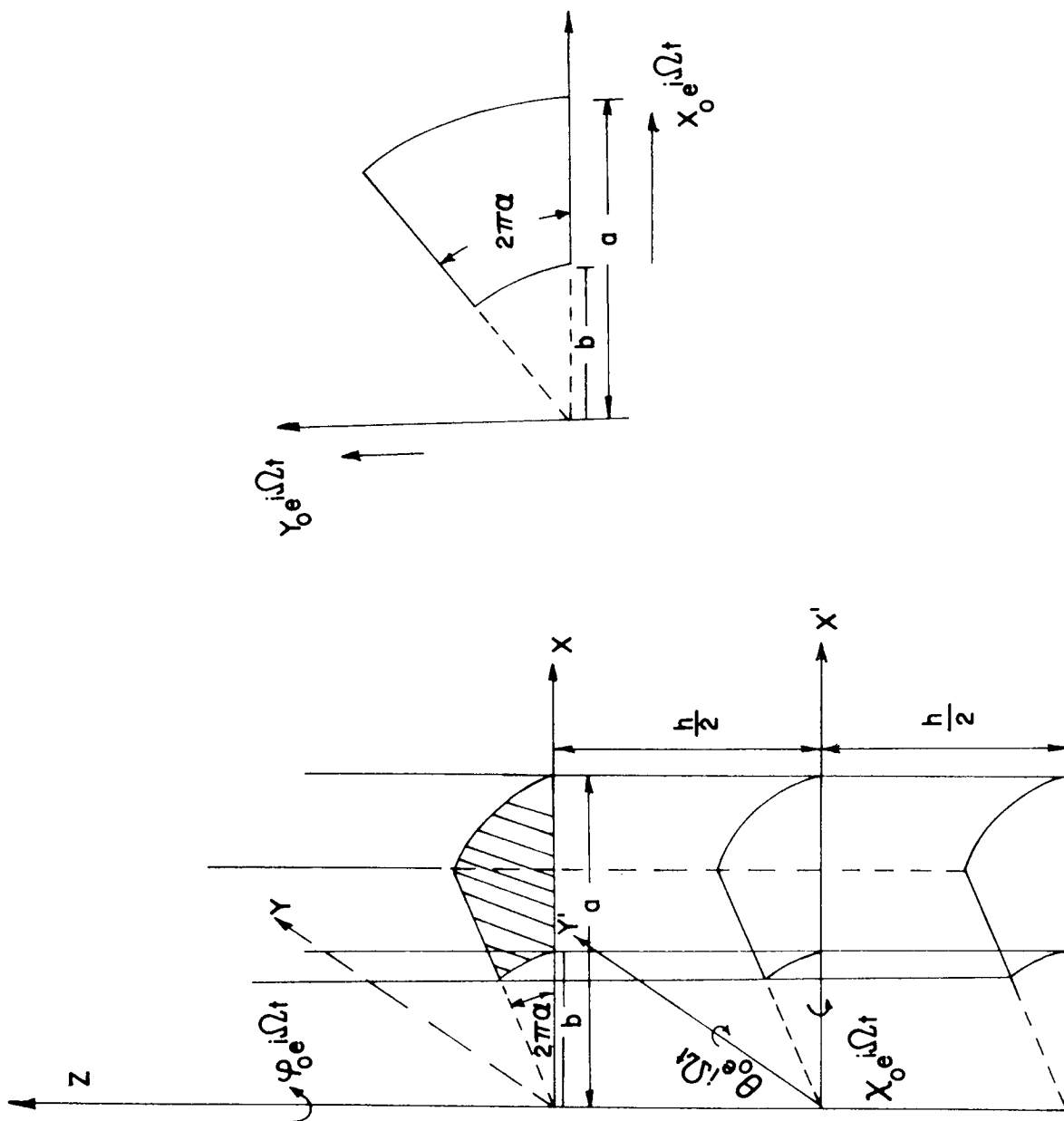


FIGURE 1. COORDINATE SYSTEM AND TANK GEOMETRY

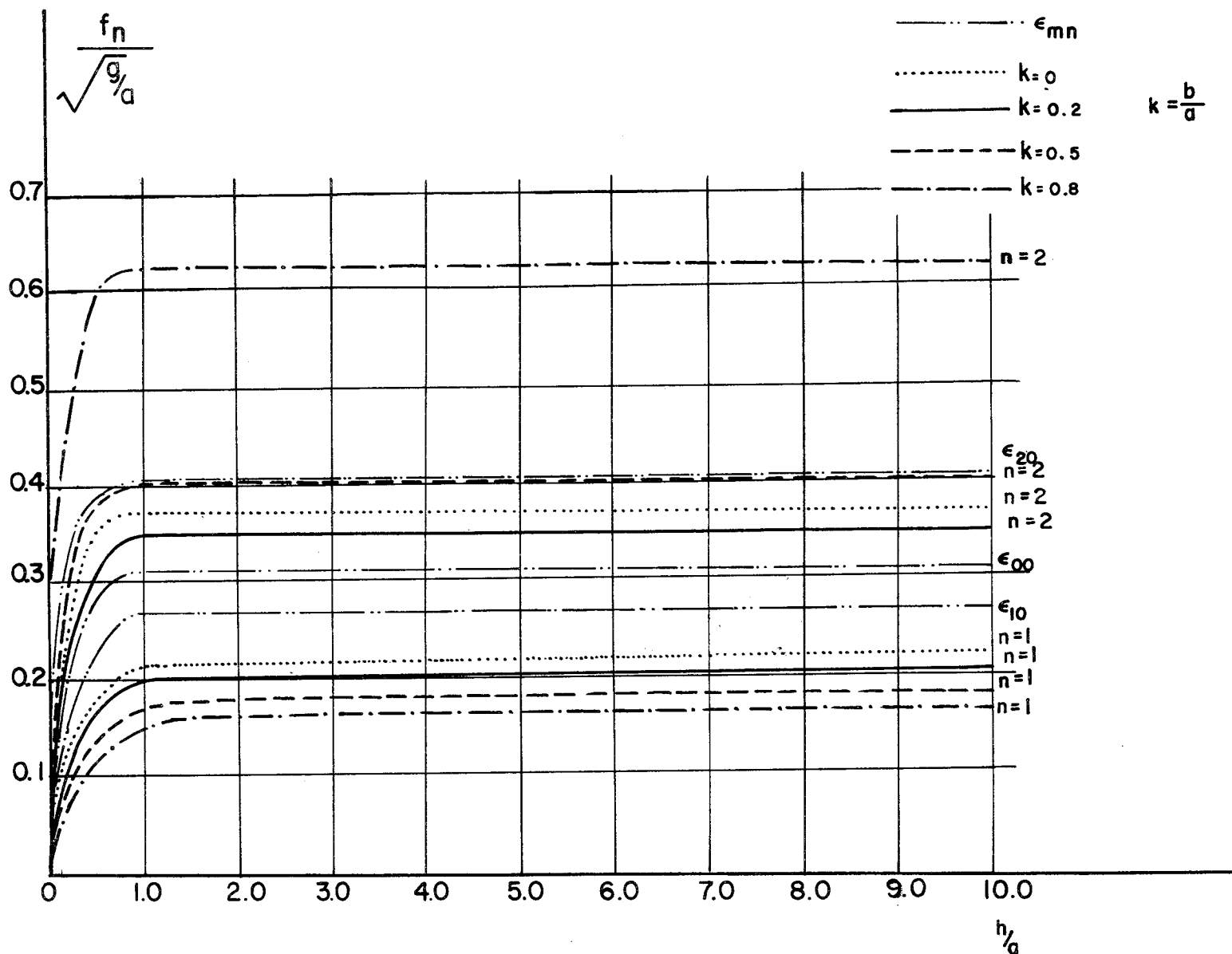
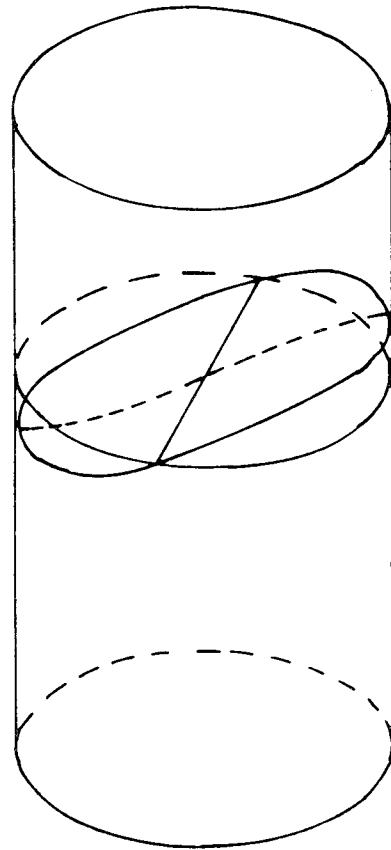
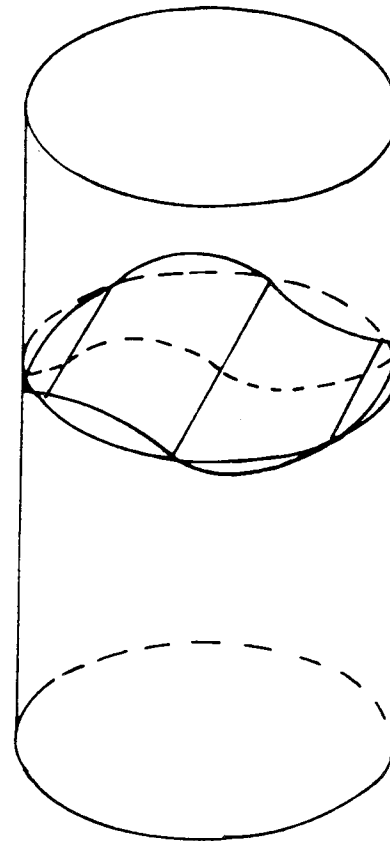


FIGURE 2. EIGEN FREQUENCY PARAMETER FOR CONTAINERS OF CIRCULAR, ANNULAR AND QUARTER-CIRCULAR CROSS SECTION (ξ_{mn})



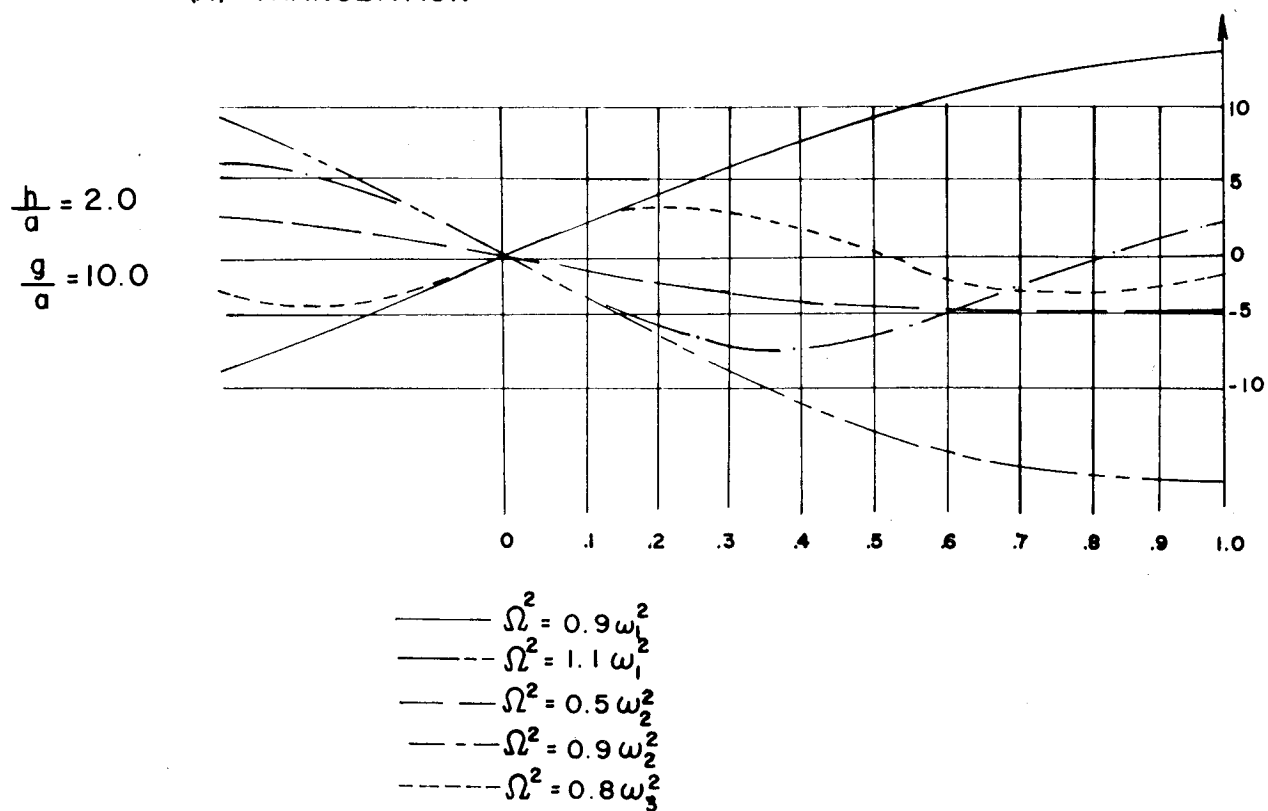
BEFORE FIRST RESONANCE



AFTER FIRST RESONANCE

FIGURE 3. WAVE FORM OF FREE FLUID SURFACE BEFORE FIRST AND SECOND RESONANCE

(A) TRANSLATION



(B) ROTATION

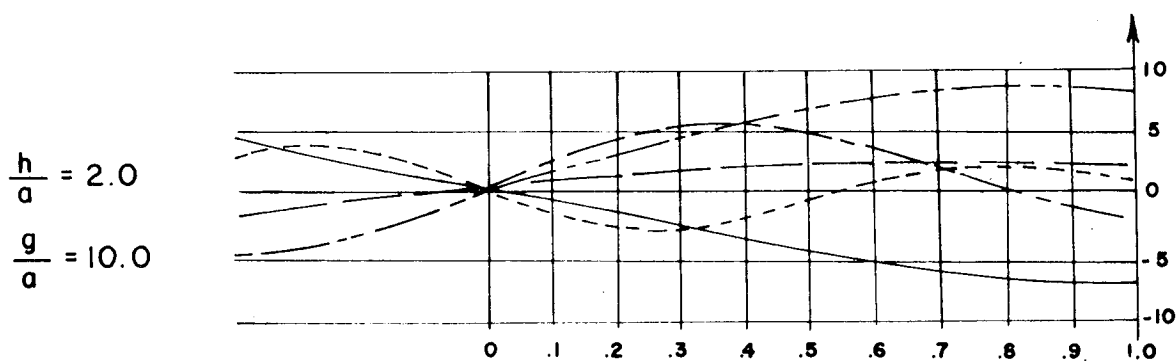


FIGURE 4. FREE SURFACE DISPLACEMENT FOR VARIOUS EXCITATION FREQUENCY RATIOS (IN CIRCULAR CYLINDRICAL CONTAINER)

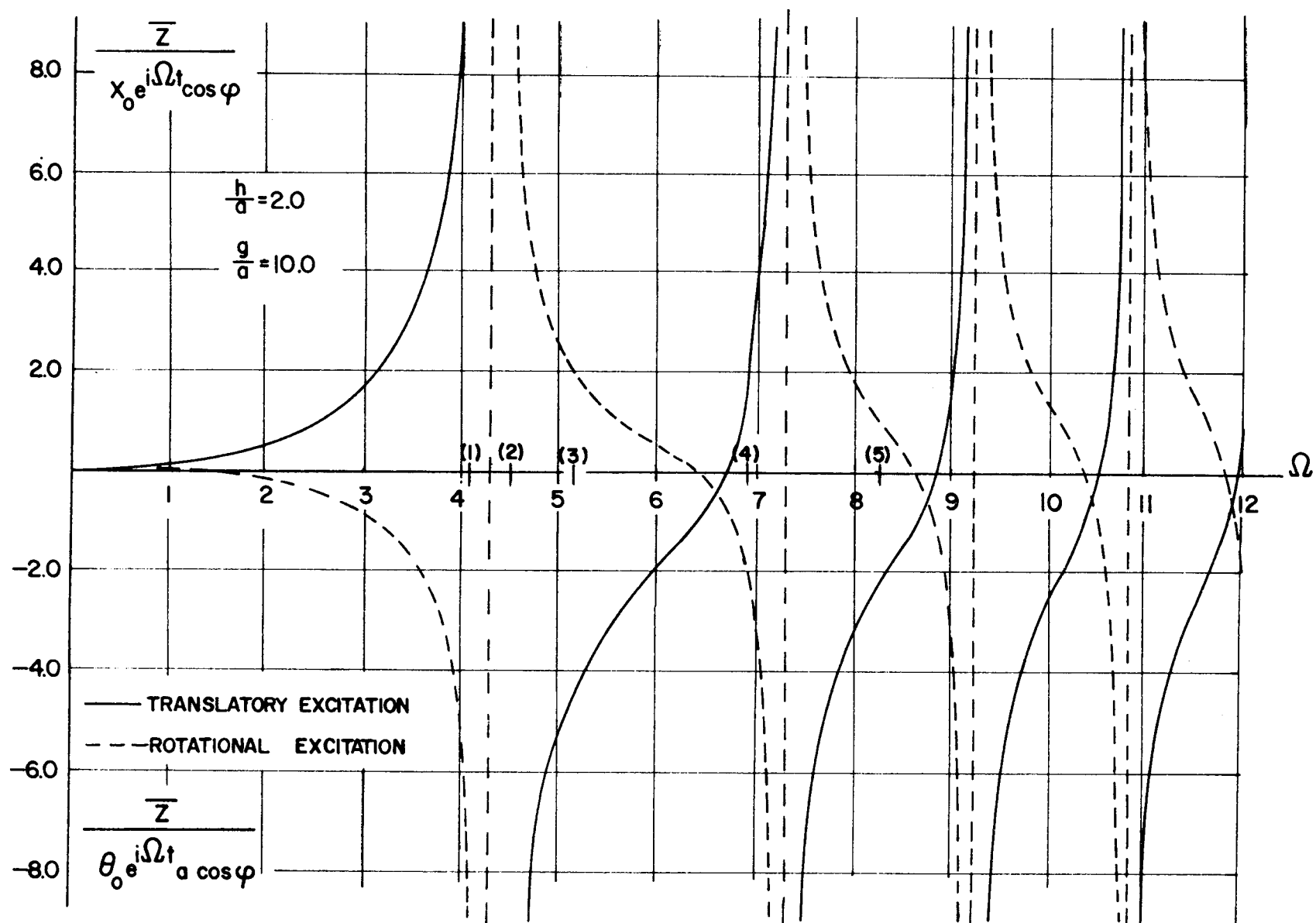


FIGURE 5. MAGNIFICATION FUNCTION OF FREE SURFACE DISPLACEMENT OF A LIQUID IN A CIRCULAR CYLINDRICAL CONTAINER.

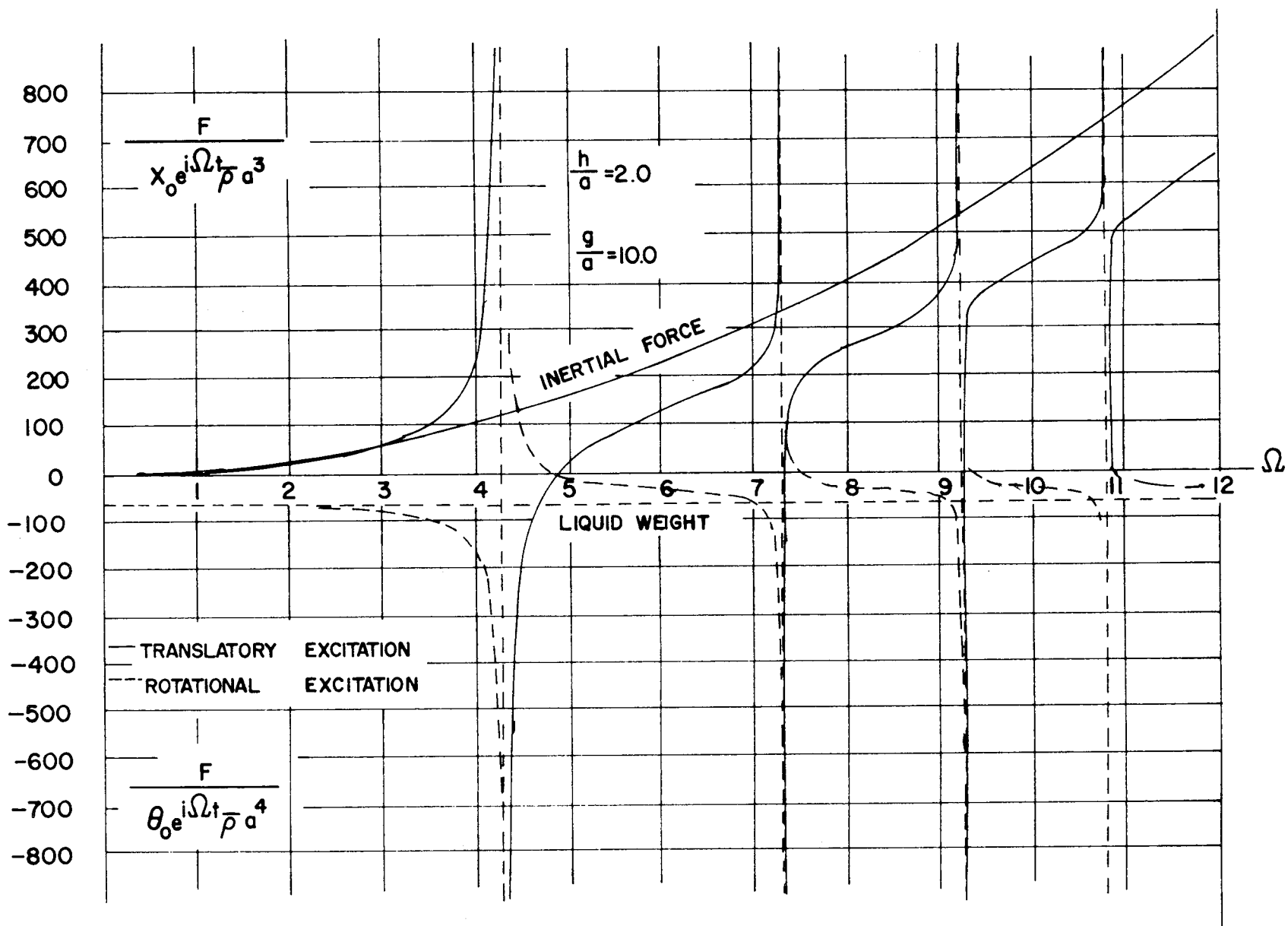


FIGURE 6. MAGNIFICATION FUNCTION OF THE LIQUID FORCE IN A CIRCULAR CYLINDRICAL CONTAINER

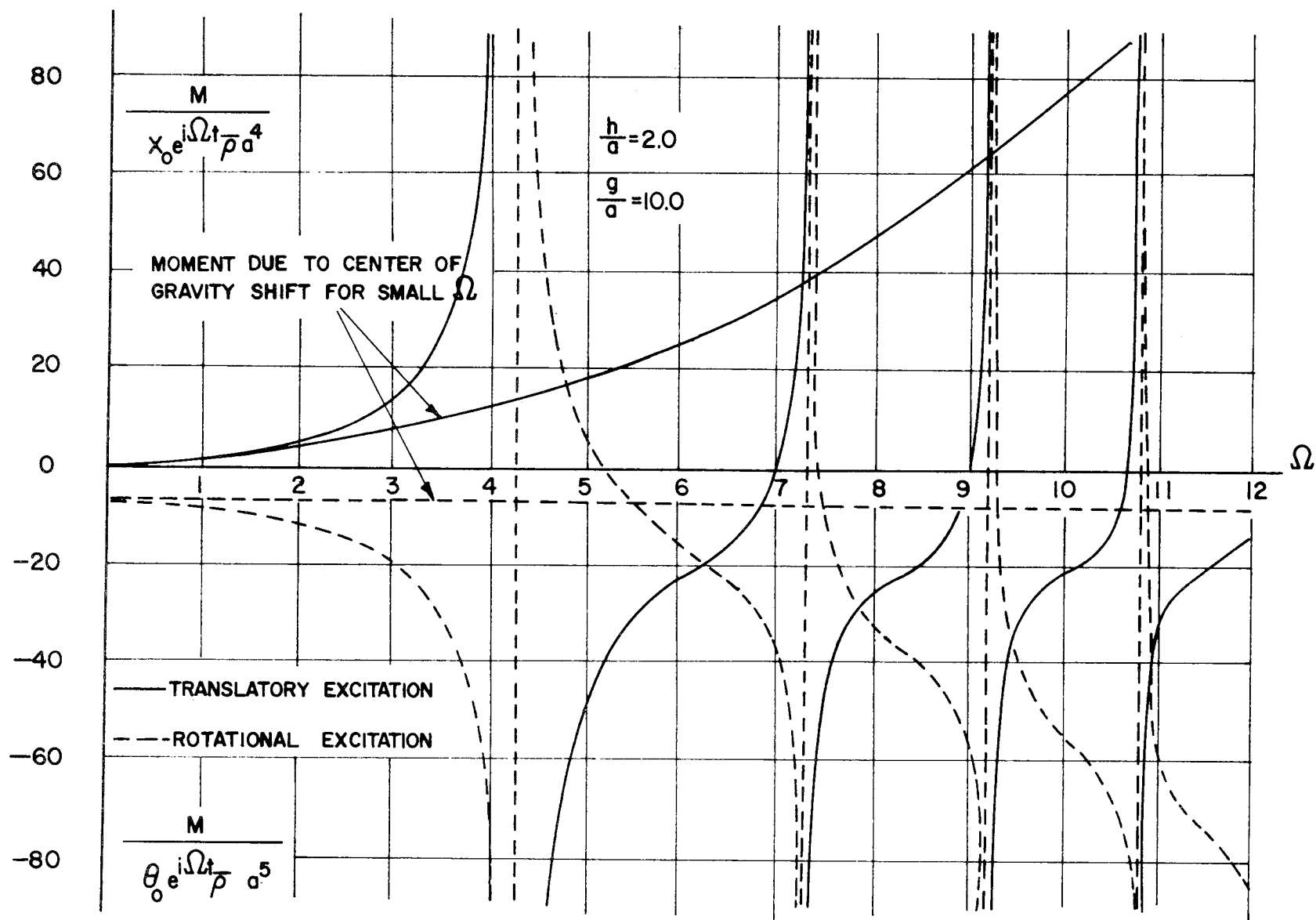


FIGURE 7. MAGNIFICATION FUNCTION OF THE LIQUID MOMENT IN A CIRCULAR CYLINDRICAL CONTAINER

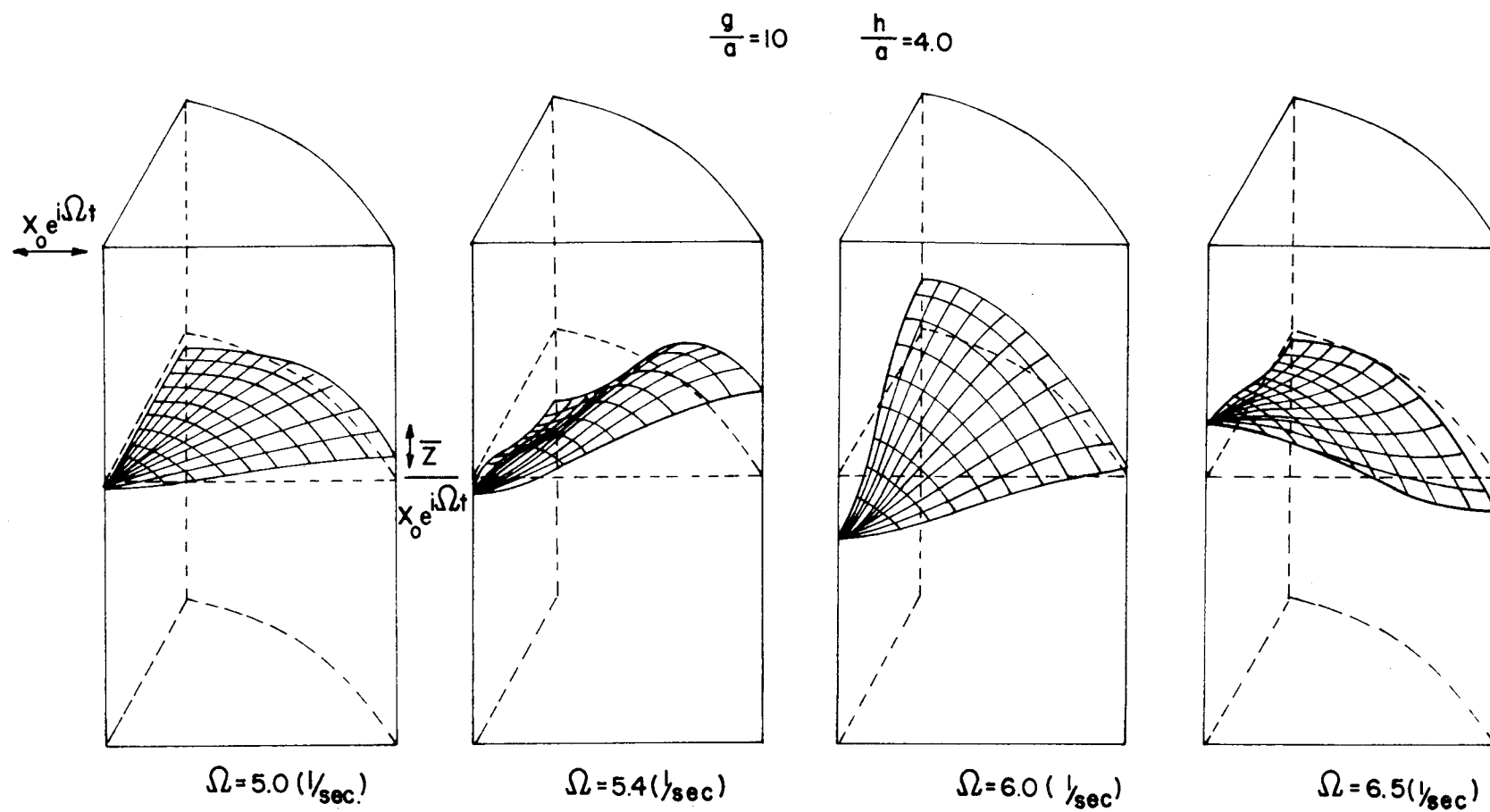


FIGURE 8. WAVE FORM OF THE FREE FLUID SURFACE IN A CIRCULAR CYLINDRICAL QUARTER CONTAINER. (FIRST EIGENFREQUENCY AT 5.5 rad/sec, SECOND EIGENFREQUENCY AT 6.2 rad/sec)

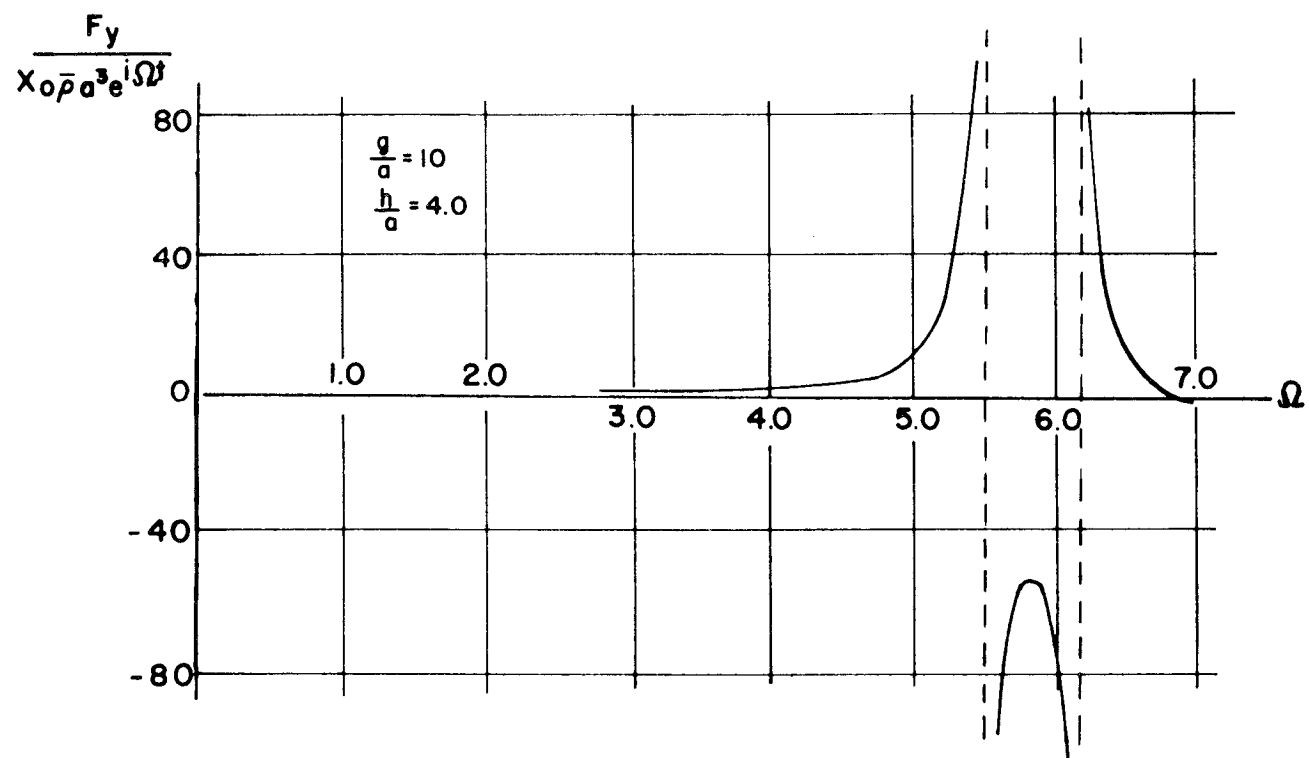
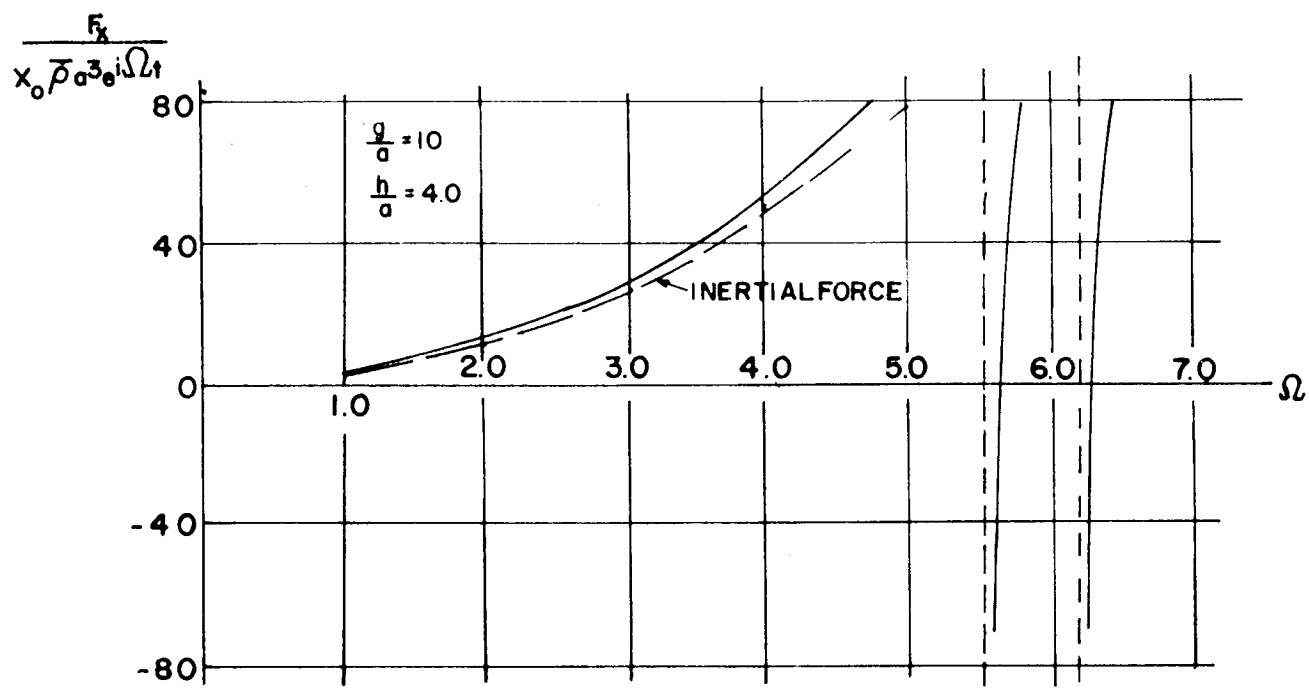


FIGURE 9. MAGNIFICATION FUNCTION OF LIQUID FORCE IN A CIRCULAR CYLINDRICAL QUARTER CONTAINER (EXCITATION ALONG X-AXIS)

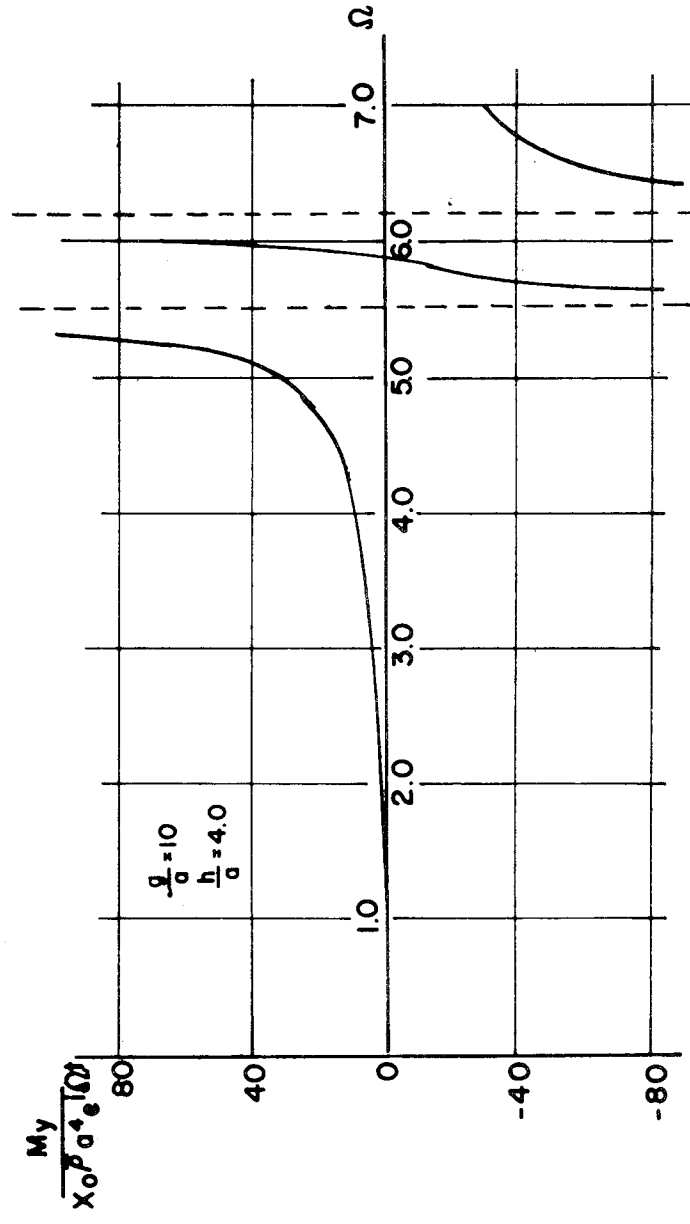
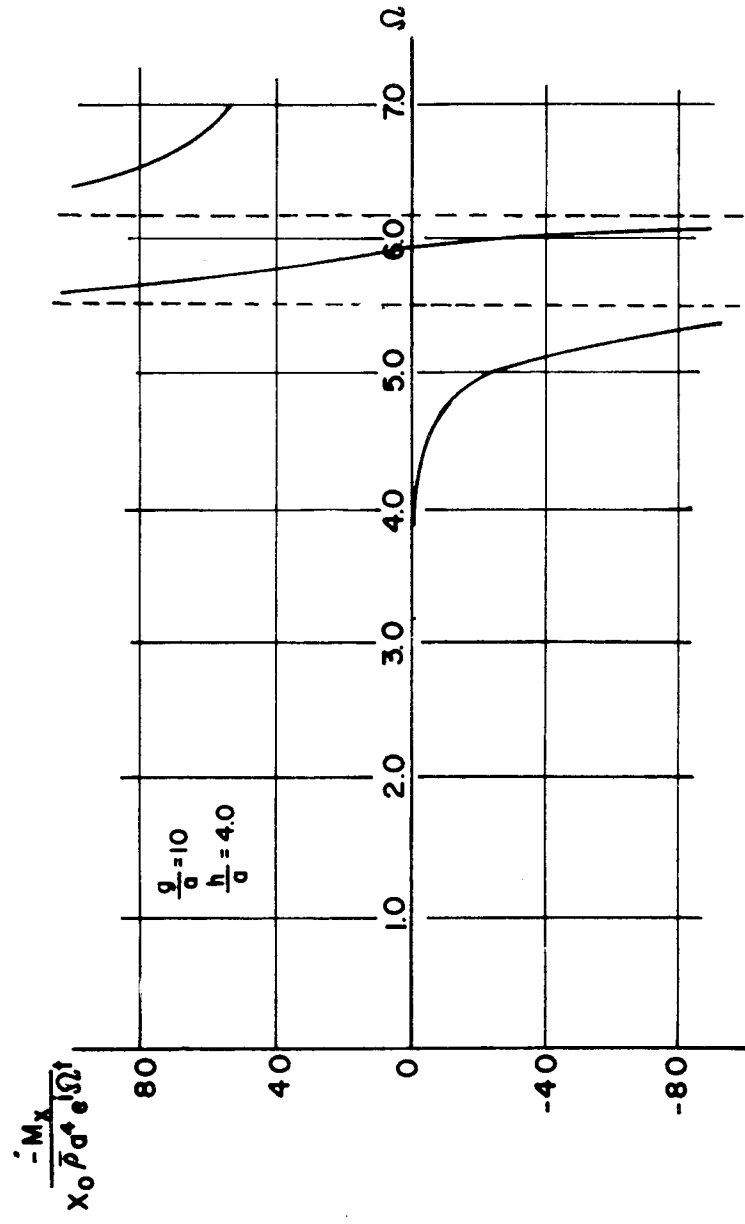


FIGURE 10. MAGNIFICATION FUNCTION OF LIQUID MOMENT IN A CIRCULAR CYLINDRICAL QUARTER CONTAINER (EXCITATION ALONG X-AXIS)

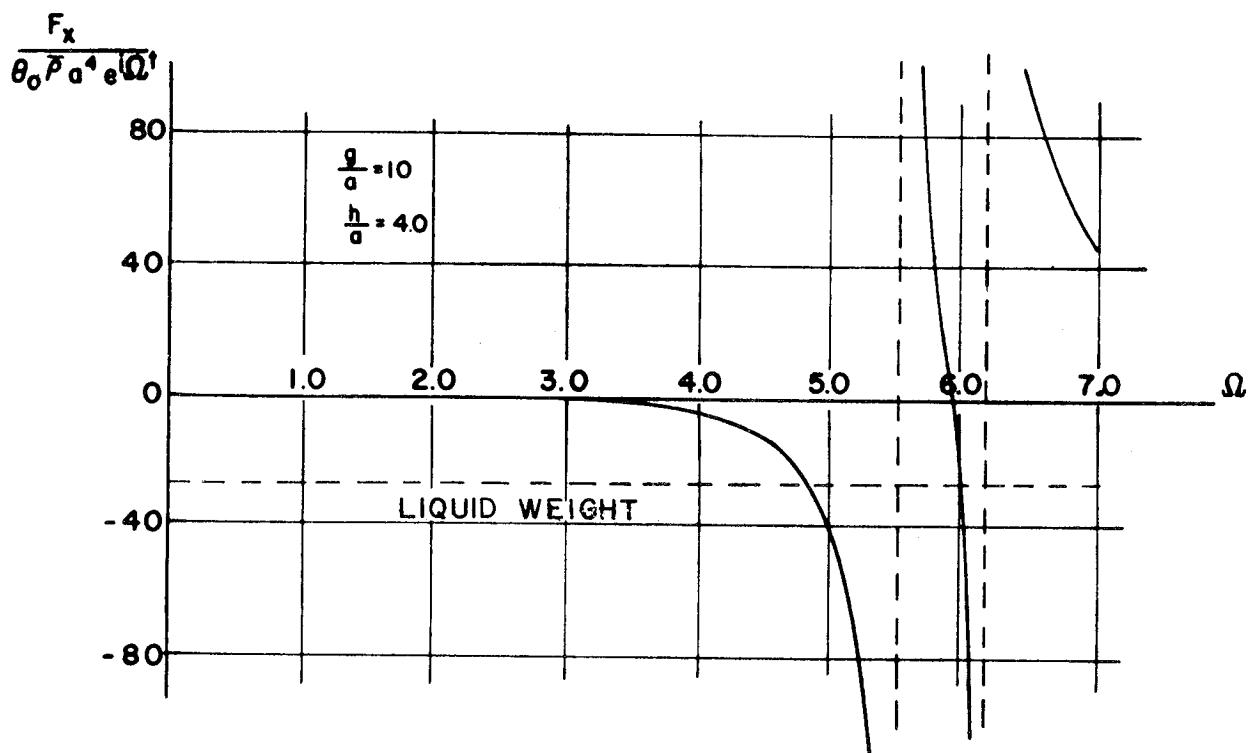
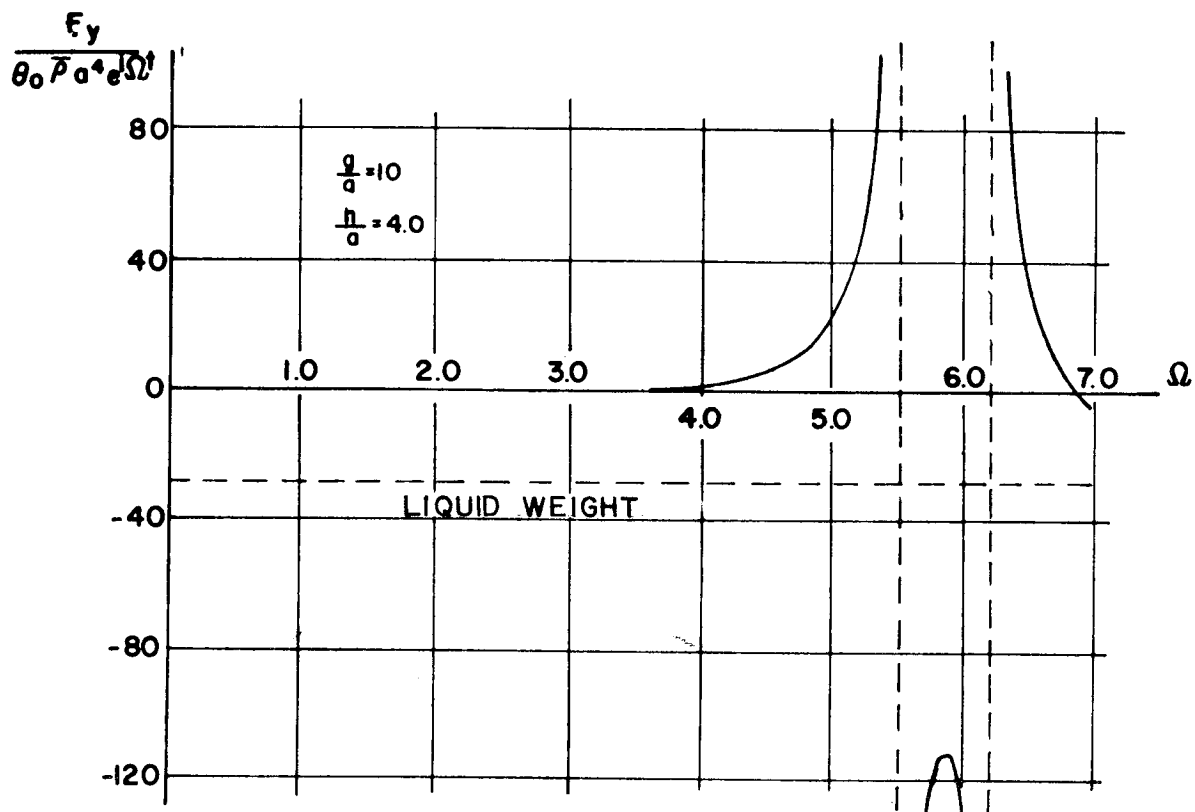


FIGURE 11. MAGNIFICATION FUNCTION OF LIQUID FORCE IN CIRCULAR CYLINDRICAL QUARTER CONTAINER (ROTATIONAL EXCITATION ABOUT Y-AXIS)

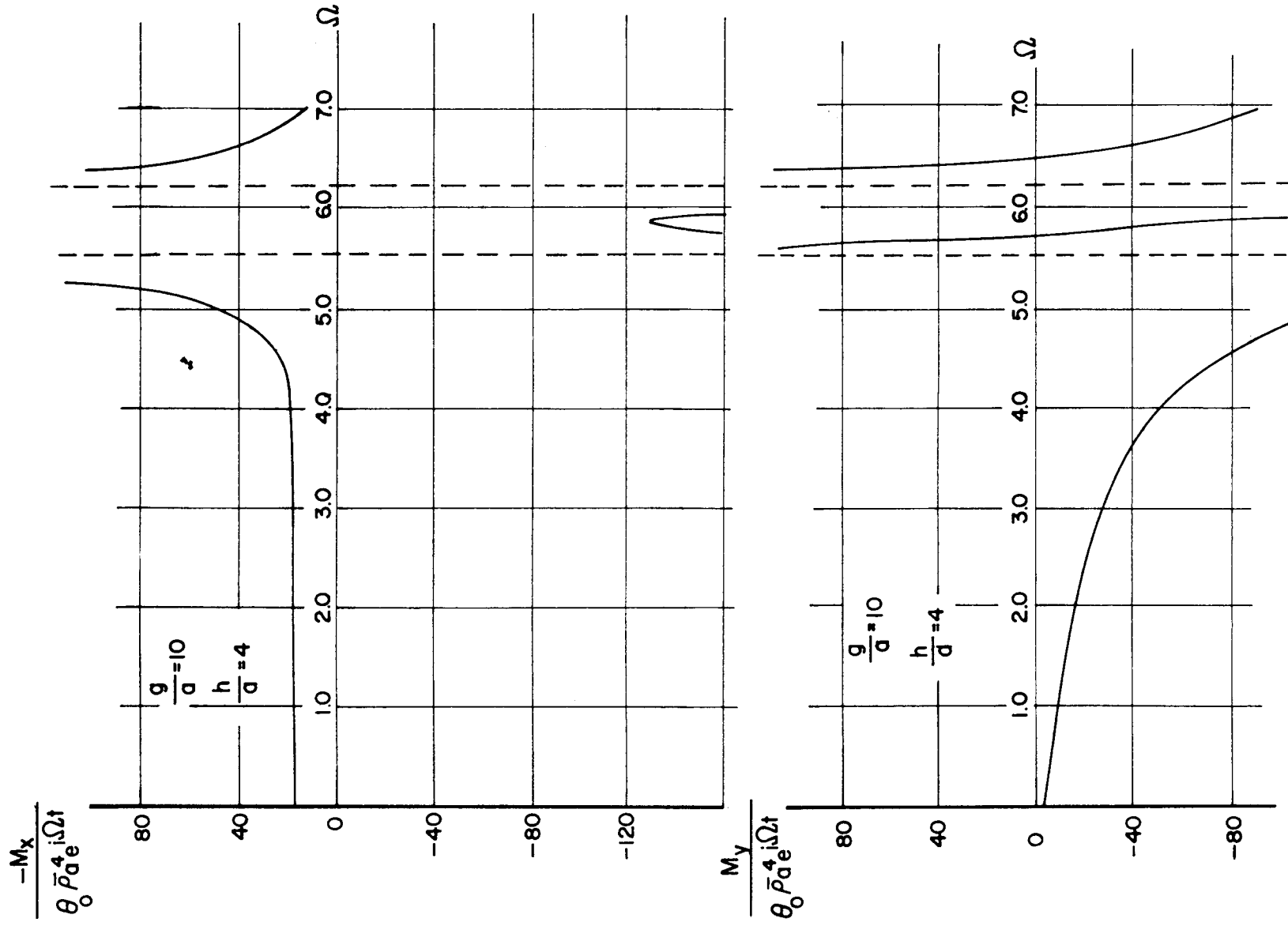


FIGURE 12. MAGNIFICATION FUNCTION OF LIQUID MOMENT IN CIRCULAR CYLINDRICAL QUARTER CONTAINER (ROTATIONAL EXCITATION ABOUT Y-AXIS).

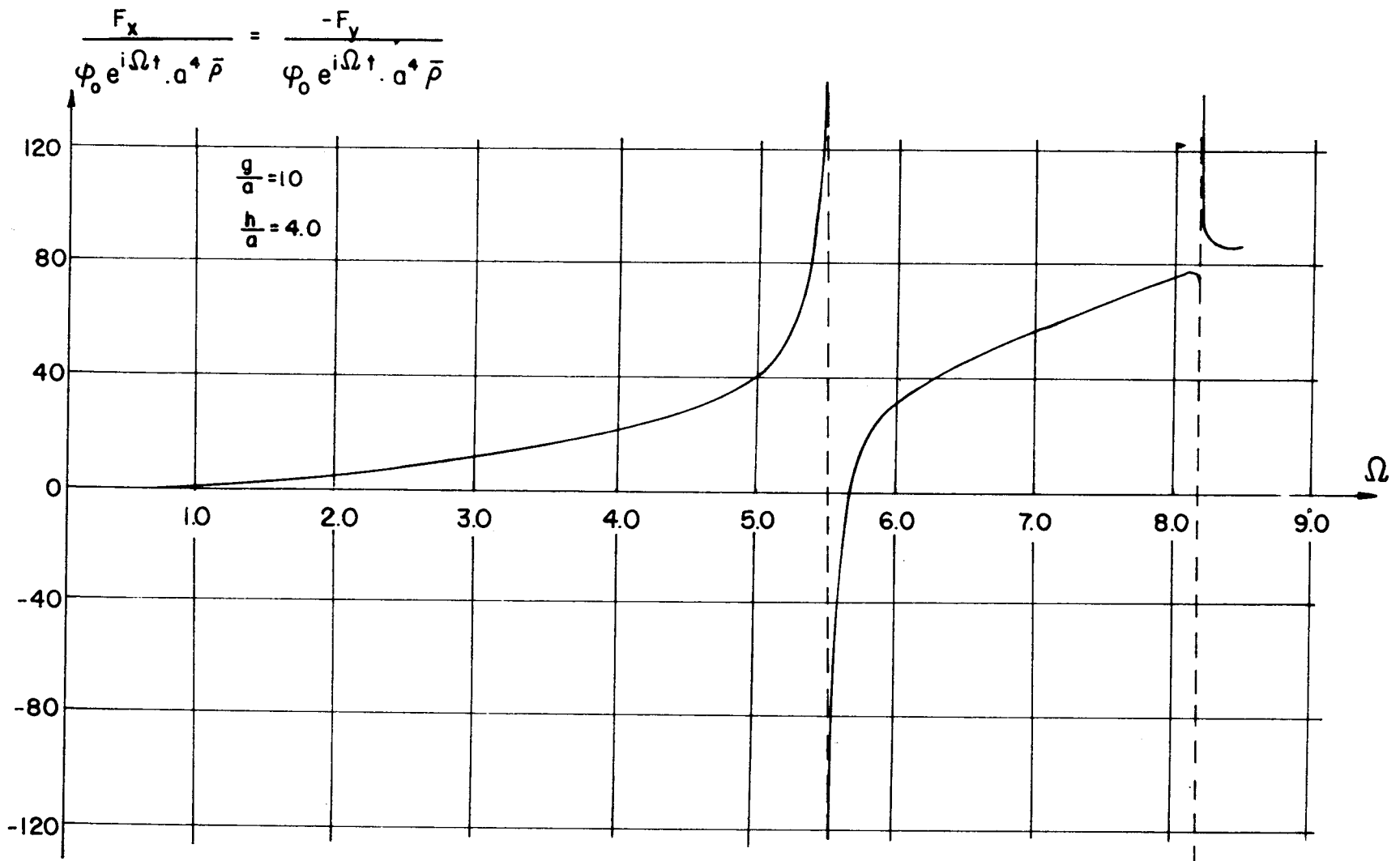


FIGURE 13. MAGNIFICATION FUNCTION OF LIQUID FORCE IN A CIRCULAR CYLINDRICAL QUARTER CONTAINER (ROLL EXCITATION ABOUT Z-AXIS)

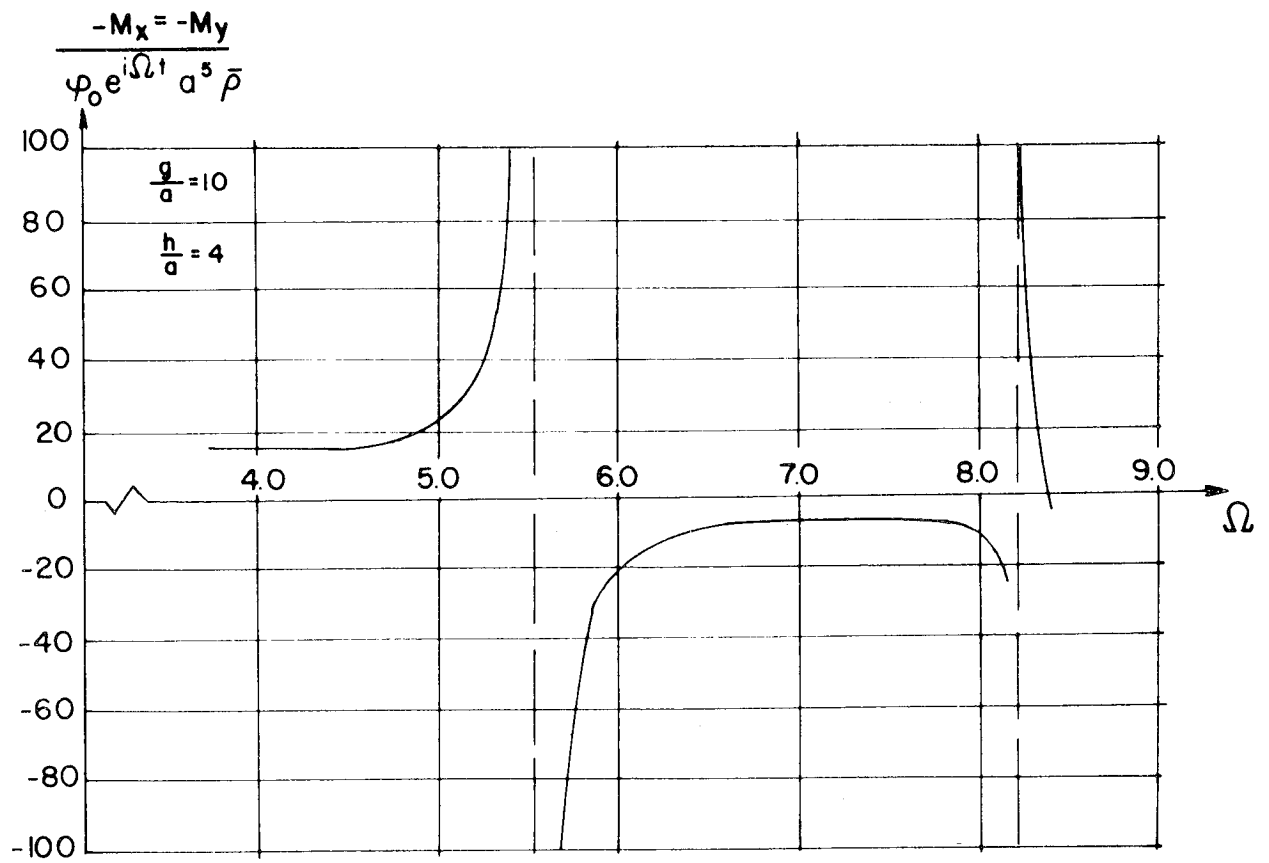


FIGURE 14. MAGNIFICATION FUNCTION OF LIQUID MOMENT IN A CIRCULAR CYLINDRICAL QUARTER CONTAINER (ROLL EXCITATION ABOUT Z-AXIS)

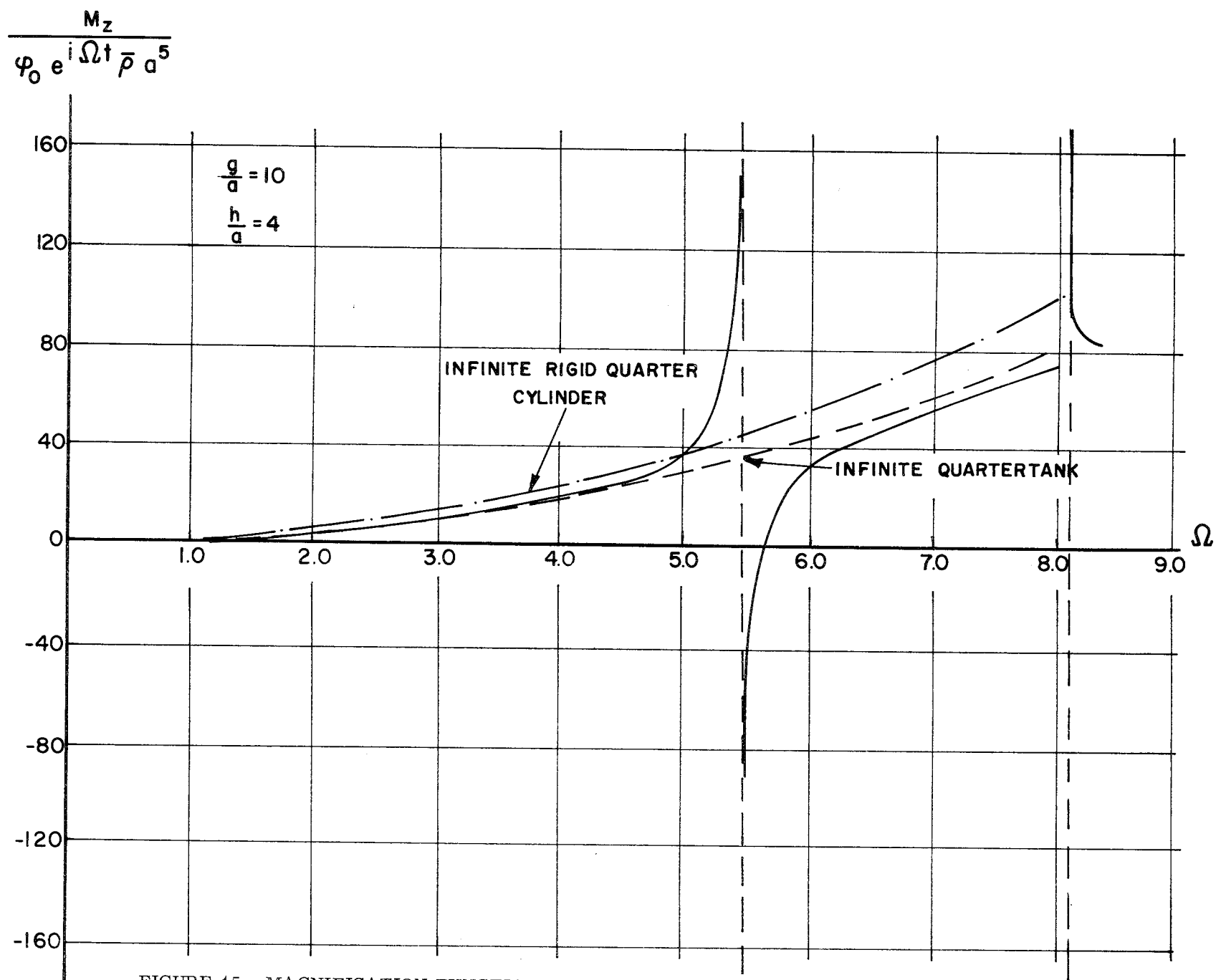
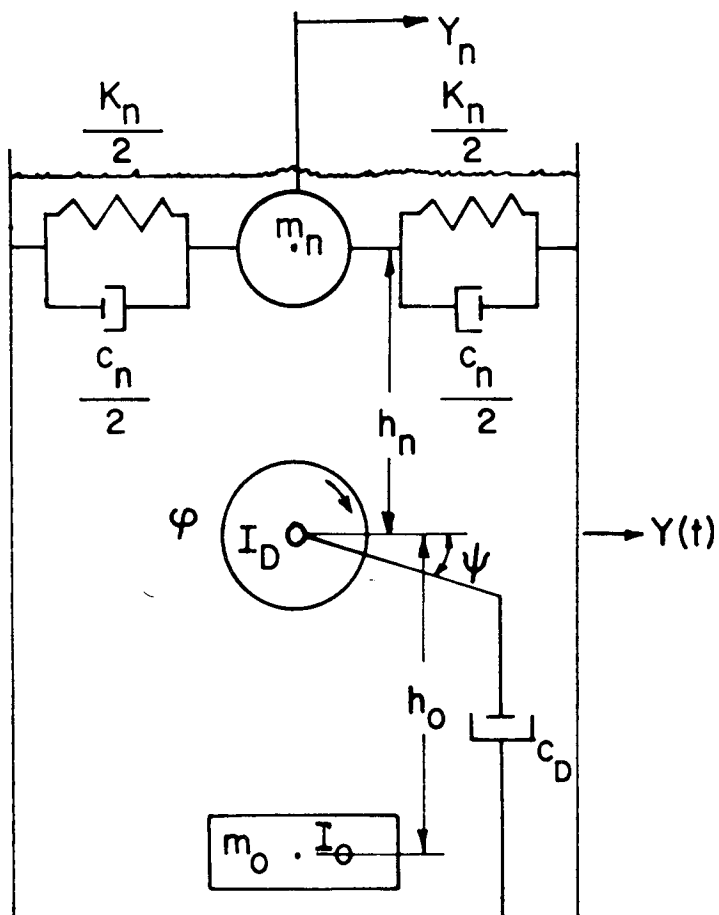


FIGURE 15. MAGNIFICATION FUNCTION OF LIQUID MOMENT IN A CIRCULAR CYLINDRICAL QUARTER CONTAINER (ROLL EXCITATION ABOUT Z-AXIS)

SPRING MASS MODEL



PENDULUM

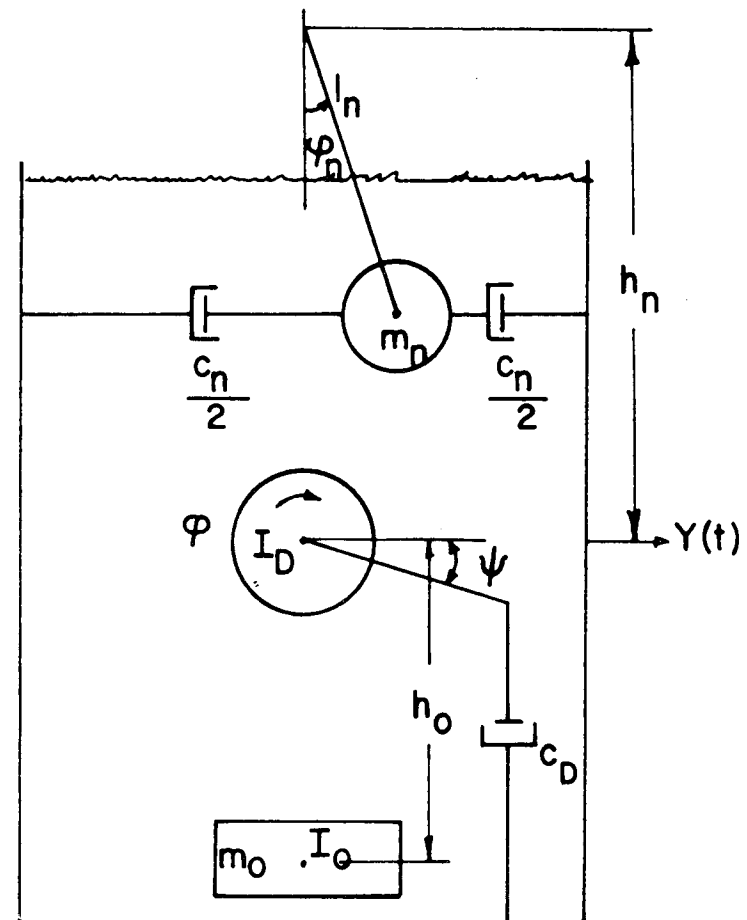


FIGURE 16. MECHANICAL MODEL

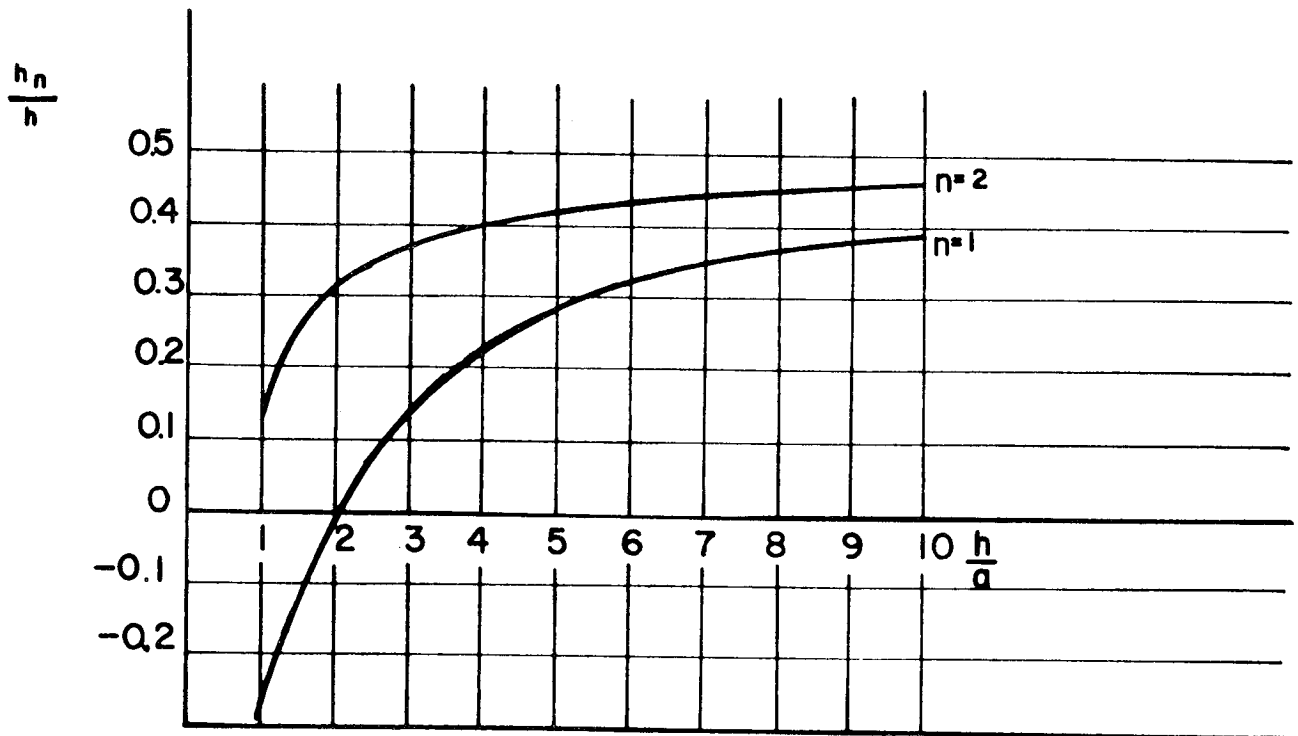
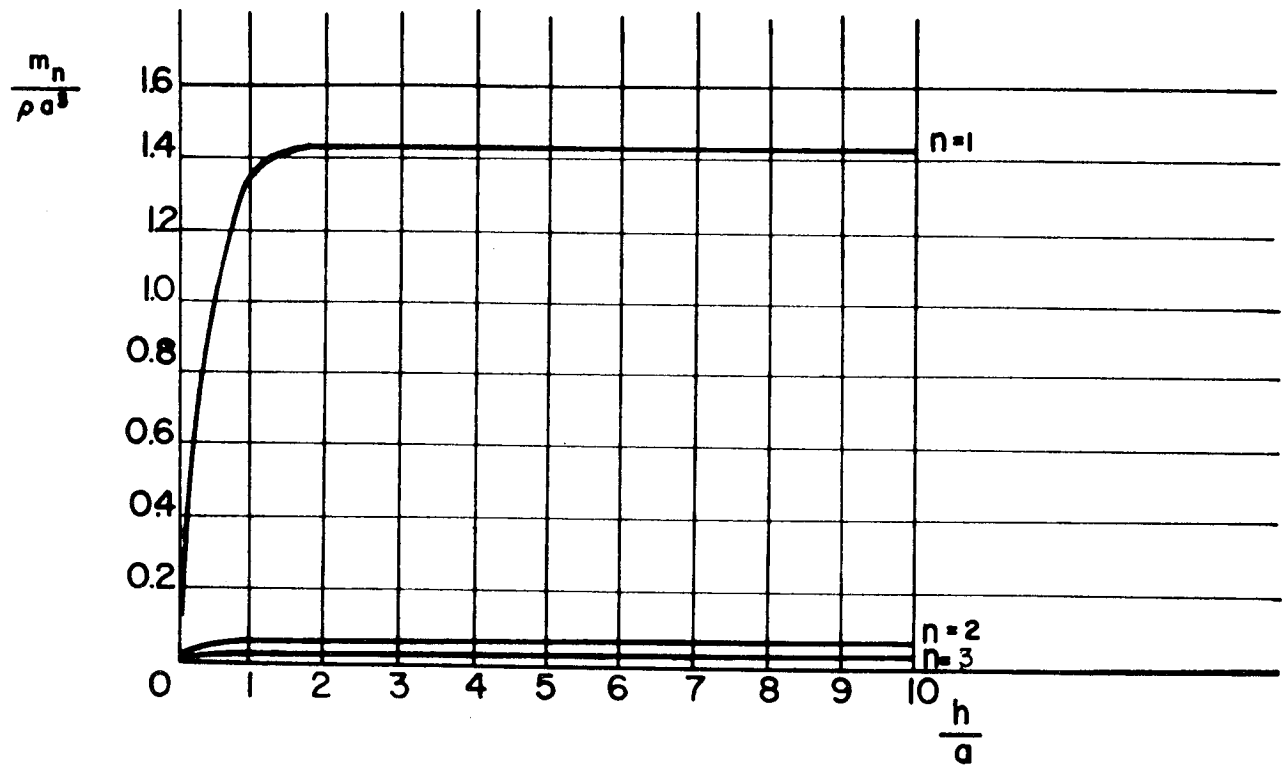


FIGURE 17. MAGNITUDE AND LOCATION OF SLOSHING (MODAL) MASSES FOR CIRCULAR CYLINDRICAL CONTAINER.

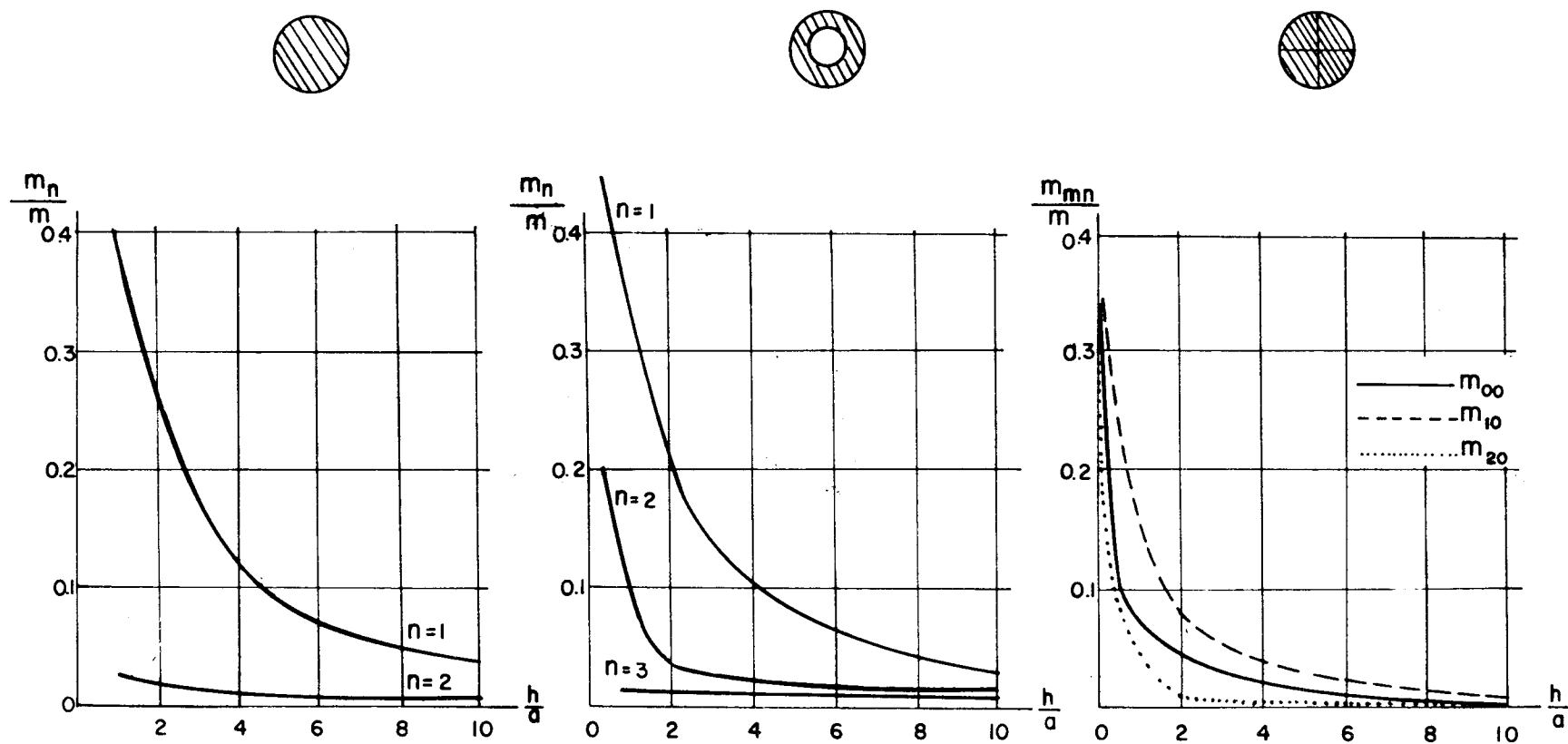


FIGURE 18. RATIO OF MODAL MASSES TO LIQUID MASS.

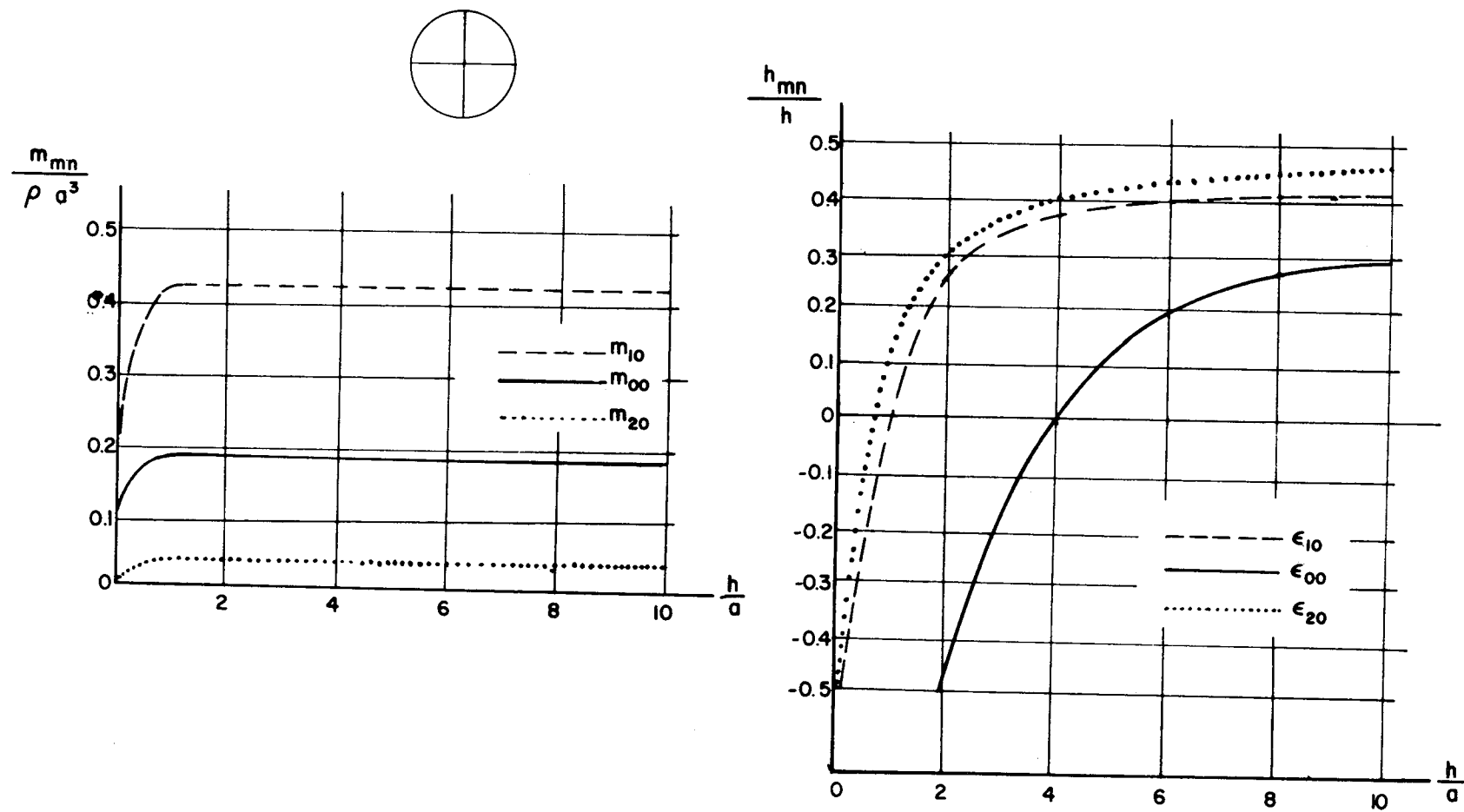


FIGURE 19. MAGNITUDE AND LOCATION OF SLOSHING (MODAL) MASSES FOR CIRCULAR CYLINDRICAL QUARTER CONTAINER

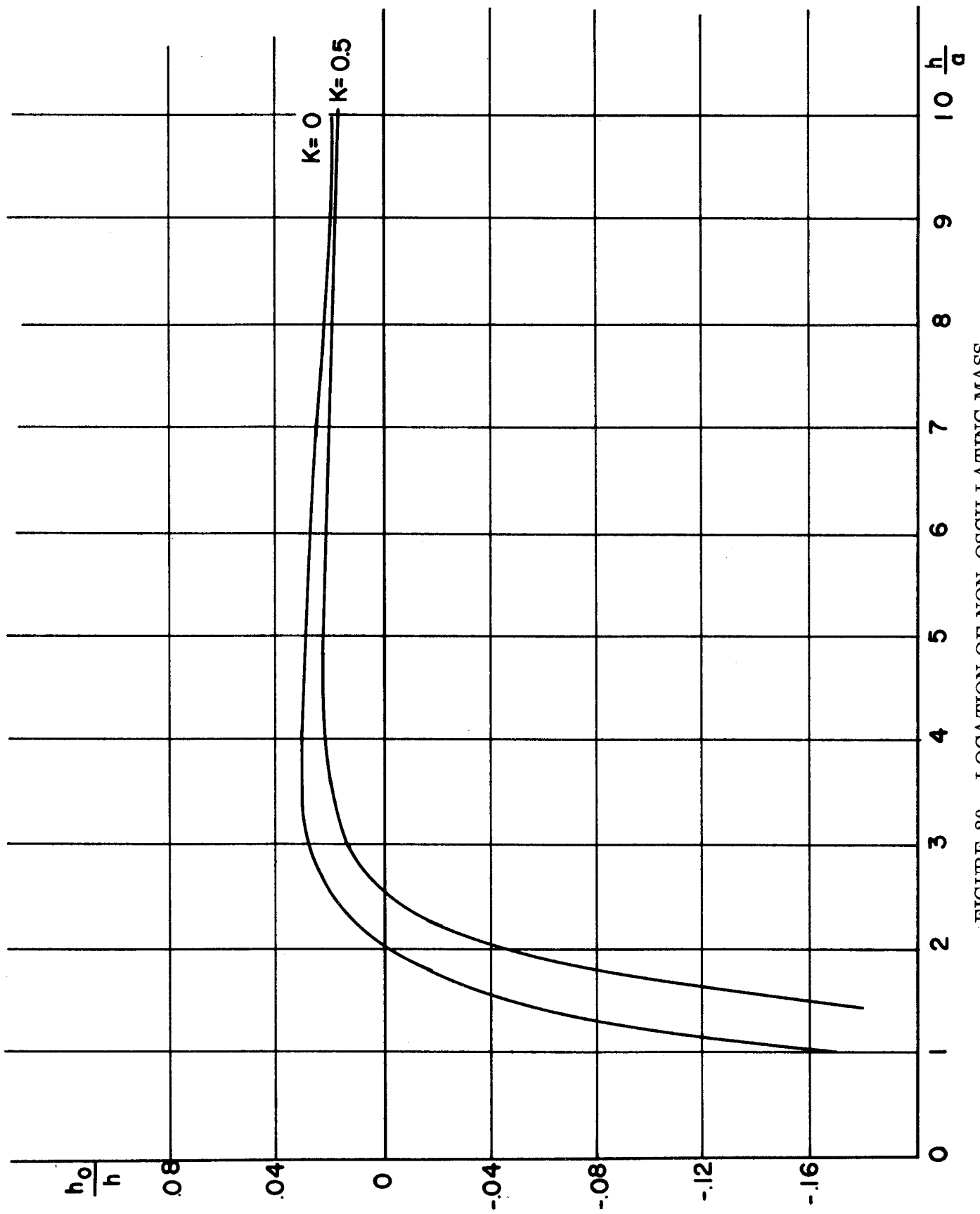


FIGURE 20. LOCATION OF NON-OSCILLATING MASS.

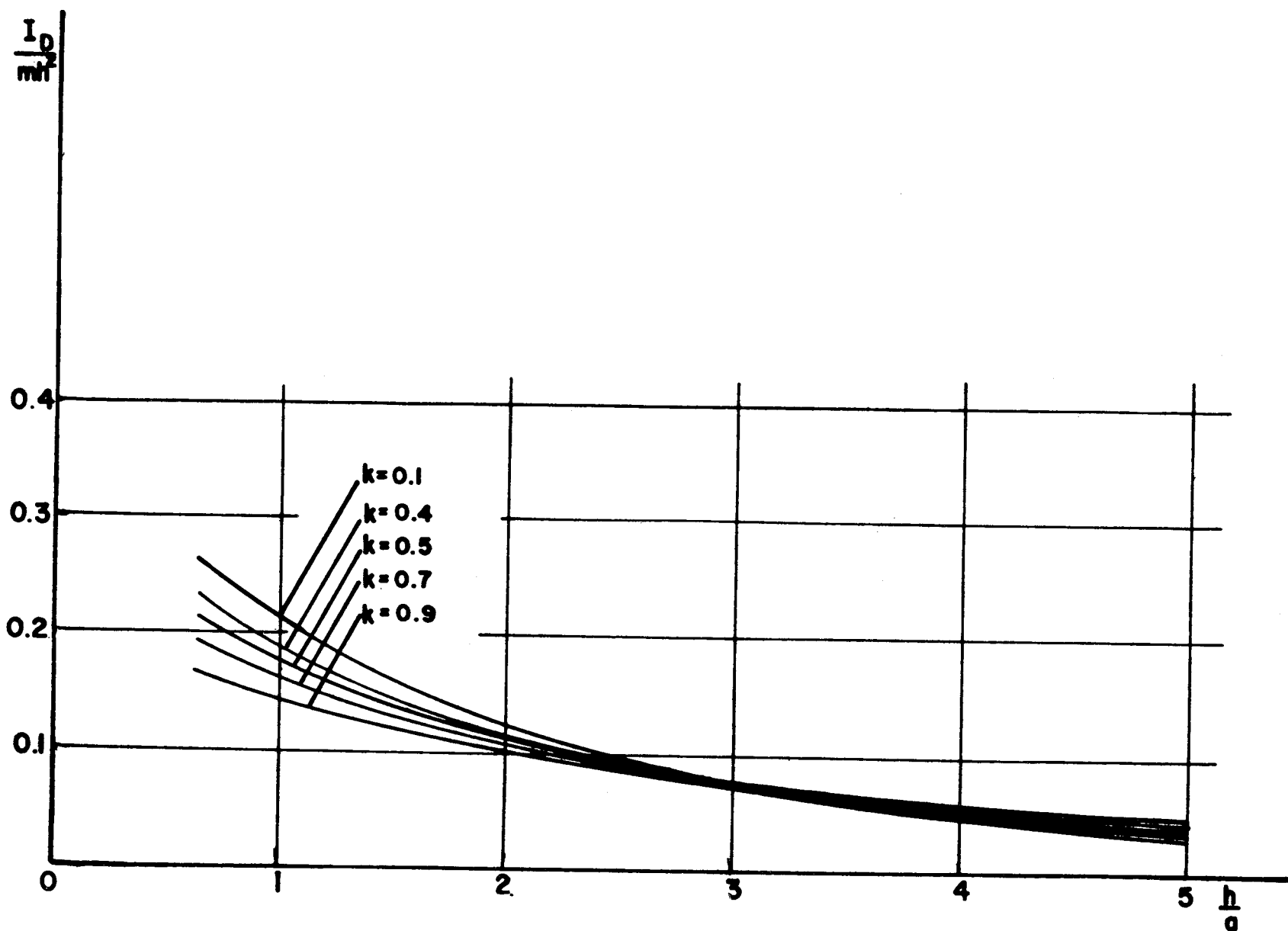


FIGURE 21. MOMENT OF INERTIA OF DISK.

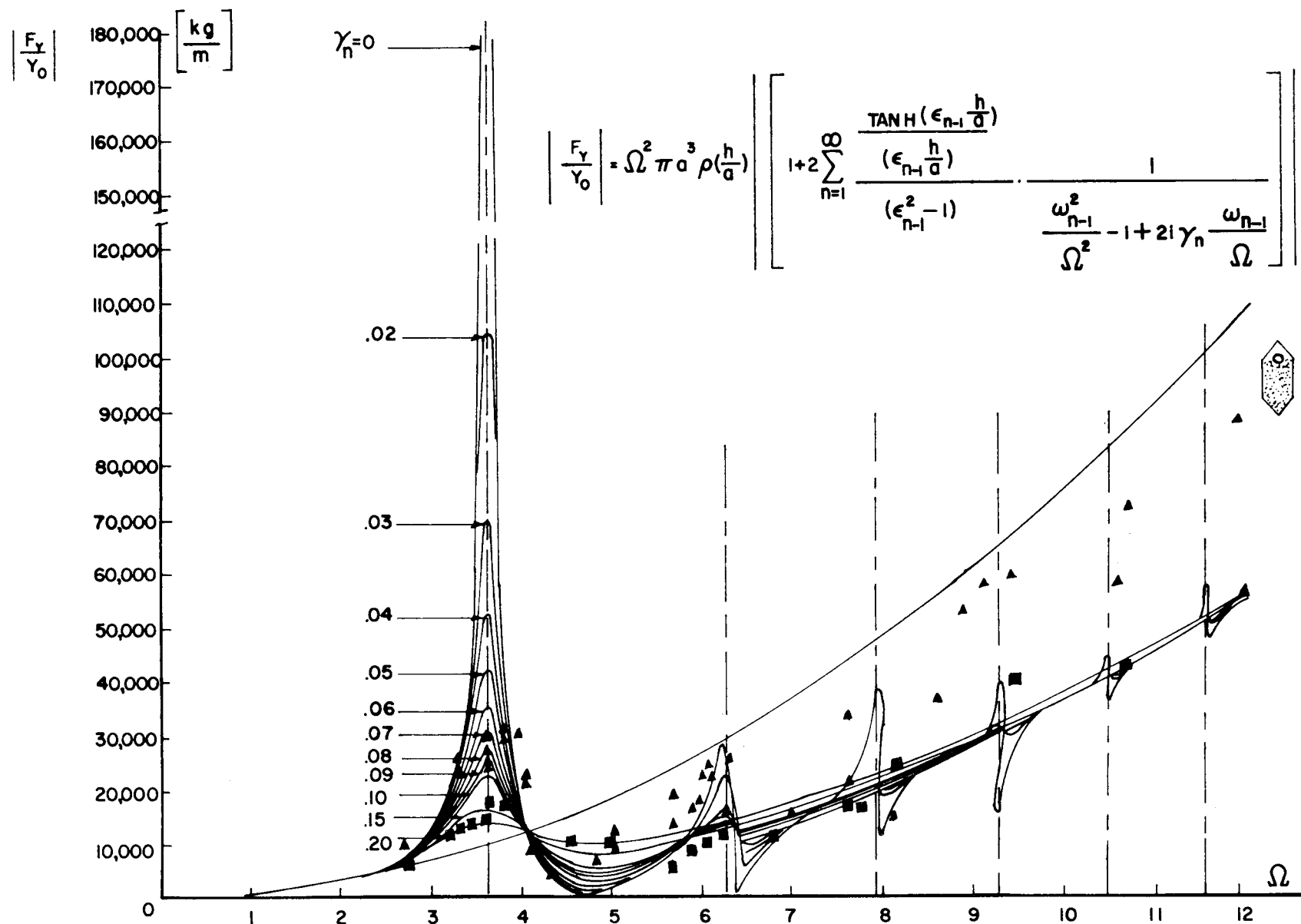


FIGURE 22. MAGNIFICATION FUNCTION OF LIQUID FORCE IN CIRCULAR CYLINDRICAL CONTAINER. (LIQUID HEIGHT $h = 1.40$ m, \blacktriangle FLOATING BAFFLES, \blacksquare RING BAFFLES.)

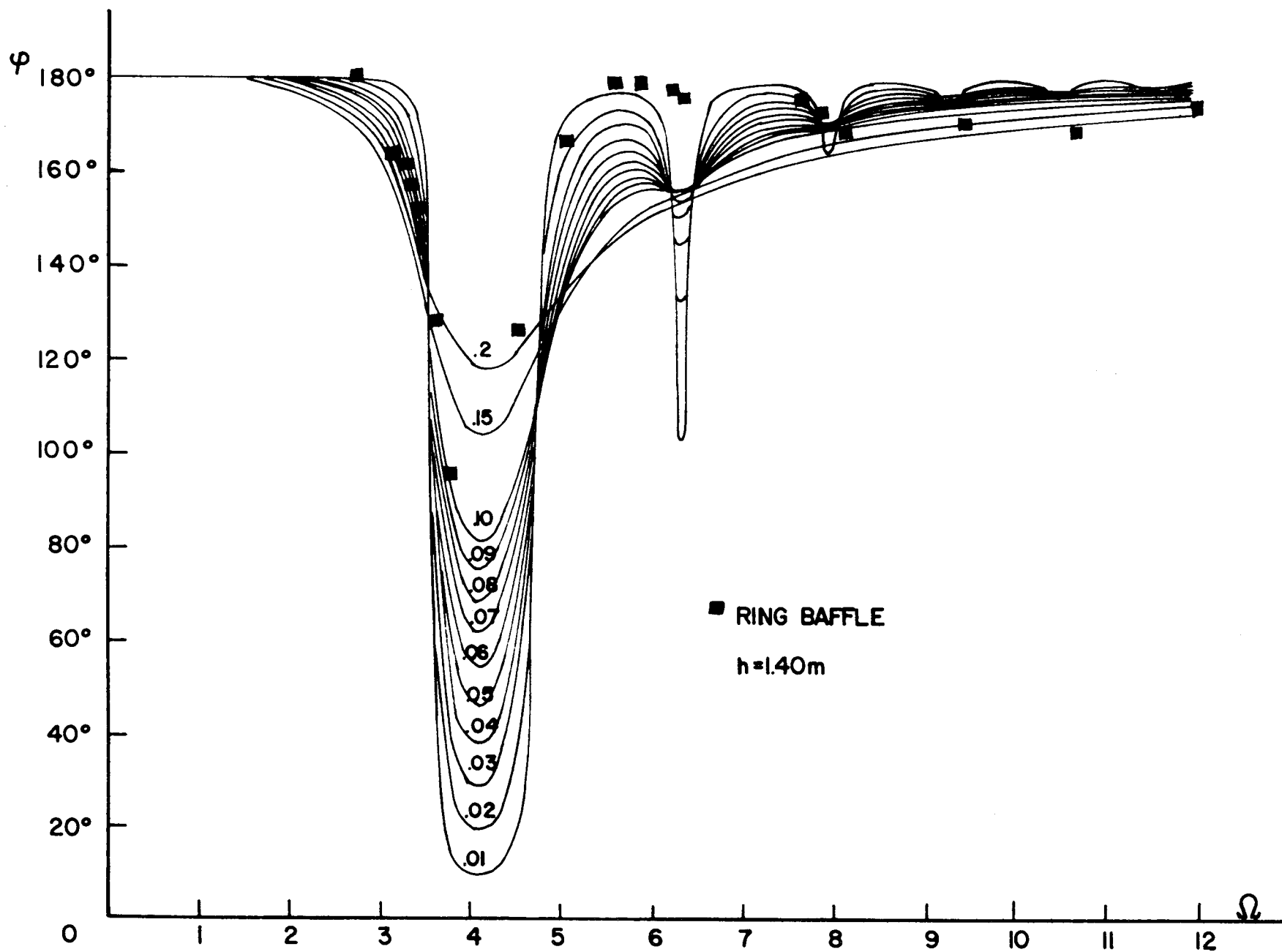
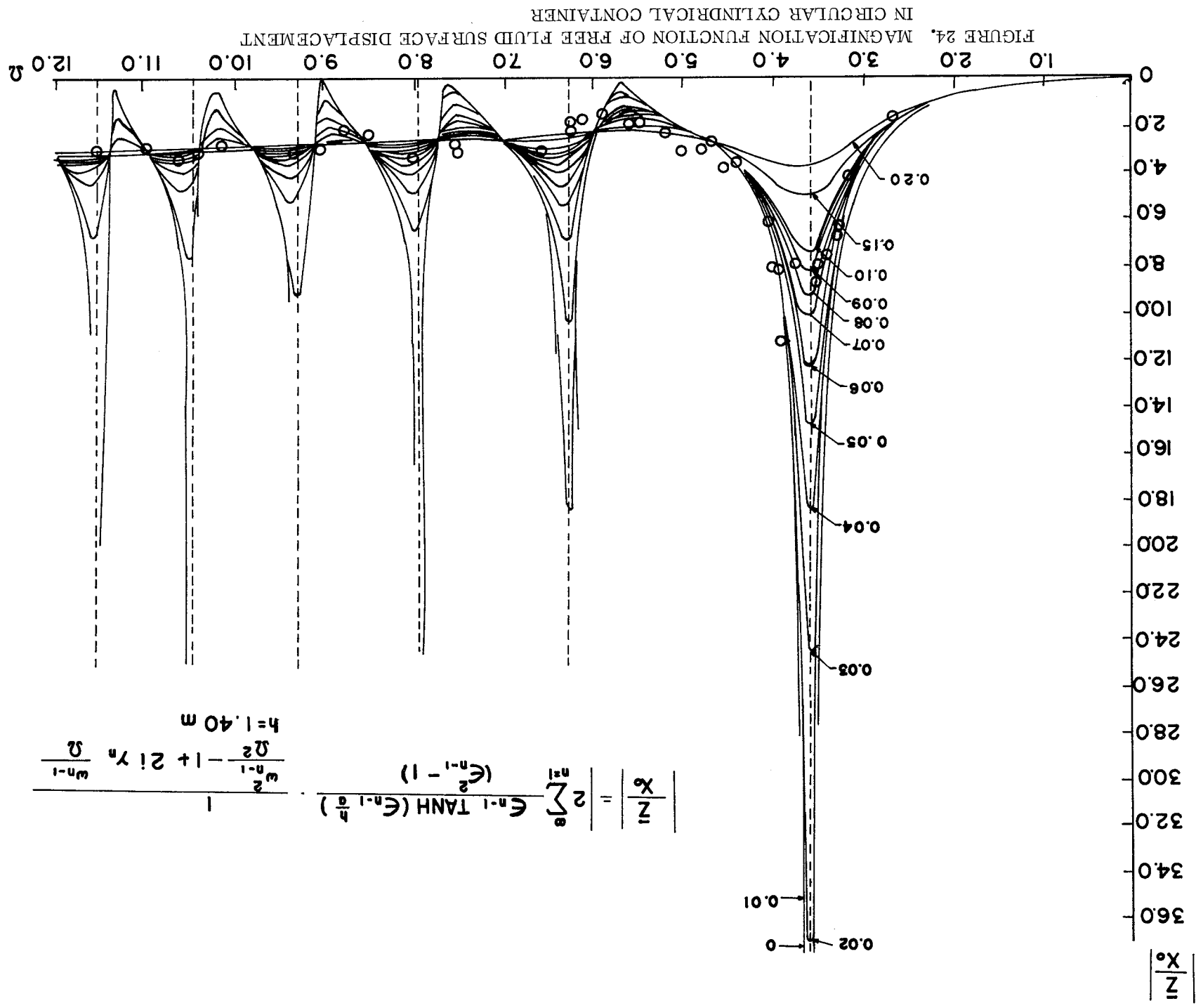


FIGURE 23. PHASE OF LIQUID FORCE IN CIRCULAR CYLINDRICAL CONTAINER



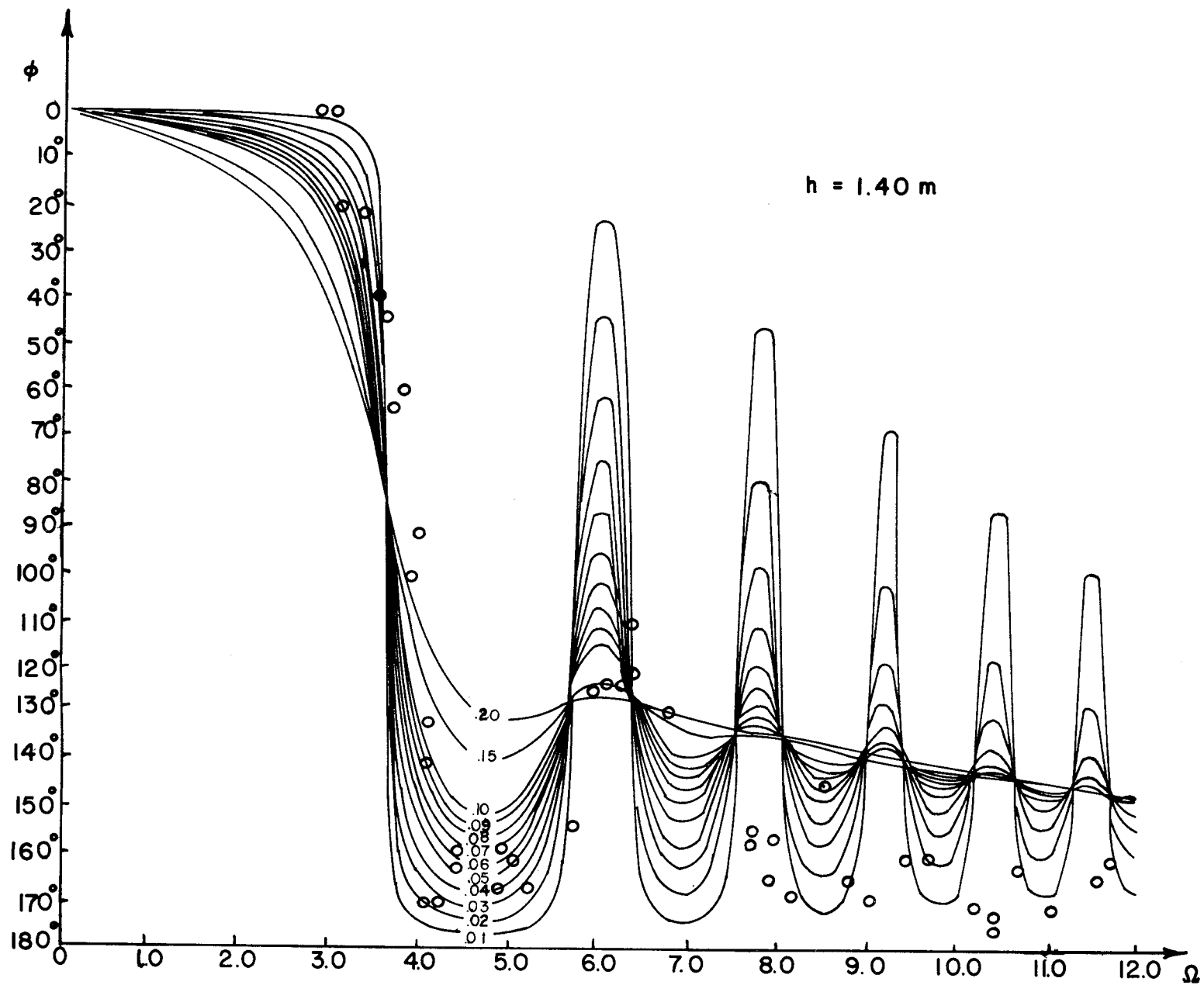


FIGURE 25. PHASE OF FREE FLUID SURFACE DISPLACEMENT IN CIRCULAR CYLINDRICAL CONTAINER

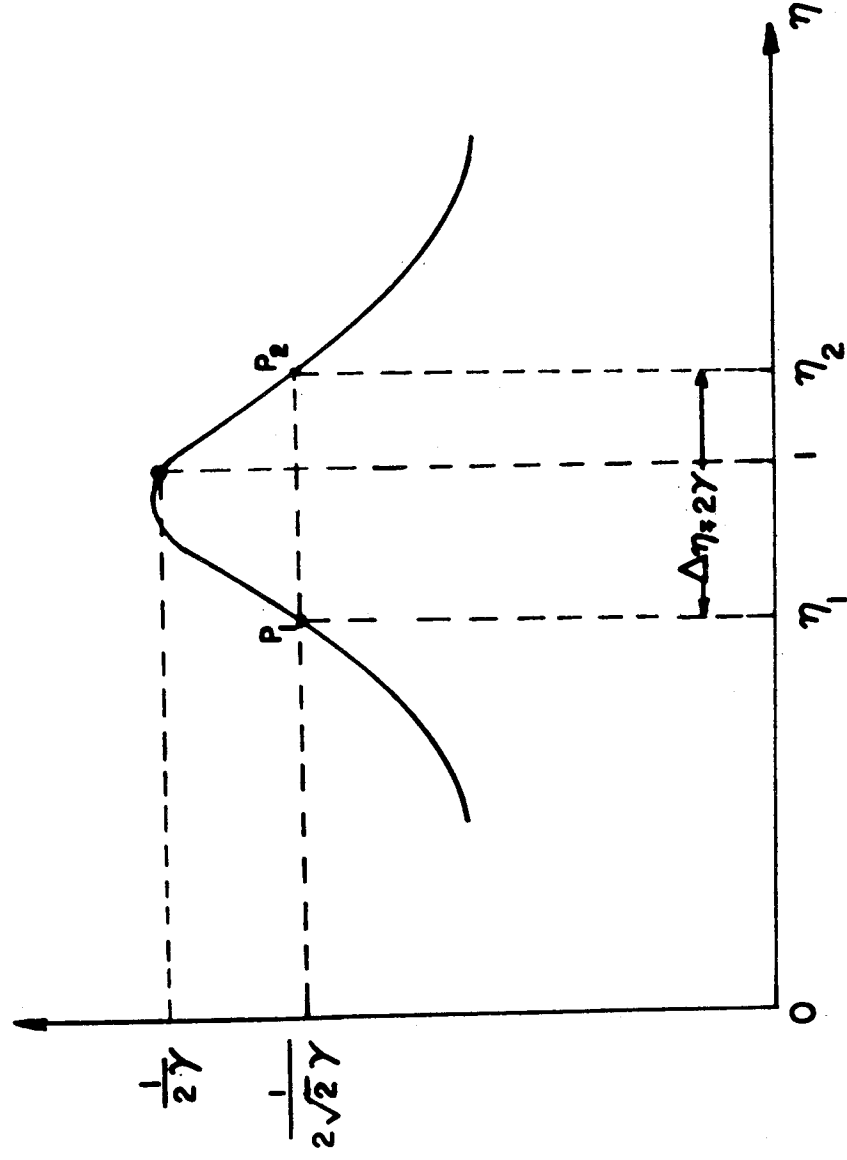


FIGURE 26. FOR THE DETERMINATION OF THE DAMPING FACTOR

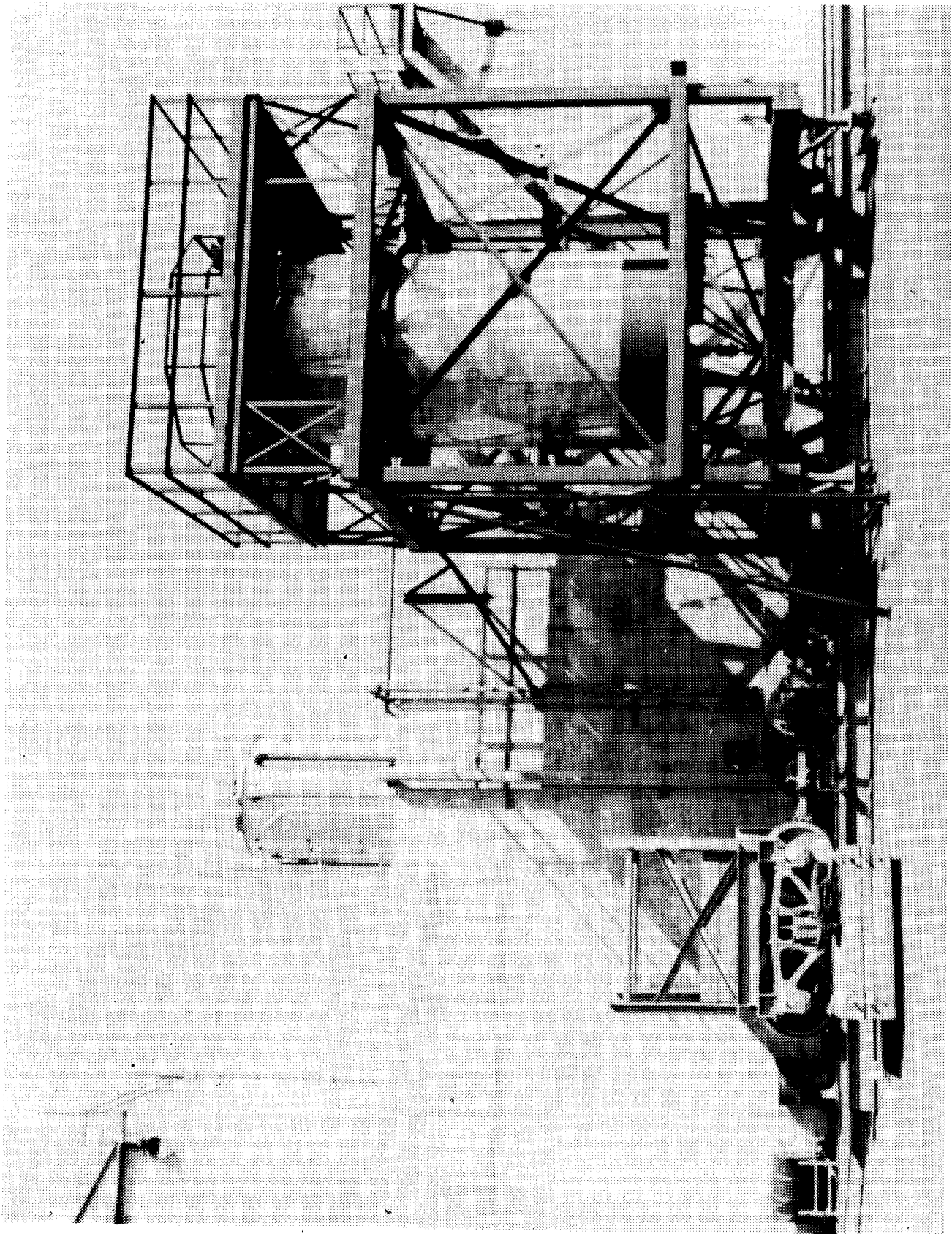
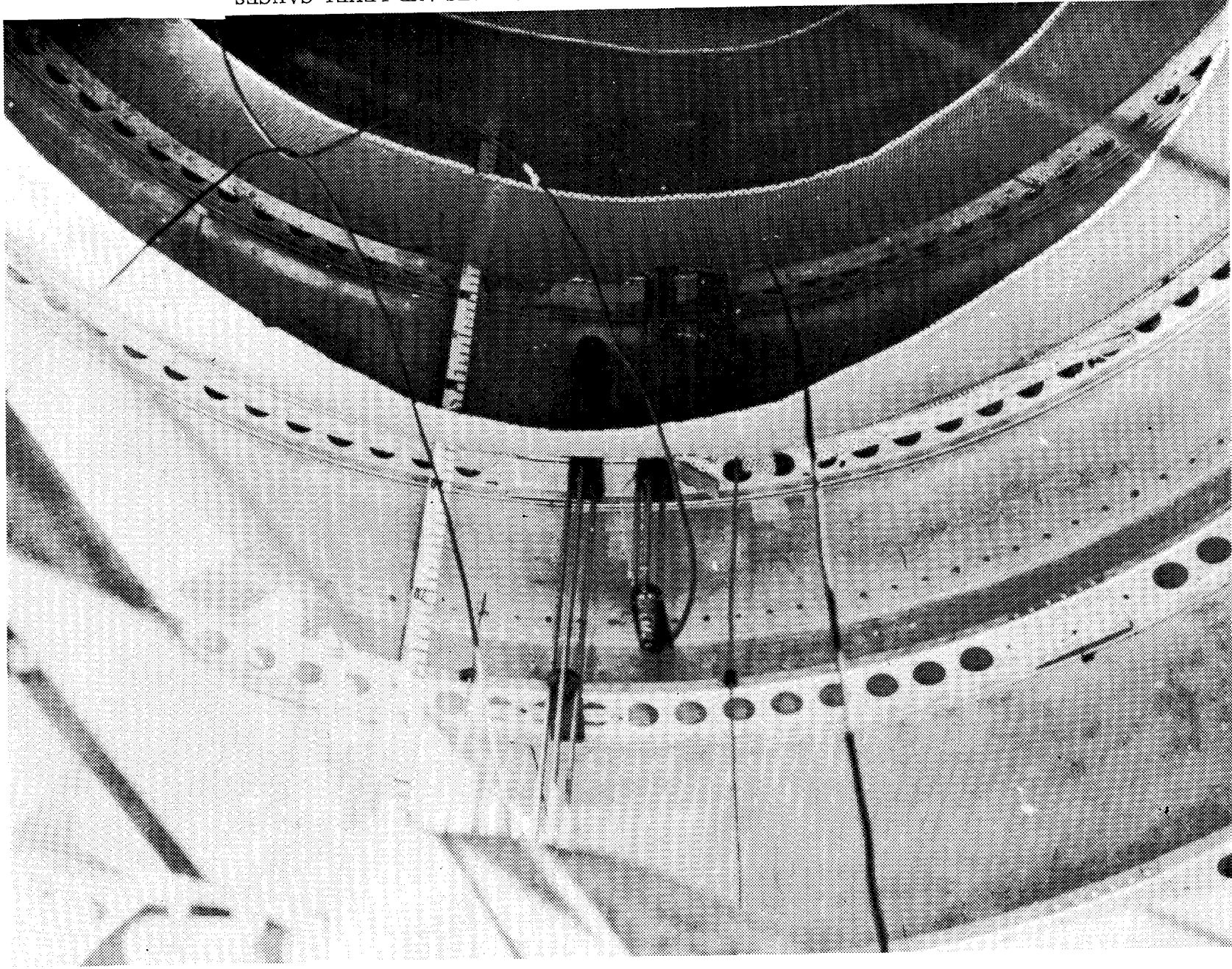


FIGURE 27. TEST SET-UP

FIGURE 28. VIEW INSIDE THE CONTAINER WITH Baffles AND LEVEL GAUGES



$$\frac{I_f}{I_{\text{RIGID}}} = 1 - \frac{\frac{(1+k^2)}{2} + 2 \sum_{n=0}^{\infty} \bar{A}_n \left[\frac{2}{\pi \xi_n} - K C_1(k \xi_n) \right]}{\frac{1}{12} \left(\frac{h}{a} \right)^2 + \frac{(1+k)^2}{4}} \cdot \left[1 - \frac{4}{\xi_n \frac{h}{a}} \tanh \left(\frac{\xi_n}{2} \frac{h}{a} \right) \right]$$

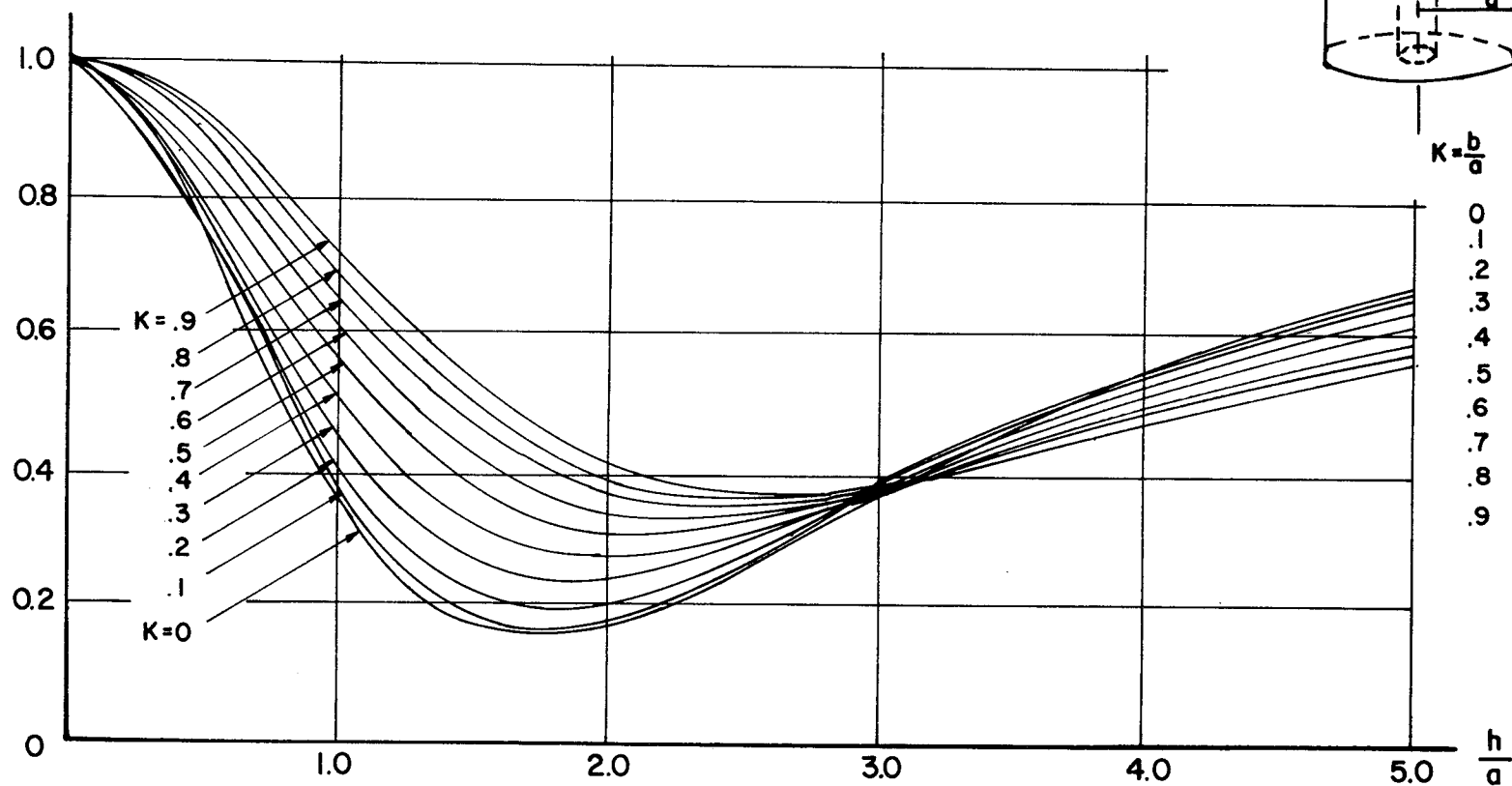


FIGURE 29. EFFECTIVE MOMENT OF INERTIA OF LIQUID IN COMPLETELY FILLED CLOSED CONTAINER

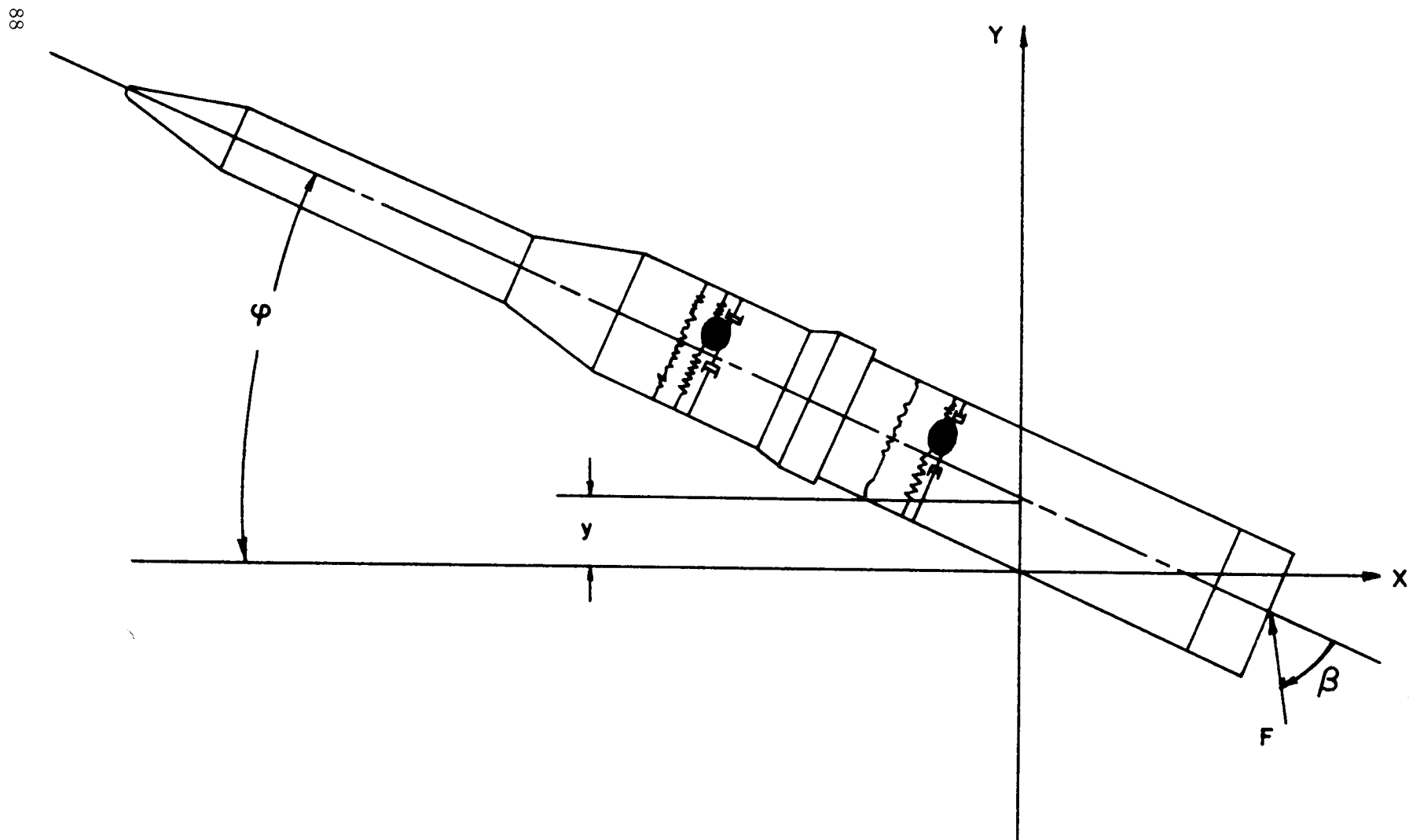


FIGURE 30. COORDINATE SYSTEM OF SPACE VEHICLE

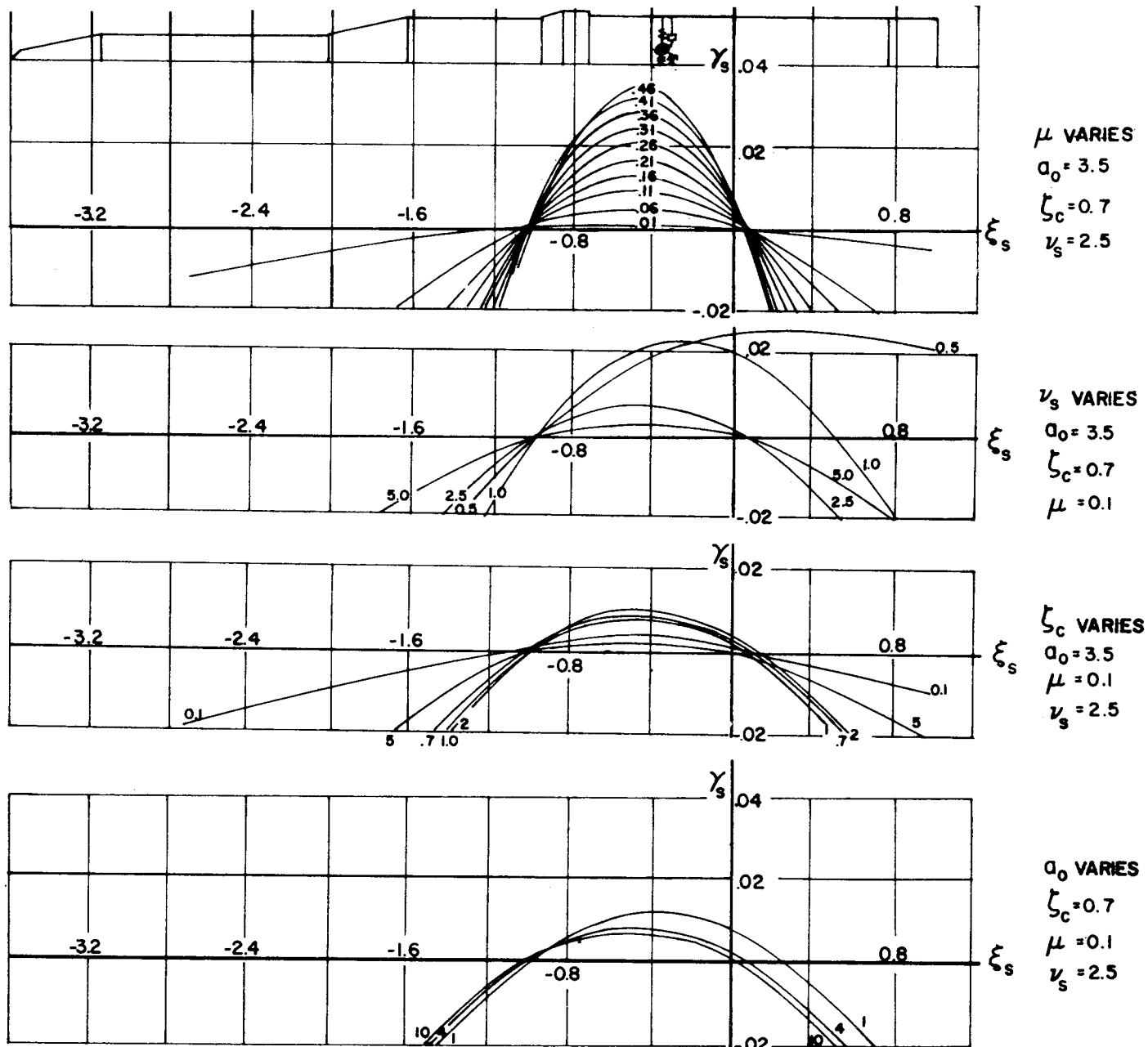


FIGURE 31. STABILITY BOUNDARIES OF RIGID SPACE VEHICLE WITH SIMPLE CONTROL SYSTEM

$$\zeta_c = 0.7$$
$$\mu = 0.1$$
$$\nu_s = 2.5$$
$$a_0 = 3.5$$

FIGURE 32. STABILITY BOUNDARIES OF RIGID SPACE VEHICLE WITH ADDITIONAL IDEAL ACCELEROMETER CONTROL. (INFLUENCE OF GAIN VALUE OF THE ACCELEROMETER)

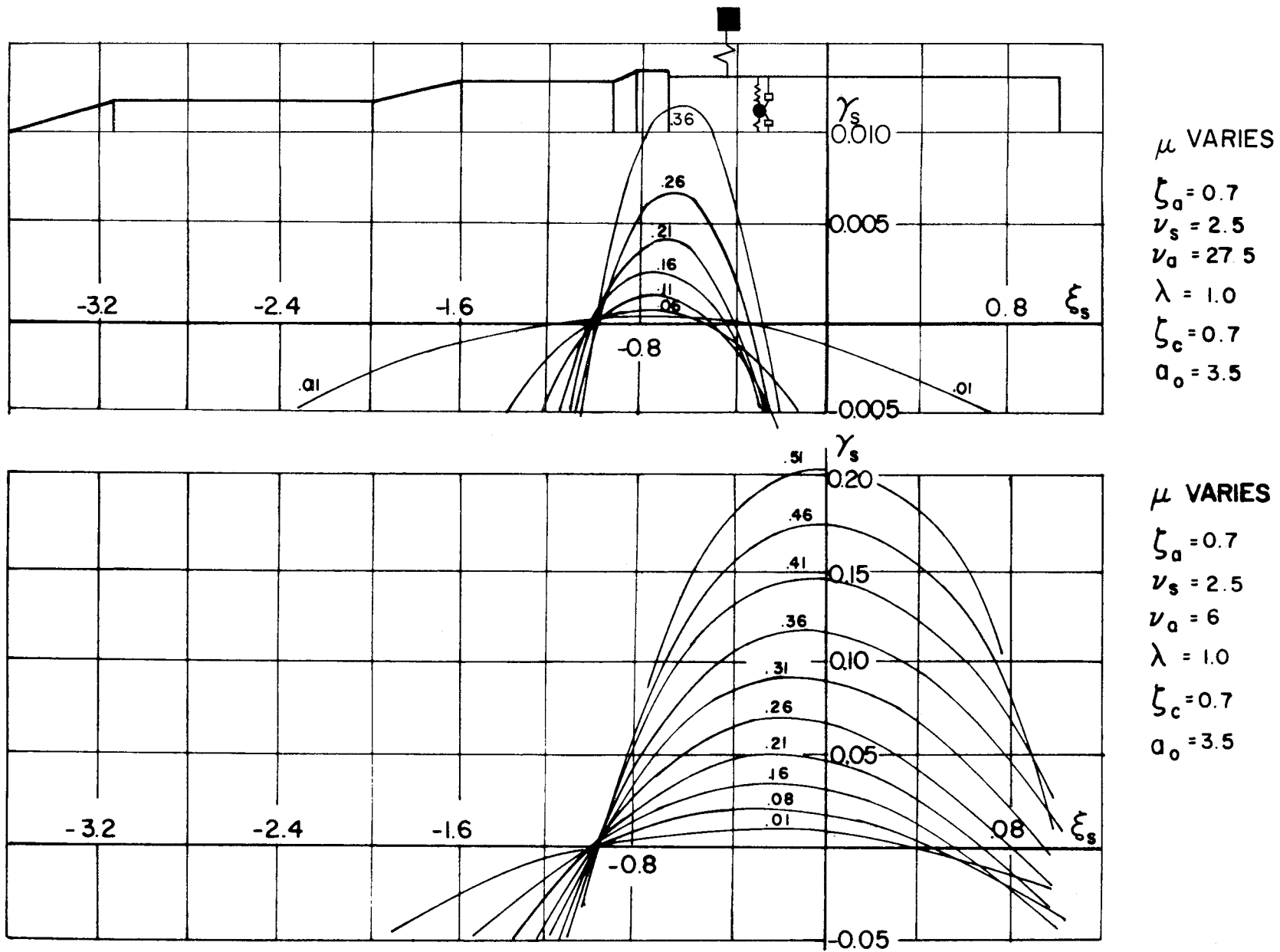


FIGURE 33. STABILITY BOUNDARIES OF RIGID SPACE VEHICLE WITH ADDITIONAL ACCELEROMETER CONTROL OF VARIOUS EIGEN FREQUENCIES

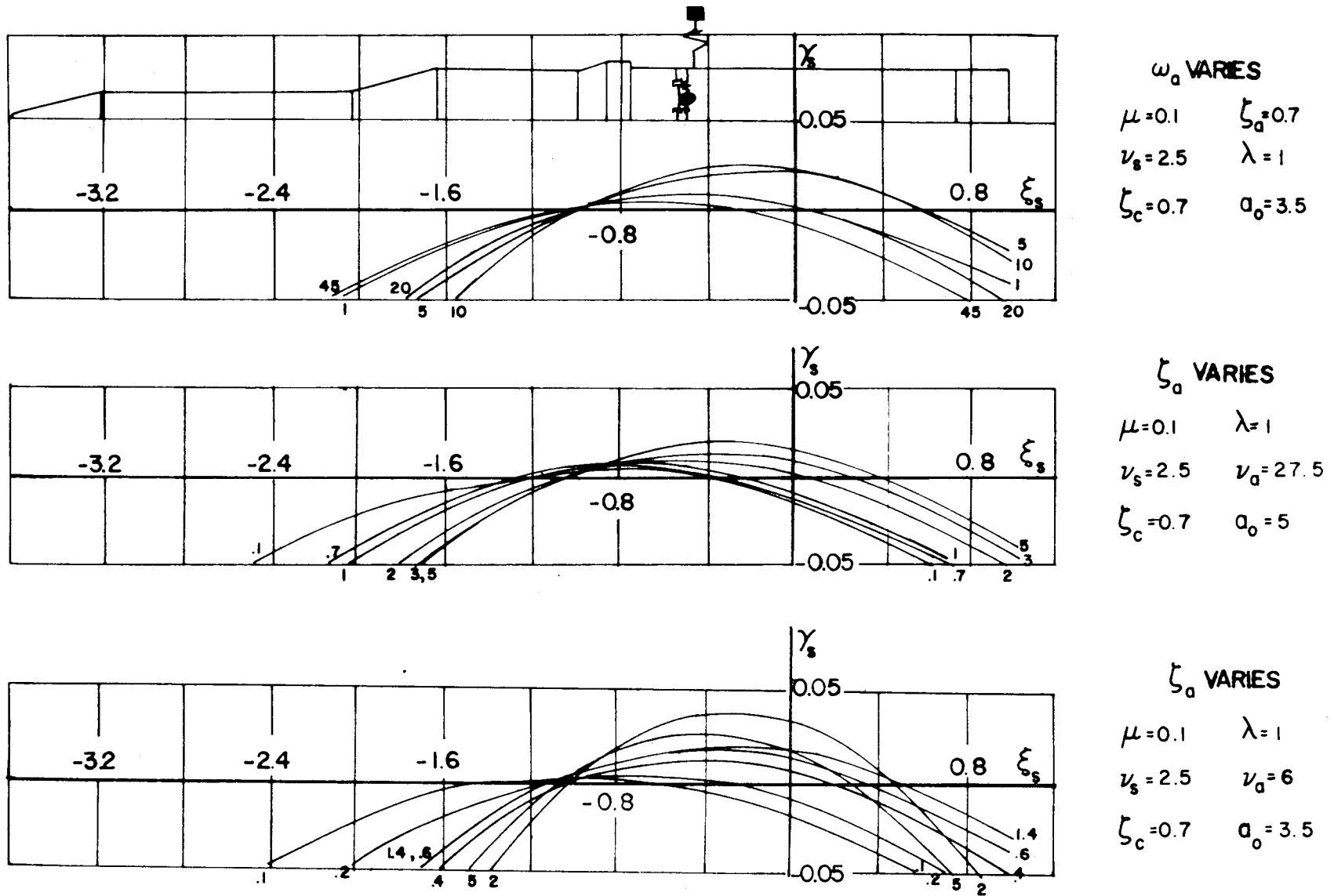


FIGURE 34. STABILITY BOUNDARIES OF RIGID SPACE VEHICLE WITH ADDITIONAL ACCELEROMETER CONTROL OF VARIOUS VIBRATIONAL CHARACTERISTICS

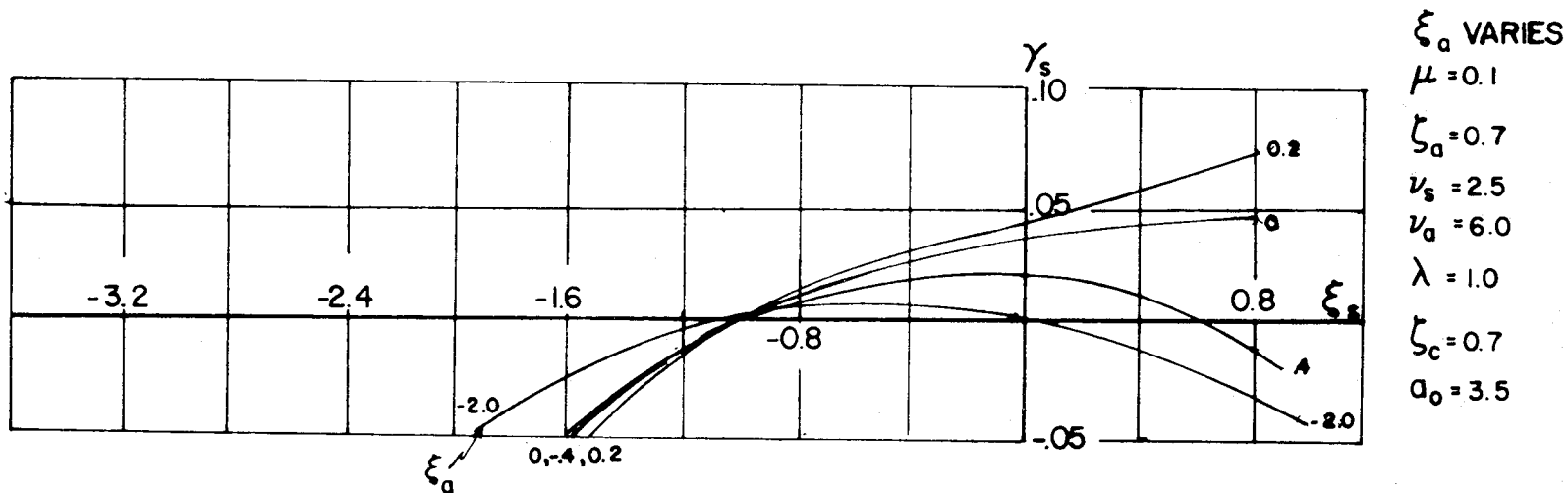
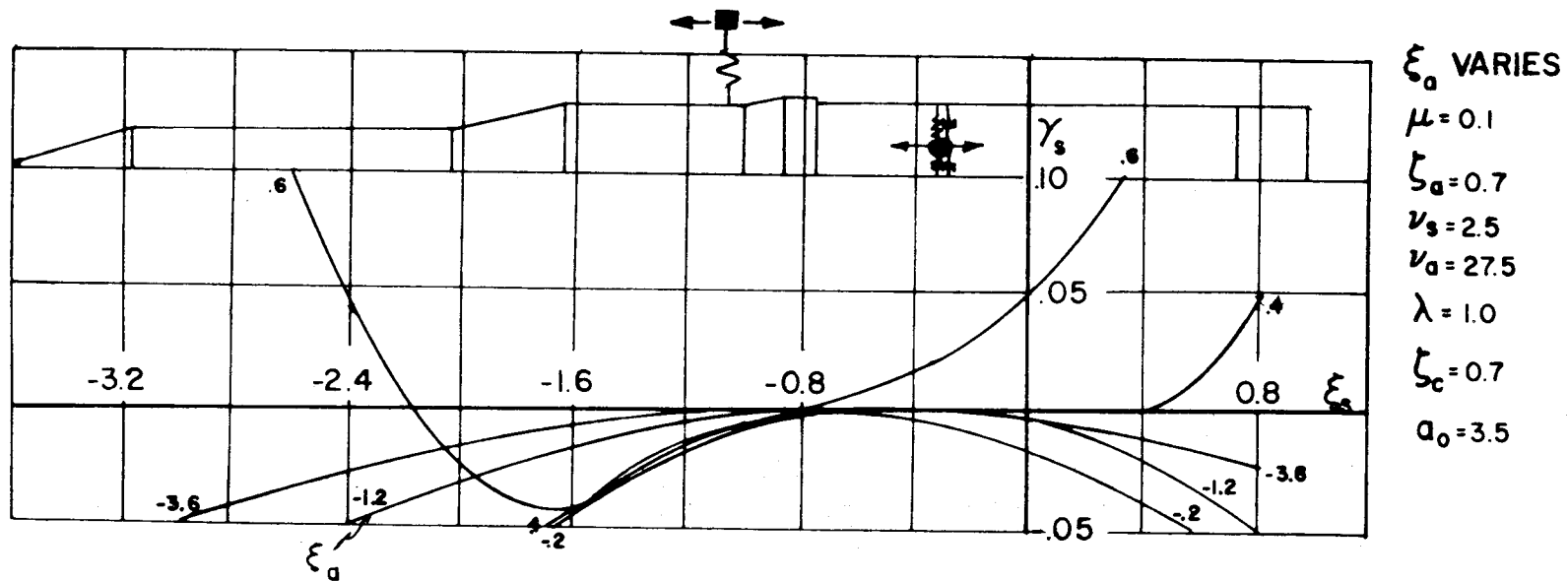


FIGURE 35. STABILITY BOUNDARIES OF RIGID SPACE VEHICLE WITH ADDITIONAL ACCELEROMETER CONTROL (INFLUENCE OF THE LOCATION OF THE ACCELEROMETER)

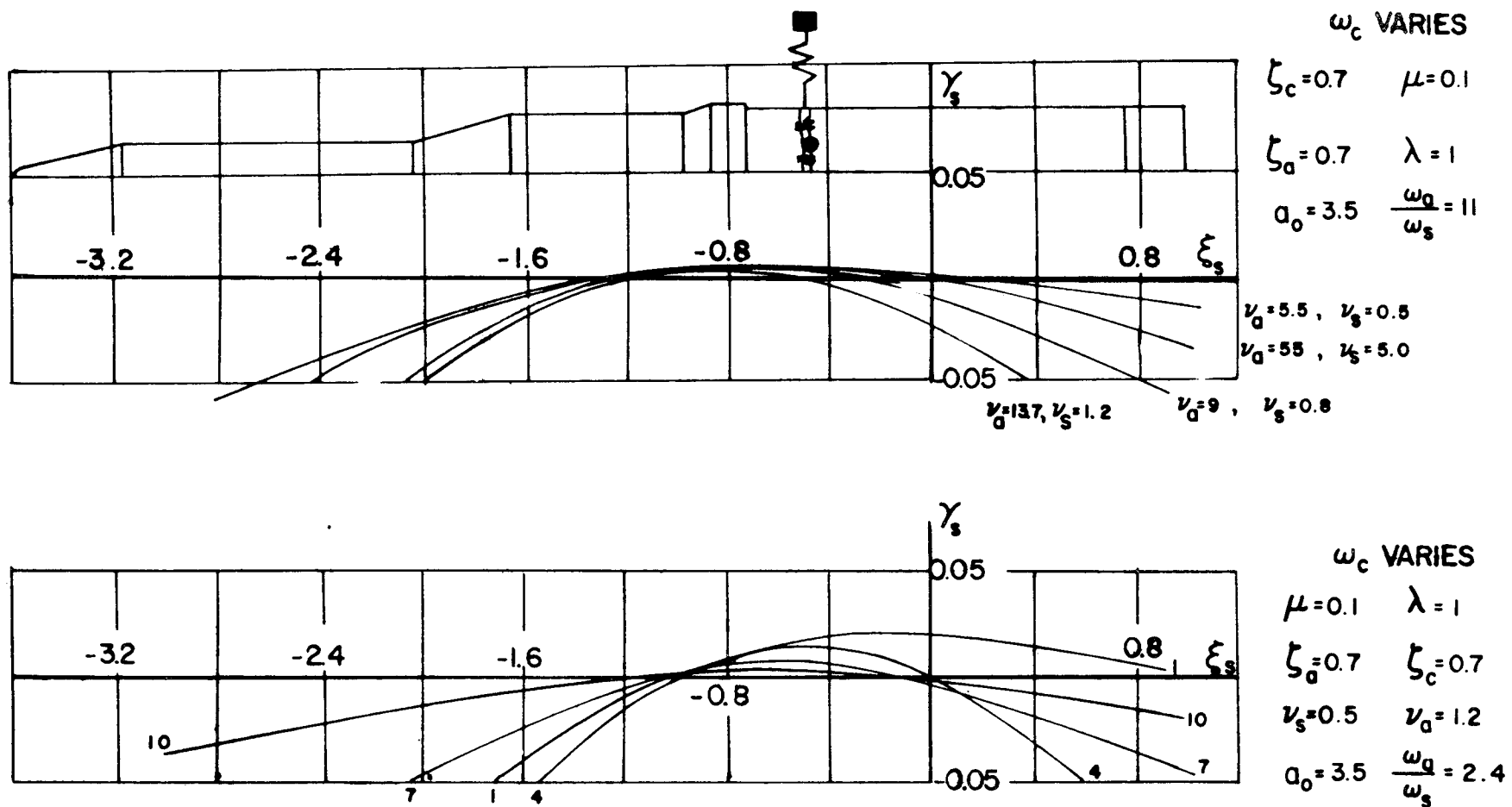


FIGURE 36. STABILITY BOUNDARIES OF A RIGID SPACE VEHICLE WITH ADDITIONAL ACCELEROMETER CONTROL. (INFLUENCE OF THE CONTROL FREQUENCY)

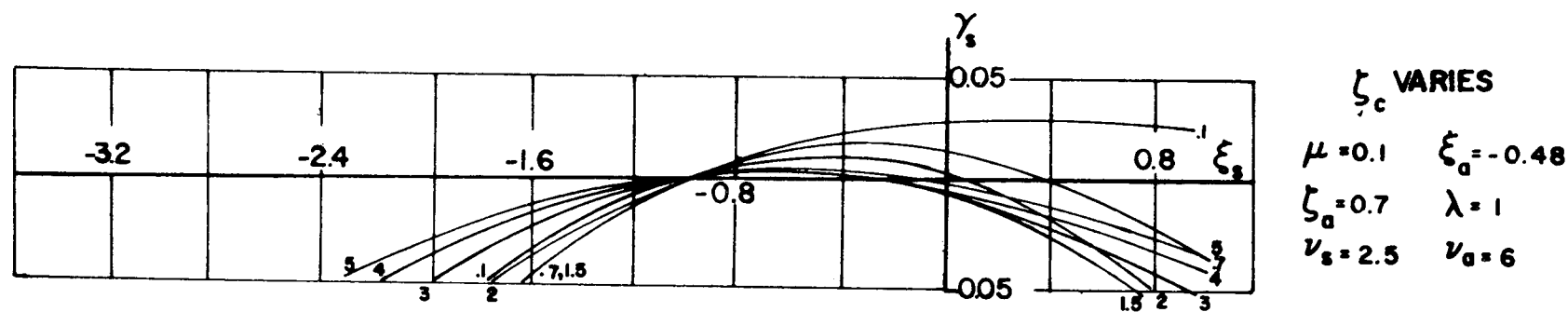
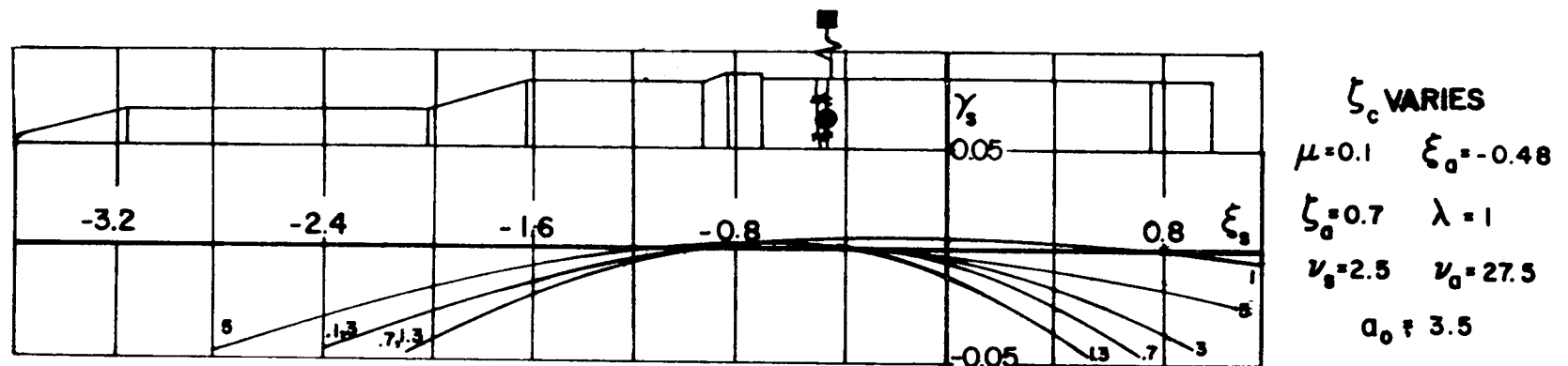


FIGURE 37. STABILITY BOUNDARIES OF A RIGID SPACE VEHICLE WITH ADDITIONAL ACCELEROMETER CONTROL. (INFLUENCE OF THE CONTROL DAMPING)

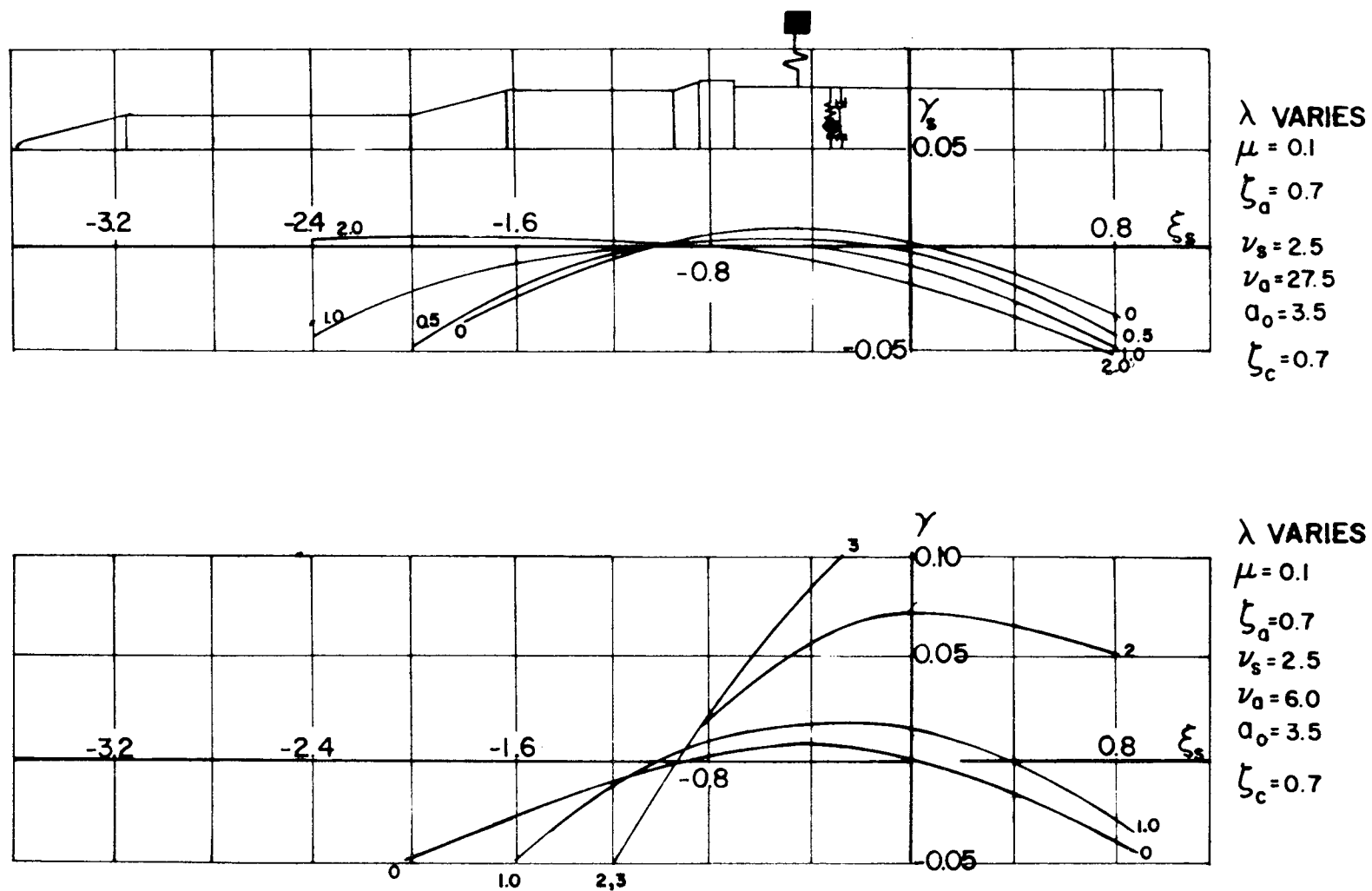


FIGURE 38. STABILITY BOUNDARIES OF A RIGID SPACE VEHICLE WITH ADDITIONAL ACCELEROMETER CONTROL. (INFLUENCE OF THE GAIN VALUE OF THE ACCELEROMETER)

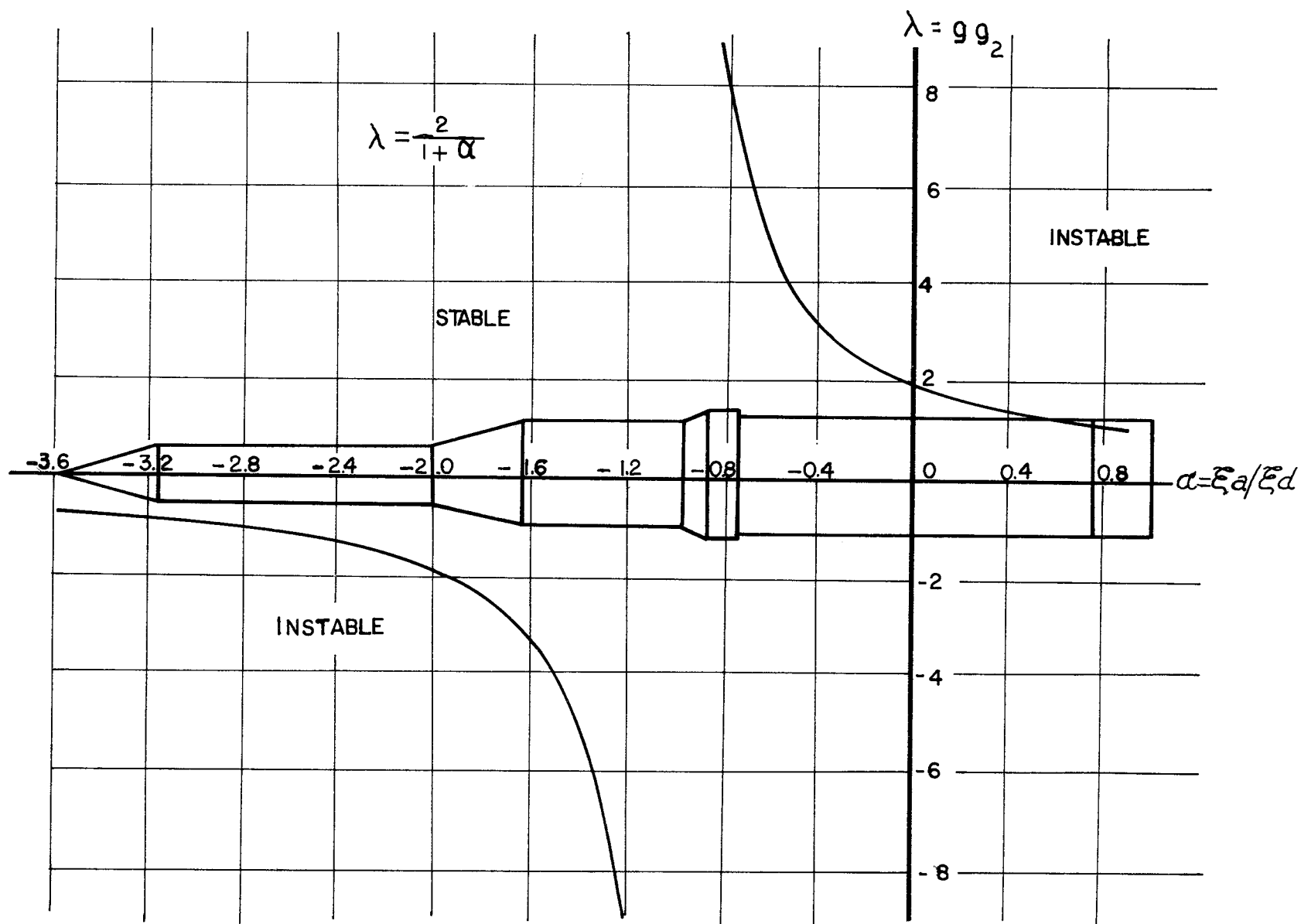


FIGURE 39. STABILITY BOUNDARIES OF A RIGID SPACE VEHICLE WITH ADDITIONAL ACCELEROMETER CONTROL (WITHOUT SLOSHING OF THE PROPELLANT)

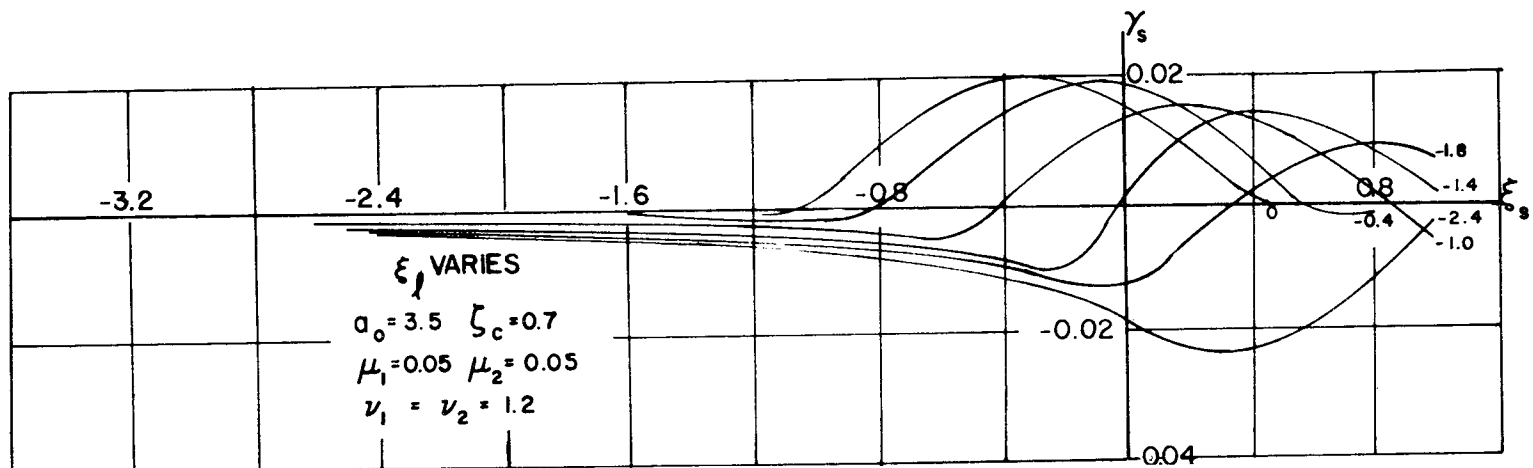
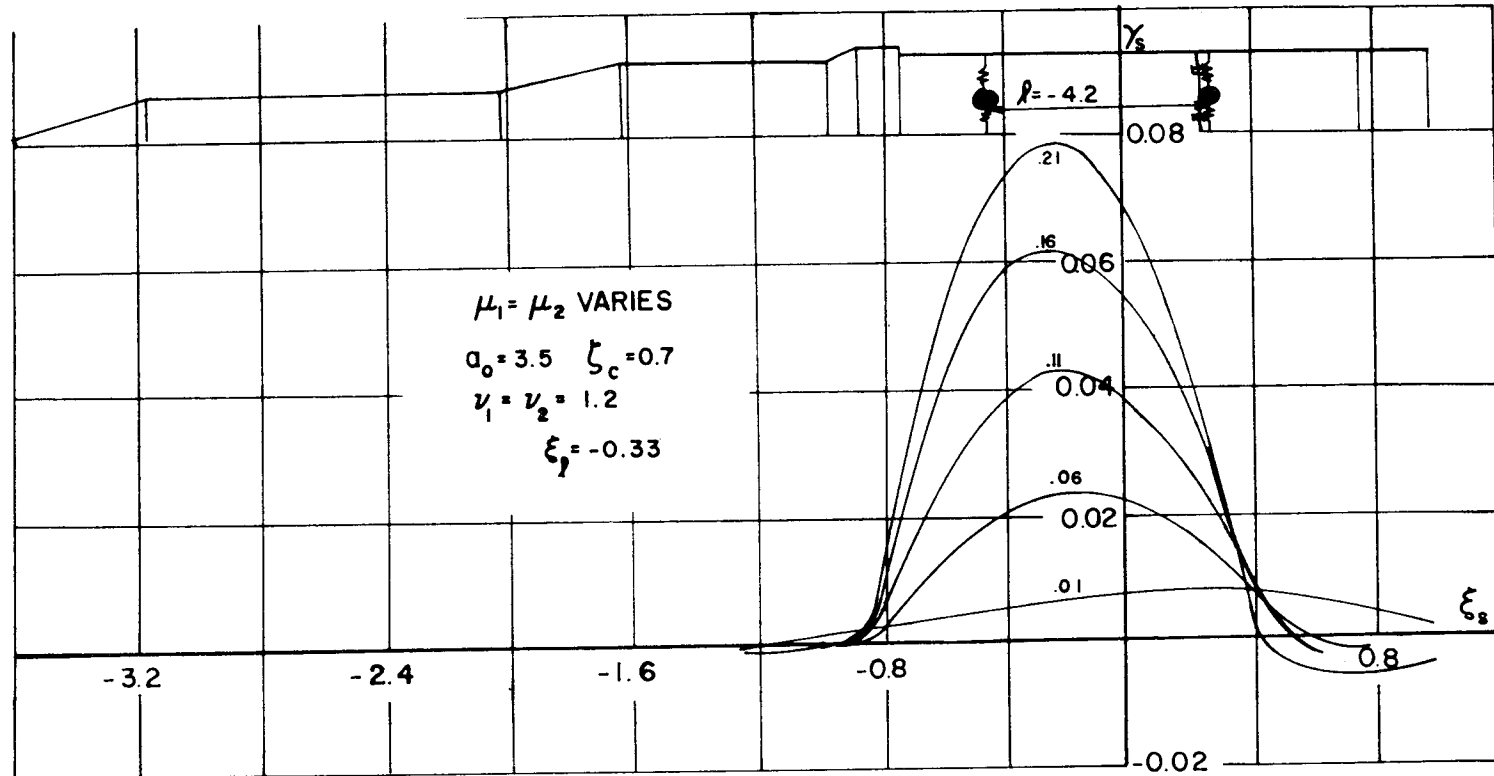


FIGURE 40. STABILITY BOUNDARIES OF A RIGID SPACE VEHICLE WITH SIMPLE CONTROL SYSTEM AND PROPELLANT SLOSHING IN TWO TANKS

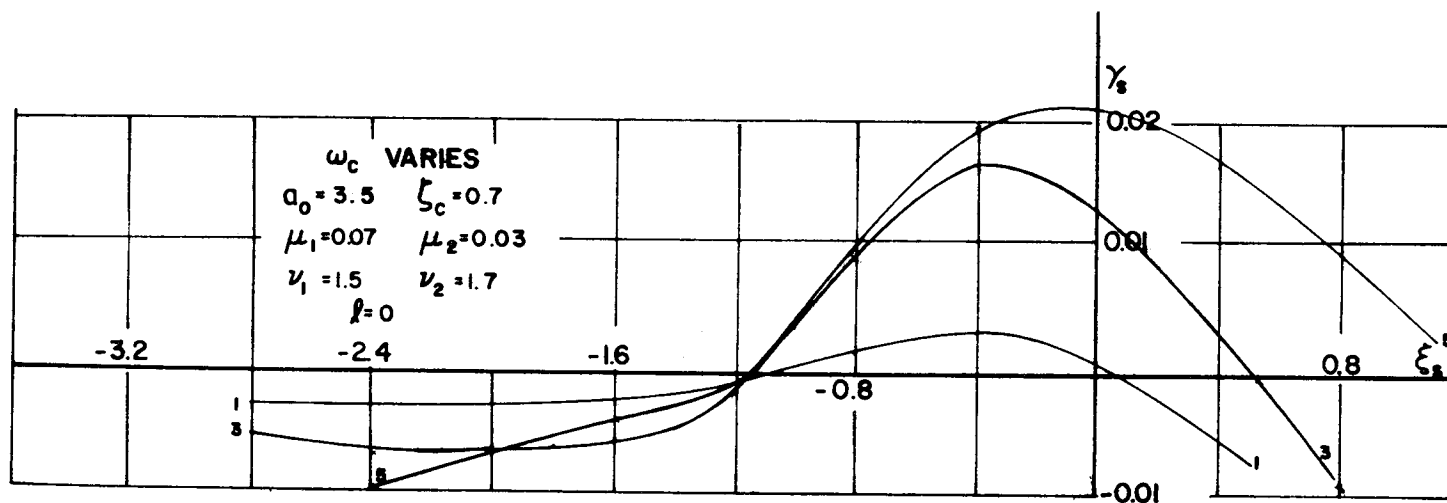
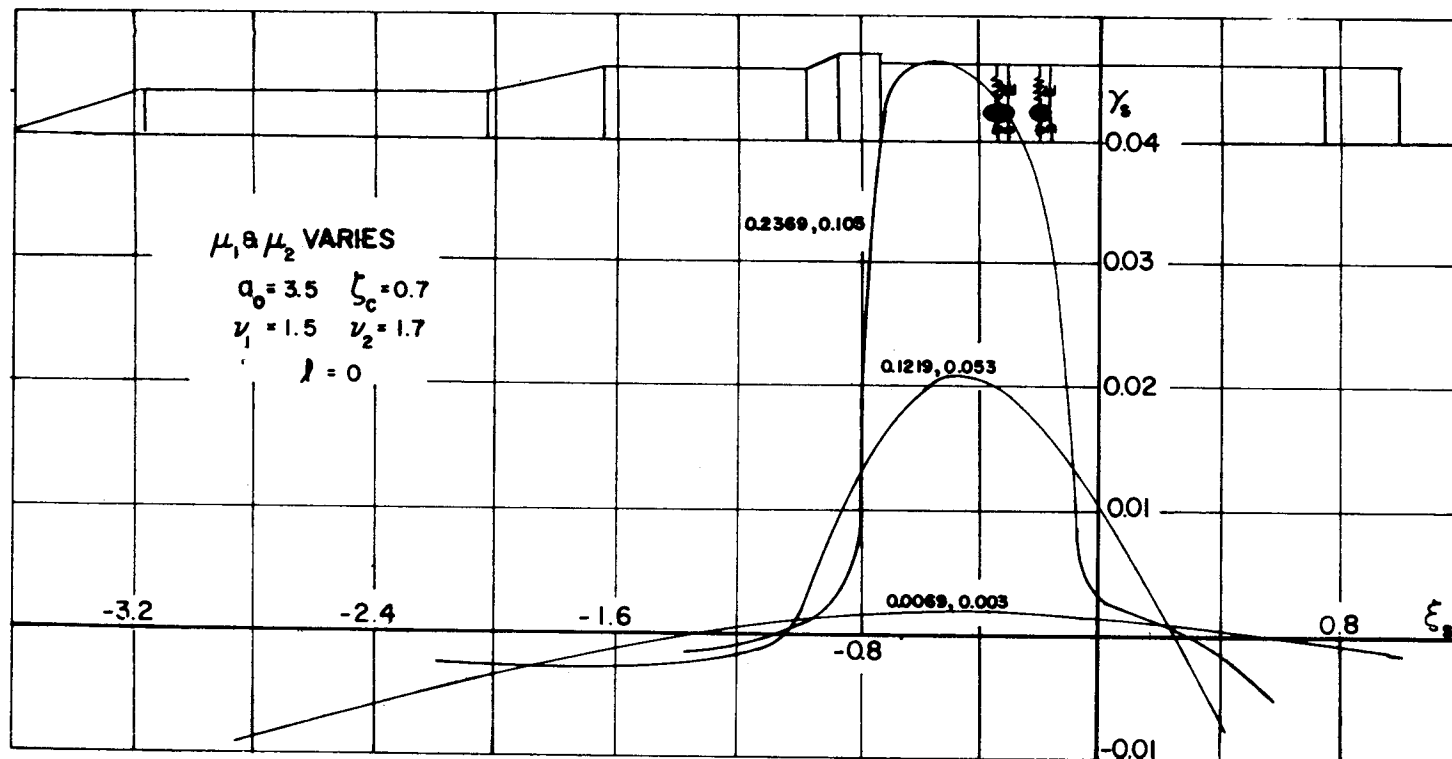


FIGURE 41. STABILITY BOUNDARIES OF A RIGID SPACE VEHICLE WITH SIMPLE CONTROL SYSTEM IN FOUR TANKS

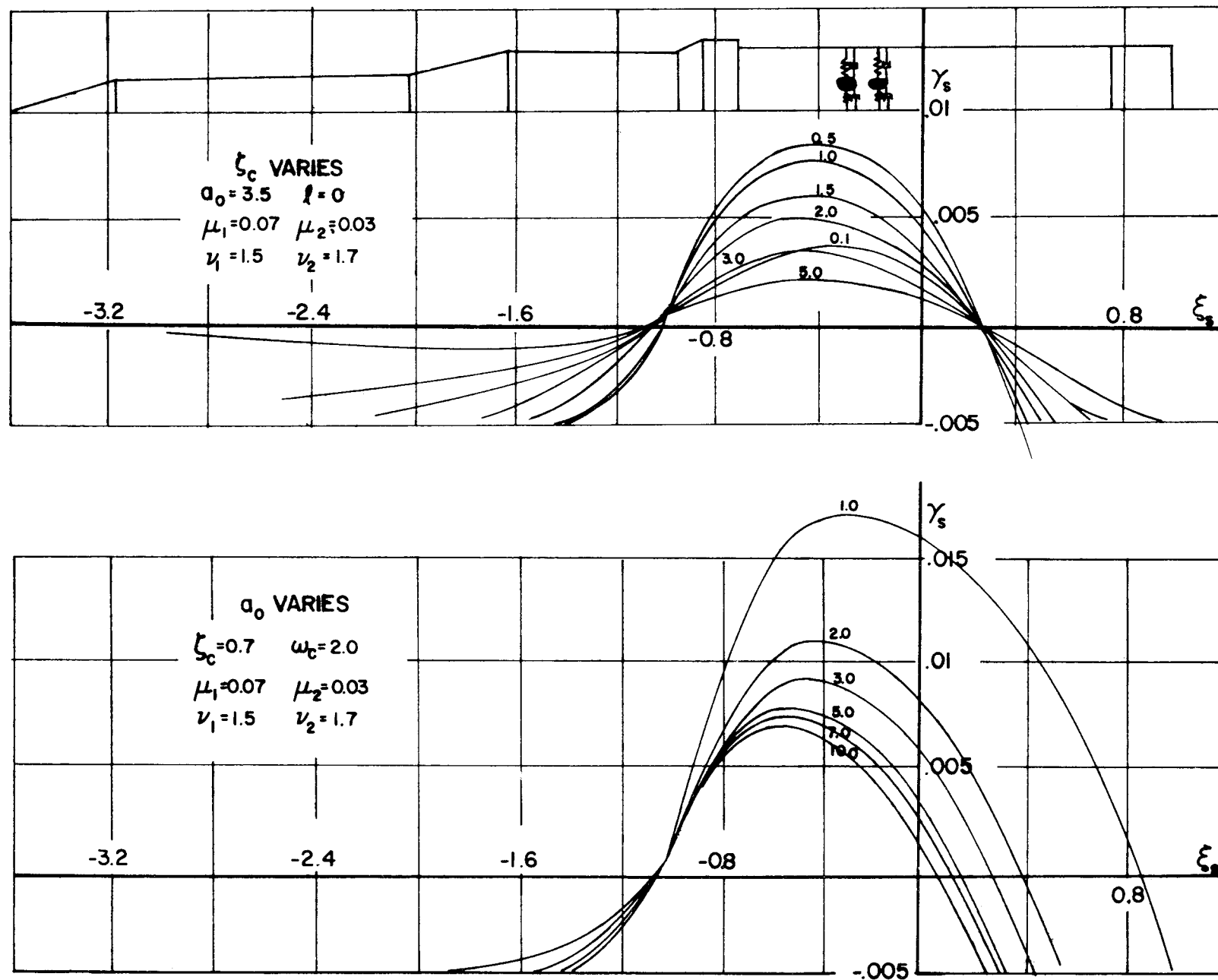


FIGURE 42. STABILITY BOUNDARIES OF A RIGID SPACE VEHICLE WITH SIMPLE CONTROL SYSTEM IN FOUR TANKS

APPENDIX

A. ROOTS OF CERTAIN BESSEL FUNCTIONS.

For the previous results, the roots of

$$\Delta_{\frac{m}{2\alpha}}(\xi) = \begin{vmatrix} J'_{\frac{m}{2\alpha}}(\xi) & Y'_{\frac{m}{2\alpha}}(\xi) \\ J'_{\frac{m}{2\alpha}}(k\xi) & Y'_{\frac{m}{2\alpha}}(k\xi) \end{vmatrix} = 0$$

for $m = 0, 1, 2, \dots$ and arbitrary $0 \leq k < 1$, must be known. For most of these roots J. McMahon represents an asymptotic expansion [16].

The lowest root, however, was not known, until H. Buchholz pointed out its existence [17]. In Reference [18] D. Kirkman represents the roots of the above determinant for $m/2\alpha = 0, 1, 2, 3$ and 4. In the numerical evaluation of fluid oscillations in circular cylindrical containers one needs to know the roots of $J'_{\frac{m}{2\alpha}}(\epsilon) = 0$ and $\Delta_{\frac{m}{2\alpha}}(\xi) = 0$

for various diameter ratios $0 \leq k < 1$. For $\Delta_1(\xi) = 0$ the roots have been numerically determined and are represented for $0 \leq k \leq 0.9$ in steps of $\Delta k = 0.1$ [10]. The roots of $J'_{\frac{2m}{2\alpha}}(\epsilon) = 0$ which occur in the case of a container of circular quarter cross sections are given in Table 4.

1. The Representation of Various Functions $f(r)$ in Bessel Series:

The determinant $C_{m/2\alpha}$ is

$$C_{\frac{m}{2\alpha}}(\lambda_{mn} r) = \begin{vmatrix} J_{\frac{m}{2\alpha}}(\lambda_{mn} r) & Y_{\frac{m}{2\alpha}}(\lambda_{mn} r) \\ J'_{\frac{m}{2\alpha}}(\lambda_{mn} a) & Y'_{\frac{m}{2\alpha}}(\lambda_{mn} a) \end{vmatrix}$$

Its derivative

$$C'_{\frac{m}{2\alpha}}(\lambda_{mn} r) = \begin{vmatrix} J'_{\frac{m}{2\alpha}}(\lambda_{mn} r) & Y'_{\frac{m}{2\alpha}}(\lambda_{mn} r) \\ J'_{\frac{m}{2\alpha}}(\lambda_{mn} a) & Y'_{\frac{m}{2\alpha}}(\lambda_{mn} a) \end{vmatrix}$$

is equal to zero for $r = a$ and for $r = b$. For $r = a$ it vanishes identically and for $r = b$ because of the roots $\xi_{mn} = \lambda_{mn} a$.

A function $f(r)$ being piecewise regular in $b \leq r \leq a$, is satisfying the Dirichlet Conditions, can be expanded in a Bessel-Fourier series

$$f(r) \approx \sum_{n=0}^{\infty} b_{mn} C_{\frac{m}{2\alpha}}(\lambda_{mn} r) \quad m = 0, 1, 2 \dots$$

The unknown coefficients of the expansion are obtained by multiplying both sides of this equation with $r C_{\frac{m}{2\alpha}}(\lambda_{mp} r)$ and integrating from $r = b$ to $r = a$, ($\lambda_{mp} \neq \lambda_{mn}$).

With the integral of Lommel the integral of the right hand side becomes

$$\int r C_{\frac{m}{2\alpha}}(\lambda_{mn} r) C_{\frac{m}{2\alpha}}(\lambda_{mp} r) dr = \frac{r}{(\lambda_{mn}^2 - \lambda_{mp}^2)} \left\{ \lambda_{mp} C_{\frac{m}{2\alpha}}(\lambda_{mn} r) C'_{\frac{m}{2\alpha}}(\lambda_{mp} r) - \lambda_{mn} C_{\frac{m}{2\alpha}}(\lambda_{mp} r) C'_{\frac{m}{2\alpha}}(\lambda_{mn} r) \right\} \quad (B1)$$

It vanishes, if one of the following conditions are satisfied:

$$1) \quad C_{\frac{m}{2\alpha}}(\lambda_{mn} a) = C_{\frac{m}{2\alpha}}(\lambda_{mp} a) = C_{\frac{m}{2\alpha}}(\lambda_{mn} b) = C_{\frac{m}{2\alpha}}(\lambda_{mp} b) = 0$$

$$2) \quad C'_{\frac{m}{2\alpha}}(\lambda_{mn} a) = C'_{\frac{m}{2\alpha}}(\lambda_{mp} a) = C'_{\frac{m}{2\alpha}}(\lambda_{mn} b) = C'_{\frac{m}{2\alpha}}(\lambda_{mp} b) = 0$$

$$3) \quad \lambda_{mp} C_{\frac{m}{2\alpha}}(\lambda_{mn} a) C'_{\frac{m}{2\alpha}}(\lambda_{mp} a) = \lambda_{mn} C_{\frac{m}{2\alpha}}(\lambda_{mp} a) C'_{\frac{m}{2\alpha}}(\lambda_{mn} a)$$

$$\lambda_{mp} C_{\frac{m}{2\alpha}}(\lambda_{mn} b) C'_{\frac{m}{2\alpha}}(\lambda_{mp} b) = \lambda_{mn} C_{\frac{m}{2\alpha}}(\lambda_{mp} b) C'_{\frac{m}{2\alpha}}(\lambda_{mn} b)$$

In the here treated fluid oscillations the second condition is satisfied, since $\lambda_{mn} a$ and $\lambda_{mn} b$ are roots of the equation $\Delta_{\frac{m}{2\alpha}} = 0$. Therefore those terms vanish for which λ_{mn}

$\neq \lambda_{mp}$ ($n \neq p$) and the coefficients of the expansion are:

$$b_{mn} = \frac{\int_b^a r f(r) C_{\frac{m}{2\alpha}}(\lambda_{mn} r) dr}{\int_b^a r C_{\frac{m}{2\alpha}}^2(\lambda_{mn} r) dr} \quad (B2)$$

For $p = n$ the equation (B1) assumes an undeterminant form of which the value can be obtained either by Taylor series expansion or the rule of L'Hospital and the Bessel differential equation for $C_{m/2\alpha}$.

$$\int r C_{\frac{m}{2\alpha}}^2(\lambda_{mn} r) dr = \frac{r^2}{2} \left\{ C_{\frac{m}{2\alpha}}^2(\lambda_{mn} r) \left[1 - \frac{m^2}{4\alpha^2 \lambda_{mn}^2 r^2} \right] + C_{\frac{m}{2\alpha}}'^2(\lambda_{mn} r) \right\}$$

and it is

$$\int_b^a r \frac{C_m^2}{2\alpha} (\lambda_{mn} r) dr = \frac{a^2}{2} \left[\frac{C_m^2}{2\alpha} (\lambda_{mn} a) \left[1 - \frac{m^2}{4\alpha^2 \lambda_{mn}^2 a^2} \right] + \frac{C_m'^2}{2\alpha} (\lambda_{mn} a) \right] \\ - \frac{b^2}{2} \left[\frac{C_m^2}{2\alpha} (\lambda_{mn} b) \left[1 - \frac{m^2}{4\alpha^2 \lambda_{mn}^2 b^2} \right] + \frac{C_m'^2}{2\alpha} (\lambda_{mn} b) \right]$$

Because of the second boundary condition this integral becomes with $\lambda_{mn} a = \xi_{mn}$

$$\int_b^a r \frac{C_m^2}{2\alpha} (\xi_{mn} \frac{r}{a}) dr = \frac{a^2}{2 \xi_{mn}^2} \left\{ \frac{4}{\pi^2 \xi_{mn}^2} (\xi_{mn}^2 - \frac{m^2}{4\alpha^2}) - \frac{C_m^2}{2\alpha} (k \xi_{mn}) \left(k^2 \xi_{mn}^2 - \frac{m^2}{4\alpha^2} \right) \right\} \quad (B3)$$

Here the value $\frac{C_m}{2\alpha} (\xi_{mn}) = 2/\pi \xi_{mn}$ is the Wronskian Determinant. The coefficient

b_{mn} of the series expansion can therefore be determined from

$$b_{mn} = \frac{2 \xi_{mn}^2 \int_b^a r f(r) \frac{C_m}{2\alpha} (\xi_{mn} \frac{r}{a}) dr}{a^2 \left\{ \frac{4}{\pi^2 \xi_{mn}^2} (\xi_{mn}^2 - \frac{m^2}{4\alpha^2}) - \frac{C_m^2}{2\alpha} (k \xi_{mn}) (k^2 \xi_{mn}^2 - \frac{m^2}{4\alpha^2}) \right\}} \quad (B4)$$

The problem that remains is the solution of the integral

$$\int_b^a r f(r) \frac{C_m}{2\alpha} (\xi_{mn} \frac{r}{a}) dr.$$

Most of the integrals of the previous treatment are of the form

$$\int z^\kappa C_\nu(z) dz.$$

These can be obtained with the help of the Lommel function

$$\int z^{\kappa} C_{\nu}(z) dz = (\kappa + \nu - 1) z C_{\nu}(z) S_{\kappa-1, \nu-1}(z) - z C_{\nu-1}(z) S_{\kappa \nu}(z).$$

The Lommel function is

$$S_{\kappa \nu}(z) = s_{\kappa \nu}(z) + 2^{\kappa-1} \Gamma\left(\frac{\kappa-\nu+1}{2}\right) \Gamma\left(\frac{\kappa+\nu+1}{2}\right) \left\{ \sin\left(\frac{\kappa-\nu}{2} \pi\right) J_{\nu}(z) - \cos\left(\frac{\kappa-\nu}{2} \pi\right) Y_{\nu}(z) \right\},$$

where $s_{\kappa \nu}$ is the particular solution of the nonhomogeneous Bessel equation

$$z^2 \frac{d^2 w}{dz^2} + z \frac{dw}{dz} + (z^2 - \nu^2) w = z^{\kappa+1}$$

and can be represented as

$$s_{\kappa \nu}(z) = z^{\kappa-1} \sum_{\mu=0}^{\infty} \frac{(-1)^{\mu} \left(\frac{z}{2}\right)^{2\mu+2} \Gamma\left(\frac{\kappa-\nu+1}{2}\right) \Gamma\left(\frac{\kappa+\nu+1}{2}\right)}{\Gamma\left(\frac{\kappa-\nu+3}{2} + \mu\right) \Gamma\left(\frac{\kappa+\nu+3}{2} + \mu\right)}.$$

With the recursion formula

$$C_{\nu-1}(z) = C'_{\nu}(z) + \frac{\nu}{z} C_{\nu}(z),$$

we obtain

$$\int z^{\kappa} C_{\nu}(z) dz = (\kappa + \nu - 1) z C_{\nu}(z) S_{\kappa-1, \nu-1}(z) - z S_{\kappa \nu}(z) \left\{ C'_{\nu}(z) + \frac{\nu}{z} C_{\nu}(z) \right\}$$

which results for the integration from

$$z_1 = \xi_{\nu n} \quad \text{to} \quad z_2 = k \xi_{\nu n} \quad (z = \xi_{\nu n} r/a)$$

because of

$$C'_{\nu}(\xi_{\nu n}) = C'_{\nu}(k \xi_{\nu n}) = 0$$

in

$$\int_{k\xi_{\nu n}}^{\xi_{\nu n}} z^{\kappa} C_{\nu}(z) dz = (\kappa + \nu - 1) \xi_{\nu n} \left[S_{\kappa-1, \nu-1}(\xi_{\nu n}) C_{\nu}(\xi_{\nu n}) \right. \\ \left. - k S_{\kappa-1, \nu-1}(k \xi_{\nu n}) C_{\nu}(k \xi_{\nu n}) \right] - \nu \left[S_{\kappa \nu}(\xi_{\nu n}) C_{\nu}(\xi_{\nu n}) \right. \\ \left. - S_{\kappa \nu}(k \xi_{\nu n}) C_{\nu}(k \xi_{\nu n}) \right].$$

We obtain

$$\int_b^a r^{\kappa} C_{\nu}(\xi_{\nu n} \frac{r}{a}) dr = \frac{a^{\kappa+1}}{\xi_{\nu n}^{\kappa}} \left[S_{\kappa-1, \nu-1}(\xi_{\nu n}) \frac{2}{\pi \xi_{\nu n}} - k S_{\kappa-1, \nu-1}(k \xi_{\nu n}) C_{\nu}(k \xi_{\nu n}) \right] \\ - \frac{\nu a^{\kappa+1}}{\xi_{\nu n}^{\kappa+1}} \left[S_{\kappa \nu}(\xi_{\nu n}) \frac{2}{\pi \xi_{\nu n}} - S_{\kappa \nu}(k \xi_{\nu n}) C_{\nu}(k \xi_{\nu n}) \right]. \quad (B5)$$

The representation of the integrals can also be performed by integration of the series expansions

$$\int z^{\kappa} C_{\nu}(z) dz = Y'_{\nu}(\xi_{\nu n}) \int z^{\kappa} J_{\nu}(z) dz - J'_{\nu}(\xi_{\nu n}) \int z^{\kappa} Y_{\nu}(z) dz.$$

Integrating the first integral term by term and collecting terms of $J_{\nu+2\mu+1}$ one obtains

$$\int z^{\kappa} J_{\nu}(z) dz = z^{\kappa} \frac{\Gamma\left(\frac{\kappa+\nu+1}{2}\right)}{\Gamma\left(\frac{\nu-\kappa+1}{2}\right)} \sum_{\mu=0}^{\infty} \frac{(\nu+2\mu+1) \Gamma\left(\frac{\nu-\kappa+1}{2} + \mu\right)}{\Gamma\left(\frac{\nu+\kappa+3}{2} + \mu\right)} J_{\nu+2\mu+1}(z) \quad (B6)$$

where $\text{Re}(\kappa + 2\mu + 1) > 0$ if we integrate from $z = 0$. The second integral is obtained by termwise integration of the series expansion of the Bessel function of second kind.

It is for ($\frac{m}{2\alpha}$ integer)

$$\begin{aligned}
\int z^{\kappa} Y_{\frac{m}{2\alpha}}(z) dz = & - \frac{z^{\kappa+1}}{\pi} \sum_{\mu=0}^{\frac{m}{2\alpha}-1} \frac{(\frac{m}{2\alpha}-\mu-1)! (\frac{z}{2})^{2\mu-\frac{m}{2\alpha}}}{\mu! (\kappa+2\mu-\frac{m}{2\alpha}+1)} \\
& + \frac{2z^{\kappa+1}}{\pi} \sum_{\mu=0}^{\infty} \frac{(-1)^{\mu} (\frac{z}{2})^{\frac{m}{2\alpha}+2\mu}}{\mu! (\frac{m}{2\alpha}+\mu)! (\frac{m}{2\alpha}+\kappa+2\mu+1)} \cdot \left\{ \ln \frac{z}{2} - \frac{1}{2} \psi(\mu+1) \right. \\
& \left. - \frac{1}{2} \psi\left(\mu + \frac{m}{2\alpha} + 1\right) \right\} - \frac{2z^{\kappa+1}}{\pi} \sum_{\mu=0}^{\infty} \frac{(-1)^{\mu} (\frac{z}{2})^{\frac{m}{2\alpha}+2\mu}}{\mu! (\frac{m}{2\alpha}+\mu)! (\frac{m}{2\alpha}+\kappa+2\mu+1)^2}
\end{aligned} \tag{B7}$$

where $\psi(z)$ represents the logarithmic derivative of the gamma function

$$\psi(z) = \frac{d(\ln \Gamma(z))}{dz} = -\gamma + (z-1) \sum_{\lambda=0}^{\infty} \frac{1}{(\lambda+1)(z+\lambda)} .$$

γ is the Euler constant.

It is:

$$\begin{aligned}
& \int_{k \xi_{mn}}^{\xi_{mn}} z^{\kappa} C_{\frac{m}{2\alpha}}(z) dz = Y'_{\frac{m}{2\alpha}}(\xi_{mn}) \xi_{mn}^{\kappa} \frac{\Gamma\left(\frac{m}{4\alpha} + \frac{\kappa}{2} + \frac{1}{2}\right)}{\Gamma\left(\frac{m}{4\alpha} - \frac{\kappa}{2} + \frac{1}{2}\right)} \\
& \sum_{\mu=0}^{\infty} \frac{\left(\frac{m}{2\alpha} + 2\mu + 1\right) \Gamma\left(\frac{m}{4\alpha} - \frac{\kappa}{2} + \frac{1}{2} + \mu\right)}{\Gamma\left(\frac{m}{4\alpha} + \frac{\kappa}{2} + \frac{3}{2} + \mu\right)} \cdot \left[J_{\frac{m}{2\alpha} + 2\mu + 1}(\xi_{mn}) \right. \\
& \left. - k^{\kappa} J_{\frac{m}{2\alpha} + 2\mu + 1}(k\xi_{mn}) \right] - J'_{\frac{m}{2\alpha}}(\xi_{mn}) \left\{ -\frac{\xi_{mn}^{\kappa+1}}{\pi} \cdot \right. \\
& \sum_{\mu=0}^{\left(\frac{m}{2\alpha} - 1\right) \left(\frac{m}{2\alpha} - \mu - 1\right)!} \frac{\xi_{mn}^{2\mu - \frac{m}{2\alpha}} (1 - k^{\kappa + 2\mu - \frac{m}{2\alpha} + 1})}{2^{2\mu - \frac{m}{2\alpha}} (\kappa + 2\mu + 1 - \frac{m}{2\alpha})} - \frac{2 \xi_{mn}^{\kappa+1}}{\pi} \cdot \\
& \sum_{\mu=0}^{\infty} \frac{(-1)^{\mu} \xi_{mn}^{2\mu + \frac{m}{2\alpha}} \left(1 - k^{\kappa + 2\mu + \frac{m}{2\alpha} - 1}\right)}{2^{2\mu + m/2\alpha} \mu! \left(\mu + \frac{m}{2\alpha}\right)! \left(\frac{m}{2\alpha} + \kappa + 2\mu + 1\right)^2} - \frac{2 k^{\kappa+1} \xi_{mn}^{\kappa+1}}{\pi} \cdot \\
& \sum_{\mu=0}^{\infty} \frac{(-1)^{\mu} k^{\frac{m}{2\alpha} + 2\mu} \xi_{mn}^{\frac{m}{2\alpha} + 2\mu}}{2^{2\mu + m/2\alpha} \mu! \left(\mu + \frac{m}{2\alpha}\right)! \left(\frac{m}{2\alpha} + \kappa + 2\mu + 1\right)} \left[\ln\left(\frac{k \xi_{mn}}{2}\right) - \frac{1}{2} \psi(\mu + 1) \right. \\
& \left. - \frac{1}{2} \psi\left(\mu + \frac{m}{2\alpha} + 1\right) \right] + \frac{2 \xi_{mn}^{\kappa+1}}{\pi} \sum_{\mu=0}^{\infty} \frac{(-1)^{\mu} \xi_{mn}^{2\mu + m/2\alpha}}{2^{2\mu + m/2\alpha} \mu! \left(\mu + \frac{m}{2\alpha}\right)! \left(2\mu + \frac{m}{2\alpha} + \kappa + 1\right)} \left[\ln\left(\frac{\xi_{mn}}{2}\right) \right. \\
& \left. - \frac{1}{2} \psi(\mu + 1) - \frac{1}{2} \psi\left(\mu + \frac{m}{2\alpha} + 1\right) \right] \left. \right\}
\end{aligned} \tag{B8}$$

If one has for $f(r) = \frac{m}{r^{2\alpha}}$ then the integral in the numerator is

$$\int_b^a r^{\frac{m}{2\alpha} + 1} C_{\frac{m}{2\alpha}} \left(\xi_{mn} \frac{r}{a} \right) dr = \frac{a^{\frac{m}{2\alpha} + 2}}{\xi_{mn}^2} \left\{ \frac{2}{\pi \xi_{mn}} - k^{\frac{m}{2\alpha}} C_{\frac{m}{2\alpha}} (k \xi_{mn}) \right\} \quad (B9)$$

and the coefficients of the expansion $r^{m/2\alpha}$

$$r^{\frac{m}{2\alpha}} = \sum_{n=0}^{\infty} d_{mn} C_{\frac{m}{2\alpha}} \left(\xi_{mn} \frac{r}{a} \right)$$

are

$$d_{mn} = \frac{2 \left(\frac{m}{2\alpha} \right) a^{\frac{m}{2\alpha}} \left\{ \frac{2}{\pi \xi_{mn}} - k^{\frac{m}{2\alpha}} C_{\frac{m}{2\alpha}} (k \xi_{mn}) \right\}}{\left\{ \frac{4}{\pi^2 \xi_{mn}^2} \left(\xi_{mn}^2 - \frac{m^2}{4\alpha^2} \right) - C_{\frac{m}{2\alpha}}^2 (k \xi_{mn}) \left(k^2 \xi_{mn}^2 - \frac{m^2}{4\alpha^2} \right) \right\}} \quad (B10)$$

These results were obtained from

$$\begin{aligned} \int z^{\nu+1} C_{\nu}(z) dz &= Y'_{\nu}(\xi_{\nu n}) \int z^{\nu+1} J_{\nu}(z) dz - J'_{\nu}(\xi_{\nu n}) \int z^{\nu+1} Y_{\nu}(z) dz \\ &= Y'_{\nu}(\xi_{\nu n}) z^{\nu+1} J_{\nu+1}(z) - J'_{\nu}(\xi_{\nu n}) z^{\nu+1} Y_{\nu+1}(z) \end{aligned}$$

which can be expressed with the recursion formulas

$$z J_{\nu+1}(z) = \nu J_{\nu}(z) - z J'_{\nu}(z)$$

$$z Y_{\nu+1}(z) = \nu Y_{\nu}(z) - z Y'_{\nu}(z)$$

as

$$\int z^{\nu+1} C_{\nu}(z) dz = \nu z^{\nu} C_{\nu}(z) - z^{\nu+1} C'_{\nu}(z).$$

Introducing the integral limits, we obtain with $C'_\nu(\xi_{\nu n}) = C'_\nu(k \xi_{\nu n}) = 0$

$$\int_{k \xi_{\nu n}}^{\xi_{\nu n}} z^{\nu+1} C_\nu(z) dz = \nu \xi_{\nu n}^\nu \left\{ C_\nu(\xi_{\nu n}) - k^\nu C_\nu(k \xi_{\nu n}) \right\}.$$

Therefore it is

$$\int_b^a r^{\nu+1} C_\nu\left(\xi_{\nu n} \frac{r}{a}\right) dr = \frac{\nu a}{\xi_{\nu n}^2} \left\{ C_\nu(\xi_{\nu n}) - k^\nu C_\nu(k \xi_{\nu n}) \right\} \quad (\text{B11})$$

with which one obtains the integrals of the text:

$$\int_b^a r^2 C_{\frac{m}{2\alpha}}\left(\xi_{mn} \frac{r}{a}\right) dr = a^3 N_2(\xi_{mn}); \quad \int_b^a r C_{\frac{2m-1}{2\alpha}}\left(\xi_{2m-1n} \frac{r}{a}\right) dr = a^2 N_1(\xi_{2m-1n});$$

$$\int_b^a C_{\frac{m}{2\alpha}}\left(\xi_{mn} \frac{r}{a}\right) dr = a N_0(\xi_{mn}).$$

For roll excitation we used the series expansions for $\left(\frac{r}{a}\right)^{\pm 2}$, $\left(\frac{r}{a}\right)^{\pm \left(\frac{2m-1}{2\alpha}\right)}$ in which integrals of the form

$$\int_b^a r^{1-\frac{2m-1}{2\alpha}} C_{\frac{2m-1}{2\alpha}}\left(\xi_{2m-1n} \frac{r}{a}\right) dr, \quad \int_b^a r^3 C_{\frac{2m-1}{2\alpha}}\left(\xi_{2m-1n} \frac{r}{a}\right) dr,$$

$$\int_b^a r^{\frac{2m-1}{2\alpha}+1} C_{\frac{2m-1}{2\alpha}}\left(\xi_{2m-1n} \frac{r}{a}\right) dr, \quad \int_b^a \frac{1}{r} C_{\frac{2m-1}{2\alpha}}\left(\xi_{2m-1n} \frac{r}{a}\right) dr$$

occur. The first two integrals can be determined with the recursion formulas

$$\int z^{1-\nu} C_\nu(z) dz = -z^{1-\nu} C_{\nu-1}(z) = -z^{1-\nu} C'_\nu(z) - z^{-\nu} \nu C_\nu(z)$$

$$\int z^{\nu+1} C_\nu(z) dz = z^{\nu+1} C_{\nu+1}(z) = \nu z^\nu C_\nu(z) - z^{\nu+1} C'_\nu(z)$$

and are with

$$\frac{C'_{\frac{2m-1}{2\alpha}}(\xi_{2m-1n})}{2\alpha} = 0$$

and

$$\frac{C'_{\frac{2m-1}{2\alpha}}(k \xi_{2m-1n})}{2\alpha} = 0$$

$$\int_b^a r^{1-\frac{2m-1}{2\alpha}} C_{\frac{2m-1}{2\alpha}}(\xi_{2m-1n} \frac{r}{a}) dr = - \frac{\left(\frac{2m-1}{2\alpha}\right) a^{2-\frac{2m-1}{2\alpha}}}{\xi_{2m-1n}^2} \left[\frac{2}{\pi \xi_{2m-1n}} - k^{-\frac{2m-1}{2\alpha}} C_{\frac{2m-1}{2\alpha}}(k \xi_{2m-1n}) \right] \quad (B12)$$

$$\int_b^a r^{\frac{2m-1}{2\alpha}+1} C_{\frac{2m-1}{2\alpha}}(\xi_{2m-1n} \frac{r}{a}) dr = \frac{\left(\frac{2m-1}{2\alpha}\right) a^{\frac{2m-1}{2\alpha}+2}}{\xi_{2m-1n}^2} \left[\frac{2}{\pi \xi_{2m-1n}} - k^{\frac{2m-1}{2\alpha}} C_{\frac{2m-1}{2\alpha}}(k \xi_{2m-1n}) \right] \quad (B13)$$

The third and fourth integral is obtained from (B8) by substituting $\nu = m/2\alpha$ by $(2m-1)/2\alpha$ and $\kappa = 3$ and $\kappa = 1$ respectively. In the denominator there appear integrals belonging to the series expansions $(r/a)^{\pm 2}$ and $(r/a)^{\pm \frac{2m-1}{2\alpha}}$. These are obtained with (B3) by substituting $m/2\alpha$ for the values $2m-1/2\alpha$. With this one can determine the coefficient g_{2m-1n} , h_{2m-1n} , l_{2m-1n} and q_{2m-1n} . For $\alpha = 1/4$ there appear series expansions of the form

$$\begin{aligned} \left(\frac{r}{a}\right)^2 \ln\left(\frac{r}{a}\right) &= \sum_{n=0}^{\infty} \beta_n C_2\left(\xi_{2n} \frac{r}{a}\right) \\ \left(\frac{r}{a}\right)^{-2} &= \sum_{n=0}^{\infty} h_n C_2\left(\xi_{2n} \frac{r}{a}\right) \\ \left(\frac{r}{a}\right)^2 &= \sum_{n=0}^{\infty} g_n C_2\left(\xi_{2n} \frac{r}{a}\right) \end{aligned} \quad (B14)$$

The numerator integral for β_n is obtained by integration by parts

$$\begin{aligned} \int_b^a r^3 \ln\left(\frac{r}{a}\right) C_2\left(\xi_{2n} \frac{r}{a}\right) dr &= -\frac{2a^4 k^2 \ln k}{\xi_{2n}^2} C_2(k \xi_{2n}) + \frac{a^4}{\xi_{2n}^2} \left[C_2(\xi_{2n}) - k^2 C_2(k \xi_{2n}) \right] \\ &\quad - \frac{4a^4}{\xi_{2n}^4} \int_{k \xi_{2n}}^{\xi_{2n}} z C_2(z) dz \end{aligned} \quad (B15)$$

The integral

$$\int z C_2(z) dz = Y_2'(\xi_{2n}) \int z J_2(z) dz - J_2'(\xi_{2n}) \int z Y_2(z) dz$$

is with

$$\int z^{\mu+1} \begin{Bmatrix} J_{\nu}(z) \\ Y_{\nu}(z) \end{Bmatrix} dz = -(\mu^2 - \nu^2) \int z^{\mu-1} \begin{Bmatrix} J_{\nu}(z) \\ Y_{\nu}(z) \end{Bmatrix} dz + z^{\mu+1} \begin{Bmatrix} J_{\nu+1}(z) \\ Y_{\nu+1}(z) \end{Bmatrix} + (\mu - \nu) z^{\mu} \begin{Bmatrix} J_{\nu}(z) \\ Y_{\nu}(z) \end{Bmatrix} \quad (\text{B16})$$

and the recursion formula for J_{ν} and Y_{ν}

$$\begin{aligned} \int z C_2(z) dz &= -Y_2'(\xi_{2n}) \left[\frac{4}{z} J_1(z) - z J_2'(z) \right] + J_2'(\xi_{2n}) \left[\frac{4}{z} Y_1(z) - z Y_2'(z) \right] \\ &= z C_2(z) - \frac{4}{z} \left[J_1(z) Y_2'(\xi_{2n}) - Y_1(z) J_2'(\xi_{2n}) \right] \end{aligned} \quad (\text{B17})$$

Applying the recursion formulas

$$z J_{\nu-1}(z) = z J_{\nu}'(z) + \nu J_{\nu}(z)$$

$$z Y_{\nu-1}(z) = z Y_{\nu}'(z) + \nu Y_{\nu}(z)$$

we obtain

$$\int z C_2(z) dz = \frac{4}{z} C_2'(z) + \frac{8}{z^2} C_2(z) \quad (\text{B18})$$

Finally the integral is

$$\begin{aligned} \int_b^a r^3 \ln\left(\frac{r}{a}\right) C_2(\xi_{2n} \frac{r}{a}) dr &= -\frac{2 a^4 k^2 \ln k}{\xi_{2n}^2} C_2(k \xi_{2n}) + \frac{a^4}{\xi_{2n}^2} \left[\frac{2}{\pi \xi_{2n}} - k^2 C_2(k \xi_{2n}) \right] \\ &\quad - \frac{32 a^4}{\xi_{2n}^6} \left[\frac{2}{\pi \xi_{2n}} - k^{-2} C_2(k \xi_{2n}) \right]. \end{aligned} \quad (\text{B19})$$

The values g_n and h_n are obtained from l_{2m-1n} and q_{2m-1n} , if $(2m-1)/2\alpha$ is substituted by 2 and the index $2m-1$ is taken to be 2. The integral in the denominator of the coefficient (β_n, h_n, g_n) is

$$\int_b^a r C_2(\xi_{2n} \frac{r}{a}) dr = \frac{a^2}{2 \xi_{2n}^2} \left[\frac{4}{\pi^2 \xi_{2n}^2} (\xi_{2n}^2 - 4) - C_2^2(k \xi_{2n}) (k^2 \xi_{2n}^2 - 4) \right] \quad (B20)$$

2. Limits for $k \rightarrow 0$. For the determination of the zeros of the function $\Delta_{m/2\alpha}(\xi) = 0$ for $k = b/a \rightarrow 0$ we substitute $m/2\alpha = \nu$ for noninteger values and $m/2\alpha = n$ for integers. The determinant is then

$$\Delta_{\nu}(\xi) = \begin{vmatrix} J'_{\nu}(\xi) & Y'_{\nu}(\xi) \\ J'_{\nu}(k\xi) & Y'_{\nu}(k\xi) \end{vmatrix} = 0.$$

It is

$$J'_{\nu}(\xi) = \frac{J'_{\nu}(k\xi) Y'_{\nu}(\xi)}{Y'_{\nu}(k\xi)}$$

the equation from which the roots are found. For the limit $k \rightarrow 0$, we need the ratio of

$$\lim_{x \rightarrow 0} \left\{ \frac{J'_{\nu}(x)}{Y'_{\nu}(x)} \right\}.$$

For small x

$$J_{\nu}(x) = \sum_{\lambda=0}^{\infty} \frac{(-1)^{\lambda} (x/2)^{\nu+2\lambda}}{\lambda! \Gamma(\nu+\lambda+1)} \simeq \frac{x^{\nu}}{2^{\nu} \Gamma(\nu+1)}$$

for integer and noninteger values of ν . It is

$$J_{-\nu}(x) = \sum_{\lambda=0}^{\infty} \frac{(-1)^{\lambda} (x/2)^{-\nu+2\lambda}}{\lambda! \Gamma(\lambda-\nu+1)} \simeq \frac{x^{-\nu}}{2^{-\nu} \Gamma(1-\nu)}$$

From the definition of the Bessel function of second kind

$$Y_{\nu} = \frac{J_{\nu} \cos \nu \pi - J_{-\nu}}{\sin \nu \pi}$$

and the relation of the gamma function

$$\Gamma(\nu) \cdot \Gamma(1 - \nu) = \frac{\pi}{\sin \pi \nu}$$

we obtain for Y_{ν} for small values x

$$Y_{\nu}(x) \simeq \frac{-2^{\nu} \Gamma(\nu)}{\pi x^{\nu}} \quad \text{for } \nu > 0$$

For integer indices n the Bessel function of the second kind is given by the series expansion

$$Y_n(x) = \frac{2}{\pi} \left\{ \left(\gamma + \ln \frac{x}{2} \right) J_n(x) - \frac{1}{2} \sum_{\lambda=0}^{n-1} \frac{(n-\lambda-1)!}{\lambda!} \left(\frac{2}{x} \right)^{n-2\lambda} - \frac{1}{2} \sum_{\lambda=0}^{\infty} \frac{(-1)^{\lambda} (x/2)^{n+2\lambda}}{\lambda! (n+\lambda)!} \left\{ \psi(\lambda) + \psi(\lambda+n) \right\} \right\}$$

with $\gamma = \lim_{n \rightarrow \infty} \left\{ 1 + \frac{1}{2} + \frac{1}{3} + \dots + \frac{1}{n} - \ln n \right\} \approx 0.5772$ as the Euler constant. The expression $\psi(\lambda)$ is defined by

$$\psi(\lambda) = \sum_{\mu=0}^{\lambda} \frac{1}{\mu}, \quad \psi(0) = 1$$

For small values we obtain, because of $\lim_{x \rightarrow 0} [x^n \cdot \ln x] = 0$ for $n > 0$ the approximated value

$$Y_n(x) \approx \frac{-2^n (n-1)!}{\pi x^n} \quad n = 1, 2, 3, \dots$$

With the recurrence formulas

$$J'_\nu(x) = \frac{1}{2} [J_{\nu-1}(x) - J_{\nu+1}(x)]$$

$$Y'_\nu(x) = \frac{1}{2} [Y_{\nu-1}(x) - Y_{\nu+1}(x)]$$

the derivatives for small values of x are

$$J'_\nu(x) \approx \frac{x^{\nu-1}}{2^{\nu+2}} \left[\frac{4}{\Gamma(\nu)} - \frac{x^2}{\Gamma(\nu+2)} \right] \approx \frac{x^{\nu-1}}{2^\nu \Gamma(\nu)}$$

$$Y'_\nu(x) \approx \frac{2^{\nu-2}}{\pi x^{\nu+1}} \left[4 \Gamma(\nu+1) - x^2 \Gamma(\nu-1) \right] \approx \frac{2^\nu \Gamma(\nu+1)}{\pi x^{\nu+1}}$$

Therefore the ratio becomes

$$\frac{J'_\nu(x)}{Y'_\nu(x)} \approx \frac{\pi x^\nu}{2^{2\nu} \Gamma(\nu) \Gamma(\nu+1)}$$

For the limit $x \rightarrow 0$ ($k \rightarrow 0$) we obtain

$$J'_{m/2\alpha}(\xi) = 0$$

The roots of this equation are expressed by ϵ_{mn} . This means that in the limit $k \rightarrow 0$ the roots $\xi_{mn} \rightarrow \epsilon_{mn}$. It is

$$\lim_{k \rightarrow 0} \left\{ \Delta_{m/2\alpha}(\xi) \right\} = J'_{m/2\alpha}(\xi) \quad \text{and} \quad \lim_{k \rightarrow 0} \xi_{mn} = \epsilon_{mn} \quad (\text{B21})$$

3. $Y'_{m/2\alpha}(\xi_{mn})$ has been taken into the integration constant A_{mn} , B_{mn} .

Therefore we have to consider the limit of

$$\frac{C_{\frac{m}{2\alpha}}(\xi_{mn} \frac{r}{a})}{Y'_{\frac{m}{2\alpha}}(\xi_{mn})}$$

It is

$$\frac{C_{\frac{m}{2\alpha}}(\xi_{mn} \frac{r}{a})}{Y'_{\frac{m}{2\alpha}}(\xi_{mn})} = J_{\frac{m}{2\alpha}}(\xi_{mn} \frac{r}{a}) - \frac{Y_{\frac{m}{2\alpha}}(\xi_{mn} \frac{r}{a}) \cdot J'_{\frac{m}{2\alpha}}(\xi_{mn})}{Y'_{\frac{m}{2\alpha}}(\xi_{mn})}$$

For the limit $k \rightarrow 0$ we obtain, because of (B21) the value

$$\lim_{k \rightarrow 0} \left\{ \frac{C_{\frac{m}{2\alpha}}(\xi_{mn} \frac{r}{a})}{Y'_{\frac{m}{2\alpha}}(\xi_{mn})} \right\} = J_{\frac{m}{2\alpha}}(\epsilon_{mn} \frac{r}{a})$$

This expresses that in the results of the circular cylindrical ring sector container in the limit for the sector tank instead of $C_{\frac{m}{2\alpha}}$ the function $J_{\frac{m}{2\alpha}}$ has to be substituted.

From (B6) we obtain the needed values for a sector tank:

$$L_0(\epsilon_{mn}) = \frac{2}{\epsilon_{mn}} \sum_{\mu=0}^{\infty} J_{2\mu+m/2\alpha+1}(\epsilon_{mn}) \quad (\operatorname{Re} \frac{m}{2\alpha} > -1) \quad (\text{B22})$$

$$L_1(\epsilon_{2m-1n}) = \frac{2m-1}{4\alpha \epsilon_{2m-1n}} \sum_{\mu=0}^{\infty} \frac{\left(\frac{2m-1}{2\alpha} + 2\mu+1 \right)}{\left(\frac{2m-1}{4\alpha} + \mu \right) \left(\frac{2m-1}{4\alpha} + \mu+1 \right)} J_{\frac{2m-1}{2\alpha} + 2\mu+1}(\epsilon_{2m-1n}) \quad (\text{B23})$$

$$L_2(\epsilon_{mn}) = \frac{\Gamma\left(\frac{m}{2\alpha} + \frac{3}{2}\right)}{\epsilon_{mn} \Gamma\left(\frac{m}{4\alpha} - \frac{1}{2}\right)} \sum_{\mu=0}^{\infty} \frac{\left(\frac{m}{2\alpha} + 2\mu + 1\right) \Gamma\left(\frac{m}{2\alpha} + \mu - \frac{1}{2}\right)}{\Gamma\left(\frac{m}{4\alpha} + \mu + \frac{5}{2}\right)} J_{\frac{m}{2\alpha} + 2\mu + 1}(\epsilon_{mn}) \quad (B24)$$

The values f_{2m-1n} are obtained from

$$f_{2m-1n} = \frac{\int_0^a r^{\frac{2m-1}{2\alpha} + 1} J_{\frac{2m-1}{2\alpha}}\left(\epsilon_{2m-1n} \frac{r}{a}\right) dr}{a^{\frac{2m-1}{2\alpha}} \int_0^a r J_{\frac{2m-1}{2\alpha}}^2\left(\epsilon_{2m-1n} \frac{r}{a}\right) dr}.$$

Here it is

$$\int_0^a r J^2(\rho^*) dr = \frac{a^2}{2} \left[1 - \frac{(2m-1)^2}{4\alpha^2 \epsilon_{2m-1n}^2} \right] \frac{J_{\frac{2m-1}{2\alpha}}^2(\epsilon_{2m-1n})}{2\alpha}$$

and

$$\int_0^a r^{\frac{2m-1}{2\alpha} + 1} J(\rho^*) dr = \frac{\left(\frac{2m-1}{2\alpha}\right) a^{\frac{2m-1}{2\alpha} + 2}}{\epsilon_{2m-1n}^2} J_{\frac{2m-1}{2\alpha}}(\epsilon_{2m-1n}).$$

It is therefore

$$f_{2m-1n} = \frac{2 \left(\frac{2m-1}{2\alpha}\right)}{\left[\epsilon_{2m-1n}^2 - \left(\frac{2m-1}{2\alpha}\right)^2 \right] \frac{J_{\frac{2m-1}{2\alpha}}(\epsilon_{2m-1n})}{2\alpha}}. \quad (B25)$$

The values e_{2m-1n} in the series expansion

$$\left(\frac{r}{a}\right)^2 = \sum_{n=0}^{\infty} e_{2m-1n} \frac{J_{\frac{2m-1}{2\alpha}}(\epsilon_{2m-1n} \frac{r}{a})}{\frac{2m-1}{2\alpha}}$$

are

$$e_{2m-1n} = \frac{\int_0^a r^3 J_{\frac{2m-1}{2\alpha}}(\epsilon_{2m-1n} \frac{r}{a}) dr}{a^2 \int_0^a r J_{\frac{2m-1}{2\alpha}}^2(\epsilon_{2m-1n} \frac{r}{a}) dr}$$

The numerator integral is obtained from (B6) and e_{2m-1n} is therefore

$$e_{2m-1n} = \frac{2 \epsilon_{2m-1n} \left(\frac{2m-1}{4\alpha}\right) \left(\frac{2m-1}{4\alpha} - 1\right) \left(\frac{2m-1}{4\alpha} + 1\right)}{\left[\epsilon_{2m-1n}^2 - \left(\frac{2m-1}{2\alpha}\right)^2\right] \frac{J_{\frac{2m-1}{2\alpha}}^2(\epsilon_{2m-1n})}{\frac{2m-1}{2\alpha}}} \sum_{\mu=0}^{\infty} \frac{\left(\frac{2m-1}{2\alpha} + 2\mu + 1\right) J_{\frac{2m-1}{2\alpha} + 2\mu + 1}(\epsilon_{2m-1n})}{\left(\frac{2m-1}{4\alpha} + \mu - 1\right) \left(\frac{2m-1}{2\alpha} + \mu\right) \left(\frac{2m-1}{2\alpha} + \mu + 1\right) \left(\frac{2m-1}{2\alpha} + \mu + 2\right)} \quad (B26)$$

In a quarter tank the values f_n and e_n require the integrals

$$\begin{aligned} \int_0^a r^3 \ln\left(\frac{r}{a}\right) J_2(\epsilon_{2n} \frac{r}{a}) dr \\ \int_0^a r^3 J_2(\epsilon_{2n} \frac{r}{a}) dr &= \frac{2a^4}{\epsilon_{2n}^2} J_2(\epsilon_{2n}) \\ \int_0^a r J_2^2(\epsilon_{2n} \frac{r}{a}) dr &= \frac{a^2}{2\epsilon_{2n}^2} (\epsilon_{2n}^2 - 4) J_2^2(\epsilon_{2n}) . \end{aligned}$$

The first integral is obtained by integration by parts and application of (B6)

$$\int_0^a r^3 \ln \left(\frac{r}{a} \right) J_2 \left(\epsilon_{2n} \frac{r}{a} \right) dr = - \frac{4a^4}{\epsilon_{2n}^2} \sum_{\mu=0}^{\infty} \frac{J_{2\mu+4}(\epsilon_{2n})}{(\mu+1)(\mu+3)} \quad (\text{B27})$$

The remaining integrals are obtained from (B6).

4. Some Series of the Roots of Bessel Functions. During the course of the introduction of equivalent damping into the result of the ideal fluid theory a few formulas had to be brought into the form of those of the mechanical model. Certain series expansions of the roots of Bessel functions had been used, which will be derived here. The expansion of r/a into a Bessel Fourier-Series was (B6)

$$\frac{r}{a} = 2 \sum_{n=0}^{\infty} \frac{J_1 \left(\epsilon_n \frac{r}{a} \right)}{(\epsilon_n^2 - 1) J_1(\epsilon_n)} \quad (\text{B28})$$

with which we obtain for $r = a$

$$\sum_{n=0}^{\infty} \frac{1}{(\epsilon_n^2 - 1)} = \frac{1}{2} \quad (\text{B29})$$

Expansion of r^3 in a Bessel-Fourier Series in the Interval $0 \leq r \leq a$ results in

$$r^3 = \sum_{n=0}^{\infty} \alpha_n J_1 \left(\epsilon_n \frac{r}{a} \right)$$

where

$$\alpha_n = \frac{\int_0^a r^4 J_1 \left(\epsilon_n \frac{r}{a} \right) dr}{\int_0^a r J_1^2 \left(\epsilon_n \frac{r}{a} \right) dr} .$$

The integral of the numerator can be obtained from (B6) if one takes $\kappa = 4$ and $\nu = 1$ with the recursion formulas of the Bessel functions and $J_1(\epsilon_n) = 0$ it is

$$\int_0^a r^4 J_1\left(\epsilon_n \frac{r}{a}\right) dr = \frac{a^5}{\epsilon_n^4} (3 \epsilon_n^2 - 8) J_1(\epsilon_n). \quad (\text{B30})$$

Therefore

$$\alpha_n = 2 a^3 \frac{3 \epsilon_n^2 - 8}{\epsilon_n^2 (\epsilon_n^2 - 1) J_1(\epsilon_n)}$$

the series expansion of the function $(r/a)^3$ is

$$\left(\frac{r}{a}\right)^3 = 2 \sum_{n=0}^{\infty} \frac{(3 \epsilon_n^2 - 8) J_1\left(\epsilon_n \frac{r}{a}\right)}{\epsilon_n^2 (\epsilon_n^2 - 1) J_1(\epsilon_n)}. \quad (\text{B31})$$

For $r = a$ we obtain

$$1 = 2 \left\{ \frac{3}{2} - 8 \sum_{n=0}^{\infty} \frac{1}{\epsilon_n^2 (\epsilon_n^2 - 1)} \right\}$$

from which we conclude that

$$\sum_{n=0}^{\infty} \frac{1}{\epsilon_n^2 (\epsilon_n^2 - 1)} = \frac{1}{8} \quad (\text{B32})$$

and

$$\sum_{n=0}^{\infty} \frac{1}{\epsilon_n^2} = \frac{3}{8} \quad (\text{B33})$$

B. EFFECTIVE MOMENT OF INERTIA OF THE LIQUID

In the description of liquid oscillations as a mechanical model, the effective moment of the fluid in a completely filled and closed container has to be known. This problem can be solved by oscillating the completely closed container about the coordinate

axis. The solution is obtained from the Laplace equation with the boundary conditions (for excitation about the y-axis)

$$\frac{\partial \Phi}{\partial r} = i \Omega \Theta_o e^{i \Omega t} z \cos \varphi \quad \text{at the tank walls } r = a, b$$

$$\frac{\partial \Phi}{\partial z} = i \Omega \Theta_o e^{i \Omega t} r \cos \varphi \quad \text{at the tank bottom and tank top } z = -h/2 \\ z = h/2$$

$$\frac{\partial \Phi}{r \partial \varphi} = 0 \quad \text{at the sector wall } \varphi = 0$$

$$\frac{\partial \Phi}{r \partial \varphi} = i \Omega \Theta_o e^{i \Omega t} z \sin \bar{\alpha} \quad \text{at the sector wall } \varphi = \bar{\alpha}.$$

The velocity potential is

$$\Phi(r, \varphi, z, t) = i \Omega \Theta_o e^{i \Omega t} \left\{ -r z \cos \varphi + \frac{2a a_m b_{mn} \sin h \zeta \cos \bar{\varphi}}{\xi_{mn} \cos h(\kappa/2)} C_{\frac{m}{2} \alpha}(\rho) \right\}. \quad (C1)$$

The pressure distribution is obtained from

$$p = -\bar{\rho} \frac{\partial \Phi}{\partial t} + g \bar{\rho} \left[\left(\frac{h}{2} \right) - z + \Theta_o e^{i \Omega t} (a - r \cos \varphi) \right]$$

and is

$$p = \bar{\rho} \Omega^2 \Theta_o e^{i \Omega t} \left\{ -r z \cos \varphi + \frac{2a a_m b_{mn} \sin h \zeta \cos \bar{\varphi} C(\rho)}{\xi_{mn} \cos h(\kappa/2)} \right\} \\ + \bar{\rho} g \left[\frac{h}{2} - z + \Theta_o e^{i \Omega t} (a - r \cos \varphi) \right]. \quad (C2)$$

With this the various pressure distributions at the tank wall can be obtained. The following represent the various moments

$$M_x = - \int_0^{\bar{\alpha}} \int_{-h/2}^{+h/2} [ap_a - bp_b] z \sin \varphi d\varphi dz - \int_0^{\bar{\alpha}} \int_b^a (p_u - p_o) r^2 \sin \varphi d\varphi dr$$

$$+ \int_b^a \int_{-h/2}^{+h/2} z p_{\varphi=o} dr dz - \int_b^a \int_{-h/2}^{+h/2} z p_{\varphi=\bar{\alpha}} \cos \bar{\alpha} dr dz$$

$$M_y = \int_0^{\bar{\alpha}} \int_{-b/2}^{+b/2} [ap_a - bp_b] z \cos \varphi d\varphi dz + \int_0^{\bar{\alpha}} \int_b^a (p_u - p_o) r^2 \cos \varphi d\varphi dr$$

$$- \int_b^a \int_{-h/2}^{+h/2} p_{\varphi=\bar{\alpha}} z \sin \bar{\alpha} dr dz.$$

They are

$$M_x = -m \Omega^2 \Theta_o e^{i\Omega t} a^2 \left\{ \frac{1}{4} (1+k^2) \frac{\sin^2 \bar{\alpha}}{\bar{\alpha}} + \frac{4a_m b_{mn} [(-1)^m \cos \bar{\alpha} - 1]}{a \bar{\alpha} (1-k^2) \xi_{mn}^2} \right.$$

$$\left[\left(1 - \frac{2 \tanh h(\kappa/2)}{\kappa} \right) \cdot \left(\frac{\bar{\alpha}^2}{m^2 \pi^2 - \bar{\alpha}^2} \left[\frac{2}{\pi \xi_{mn}} - k C_{\frac{m}{2\alpha}} (k \xi_{mn}) \right] + N_o (\xi_{mn}) \right) \right.$$

$$\left. \left. - \frac{2 \bar{\alpha}^2 \xi_{mn}^2 N_2 (\xi_{mn})}{(m^2 \pi^2 - \bar{\alpha}^2) \kappa} \tanh h(\kappa/2) \right] \right\} - \frac{2 m g a}{3} \frac{(1 - \cos \bar{\alpha})}{\bar{\alpha}} \frac{(1+k+k^2)}{(1+k)} . \quad (C3)$$

and

$$M_y = -m\Omega^2 \Theta_o e^{i\Omega t} a^2 \left\{ \frac{1}{12} \left(\frac{h}{a} \right)^2 \frac{(1+k^2)}{4} \left(1 + \frac{\sin \bar{\alpha} \cos \bar{\alpha}}{\bar{\alpha}} \right) + \frac{4a_m b_{mn} (-1)^m \sin \bar{\alpha}}{\bar{\alpha} a (1-k^2) \xi_{mn}^2} \right. \\ \left. \left[\left(1 - \frac{2 \tan h (\kappa/2)}{\kappa} \right) \left(\frac{\bar{\alpha}^2}{m^2 \pi^2 - \alpha^2} \left[\frac{2}{\pi \xi_{mn}} - k \frac{C_m}{2\alpha} (k \xi_{mn}) \right] + N_o (\xi_{mn}) \right) \right. \right. \\ \left. \left. - \frac{2\bar{\alpha}^2 \xi_{mn}^2 N_2 (\xi_{mn})}{(m^2 \pi^2 - \bar{\alpha}^2) \kappa} \tan h (\kappa/2) \right] \right\} + \frac{2 m g a}{3} \frac{\sin \bar{\alpha}}{\bar{\alpha}} \frac{(1+k+k^2)}{(1+k)} . \quad (C4)$$

For a container which is roll excited about the z-axis, the Laplace equation has to be solved with the boundary conditions

$$\frac{\partial \Phi}{\partial r} = 0 \quad \text{at the tank walls } r = a, b$$

$$\frac{\partial \Phi}{\partial z} = 0 \quad \text{at the tank bottom and top } z = -h/2 \\ z = h/2$$

$$\frac{\partial \Phi}{r \partial \varphi} = i \Omega \varphi_o \text{ re }^{i\Omega t} \quad \text{at the sector walls } \varphi = 0, \bar{\alpha}.$$

The velocity potential is given in (Eq. 41) if we omit the double summation. The moment about the z-axis is given in Table 1; therefore the effective moment of inertia of the liquid about the z-axis is

$$I_{z \text{ eff}} = m a^2 \left\{ \frac{1+k^2}{2} + \frac{32 \bar{\alpha}}{(2m-1) [(2m-1)^2 \pi^2 - \bar{\alpha}^2]} \left[\frac{\alpha (1+k^2)}{2m-1} \right. \right. \\ \left. \left. - \frac{\left(1 - k \frac{2m-1}{2\alpha} + 2 \right)^2 / \left(\frac{2m-1}{2\alpha} + 2 \right) - \left(k^2 - k \frac{2m-1}{2\alpha} \right)^2 / \left(\frac{2m-1}{2\alpha} - 2 \right)}{\left(1 - k \frac{2m-1}{2\alpha} \right) (1-k^2)} \right] \right\}$$

The first term is the moment of inertia of the rigid body and the ratio of the moment of inertia of the liquid to that of the rigid body is

$$\frac{I_{z \text{ eff}}}{I_{z0}} = 1 - \frac{64 \bar{\alpha}}{\pi} \sum_{m=1}^{\infty} \left\{ \frac{\left(\frac{2m-1}{2\alpha} + 2 \right)^2}{\left(1 - k^4 \right) \left(1 - k^{\frac{2m-1}{2\alpha}} \right) \left(\frac{2m-1}{2\alpha} + 2 \right)} - \frac{\left(k^2 - k^{\frac{2m-1}{2\alpha}} \right)^2}{(1 - k^4) \left(1 - k^{\frac{2m-1}{2\alpha}} \right) \left(\frac{2m-1}{2\alpha} - 2 \right) - \frac{\alpha}{2m-1}} \right\} \frac{1}{[(2m-1)^2 \pi^2 - 4\bar{\alpha}^2] (2m-1)} \quad (C5)$$

The last terms in equations C3 and C4 represent the static moments, because the co-ordinates of the center of gravity of the undisturbed liquid are

$$\xi_s = \frac{2}{3} a \frac{\sin \bar{\alpha}}{\bar{\alpha}} \frac{(1+k+k^2)}{(1+k)}$$

$$\eta_s = \frac{2}{3} a \frac{(1 - \cos \bar{\alpha})}{\bar{\alpha}} \frac{(1+k+k^2)}{(1+k)} .$$

The effective moment of inertia of liquid about y-axis is therefore

$$I_{y \text{ eff}} = m a^2 \left\{ \frac{1}{12} \left(\frac{h}{a} \right)^2 - \frac{(1+k^2)}{4} \left(1 + \frac{\sin \bar{\alpha} \cos \bar{\alpha}}{\bar{\alpha}} \right) + \frac{4(-1)^m a_m b_{mn} \sin \bar{\alpha}}{a \bar{\alpha} (1-k^2) \xi_{mn}^2} \right. \\ \cdot \left[\left(1 - \frac{2 \tanh (\kappa/2)}{\kappa} \right) \cdot \left(\frac{\bar{\alpha}^2}{m^2 \pi^2 - \bar{\alpha}^2} \left[\frac{2}{\pi \xi_{mn}} - k C_{\frac{m}{2\alpha}} (k \xi_{mn}) \right] + N_o (\xi_{mn}) \right) \right. \\ \left. \left. - \frac{2 \bar{\alpha}^2 \xi_{mn}^2 N_2 (\xi_{mn}) \tanh (\kappa/2)}{(m^2 \pi^2 - \bar{\alpha}^2) \kappa} \right] \right\} \quad (C6)$$

and about the x-axis

$$I_{x\text{eff}} = m a^2 \left\{ \frac{1+k^2}{4} \frac{\sin^2 \bar{\alpha}}{\bar{\alpha}} + \frac{4 a_m b_{mn} [(-1)^m \cos \bar{\alpha} - 1]}{a \bar{\alpha} (1-k^2) \xi_{mn}^2} \cdot \left[\left(1 - \frac{2 \tanh (\kappa/2)}{\kappa} \right) \right. \right. \\ \left. \cdot \left(\frac{\bar{\alpha}^2}{m^2 \pi^2 - \bar{\alpha}^2} \left[\frac{2}{\pi \xi_{mn}} - k C_{\frac{m}{2\alpha}} (k \xi_{mn}) \right] + N_o (\xi_{mn}) \right) - \frac{2 \bar{\alpha}^2 \xi_{mn}^2 N_2 (\xi_{mn}) \tanh (\kappa/2)}{(m^2 \pi^2 - \bar{\alpha}^2) \kappa} \right] \right\} \quad (C7)$$

Since the moment of inertia of the rigid body

$$I_{yo} = m a^2 \left\{ \frac{1}{12} \left(\frac{h}{a} \right)^2 + \frac{1+k^2}{4} \left(1 + \frac{\sin \bar{\alpha} \cos \bar{\alpha}}{\bar{\alpha}} \right) \right\} \\ I_{xo} = m a^2 \left\{ \frac{1}{12} \left(\frac{h}{a} \right)^2 + \frac{1+k^2}{4} \left(1 - \frac{\sin \bar{\alpha} \cos \bar{\alpha}}{\bar{\alpha}} \right) \right\}$$

The ratio of the effective moment of the liquid to that of the rigid body can be obtained easily from these results. For oscillations about the x-axis similar results can be obtained.

For a container with circular cylindrical sector cross section corresponding values for the effective moment of inertia can be obtained by substituting N_o and N_2 by L_o and L_2 . The roots ξ_{mn} transform into ϵ_{mn} and for the value $[2/\pi \xi_{mn} - k C_{\frac{m}{2\alpha}} (k \xi_{mn})]$ has to be substituted by $J_{\frac{m}{2\alpha}} (\epsilon_{mn})$. For a container of circular cross section ($\alpha = 1$) the ratio of the moment of inertia is

$$\frac{I_{y\text{eff}}}{I_{yo}} = 1 - \frac{\frac{1}{2} + 4 \sum_{n=0}^{\infty} \frac{\left[1 - \frac{4}{\epsilon_n h/a} \tanh \frac{\epsilon_n h}{2} \right]}{\epsilon_n^2 (\epsilon_n^2 - 1)}}{\frac{1}{12} \left(\frac{h}{a} \right)^2 + \frac{1}{4}} \quad (C8)$$

which approaches, for $h \rightarrow 0$ and $h \rightarrow \infty$, the value one.

CYLINDRICAL TANK WITH RING SECTOR CROSS-SECTION

Excitation in y-Direction $y(t) = y_0 e^{i\Omega t}$		Excitation in y-Direction $y(t) = y_0 e^{i\Omega t}$		Excitation About y-Axis $\Theta(t) = \Theta_0 e^{i\Omega t}$ and x-Axis $x(t) = x_0 e^{i\Omega t}$									
Fluid Force in x-Direction	$F_x = m\Omega^2 y_0 e^{i\Omega t} \frac{(-1)^{m+1} c_{mn} b_{mn} \eta^2 \sin \tilde{\alpha} \tanh \kappa}{m^2 \alpha (1-k^2) (1-\eta^2) \kappa} \cdot \left\{ \frac{\tilde{\alpha}^2}{\pi^2 \pi^2 - \tilde{\alpha}^2} \left[\frac{2}{\pi \xi_{mn}} - kC \frac{m}{2\alpha} (k\xi_{mn}) \right] + N_0(\xi_{mn}) \right\}$ $N_0(\xi_{mn}) = \frac{1}{\alpha+1} \int_b^a r \frac{C}{m} \left(\frac{\xi_{mn}}{2\alpha} \right) dr = \frac{1}{\xi_{mn}} \frac{1}{\kappa+1} \int_{k\xi_{mn}}^{\xi_{mn}} z \frac{C}{m} (z) dz$ $= \frac{Y}{m} \frac{1}{2\alpha} (\xi_{mn}) \frac{\Gamma(\frac{m}{4\alpha} + \frac{\kappa}{2} + \frac{1}{2})}{\xi_{mn} \Gamma(\frac{m}{4\alpha} - \frac{\kappa}{2} + \frac{1}{2})} \sum_{\mu=0}^{\infty} \frac{(\frac{m}{2\alpha} + 2\mu + 1) \Gamma(\frac{m}{4\alpha} - \frac{\kappa}{2} + \frac{1}{2} + \mu)}{\Gamma(\frac{m}{4\alpha} + \frac{\kappa}{2} + \frac{3}{2} + \mu)} \left[\frac{J_{\frac{m}{2\alpha} + 2\mu + 1}(\xi_{mn})}{\xi_{mn}} \right.$ $\left. - k \frac{J_{\frac{m}{2\alpha} + 2\mu + 1}(\xi_{mn})}{2\mu + 1} + \frac{J_{\frac{m}{2\alpha}}(\xi_{mn})}{2\alpha} \left(\frac{1}{\pi} \sum_{\mu=0}^{\infty} \frac{(\frac{m}{2\alpha} - 1) (\frac{m}{2\alpha} - \mu - 1)! \xi_{mn}^{2\mu - \frac{m}{2\alpha}} (1 - k^2 \mu + 2\mu - \frac{m}{2\alpha} + 1)}{2^{2\mu - \frac{m}{2\alpha}} (\kappa + 2\mu + 1 - \frac{m}{2\alpha})} \right) \right.$ $\left. + \frac{2}{\pi} \sum_{\mu=0}^{\infty} \frac{(-1)^\mu \xi_{mn}^{2\mu + \frac{m}{2\alpha}} (1 - k^2 \mu + 2\mu + \frac{m}{2\alpha} - 1)}{2^{2\mu + \frac{m}{2\alpha}} \mu! (\mu + \frac{m}{2\alpha})! (\frac{m}{2\alpha} + \kappa + 2\mu + 1)^2} + \frac{2k}{\pi} \sum_{\mu=0}^{\infty} \frac{(-1)^\mu k^{\frac{m}{2\alpha} + 2\mu} \xi_{mn}^{2\mu}}{2^{2\mu + \frac{m}{2\alpha}} \mu! (\mu + \frac{m}{2\alpha})! (\frac{m}{2\alpha} + \kappa + 2\mu + 1)} \right.$ $\left. \left[\ln \left(\frac{k\xi_{mn}}{2} \right) - \frac{1}{2} \psi(\mu + 1) - \frac{1}{2} \psi \left(\mu + \frac{m}{2\alpha} + 1 \right) \right] - \frac{2}{\pi} \sum_{\mu=0}^{\infty} \frac{(-1)^\mu \xi_{mn}^{2\mu + \frac{m}{2\alpha}}}{2^{2\mu + \frac{m}{2\alpha}} \mu! (\mu + \frac{m}{2\alpha})! (2\mu + \frac{m}{2\alpha} + \kappa + 1)} \right.$ $\left. \left[\ln \left(\frac{\xi_{mn}}{2} \right) - \frac{1}{2} \psi(\mu + 1) - \frac{1}{2} \psi \left(\mu + \frac{m}{2\alpha} + 1 \right) \right] \right\}$	Fluid Force in y-Direction	$F_y = m\Omega^2 y_0 e^{i\Omega t} \left\{ 1 - \frac{2c_{mn} b_{mn} \eta^2 [1 - (-1)^m \cos \tilde{\alpha}]}{\tilde{\alpha} \alpha (1-k^2) (1-\eta^2)} \right.$ $\frac{\tanh \kappa}{\kappa} \cdot \left(\frac{\tilde{\alpha}^2}{\pi^2 \pi^2 - \tilde{\alpha}^2} \left[\frac{2}{\pi \xi_{mn}} - kC \frac{m}{2\alpha} (k\xi_{mn}) \right] + N_0(\xi_{mn}) \right) \left. \right\}$	Moment About y-Axis	$M_y = m\Omega^2 a y_0 e^{i\Omega t} \left\{ \left(\frac{1+k^2}{4} \right) \frac{\sin^2 \tilde{\alpha}}{\tilde{\alpha}} + \frac{\sin \tilde{\alpha}}{\tilde{\alpha} \alpha} \right.$ $\frac{(-1)^{m+1} c_{mn} b_{mn} \eta^2}{(1-k^2) \xi_{mn} (1-\eta^2)} \cdot \left(\left[\tanh \kappa + \frac{2}{\kappa} \right] \cdot \left(\frac{1}{\cosh \kappa} - 1 \right) \cdot \left[\frac{\tilde{\alpha}^2}{(m^2 \pi^2 - \tilde{\alpha}^2)} \left(\frac{2}{\pi \xi_{mn}} - kC \frac{m}{2\alpha} (k\xi_{mn}) \right) + N_0(\xi_{mn}) \right] + \frac{2\tilde{\alpha}^2 \xi_{mn}^2}{(m^2 \pi^2 - \tilde{\alpha}^2) \kappa \cosh \kappa} \right.$ $\left. \frac{N_2(\xi_{mn})}{\kappa \cosh \kappa} \right\} + 2mg \frac{a}{3} \frac{\sin \tilde{\alpha}}{\tilde{\alpha}} \cdot \frac{(1-k^2)}{(1-k^2)} \left. \right\}$	Moment About x-Axis	$M_x = -m\Omega^2 a y_0 e^{i\Omega t} \left\{ \left(\frac{1+k^2}{4} \right) \left(1 + \frac{\sin \tilde{\alpha} \cos \tilde{\alpha}}{2} \right) - \frac{1}{\tilde{\alpha} \alpha} \right.$ $\frac{c_{mn} b_{mn} [1 - (-1)^m \cos \tilde{\alpha}] \eta^2}{(1-k^2) \xi_{mn} (1-\eta^2)} \cdot \left(\left[\tanh \kappa + \frac{2}{\kappa} \right] \cdot \left(\frac{1}{\cosh \kappa} - 1 \right) \cdot \left[\frac{\tilde{\alpha}^2}{(m^2 \pi^2 - \tilde{\alpha}^2)} \left(\frac{2}{\pi \xi_{mn}} - kC \frac{m}{2\alpha} (k\xi_{mn}) \right) + N_0(\xi_{mn}) \right] + \frac{2\tilde{\alpha}^2 \xi_{mn}^2}{(m^2 \pi^2 - \tilde{\alpha}^2) \kappa \cosh \kappa} \right.$ $\left. \frac{N_2(\xi_{mn})}{\kappa \cosh \kappa} \right\} - 2mg \frac{a}{3} \frac{(1 - \cos \tilde{\alpha})}{\tilde{\alpha}} \cdot \frac{(1-k^2)}{(1-k^2)} \left. \right\}$		$F_y = -mg \left\{ \frac{0}{x_0} \frac{i\Omega t}{4m\Omega^2} \left(\frac{\Theta_0}{x_0} \right) e^{i\Omega t} \frac{A_{mn} \sinh \left(\frac{\kappa}{2} \right) [1 - (-1)^m \cos \tilde{\alpha}]}{\kappa (1-k^2) \tilde{\alpha} \alpha} \right.$ $\left[N_0(\xi_{mn}) + \frac{\tilde{\alpha}^2}{(m^2 \pi^2 - \tilde{\alpha}^2)} \left(\frac{2}{\pi \xi_{mn}} - kC \frac{m}{2\alpha} (k\xi_{mn}) \right) \right] \left. \right\}$		$M_y = -\frac{mg e^{i\Omega t} a (1+k^2)}{4 \frac{h}{a}} \left\{ \frac{\Theta_0}{x_0} \frac{1 + \sin \tilde{\alpha} \cos \tilde{\alpha}}{\tilde{\alpha}} \right.$ $\left[\frac{(1+k^2)}{8} \left(1 + \frac{\sin \tilde{\alpha} \cos \tilde{\alpha}}{\tilde{\alpha}} \right) - \frac{1}{12} \left(\frac{h}{a} \right)^2 \right] + \frac{2(-1)^{m+1} \sin \tilde{\alpha}}{a^2 \tilde{\alpha}^2 \xi_{mn} (1-k^2)} \left.$ $\left[B_{mn} \left\{ \cosh \left(\frac{\kappa}{2} \right) - \frac{2}{\kappa} \sinh \left(\frac{\kappa}{2} \right) \right\} \cdot \left\{ \frac{\tilde{\alpha}^2}{(m^2 \pi^2 - \tilde{\alpha}^2)} \left(\frac{2}{\pi \xi_{mn}} - kC \frac{m}{2\alpha} (k\xi_{mn}) \right) + N_0(\xi_{mn}) \right\} + \frac{\tilde{\alpha}^2 \xi_{mn}^2 N_2(\xi_{mn})}{(\pi^2 m^2 - \tilde{\alpha}^2) \kappa} \right] - \frac{B_{mn} \sinh \left(\frac{\kappa}{2} \right)}{a^2 \tilde{\alpha}^2 \xi_{mn} (1-k^2)} \right] +$ $2mg \frac{a}{3} \frac{\sin \tilde{\alpha}}{\tilde{\alpha}} \cdot \frac{(1-k^2)}{(1-k^2)} \left. \right\}$		$M_x = + \frac{mg e^{i\Omega t} a (1+k^2)}{4 \frac{h}{a}} \left\{ \frac{\Theta_0}{x_0} \frac{1 - \sin \tilde{\alpha} \cos \tilde{\alpha}}{\tilde{\alpha}} \right.$ $\left[\frac{(1+k^2)}{8} \frac{\sin^2 \tilde{\alpha}}{\tilde{\alpha}} \right] - \frac{2[1 - (-1)^m \cos \tilde{\alpha}]}{a^2 \tilde{\alpha}^2 \xi_{mn} (1+k^2)} \left[B_{mn} \left\{ \cosh \left(\frac{\kappa}{2} \right) - \frac{2}{\kappa} \sinh \left(\frac{\kappa}{2} \right) \right\} \cdot \left\{ \frac{\tilde{\alpha}^2}{(\pi^2 m^2 - \tilde{\alpha}^2)} \left(\frac{2}{\pi \xi_{mn}} - kC \frac{m}{2\alpha} (k\xi_{mn}) \right) + N_0(\xi_{mn}) \right\} + \frac{\tilde{\alpha}^2 \xi_{mn}^2 N_2(\xi_{mn})}{(\pi^2 m^2 - \tilde{\alpha}^2) \kappa} \right] - \frac{A_{mn} \cosh \left(\frac{\kappa}{2} \right)}{a^2 \tilde{\alpha}^2 \xi_{mn} (1-k^2)} \right] - 2mg \frac{a}{3} \frac{[1 - \cos \tilde{\alpha}]}{\tilde{\alpha}} \cdot \frac{(1-k^2)}{(1-k^2)} \left. \right\}$

Table 2
CIRCULAR CYLINDRICAL SECTOR TANK

Excitation in x- and y- Direction: $x(t) = x_0 e^{i\Omega t}$ $y(t) = y_0 e^{i\Omega t}$		Excitation About y-Axis and x-Axis $\theta(t) = \theta_0 e^{i\Omega t}$ $\chi(t) = \chi_0 e^{i\Omega t}$	
Velocity Potential	$\phi = \left\{ \begin{matrix} i\Omega x_0 \\ i\Omega y_0 \end{matrix} \right\} e^{i\Omega t} \left[\begin{matrix} r \cos \varphi \\ r \sin \varphi \end{matrix} \right] + \frac{b_{mn} \eta^2}{(1-\eta^2)} \left\{ \begin{matrix} a_m \\ c_m \end{matrix} \right\} \cos(\varphi) \frac{\cosh(\kappa r)}{\cosh \kappa} J(\rho)$	$\phi = (r, \varphi, z, t) = - \left\{ \begin{matrix} i\Omega \theta_0 \\ i\Omega \chi_0 \end{matrix} \right\} e^{i\Omega t} \left[\begin{matrix} rz \cos \varphi \\ rz \sin \varphi \end{matrix} \right] - \left\{ A_{mn} \cosh(\xi) + B_{mn} \sinh(\xi) \right\} \cos \varphi J(\xi)$	
Fluid Force in x-Direction	$F_x = m\Omega^2 e^{i\Omega t} \left\{ \begin{matrix} x_0 \\ y_0 \end{matrix} \right\} \left[\begin{matrix} 1 \\ 0 \end{matrix} \right] + \frac{2 \sin \tilde{\alpha}}{\tilde{\alpha} a} \frac{b_{mn} \eta^2}{(1-\eta^2)} \left\{ \begin{matrix} a_m \\ c_m \end{matrix} \right\} (-1)^{m+1} \frac{\tanh \kappa}{\kappa} \cdot \left\{ \frac{\tilde{\alpha}^2}{(\pi^2 m^2 - \tilde{\alpha}^2)} J(\epsilon_{mn}) + L_0(\epsilon_{mn}) \right\}$	$F_x = -mg \left\{ \begin{matrix} \theta_0 \\ \chi_0 \end{matrix} \right\} e^{i\Omega t} + m\Omega^2 e^{i\Omega t} \left\{ \begin{matrix} \theta_0 \\ \chi_0 \end{matrix} \right\} \frac{4 \sinh(\frac{\kappa}{2}) (-1)^{m+1} A_{mn} \sin \tilde{\alpha}}{\kappa \tilde{\alpha} a} \cdot \left[\frac{\tilde{\alpha}^2}{(\pi^2 m^2 - \tilde{\alpha}^2)} J(\epsilon_{mn}) + L_0(\epsilon_{mn}) \right]$	
Fluid Force in y-Direction	$F_y = m\Omega^2 e^{i\Omega t} \left\{ \begin{matrix} x_0 \\ y_0 \end{matrix} \right\} \left[\begin{matrix} 0 \\ 1 \end{matrix} \right] - \frac{2 \sin \tilde{\alpha}}{\tilde{\alpha} a} \frac{b_{mn} \eta^2}{(1-\eta^2)} \left\{ \begin{matrix} a_m \\ c_m \end{matrix} \right\} [1 - (-1)^m \cos \tilde{\alpha}] \frac{\tanh \kappa}{\kappa} \cdot \left\{ \frac{\tilde{\alpha}^2}{(\pi^2 m^2 - \tilde{\alpha}^2)} J(\epsilon_{mn}) + L_0(\epsilon_{mn}) \right\}$	$F_y = -mg \left\{ \begin{matrix} \theta_0 \\ \chi_0 \end{matrix} \right\} e^{i\Omega t} - m\Omega^2 e^{i\Omega t} \left\{ \begin{matrix} \theta_0 \\ \chi_0 \end{matrix} \right\} \frac{4 \sinh(\frac{\kappa}{2}) A_{mn}}{\kappa \tilde{\alpha} a} [1 - (-1)^m \cos \tilde{\alpha}] \cdot \left[\frac{\tilde{\alpha}^2}{(\pi^2 m^2 - \tilde{\alpha}^2)} J(\epsilon_{mn}) + L_0(\epsilon_{mn}) \right]$	
Moment About y-Axis	$M_y = m\Omega^2 e^{i\Omega t} a \left\{ \begin{matrix} x_0 \\ y_0 \end{matrix} \right\} \left[\begin{matrix} \frac{1}{4h/a} \cdot \frac{2 \sin \tilde{\alpha}}{\tilde{\alpha}} \cdot \left(1 + \frac{\sin \tilde{\alpha} \cos \tilde{\alpha}}{\tilde{\alpha}} \right) \\ \frac{1}{4h/a} \cdot \frac{\sin^2 \tilde{\alpha}}{\tilde{\alpha}} \end{matrix} \right] + \frac{\sin \tilde{\alpha}}{a \tilde{\alpha}} \frac{(-1)^{m+1} b_{mn} \eta^2}{\epsilon_{mn} (1-\eta^2)} \cdot \left\{ \begin{matrix} a_m \\ c_m \end{matrix} \right\} \left\{ \frac{\tilde{\alpha}^2}{(\pi^2 m^2 - \tilde{\alpha}^2)} J(\epsilon_{mn}) + L_0(\epsilon_{mn}) \right\} \cdot \left\{ \tanh \kappa + \frac{2}{\kappa} \left(\frac{1}{\cosh \kappa} - 1 \right) \right\} + \frac{2 \tilde{\alpha}^2 \epsilon_{mn}^2}{(\pi^2 m^2 - \tilde{\alpha}^2)} \cdot \frac{L_2(\epsilon_{mn})}{\kappa \cosh \kappa} \right] + 2mg \frac{a}{3} \frac{\sin \tilde{\alpha}}{\tilde{\alpha}}$	$M_y = - \frac{m(g/a)}{(4h/a)} e^{i\Omega t} \left\{ \begin{matrix} \theta_0 \\ \chi_0 \end{matrix} \right\} \left[\begin{matrix} 1 + \frac{\sin \tilde{\alpha} \cos \tilde{\alpha}}{\tilde{\alpha}} \\ \frac{\sin^2 \tilde{\alpha}}{\tilde{\alpha}} \end{matrix} \right] + ma^2 \Omega^2 e^{i\Omega t} \left\{ \begin{matrix} \theta_0 \\ \chi_0 \end{matrix} \right\} \left[\begin{matrix} \frac{1}{8} \left(1 + \frac{\sin \tilde{\alpha} \cos \tilde{\alpha}}{\tilde{\alpha}} \right) - \frac{1}{12} \left(\frac{1}{a} \right)^2 \\ \frac{1}{8} \frac{\sin^2 \tilde{\alpha}}{\tilde{\alpha}} \end{matrix} \right] + \frac{2(-1)^{m+1} \sin \tilde{\alpha}}{a^2 \tilde{\alpha} \epsilon_{mn}} \left[B_{mn} \left\{ \cosh(\frac{\kappa}{2}) - \frac{2}{\kappa} \sinh(\frac{\kappa}{2}) \right\} \cdot \left\{ \frac{\tilde{\alpha}^2}{(\pi^2 m^2 - \tilde{\alpha}^2)} J(\epsilon_{mn}) + L_0(\epsilon_{mn}) \right\} + \frac{\tilde{\alpha}^2 L_2(\epsilon_{mn}) \epsilon_{mn}^2}{(\pi^2 m^2 - \tilde{\alpha}^2) \kappa} \cdot \left\{ A_{mn} \cosh(\frac{\kappa}{2}) - B_{mn} \sinh(\frac{\kappa}{2}) \right\} \right] + 2mg \frac{a}{3} \cdot \frac{\sin \tilde{\alpha}}{\tilde{\alpha}}$	
Moment About x-Axis	$M_x = -m\Omega^2 e^{i\Omega t} a \left\{ \begin{matrix} x_0 \\ y_0 \end{matrix} \right\} \left[\begin{matrix} \frac{1}{4h/a} \cdot \frac{2 \sin \tilde{\alpha}}{\tilde{\alpha}} \cdot \left(1 - \frac{\sin \tilde{\alpha} \cos \tilde{\alpha}}{\tilde{\alpha}} \right) \\ \frac{1}{4h/a} \left(1 - \frac{\sin \tilde{\alpha} \cos \tilde{\alpha}}{\tilde{\alpha}} \right) \end{matrix} \right] - \frac{1}{\tilde{\alpha} a} \frac{b_{mn} \eta^2}{(1-\eta^2)} \left\{ \begin{matrix} a_m \\ c_m \end{matrix} \right\} \frac{1}{\epsilon_{mn}} \cdot [1 - (-1)^m \cos \tilde{\alpha}] \cdot \left\{ \frac{\tilde{\alpha}^2}{(\pi^2 m^2 - \tilde{\alpha}^2)} J(\epsilon_{mn}) + L_0(\epsilon_{mn}) \right\} \left[\tanh \kappa + \frac{2}{\kappa} \left(\frac{1}{\cosh \kappa} - 1 \right) \right] + \frac{2 \tilde{\alpha}^2 \epsilon_{mn}^2}{(\pi^2 m^2 - \tilde{\alpha}^2)} \cdot \frac{L_2(\epsilon_{mn})}{\kappa \cosh \kappa} \right] - 2mg \frac{a}{3} \cdot \frac{[1 - \cos \tilde{\alpha}]}{\tilde{\alpha}}$	$M_x = \frac{g}{(4h/a)} e^{i\Omega t} a^2 \left\{ \begin{matrix} \theta_0 \\ \chi_0 \end{matrix} \right\} \left[\begin{matrix} \frac{1}{8} \frac{\sin^2 \tilde{\alpha}}{\tilde{\alpha}} \\ \frac{1}{8} \left(1 - \frac{\sin \tilde{\alpha} \cos \tilde{\alpha}}{\tilde{\alpha}} \right) \end{matrix} \right] - m\Omega^2 e^{i\Omega t} a^2 \left\{ \begin{matrix} \theta_0 \\ \chi_0 \end{matrix} \right\} \cdot \left[\begin{matrix} \frac{1}{8} \frac{\sin^2 \tilde{\alpha}}{\tilde{\alpha}} \\ \frac{1}{8} \left(1 - \frac{\sin \tilde{\alpha} \cos \tilde{\alpha}}{\tilde{\alpha}} \right) \end{matrix} \right] - \frac{2[1 - (-1)^m \cos \tilde{\alpha}]}{a^2 \tilde{\alpha} \epsilon_{mn}} \left[B_{mn} \cdot \left\{ \cosh(\frac{\kappa}{2}) - \frac{2}{\kappa} \sinh(\frac{\kappa}{2}) \right\} \cdot \left\{ \frac{\tilde{\alpha}^2}{(\pi^2 m^2 - \tilde{\alpha}^2)} J(\epsilon_{mn}) + L_0(\epsilon_{mn}) \right\} + \frac{\tilde{\alpha}^2 L_2(\epsilon_{mn}) \epsilon_{mn}^2}{\kappa (\pi^2 m^2 - \tilde{\alpha}^2)} \cdot \left\{ A_{mn} \cosh(\frac{\kappa}{2}) - B_{mn} \sinh(\frac{\kappa}{2}) \right\} \right] - 2mg \frac{a}{3} \cdot \frac{(1 - \cos \tilde{\alpha})}{\tilde{\alpha}}$	
Moment About z-Axis			

Roll Excitation $\varphi = \varphi_0 e^{i\Omega t}$

$$\begin{aligned} \begin{Bmatrix} \dot{M}_x \\ \dot{M}_y \end{Bmatrix} &= m a^2 \ddot{\varphi}_0 e^{i\Omega t} \begin{Bmatrix} \frac{1}{5} \frac{1-k^2}{1-k^2} \left\{ \frac{\sin \bar{\alpha}}{\bar{\alpha}} + 2 \frac{(\cos \bar{\alpha} - 1)}{\bar{\alpha}^2} \right\} + \frac{16 \bar{\alpha} \sin \bar{\alpha}}{\pi} \\ \frac{2}{3} \frac{\sin \bar{\alpha}}{\bar{\alpha}} - \frac{2}{3} (1 + \cos \bar{\alpha}) \end{Bmatrix} - \begin{Bmatrix} \frac{16 \bar{\alpha} \sin \bar{\alpha}}{\pi} \\ \frac{16 \bar{\alpha} (1 + \cos \bar{\alpha})}{\pi} \end{Bmatrix} \\ &\cdot \frac{1}{(2m-1) [(2m-1)^2 \pi^2 - 4\bar{\alpha}^2] (1-k^2)} \left[\frac{\bar{\alpha}^2}{[(2m-1)^2 \pi^2 - 4\bar{\alpha}^2]} \cdot \left\{ \frac{2m-1}{1-k} + 2 + k \frac{2m-1}{2\bar{\alpha}} - \frac{2m-1}{2\bar{\alpha}} + 1 + k \frac{2m-1}{\bar{\alpha}} + 3 \right\} \right. \\ &\left. - \frac{4\bar{\alpha}(1-k^2)}{(2m-1)} \right] + \frac{\bar{\alpha}^2}{(2m-1)^2 \pi^2 - 4\bar{\alpha}^2} \left\{ \left(\frac{2m-1}{2\bar{\alpha}} - 1 \right) \left(1 - k \frac{2m-1}{2\bar{\alpha}} + 1 \right) \left(1 - k \frac{2m-1}{2\bar{\alpha}} + 2 \right) + \left(\frac{2m-1}{2\bar{\alpha}} + 1 \right) \left(k \frac{2m-1}{2\bar{\alpha}} - k \right) \left(k - k \frac{2m-1}{2} \right) \right\} \\ &\cdot \frac{2m-1}{1-k} \frac{1}{\bar{\alpha}} \\ &\cdot \frac{4\bar{\alpha}(1-k^2)}{3(2m-1)} \pm \frac{16\bar{\alpha} \sin \bar{\alpha}}{\pi [1 + \cos \bar{\alpha}]} \cdot \frac{\tanh \kappa^* \left[\frac{\bar{\alpha}^2}{\pi^2 (2m-1)^2 - 4\bar{\alpha}^2} - \frac{2}{\pi^2 (2m-1)^2} - k C^* (k \frac{2m-1}{2\bar{\alpha}} - 1) + N_0 \right]}{\kappa^* (2m-1) [(2m-1)^2 \pi^2 - 4\bar{\alpha}^2] (1-\eta^*) (1-k^2)} \\ &\cdot \left\{ \frac{2m-1}{1-k} \frac{1}{\bar{\alpha}} \left(\frac{2m-1}{2\bar{\alpha}} + 2 \right) - q_{2m-1n} \left(k - k \frac{2m-1}{2\bar{\alpha}} \right) k \frac{2m-1}{2\bar{\alpha}} - \frac{(2m-1)}{4\bar{\alpha}} s_{2m-1n} \right\} \end{aligned}$$

Roll Excitation $\varphi = \varphi_0 e^{i\Omega t}$

$$\begin{aligned} \begin{Bmatrix} \dot{M}_x \\ \dot{M}_y \end{Bmatrix} &= m a^2 \ddot{\varphi}_0 e^{i\Omega t} \begin{Bmatrix} \frac{1}{5} \frac{1-k^2}{1-k^2} \left\{ \frac{\sin \bar{\alpha}}{\bar{\alpha}} + 2 \frac{(\cos \bar{\alpha} - 1)}{\bar{\alpha}^2} \right\} \\ \frac{2}{3} \frac{\sin \bar{\alpha}}{\bar{\alpha}} - \frac{2}{3} (1 + \cos \bar{\alpha}) \end{Bmatrix} \\ &+ \frac{16 \bar{\alpha}}{\pi (1-k^2)} \left\{ \frac{\sin \bar{\alpha}}{1 + \cos \bar{\alpha}} \right\} \frac{1}{(2m-1) [(2m-1)^2 \pi^2 - 4\bar{\alpha}^2]} \\ &\cdot \frac{\bar{\alpha}^2}{\pi^2 (2m-1)^2 - 4\bar{\alpha}^2} \\ &\cdot \left\{ \frac{(2m-1)}{1-k} \frac{1}{2\bar{\alpha}} + 2 + \frac{(2m-1)}{1-k} \frac{1}{2\bar{\alpha}} + 3 \right\} + \frac{(2m-1)}{2\bar{\alpha}} \frac{1}{2\bar{\alpha}} - 3 \\ &\cdot \frac{4\bar{\alpha}(1-k^2)}{5(2m-1)} \left\{ \frac{\sin \bar{\alpha}}{1 + \cos \bar{\alpha}} \right\} \\ &\cdot \frac{1-k}{1-k} \frac{2m-1}{\bar{\alpha}} \\ &\cdot \frac{1}{\eta^*} \left[\frac{2m-1}{1-k} \frac{1}{2\bar{\alpha}} - q_{2m-1n} \left(k \frac{2m-1}{2\bar{\alpha}} - k \frac{2m-1}{2\bar{\alpha}} \right) k \frac{2m-1}{2\bar{\alpha}} - \frac{2m-1}{1-k} \frac{1}{\bar{\alpha}} \right] \\ &\cdot \frac{2m-1}{1-k} \frac{1}{\bar{\alpha}} \cdot \frac{1}{\pi^2 (2m-1)^2 - 4\bar{\alpha}^2} (1-\eta^*) (1-k^2) \\ &\cdot \frac{2m-1}{4\bar{\alpha}} s_{2m-1n} \\ &\cdot \left[\tanh \kappa^* + \frac{2}{\kappa^*} \left(\frac{1}{\cosh \kappa^*} - 1 \right) \right] \cdot \frac{\bar{\alpha}^2}{\pi^2 (2m-1)^2 - 4\bar{\alpha}^2} \\ &\cdot \left(\frac{2}{\pi^2 (2m-1)^2} - k C_{2m-1} \left(k \frac{2m-1}{2\bar{\alpha}} - k \frac{2m-1}{2\bar{\alpha}} \right) + N_0 \left(k \frac{2m-1}{2\bar{\alpha}} - 1 \right) \right) + \\ &\cdot \frac{\bar{\alpha}^2}{\pi^2 (2m-1)^2 - 4\bar{\alpha}^2} \cdot \frac{2\bar{\alpha}^2}{\kappa^* \cosh \kappa^*} \left(\frac{2m-1}{2\bar{\alpha}} - 1 \right) N_0 \left(k \frac{2m-1}{2\bar{\alpha}} - 1 \right) \right\} \cdot \\ &\cdot 2m g \frac{a}{3} \frac{1-k^2}{1-k^2} \left\{ \frac{\sin \bar{\alpha}}{\bar{\alpha}} \right\} \end{aligned}$$

Moment About z-Axis

Roll Excitation $\varphi = \varphi_0 e^{i\Omega t}$

$$\begin{aligned} M_z &= m a^2 \ddot{\varphi}_0 e^{i\Omega t} \left\{ \frac{1+k^2}{2} + \frac{32\bar{\alpha}}{\pi} \right. \\ &\cdot \frac{1}{(1-k^2) (2m-1) [(2m-1)^2 \pi^2 - 4\bar{\alpha}^2]} \\ &\cdot \left(\frac{2m-1}{1-k} \frac{1}{2\bar{\alpha}} + 2 \right) \left(k \frac{2m-1}{2\bar{\alpha}} - k \frac{2m-1}{2\bar{\alpha}} \right) \\ &\cdot \left[\frac{\bar{\alpha}(1-k^2)}{(2m-1)} - \frac{2m-1}{2\bar{\alpha}} + 2 \right] \cdot \frac{2m-1}{2\bar{\alpha}} - 2 \\ &\cdot \left. \frac{1-k}{\bar{\alpha}} \frac{2m-1}{\bar{\alpha}} \right] + \\ &+ \frac{32\bar{\alpha}}{\pi} \frac{N_1 \left(k \frac{2m-1}{2\bar{\alpha}} \right)}{\kappa^*} \frac{\tanh \kappa^* \eta^*}{(2m-1) [(2m-1)^2 \pi^2 - 4\bar{\alpha}^2] (1-\eta^*)} \\ &\cdot \left[\frac{2m-1}{1-k} \frac{1}{2\bar{\alpha}} + 2 \right] - q_{2m-1n} \left(k \frac{2m-1}{2\bar{\alpha}} - k \frac{2m-1}{2\bar{\alpha}} \right) k \frac{2m-1}{2\bar{\alpha}} \\ &\cdot \left. \frac{2m-1}{4\bar{\alpha}} s_{2m-1n} \right] \end{aligned}$$

TABLE 3. CYLINDRICAL CONTAINER WITH CIRCULAR AND QUARTER CROSS SECTION

Circular Cylindrical Tank		Cylindrical Quarter Tank	
Excitation in x-Direction $x = x_0 e^{i\Omega t}$			
Displacement of Free Fluid Surface	$\bar{z} = \frac{\Omega^2}{g/a} x_0 e^{i\Omega t} \cos \varphi \left\{ \frac{1}{2} + 2 \frac{J_1(\rho)\eta^2}{(\epsilon_n^2 - 1)J_1(\epsilon_n)(1 - \eta^2)} \right\}$		$\bar{z} = \frac{x_0 \Omega^2 e^{i\Omega t}}{g/a} \left[\frac{1}{2} \cos \varphi + \frac{a}{\pi} \frac{b}{mn} \frac{\eta^2 J_{2m}(\rho) \cos 2m\varphi}{a(1 - \eta^2)} \right]$
Fluid Force	$F_x = m\Omega^2 x_0 e^{i\Omega t} \left\{ 1 + 2 \frac{\eta^2 \tanh \kappa}{\kappa(\epsilon_n^2 - 1)(1 - \eta^2)} \right\}$		$F_x = m\Omega^2 x_0 e^{i\Omega t} \left[1 + \frac{4\eta^2}{\pi a} \frac{(-1)^{m+1} a}{mn} \frac{b}{\eta^2} \frac{\tanh \kappa}{(1 - \eta^2)\kappa} \left\{ \frac{J_{2m}(\epsilon_{mn})}{(4m^2 - 1)} + L_0(\epsilon_{mn}) \right\} \right]$ $F_y = m\Omega^2 x_0 e^{i\Omega t} \frac{4a}{\pi a \kappa (1 - \eta^2)} \frac{b}{mn} \frac{\eta^2 \tanh \kappa}{\eta^2} \left\{ \frac{J_{2m}(\epsilon_{mn})}{(4m^2 - 1)} + L_0(\epsilon_{mn}) \right\}$
Moment	$M_y = m\Omega^2 a x_0 e^{i\Omega t} \left\{ \frac{1}{4h/a} + 2 \frac{\frac{1}{\kappa} \left(\frac{2}{\cosh \kappa} - 1 \right) + \frac{1}{2} \tanh \kappa}{\epsilon_n (\epsilon_n^2 - 1)(1 - \eta^2)} \eta^2 \right\}$		$M_x = -m\Omega^2 a x_0 e^{i\Omega t} \left[\frac{1}{\pi h/a} - \frac{2}{\pi} \frac{a}{mn} \frac{b}{\eta^2} \frac{\eta^2}{(1 - \eta^2)} \left\{ \left[\frac{J_{2m}(\epsilon_{mn})}{(4m^2 - 1)} + L_0(\epsilon_{mn}) \right] \left[\tanh \kappa + \frac{2}{\kappa} \left(\frac{1}{\cosh \kappa} - 1 \right) \right] \right. \right.$ $\left. \left. + \frac{2\epsilon_{mn}^2 L_0(\epsilon_{mn})}{(4m^2 - 1)\kappa \cosh \kappa} \right\} \right] - \frac{4mga}{3\pi}$ $M_y = m\Omega^2 a x_0 e^{i\Omega t} \left[\frac{1}{4h/a} + \frac{2}{\pi} \frac{(-1)^{m+1} a}{mn} \frac{b}{\eta^2} \frac{\eta^2}{(1 - \eta^2)} \left\{ \left[\frac{J_{2m}(\epsilon_{mn})}{(4m^2 - 1)} + L_0(\epsilon_{mn}) \right] \left[\tanh \kappa + \frac{2}{\kappa} \left(\frac{1}{\cosh \kappa} - 1 \right) \right] \right. \right.$ $\left. \left. + \frac{2\epsilon_{mn}^2 L_0(\epsilon_{mn})}{(4m^2 - 1)\kappa \cosh \kappa} \right\} \right] + \frac{4mga}{3\pi}$
Rotational Excitation $\theta = \theta_0 e^{i\Omega t}$			
Displacement of Free Fluid Surface	$\bar{z} = -\Omega^2 a \theta_0 e^{i\Omega t} \cos \varphi \left\{ \frac{1}{2} \frac{a}{b} + 2 \frac{J_1(\rho)\eta^2}{(\epsilon_n^2 - 1)J_1(\epsilon_n)(1 - \eta^2)} \left[\frac{2}{\Omega^2 \cosh \kappa} + \frac{1}{2} \frac{a}{b} - \frac{1}{\Omega^2} \right] \right\}$		$\bar{z} = -\frac{\Omega^2 \theta_0 e^{i\Omega t}}{g/a} \left\{ \frac{1}{2} \frac{a}{b} \cos \varphi - \left[A_{mn} \cosh \left(\frac{\kappa}{2} \right) + B_{mn} \sinh \left(\frac{\kappa}{2} \right) \right] J_{2m}(\rho) \cos 2m\varphi \right\}$
Fluid Force	$F_x = -mg\theta_0 e^{i\Omega t} - 2m\Omega^2 \theta_0 e^{i\Omega t} \left\{ \frac{2}{\kappa} \left(\frac{1}{\cosh \kappa} - 1 \right) + \left(\frac{\kappa}{2} + \frac{1}{2} \right) \tanh \kappa \right\} \eta^2$		$F_x = -mg\theta_0 e^{i\Omega t} + \frac{8m\Omega^2}{\pi} \theta_0 e^{i\Omega t} \frac{(-1)^{m+1} A_{mn} \sinh \left(\frac{\kappa}{2} \right)}{\kappa} \left[\frac{J_{2m}(\epsilon_{mn})}{(4m^2 - 1)} + L_0(\epsilon_{mn}) \right]$ $F_y = -mg\theta_0 e^{i\Omega t} - \frac{8m\Omega^2}{\pi} \theta_0 e^{i\Omega t} \frac{A_{mn} \sinh \left(\frac{\kappa}{2} \right)}{\kappa} \left[\frac{J_{2m}(\epsilon_{mn})}{(4m^2 - 1)} + L_0(\epsilon_{mn}) \right]$
Moment	$M_y = -\frac{mg a \theta_0 e^{i\Omega t}}{4h/a} - m\Omega^2 a^2 \theta_0 e^{i\Omega t} \left\{ \frac{1}{12} \left(\frac{b}{a} \right)^2 - \frac{1}{8} + 2 \frac{\eta^2}{\epsilon_n (\epsilon_n^2 - 1)(1 - \eta^2)} \right.$ $\left. \left[\left(2 - \frac{4\gamma}{\kappa} \right) \frac{1}{\epsilon_n \cosh \kappa} + \frac{1}{\epsilon_n} \left(\frac{3\gamma}{\kappa} + \frac{1}{2} \right) + \frac{1}{\epsilon_n} \left(\frac{\kappa}{4} - \frac{3\gamma}{2} - \frac{4}{\kappa} \right) \tanh \kappa \right] \right\}$		$M_x = -\frac{mg a \theta_0 e^{i\Omega t}}{2\pi(h/a)} - m\Omega^2 a^2 \theta_0 e^{i\Omega t} \left\{ \frac{1}{4\pi} - \frac{4}{\pi \epsilon_{mn}} \left[\frac{1}{\kappa} \left\{ \cosh \left(\frac{\kappa}{2} \right) - \frac{2}{\kappa} \sinh \left(\frac{\kappa}{2} \right) \right\} \frac{J_{2m}(\epsilon_{mn})}{(4m^2 - 1)} \right. \right.$ $\left. \left. + L_0(\epsilon_{mn}) \right\} + \frac{L_0(\epsilon_{mn}) \epsilon_{mn}^2}{(4m^2 - 1)\kappa} \left\{ A_{mn} \cosh \left(\frac{\kappa}{2} \right) + B_{mn} \sinh \left(\frac{\kappa}{2} \right) \right\} \right\} - \frac{4mga}{3\pi}$ $M_y = -\frac{mg a \theta_0 e^{i\Omega t}}{4h/a} + m\Omega^2 a^2 \theta_0 e^{i\Omega t} \left\{ \frac{1}{8} - \frac{1}{12} \left(\frac{b}{a} \right)^2 + \frac{4(-1)^{m+1}}{\pi \epsilon_{mn}} \left[\frac{1}{\kappa} \left\{ \cosh \left(\frac{\kappa}{2} \right) - \frac{2}{\kappa} \sinh \left(\frac{\kappa}{2} \right) \right\} \right. \right.$ $\left. \left. + L_0(\epsilon_{mn}) \right\} + \frac{L_0(\epsilon_{mn}) \epsilon_{mn}^2}{(4m^2 - 1)\kappa} \left\{ A_{mn} \cosh \left(\frac{\kappa}{2} \right) + B_{mn} \sinh \left(\frac{\kappa}{2} \right) \right\} \right\} + \frac{4mga}{3\pi}$

Roll Excitation: $\Psi = \varphi_0 e^{i\Omega t}$

$$\langle r, \varphi, z, t \rangle = i\Omega \varphi_0 e^{i\Omega t} a^2 \left\{ \frac{\gamma^2}{a^2} \cdot (\varphi - \pi\alpha) + \frac{8\tilde{\alpha}^2}{\pi} \cdot \frac{\cos \tilde{\varphi}}{(2m-1)[(2m-1)^2 \pi^2 - 4\tilde{\alpha}^2]} \left[\left(\frac{\gamma}{a} \right)^2 - \frac{4\alpha}{(2m-1)} \left(\frac{\gamma}{a} \right)^2 \right] + \frac{4\tilde{\alpha}^2 [4\alpha/2m - l(\epsilon_{2m-1n} - \epsilon_{2m-1n})] \cdot J_{2m-1/2\alpha}(\epsilon_{2m-1n})^2}{[(2m-1)^2 \pi^2 - 4\tilde{\alpha}^2] (1-\eta^2) \cosh \kappa^*} \cosh(\kappa^* + \kappa^*) \cdot \cos \tilde{\varphi} \right\}$$

$$= m\Omega^2 \varphi_0 e^{i\Omega t} a^2 \left\{ \left[\frac{2\cos \tilde{\alpha} - 1}{\tilde{\alpha}} + \frac{2}{3} \sin \tilde{\alpha} \right] + \frac{16\tilde{\alpha} \sin \tilde{\alpha}}{\pi} \sum_{n=1}^{\infty} \left\{ \frac{2\alpha/(2m+2\alpha-1) - 4\alpha/3(2m-1)}{(2m-1)[(2m-1)^2 \pi^2 - 4\tilde{\alpha}^2]} + \frac{\tilde{\alpha}^2}{(2m-1)^2 [(2m-1)^2 \pi^2 - \tilde{\alpha}^2] [(2m-1) + 4\alpha]} \right\} + \frac{8\sin \tilde{\alpha}}{(h/a)} \right. \\ \left. \cdot \frac{4\alpha}{(2m-1)} \frac{\epsilon_{2m-1n} - \epsilon_{2m-1n}}{(2m-1)^2 \pi^2 - 4\tilde{\alpha}^2} \tanh \kappa^* \eta^2 \right\} \left[\frac{\tilde{\alpha}^2 J_{2m-1/2\alpha}(\epsilon_{2m-1n})}{[(2m-1)^2 \pi^2 - \tilde{\alpha}^2]} + L_0(\epsilon_{2m-1n}) \right]$$

$$= m\Omega^2 \varphi_0 e^{i\Omega t} a^2 \left\{ \frac{1}{5h/a} \cdot \left[1 + \cos \tilde{\alpha} - \frac{2\sin \tilde{\alpha}}{\tilde{\alpha}} \right] \right\} + \frac{48\tilde{\alpha}^2}{5\pi^2 (h/a)} \frac{\tilde{\alpha}^2 \sin \tilde{\alpha} [(2m-1) - 4\alpha]}{[(2m-1)^2 \pi^2 - \tilde{\alpha}^2] [(2m-1)^2 \pi^2 - 4\tilde{\alpha}^2] (2m-1 + 4\alpha) (2m-1)^2} + \frac{4}{a^2} \frac{4\alpha}{(2m-1)} \frac{\epsilon_{2m-1n} - \epsilon_{2m-1n}}{(2m-1)^2 \pi^2 - 4\tilde{\alpha}^2} \frac{\sin \tilde{\alpha}}{(1-\eta^2) \cosh \kappa^*} \cdot \frac{\eta^2}{(1-\eta^2) \cosh \kappa^*} \\ \left\{ \left[\tanh \left(\frac{\kappa^*}{2} \right) + \frac{2}{\kappa^*} \left(\frac{1}{\cosh \kappa^*} - 1 \right) \right] L_0(\epsilon_{2m-1n}) + \frac{\tilde{\alpha}^2}{[(2m-1)^2 \pi^2 - \tilde{\alpha}^2]} J_{2m-1/2\alpha}(\epsilon_{2m-1n}) + \frac{2\tilde{\alpha}^2 \epsilon_{2m-1n} L_2(\epsilon_{2m-1n})}{[(2m-1)^2 \pi^2 - \tilde{\alpha}^2] [\kappa^* \cosh \kappa^*]} \right\} + \left\{ \frac{-2m\tilde{\alpha}^2}{3} \frac{(1-\cos \tilde{\alpha})}{\tilde{\alpha}} \right. \\ \left. + \frac{2m\tilde{\alpha}^2}{3} \frac{\sin \tilde{\alpha}}{\tilde{\alpha}} \right\}$$

$$L_0(\epsilon_{mn}) = \frac{2}{\epsilon_{mn}} \sum_{\mu=0}^{\infty} J_{2\mu} + \frac{m}{2\alpha} + 1 \quad (\text{Re } \frac{m}{2\alpha} > -1) \quad L_1(\epsilon_{2m-1n}) = \frac{2m-1}{4\alpha \epsilon_{2m-1n}} \sum_{\mu=0}^{\infty} \frac{\left(\frac{2m-1}{2\alpha} + 2\mu + 1 \right)}{\left(\frac{2m-1}{4\alpha} + \mu \right) \left(\frac{2m-1}{4\alpha} + \mu + 1 \right)} J_{\frac{2m-1}{2\alpha} + 2\mu + 1}(\epsilon_{2m-1n})$$

$$L_2(\epsilon_{mn}) = \frac{\Gamma(\frac{m}{4\alpha} + \frac{3}{2})}{\epsilon_{mn} \Gamma(\frac{m}{4\alpha} - \frac{1}{2})} \sum_{\mu=0}^{\infty} \frac{\left(\frac{m}{2\alpha} + 2\mu + 1 \right) \Gamma(\frac{m}{4\alpha} + \mu - \frac{1}{2})}{\Gamma(\frac{m}{4\alpha} + \mu + \frac{5}{2})} J_{\frac{m}{2\alpha} + 2\mu + 1}(\epsilon_{mn})$$

$$z = m\Omega^2 \varphi_0 e^{i\Omega t} a^2 \left[\frac{1}{2} - \frac{16\tilde{\alpha}^2}{\pi^2 (2m-1)^2 [(2m-1)\pi + 2\tilde{\alpha}]} - 16 \frac{4\alpha}{(2m-1)} \frac{\epsilon_{2m-1n} - \epsilon_{2m-1n}}{(2m-1)^2 \pi^2 - 4\tilde{\alpha}^2} \frac{L_1(\epsilon_{2m-1n}) \eta^2 \tanh \kappa^*}{[(2m-1)^2 \pi^2 - \tilde{\alpha}^2] (1-\eta^2) \cosh \kappa^*} \right]$$

Cylindrical Quarter Tank	
Roll Excitation $\varphi = \varphi_0 e^{i\Omega t}$ (for Cylindrical Quarter Tank)	
Displacement of Free Fluid Surface	$\xi = \frac{\varphi_0 e^{i\Omega t}}{g/a} \left\{ \left(\frac{r}{a} \right)^2 \left(\frac{r}{a} + \frac{\pi}{4} \right) + \frac{2}{\pi} \left(\frac{r}{a} \right)^2 \left[\ln \left(\frac{r}{a} \right) + \frac{1}{2} \right] \cos 2\varphi + \frac{2}{\pi} \frac{\cos(4m-2)\varphi}{(2m-1) [(2m-1)^2 - 1]} \left\{ \left(\frac{r}{a} \right)^{4m-2} \right. \right.$ $\left. + \frac{(r/a)^2}{(2m-1)} + \frac{\eta_1^2 (2f_n - v_n) J_2(\kappa_1^*)}{(1 - \eta_1^2)} \cos 2\varphi + \frac{2}{\pi} \right.$ $\left. \frac{(f_{2m-1n} - (2m-1)e^{2m-1n}) J_{4m-2}(\rho^*) \eta^{*2} \cos(4m-2)\varphi}{(2m-1) [(2m-1)^2 - 1] (1 - \eta^{*2})} \right\}$
Fluid Force	$F_x = m_1^2 a^2 \varphi_0 e^{i\Omega t} \left\{ \frac{2}{3} - \frac{4}{\pi} + \frac{16}{9\pi^2} + \frac{8}{\pi^2} \left[\frac{4m-1}{(2m-1)} - \frac{1}{3} \frac{1}{(2m-1)} \right] + \frac{1}{8m(2m-1)^2 [(2m-1)^2 - \frac{1}{4}]} \right.$ $\left. + \frac{4}{\pi^2} \frac{(2f_n - v_n) \tanh(\kappa_1^*) \eta_1^2}{\kappa_1^* (1 - \eta_1^2)} \cdot \left[\frac{1}{3} J_2(\bar{\kappa}_n) + L_0(\bar{\kappa}_n) \right] + \frac{8}{\pi^2 h} \right.$ $\left. \eta^{*2} \left[\frac{f_{2m-1n}}{2m-1} - e^{2m-1n} \right] \frac{\tanh \kappa^*}{e^{2m-1n} [(2m-1)^2 - 1] (1 - \eta^{*2})} \cdot \left[\frac{J_{4m-2}(\epsilon_{2m-1n})}{4[(2m-1)^2 - \frac{1}{4}]} + L_0(\epsilon_{2m-1n}) \right] \right\} = -F_y$
Moment	$M_x = m_1^2 a^2 \varphi_0 e^{i\Omega t} \left\{ \frac{1}{5} \left(1 - \frac{4}{\pi} \right) + \frac{4}{25\pi^2 h} + \frac{12}{5\pi^2 h} \frac{2(m-1)}{4[(2m-1)^2 - \frac{1}{4}][(2m-1)^2 - 1] (2m+\frac{1}{2})(2m-1)} \right.$ $\left. + \frac{2}{\pi^2} \frac{(2f_n - v_n) \eta_1^2}{\kappa_1^* (1 - \eta_1^2)} \left[\tanh(\kappa_1^*) + \frac{2}{\kappa_1^*} \left(\frac{1}{\cosh(\kappa_1^*)} - 1 \right) \right] \left[L_0(\bar{\kappa}_n) + \frac{1}{3} J_2(\bar{\kappa}_n) \right] \right.$ $\left. + \frac{2}{3} \frac{L_0(\bar{\kappa}_n)}{\kappa_1^* \cosh \kappa_1^*} + \frac{4}{\pi^2} \frac{[f_{2m-1n} - e^{2m-1n}]}{(2m-1)^2 - 1} \frac{\eta^{*2}}{e^{2m-1n} (1 - \eta^{*2})} \left\{ \tanh \kappa^* + \frac{2}{\kappa^*} \right. \left. \left(\frac{1}{\cosh(\kappa^*)} - 1 \right) \right\} \left\{ \frac{J_{4m-2}(\epsilon_{2m-1n})}{4[(2m-1)^2 - \frac{1}{4}]} + L_0(\epsilon_{2m-1n}) \right\} + \left. \frac{e^{2m-1n} L_0(\epsilon_{2m-1n})}{2[(2m-1)^2 - \frac{1}{4}](\kappa^*) \cosh(\kappa^*)} \right\} + \frac{4m+4}{3\pi} = M_y M_z = m_1^2 a^2 \varphi_0 e^{i\Omega t} \left\{ \frac{1}{2} - \frac{1}{\pi^2} + \frac{4}{\pi^2} \frac{1}{4m^2 (2m-1)^2} - \frac{8}{\pi^2} \frac{(2f_n - v_n) \tanh(\kappa_1^*) L_1(\bar{\kappa}_n) \eta_1^2}{\kappa_1^* (1 - \eta_1^2)} \right. \left. - \frac{16}{\pi^2} \frac{[f_{2m-1n} - e^{2m-1n}]}{(2m-1)^2 - 1} \frac{L_1(\epsilon_{2m-1n}) \eta^{*2} \tanh(\kappa^*)}{(\kappa^*) (1 - \eta^{*2})} \right\} $

Table 4

Roots of $J_{2m}^*(\epsilon_{mn}) = 0$


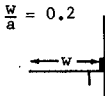
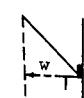
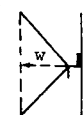
$\frac{m}{n}$	0	1	2	3	4	5	6	7	8	9
0	3.832	3.054	5.318	8.105	9.648	11.716	13.821	15.917	18.104	20.189
1	7.016	6.706	9.282	11.735	14.115	16.448	18.745	21.015	23.264	25.495
2	10.173	9.969	12.682	15.268	17.774	20.223	22.629	25.002	27.347	29.670
3	13.324	13.170	15.964	18.637	21.229	23.761	26.246	28.694	31.112	33.504
4	16.471	16.348	19.196	21.932	24.587	27.182	29.729	32.237	34.712	37.160
5	19.616	19.513	22.401	25.184	27.889	30.535	33.131	35.689	38.212	40.707
6	22.760	22.672	25.590	28.410	31.155	33.842	36.481	39.079	41.643	44.178
7	25.904	25.826	28.768	31.618	34.397	37.118	39.792	42.426	45.052	47.595
8	29.047	28.978	31.939	34.813	37.620	40.371	43.075	45.740	48.371	50.971
9	32.189	32.127	35.104	38.000	40.830	43.607	46.338	49.030	51.687	54.315

Table 5
MECHANICAL MODEL

	Circular Cylindrical Tank	Container with Annular Cross Section	Container of Four Quarter Tanks
Mass Ratio of Sloshing Mass to Liquid Mass	$\frac{m_n}{m} = \frac{2 \tanh(\kappa)}{\kappa (\epsilon_{n-1}^2 - 1)} \quad n = 1, 2, 3, \dots$	$\frac{m_n}{m} = \frac{\bar{A}_{n-1} \left[\frac{2}{\pi \epsilon_{n-1}^2} - \kappa C_1(k \epsilon_{n-1}) \right] \tanh \kappa}{(1 - k^2) \kappa}$ $\bar{A}_{n-1} = 2 \frac{\frac{2}{\pi \epsilon_{n-1}^2} - \kappa C_1(k \epsilon_{n-1})}{\frac{4}{\pi \epsilon_{n-1}^2} (\epsilon_{n-1}^2 - 1) - C_1^2(k \epsilon_{n-1}^2) (k \epsilon_{n-1}^2 - 1)}$	$\frac{m_{on}}{m} = \frac{32 \tanh \kappa}{\epsilon_{on} \pi^2 \kappa} \cdot \left[\frac{2}{\epsilon_{on}} \sum_{\mu=0}^{\infty} J_{2\mu+1}(\epsilon_{on}) - J_0(\epsilon_{on}) \right]$ $\cdot \sum_{\mu=0}^{\infty} \frac{J_{2\mu+1}(\epsilon_{on})}{(2\mu+3)(2\mu-1)}$ $\frac{m_{mn}}{m} = \frac{64 \tanh \kappa}{\pi^2 (\epsilon_{mn}^2 - 4m^2) \kappa} \left[\frac{\epsilon_{mn}}{J_{2m}(\epsilon_{mn}) (4m^2 - 1)} + \frac{2}{J_{2m}^2(\epsilon_{mn})} \sum_{\mu=0}^{\infty} \right]$ $J_{2m+2\mu+1}(\epsilon_{mn}) \cdot \sum_{\mu=0}^{\infty} \frac{J_{2m+2\mu+1}(\epsilon_{mn})}{(2m+2\mu+3)(2m+2\mu-1)}$
Ratio of Slosh Mass Location to Fluid Height	$\frac{h_n}{h} = \frac{1}{2} \left[1 - \frac{4}{\kappa} \tanh \left(\frac{\kappa}{2} \right) \right] \quad \text{for "spring-mass system"}$ $\frac{h_n}{h} = \frac{1}{h} + \frac{1}{2} \left[1 - \frac{4}{\kappa} \tanh \left(\frac{\kappa}{2} \right) \right] \quad \text{for "the oscillation system"}$	$\frac{h_n}{h} = \frac{1}{2} \left[1 - \frac{4}{\kappa} \tanh \left(\frac{\kappa}{2} \right) \right]$ $\frac{h_n}{h} = \frac{1}{h} + \frac{1}{2} \left[1 - \frac{4}{\kappa} \tanh \left(\frac{\kappa}{2} \right) \right]$	$\frac{h_n}{h} = \frac{1}{2} \left[1 - \frac{4}{\kappa} \tanh \left(\frac{\kappa}{2} \right) \right]$ $\frac{h_n}{h} = \frac{1}{h} + \frac{1}{2} \left[1 - \frac{4}{\kappa} \tanh \left(\frac{\kappa}{2} \right) \right]$
Distance of Fixed Mass Below Center of Gravity of Liquid	$h_o = \frac{1}{m_o} \sum_{n=1}^{\infty} m_n h_n \quad \text{for "spring-mass system"}$ $h_o = \frac{1}{m_o} \sum_{n=1}^{\infty} m_n (1_n - h_n) \quad \text{for "the oscillation system"}$		
Fixed Mass	$m_o = m - \sum_{n=1}^{\infty} m_n = m \left[1 - 2 \sum_{n=1}^{\infty} \frac{\tanh \kappa}{\kappa (\epsilon_{n-1}^2 - 1)} \right]$	$m_o = m - \sum_{n=1}^{\infty} \frac{\bar{A}_{n-1} \left[\frac{2}{\pi \epsilon_{n-1}^2} - \kappa C_1(k \epsilon_{n-1}) \right] \tanh \kappa}{(1 - k^2) \kappa}$	$m_o = m - \sum_{n=1}^{\infty} \sum_{m=1}^{\infty} m_{mn}$

Table 6

DAMPING FACTOR γ_s FOR CONSTANT EXCITATION AMPLITUDE $X_0 = 2.5\text{cm}$

DAMPING FACTOR γ_s FOR CONSTANT EXCITATION AMPLITUDE $X_o = 2.5\text{cm}$											Baffles
Liquid Height in Meters	Direct Method from			By Comparison with Magnification Curves and Phase Curves						Form of Baffles	
	\bar{Z}	ΔP	F	\bar{Z}	\bar{Z} Phase	ΔP	ΔP Phase	F	F Phase		
1.40	0.039	0.032	0.644	0.034	0.025	0.025	0.015	0.029	0.020		No
1.65	0.035	0.035	0.046	0.035		0.050		0.042	0.038		
2.70		0.035	0.042					0.030	0.030		
1.40	0.089	0.045	0.100	0.066	0.050	0.052	0.040	0.068	0.130		Floating Containers
1.65	0.147	0.170	0.125	0.075		0.130		0.073	0.150		
2.70		0.150	0.105					0.095	0.250		
1.40	0.130	0.170	0.120	0.180	0.050	0.150	0.120	0.100	0.250		Short Rings
1.65			0.090	0.120		0.140		0.090	0.200		
2.70			0.080					0.080			
1.40	0.120	0.130	0.120	0.400		0.200	0.150	0.140	0.130		Wide Cone Rings
1.65	0.090	0.100	0.140	0.300		0.100			0.170		
2.70		0.140	0.100					0.080	0.140		
1.40	0.120	0.120	0.080	0.130		0.110	0.120	0.090	0.160		Double Cone Rings
1.65		0.120	0.100	0.140		0.150		0.160	0.200		
2.70			0.090					0.080			

	Circular Cylindrical Tank	Container with Annular Cross Section	Container of Four Quarter Tanks
Spring Constants	$k_n = \omega_{n-1}^2 m_n$		
Length of Pendulum	$l_n = \frac{g}{\omega_{n-1}^2} = \frac{a}{\epsilon_{n-1} \tanh \kappa}$		
Damping Coefficient	$c_n = 2m_n \omega_{n-1} \gamma_n$		
Moment of Inertia of Fixed Mass	$I_o = I_{starr} - I_d - m_o h_o^2 - \sum_{n=1}^{\infty} m_n h_n^2 \quad \text{for "spring-mass system"}$ $I_o = I_{starr} - I_d - m_o h_o^2 - \sum_{n=1}^{\infty} m_n (h_n - l_n)^2 \quad \text{for "the oscillation system"}$		
Moment of Inertia of Disc	$I_d = 8ma^2 \sum_{n=1}^{\infty} \frac{\left[1 - \frac{2}{\kappa} \tanh\left(\frac{\kappa}{2}\right)\right]}{\epsilon_{n-1}^2 (\epsilon_{n-1}^2 - 1)}$ $I_d = I_{starr} - \bar{I} \left[1 + \frac{\bar{c}^2}{\omega^2 (I_{starr} - \bar{I})^2}\right] \quad \text{from experimental results}$	$I_d = 4ma^2 \sum_{n=1}^{\infty} \frac{\bar{A}_{n-1} \left[\frac{2}{\pi \epsilon_{n-1}} - k C_1 (k \epsilon_{n-1}) \right] \left[1 - \frac{2}{\kappa} \tanh\left(\frac{\kappa}{2}\right) \right]}{(1 - k^2) \epsilon_{n-1}^2}$	$I_d = ma^2 \frac{1}{2} + 8 \sum_{m=0}^{\infty} \sum_{n=0}^{\infty} \frac{(-1)^m a_m b_{mn}}{\pi a \epsilon_{mn}^2}$ $\left[\left(1 - \frac{2}{\kappa} \tanh\left(\frac{\kappa}{2}\right)\right) \cdot \left(\frac{J_{2m}(\epsilon_{mn})}{(4m^2 - 1)} + l_o(\epsilon_{mn}) \right) - \frac{2\epsilon_{mn}^2 l_o(\epsilon_{mn}) \tanh \kappa}{\kappa (4m^2 - 1)} \right]$
Damping Coefficient	$\bar{c}_d = \bar{c} \left[1 + \frac{\bar{c}^2}{\omega^2 [I_{starr} - \bar{I}]^2}\right] \quad \text{for fluid suppression}$		

REFERENCES

1. Lamb, H. , Hydrodynamics, Dover Publication, New York 1945, sixth edition. (Articles 191, 259)
2. Rayleigh, Lord, "On Waves," Phil Mag., Series 5, Vol. 1, 1876. (Seite 257 - 279)
3. Jacobson, L. S. , and Ayre, R. S. , "Hydrodynamic Experiments with Rigid Cylindrical Tanks subjected to transient Motions," Bulletin of the Seismological Society of America, Vol. 41, No. 4 (October 1951).
4. Graham, E. W. and A. M. Rodriguez, "The Characteristics of Fuel Motion, which Affect Airplane Dynamics," Journal of Applied Mechanics, Vol. 19. , No. 3 (September 1951).
5. Lorell, J. , "Forces produced by Fuel Oscillations," Jet Propulsion Laboratory, Progress Report 20 - 149 (1951).
6. Kachigan, K. , "Forced Oscillations of a Fluid in a Cylindrical Tank," Rep. No. -ZU-7-046, Convair, San Diego (1955).
7. Schmitt, A. F. , "Forced Oscillations of a Fluid in a Cylindrical Tank undergoing both Translation and Rotation," Rep. No. -ZU-7-069, Convair, San Diego (1956).
8. Miles, J. , "On the Sloshing of a Liquid in a Cylindrical Tank," Ramo - Woolridge AM-6-5, GM-TR-18 (1958).
9. Bauer, H. F. , "Fluidoscillations in a Circular Cylindrical Tank," Army Ballistic Missile Agency, Rep. No. -DA-TR-1-58 (1958).
10. Bauer, H. F. , "Theory of the Fluid Oscillations in a Circular Cylindrical Ring Tank partially filled with Liquid," NASA-TN-D-557 (1960).
11. Chu, W. , "Sloshing of Liquids in Cylindrical Tanks of Elliptic Cross-Section," Journal of the American Rocket Society, Vol. 30, No. 4. (1960).
12. Budiansky, B. , "Sloshing of Liquids in Circular Canals and Spherical Tanks," Journal of Aero Space Science, Vol. 27, (1960).

13. Bauer, H. F. , "Determination of Approximate First natural Frequencies of a Fluid in a Spherical Tank," Army Ballistic Missile Agency, Rep. No. -DA-TN-75-58 (1958).
14. Kellogg, O. D. , Foundations of Potential Theory, Verlag von Julius Springer, Berlin (1929).
15. Fuller, A. T. , "Stability Criteria for linear System and Reliability Criteria for RC Networks," Philosophical Society, Vol. 53 (1957).
16. McMahon, J. , "On the roots of the Bessel and Certain related functions," Annals of Mathematics, 9, (1894).
17. Buchholz, H. , "Besondere Reihenentwicklungen für eine häufig vorkommende zweireihige Determinante mit Zylinderfunktionen und ihre Nullstellen." Zeitschrift für Angewandte Mathematik und Mechanik No. 11/12 (1949).
18. Kirkman, D. , "Graphs and Formulas of Zeros of Cross Product Bessel Functions," Journal of Mathematics and Physics (1958).
19. Bateman, H. , Higher Transcendental Functions, Vol. II, New York, McGraw-Hill Book Company (1953).
20. Watson, G. N. , A Treatise on the Theory of Bessel Functions, Cambridge at the University Press (1952).

<p>NASA TR R-187 National Aeronautics and Space Administration. FLUID OSCILLATIONS IN THE CONTAINERS OF A SPACE VEHICLE AND THEIR INFLUENCE UPON STABILITY. Helmut F. Bauer. February 1964. xi, 138p. OTS price, \$3.00. (NASA TECHNICAL REPORT R-187)</p> <p>With the increasing size of space vehicles and their larger diameters which lower the natural frequencies of the propellants, the effects of propellant sloshing upon the vehicle stability are becoming more critical, especially since at launch a very large amount of the total weight is in the form of liquid propellant. With increasing diameters the eigenfrequencies of the propellant become smaller and shift closer to the control frequency of the space vehicle. Furthermore, the oscillating propellant masses and the corresponding forces increase considerably. A relatively simple means of avoiding strong dynamic coupling can be achieved by subdivision of the container by radial or circular walls. This results in smaller sloshing (over)</p>	<p>I. Bauer, Helmut F. II. NASA TR R-187</p> <p>NASA</p>	<p>NASA TR R-187 National Aeronautics and Space Administration. FLUID OSCILLATIONS IN THE CONTAINERS OF A SPACE VEHICLE AND THEIR INFLUENCE UPON STABILITY. Helmut F. Bauer. February 1964. xi, 138p. OTS price, \$3.00. (NASA TECHNICAL REPORT R-187)</p> <p>With the increasing size of space vehicles and their larger diameters which lower the natural frequencies of the propellants, the effects of propellant sloshing upon the vehicle stability are becoming more critical, especially since at launch a very large amount of the total weight is in the form of liquid propellant. With increasing diameters the eigenfrequencies of the propellant become smaller and shift closer to the control frequency of the space vehicle. Furthermore, the oscillating propellant masses and the corresponding forces increase considerably. A relatively simple means of avoiding strong dynamic coupling can be achieved by subdivision of the container by radial or circular walls. This results in smaller sloshing (over)</p>	<p>I. Bauer, Helmut F. II. NASA TR R-187</p> <p>NASA</p>
<p>NASA TR R-187 National Aeronautics and Space Administration. FLUID OSCILLATIONS IN THE CONTAINERS OF A SPACE VEHICLE AND THEIR INFLUENCE UPON STABILITY. Helmut F. Bauer. February 1964. xi, 138p. OTS price, \$3.00. (NASA TECHNICAL REPORT R-187)</p> <p>With the increasing size of space vehicles and their larger diameters which lower the natural frequencies of the propellants, the effects of propellant sloshing upon the vehicle stability are becoming more critical, especially since at launch a very large amount of the total weight is in the form of liquid propellant. With increasing diameters the eigenfrequencies of the propellant become smaller and shift closer to the control frequency of the space vehicle. Furthermore, the oscillating propellant masses and the corresponding forces increase considerably. A relatively simple means of avoiding strong dynamic coupling can be achieved by subdivision of the container by radial or circular walls. This results in smaller sloshing (over)</p>	<p>I. Bauer, Helmut F. II. NASA TR R-187</p> <p>NASA</p>	<p>NASA TR R-187 National Aeronautics and Space Administration. FLUID OSCILLATIONS IN THE CONTAINERS OF A SPACE VEHICLE AND THEIR INFLUENCE UPON STABILITY. Helmut F. Bauer. February 1964. xi, 138p. OTS price, \$3.00. (NASA TECHNICAL REPORT R-187)</p> <p>With the increasing size of space vehicles and their larger diameters which lower the natural frequencies of the propellants, the effects of propellant sloshing upon the vehicle stability are becoming more critical, especially since at launch a very large amount of the total weight is in the form of liquid propellant. With increasing diameters the eigenfrequencies of the propellant become smaller and shift closer to the control frequency of the space vehicle. Furthermore, the oscillating propellant masses and the corresponding forces increase considerably. A relatively simple means of avoiding strong dynamic coupling can be achieved by subdivision of the container by radial or circular walls. This results in smaller sloshing (over)</p>	<p>I. Bauer, Helmut F. II. NASA TR R-187</p> <p>NASA</p>

masses and higher eigenfrequencies. Another possibility is the clustering of tanks with small diameters which has the disadvantage of a weight penalty. For stability investigations the influence of the oscillating propellant has to be known. For this reason forces and moments of the propellant with a free fluid surface in a container of circular ring sector cross section performing forced oscillations must be determined. This will be performed with the assumption of irrotational, frictionless, and incompressible liquid. Linear equivalent damping is introduced with the help of a mechanical model describing the fluid motion. It has to be determined by experiments.

NASA

masses and higher eigenfrequencies. Another possibility is the clustering of tanks with small diameters which has the disadvantage of a weight penalty. For stability investigations the influence of the oscillating propellant has to be known. For this reason forces and moments of the propellant with a free fluid surface in a container of circular ring sector cross section performing forced oscillations must be determined. This will be performed with the assumption of irrotational, frictionless, and incompressible liquid. Linear equivalent damping is introduced with the help of a mechanical model describing the fluid motion. It has to be determined by experiments.

NASA

masses and higher eigenfrequencies. Another possibility is the clustering of tanks with small diameters which has the disadvantage of a weight penalty. For stability investigations the influence of the oscillating propellant has to be known. For this reason forces and moments of the propellant with a free fluid surface in a container of circular ring sector cross section performing forced oscillations must be determined. This will be performed with the assumption of irrotational, frictionless, and incompressible liquid. Linear equivalent damping is introduced with the help of a mechanical model describing the fluid motion. It has to be determined by experiments.

NASA

masses and higher eigenfrequencies. Another possibility is the clustering of tanks with small diameters which has the disadvantage of a weight penalty. For stability investigations the influence of the oscillating propellant has to be known. For this reason forces and moments of the propellant with a free fluid surface in a container of circular ring sector cross section performing forced oscillations must be determined. This will be performed with the assumption of irrotational, frictionless, and incompressible liquid. Linear equivalent damping is introduced with the help of a mechanical model describing the fluid motion. It has to be determined by experiments.

NASA